Effects of reaction conditions on the conversion of epoxides to cyclic carbonates through CO_2 inclusion

Thesis submitted in accordance with the regulations of the University of Cardiff for the degree of Doctor of Philosophy

By

Raiedhah Alsaiari

2017

Declaration

This work has not previously been accepted in substance for any degree and is not being concurrently submitted in candidature for any degree.

Signed……...(candidate)

Date…….

Statement 1

This thesis is the result of my own investigations, except where otherwise stated. Other sources are acknowledged by footnotes giving explicit references. A bibliography is appended.

Signed…….(candidate)

Date……..

Statement 2

I hereby give consent for my thesis, if accepted, to be available for photocopying and for inter-library loan, and for the title and summary to be made available to outside organizations.

Signed……...(candidate)

Date……...

Publication

- Raiedhah Alsaiari, Luke T. Perrott, Ewa Nowicka, Rebecca V. Engel, Peter J. Miedziak, Simon A. Kondrat, Jennifer K. Edwards, David J. Willock and Graham J. Hutchings, The effect of ring size on the selective carboxylation of cycloalkene oxides, *Catal. Sci. Technol.*, 2017, **7**, 1433.

Acknowledgements

First and foremost, all prayers and thanks are to Allah without whose help this work would have not been completed.

I would like to thank many people for their support and help throughout my PhD degree journey.

Special thanks go to my supervisor Professor Graham Hutchings for his guidance and support to complete this study. I am very fortunate and proud to be a student in his group.

I would like to thank Professor Joe Sweeney and Dr David Willock for their very useful comments on my thesis.

I take this opportunity to express my deepest sense of gratitude to Dr Rebecca Engle, Dr Ewa Nowicka, Dr Peter Miedziak, Dr Simon Kondrat and Dr Jennifer Edwards for their supervision, input, support and for giving me so much of their time.

I would like also to thank all Professional Services Staff in the CCI for their unlimited help and the department Technical Staff in chemistry school. Additionally, I would like to thank all the CCI members in lab 1.88, 1.86, 0.90 and room 0.74 for a nice time we spent together. I acknowledge my gratitude to Najran University for funding this research.

Words are not enough to express my love and gratitude to my husband Mubarak Alsaiari for his unlimited love, prayers and patience during the PhD degree journey.

Big thanks are given to my parent, especially to my mother who spent her life looking after me and praying for me all the time. Big sincere thanks must go to my brother Dr Saleh Alsaiari who gives me a special advice and encouragement during my study.

I would also like to thank my brother Mabkhoot Alsaiari for his suggestions and advice throughout this study. To all my brothers and sisters, thanks for everything.

Big thanks are given to my friends specially Dhabiah and Huda for all the amazing time that we spent together in Cardiff.

Abstract

This thesis targets to the synthesis of cyclic carbonates as they are compounds of high importance in a number of different applications. The one-pot synthesis of cyclic carbonates consists of two sequential reactions of epoxidation of the olefin and the subsequent cycloaddition reaction of CO_2 with the epoxide. To obtain more information on the roles of catalyst components, the epoxidation of 1-decene (first step) and the cycloaddition of CO_2 with epoxide (second step) were conducted individually.

The supported cobalt catalysts, prepared by a wet-impregnation method, were active in the epoxidation of 1-decene in the presence of oxygen from air as the primary oxidant and a very small amount of the radical initiator at 80°C. Using TiO_2 as a support for cobalt resulted in a significant reduction in the quantity of the leached cobalt catalyst compared with the use of MgO as a support. 1-Decene epoxidation was also performed over supported gold catalysts in the presence of a very small amount of the radical initiator using oxygen as the oxidant. Supported gold catalysts prepared by the sol-immobilisation method displayed the highest activity. Gold nanoparticles supported on TiO_2 and SiO_2 showed the highest activity.

The cycloaddition of CO_2 with different epoxides were studied using different catalysts. Tetrabutylammonium bromide (Bu_4NBr) was the most active quaternary ammonium salts. Other heterogeneous catalysts such as polydiallyldimethylammonium bromide and imidazole supported onto silica were found to be effective catalysts for this reaction. The compatibility between these two catalysts for the two different steps before coupling them in a one-pot reaction for the direct synthesis of cyclic carbonate was also investigated. The epoxide selectivity was significantly reduced in the presence of Bu_4NBr or polydiallyldimethylammonium bromide (40% PDDABr/SiO_2) or imidazole supported on silica (Imid/SiO_2). No effect of supported gold catalysts was observed on the cycloaddition of CO_2 with 1,2-epoxydecane. A simple and highly efficient preparation of cyclic carbonates from 1-decene was achieved by the use of 1%Au/support-$Bu_4NBr/ZnBr_2$ catalysts. The oxidative carboxylation process for a range of different cycloalkenes is challenging. For the epoxidation step, it was shown previously in our group that smaller ring size, such as cyclopentene, became less selective to the epoxidation. However, regarding the cycloaddition step, the opposite trend was found. Cyclopentene oxide and cyclohexene oxide gave high selectivity for cyclic carbonate, whereas the insertion of CO_2 in carbonylation of cyclooctene oxide and cyclododecane oxide to form cyclic carbonate was a challenging step and the main product was ketone.

Abbreviations

AIBN	α,α-Azoisobutyronitrile
BPO	Benzoyl peroxide
E_b	Binding energy
BET	Brunauer, Emmett and Teller
CHP	Cumene hydroperoxide
CC	Cyclic carbonate
DMF	Dimethylformamide
BHT	2,6-Di-*tert*-Butyl-4-methylpehnol
DTBP	Di-*tert*-butyl peroxide
ESCA	Electron spectroscopy for chemical analysis
FID	Flame ionization detector
FTIR	Fourier transform infrared spectroscopy
GC	Gas chromatograph
GC-MS	Gas chromatography-mass spectrometry
G	Graphite
ICP-MS	Inductivity coupled plasma-mass spectrometry
E_k	Kinetic energy
NMR	Nuclear magnetic resonance
PDDA-Br	Polydiallyldimethylammonium bromide
RI	Radical initiator
RF	Response factor
SEM	Scanning electron microscopy
TPR	Temperature programmed reduction
TBHP	*tert*-Butyl hydroperoxide
TCD	Thermal conductivity detector
TGA	Thermal gravimetric analysis
TEM	Transmission electron microscopy
PPh_3	Triphenylphosphine

XRD	X-ray diffraction
XPS	X-ray photoelectron spectroscopy

Table of contents

Chapter 1: Introduction

1.1. History of catalysis

The word catalysis is derived from the Greek language and can be divided into two parts: “cata” which means to bring down and “lysein” meaning to break. The term ‘catalysis’ was initially coined by Berzlius in 1836 during the combustion of oxygen and hydrogen over platinum in a reaction which had the ability to increase its rate without being consumed or altered itself during the reaction [1]. Using a suitable catalyst for a reaction offers an alternate, energetically more favourable pathway and therefore enables procedures to be completed under industrially feasible conditions of time, temperature and pressure. In 1825, many studies into reactions were done by Faraday [1], who explained that the activity of the platinum catalyst was involved a process of adsorption. In 1877, Lemoine [2] explained the thermodynamics of a catalyst and stated that the addition of a catalyst cannot change the equilibrium of a chemical reaction but the reaction rate would be altered.

1.2. Catalysts definition

A catalyst accelerates the rate of a chemical reaction towards chemical equilibrium, but is not altered itself. It can afford an alternative chemical pathway, which provides lower activation energy so the reaction can proceed at an accelerated rate. After the reaction is stopped, it can be recovered in its original form from the mixture without having been subjected to a chemical change [1]. For this reason, the catalytic material does not appear as one of the reactants or products in an overall balanced chemical equation. Figure 1.1 compares between the non-catalytic and catalytic reactions. For the non-catalytic reaction: the reaction proceeds when the reactants react with enough energy to overcome the activation energy barrier. The catalyst’s role is to lower the amount of energy needed to form one or more transition states between the reactants and the product. Nevertheless, both the forward and reverse reactions will be altered by a catalyst and there should be no change in the equilibrium position.

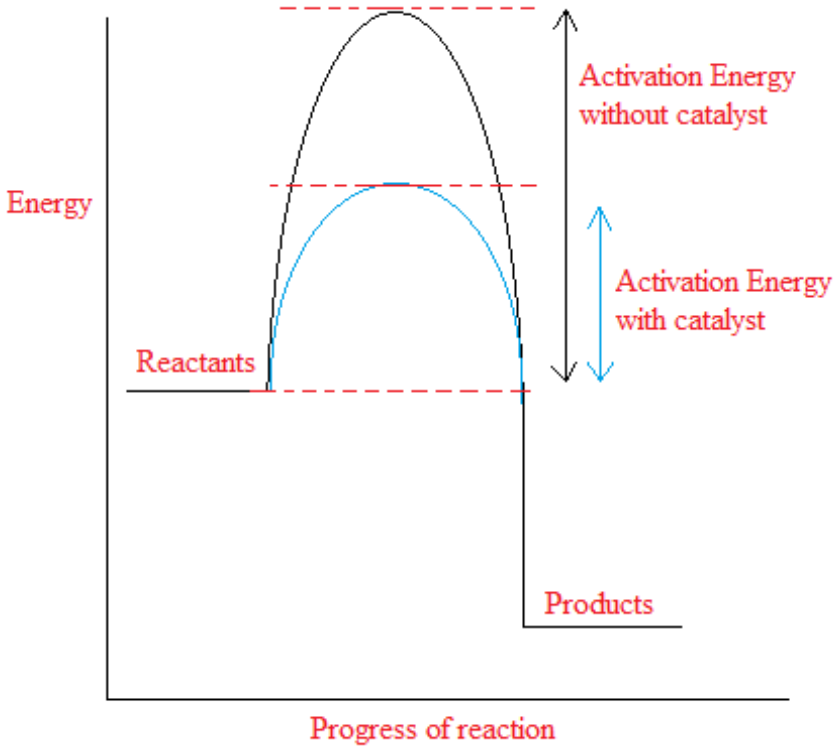

Figure 1.1: Activation energy barriers of uncatalysed/catalysed reaction. Adapted from reference [3].

1.3. Categories of catalysis

Catalysis can generally be classified into three different groups: heterogeneous catalysis, homogeneous catalysis and bio-catalysis. Heterogeneous catalysts exist in a different phase from the reactants (gas/solid or gas/liquid/solid). They are often present as metals supported on a secondary material, which help to enhance the activity of the catalyst. They are easy to separate and can have tuneable selectivity. Secondly, there are homogeneous catalysts, which are in the same phase as reactants. These can be more active than heterogeneous catalysts, and may have high selectivity but can be difficult to separate. Thirdly, there are bio-catalysts such as enzymes or bacteria [4]. The subsequent sections will briefly explain these types of catalysis.

1.3.1. Bio-catalysis

Enzyme catalysis (bio-catalysis) is an important area in catalysis. The enzyme is a natural catalyst and almost all living organisms' processes depend on it. The enzymes consist of proteins and the amino acids, which are the backbone of proteins and are linked together by peptide bonds, and these bonds form the enzyme's structure [5]. The enzyme active sites are a cleft surrounded by an array of amino acid residues, then these residues bind the substrates to the enzyme surface. Four types of interactions are used by the enzymes to bind their substrates, which are: hydrogen bonding, electronic interactions,

hydrophobic interactions and Van der Waals interactions. The bond between the substrate and the active site is relatively weak, as if the bond is strong, it may prevent the enzymes' catalytic cycle. In recent years, enzyme catalysis has become increasingly used as a catalyst for industrial processes [5].

1.3.2. Homogeneous catalysis

In homogeneous catalysis, the catalyst is in the same phase as the reaction mixture, which is generally liquid. The advantages of homogeneous catalysis are that there is a good contact between the substrates and catalyst, which results in greater selectivity. Many transition metals are used as homogeneous catalysts, stabilised by ligands. A ligand can play an essential role in homogeneous catalysis, as it can adjust the selectivity of the catalyst. Therefore, the catalytic activity and selectivity can be significantly improved by selecting appropriate metal and ligand [5]. However, as catalyst and reaction mixture exist in the same phase, the difficulties of the catalyst separation and recovery are major disadvantages of homogeneous catalysis.

1.3.3. Heterogeneous catalysis

In heterogeneous catalysis, the catalyst is usually solid, that is present at a different phase from the reaction mixture. Therefore, the ease of catalyst separation is the main advantage of heterogeneous catalysis. Most heterogeneous catalysis generally involves the three following stages of the catalytic process: first, adsorption of the reactants on to the surface of the catalyst at active sites, which is physisorption (weak adsorption) or chemisorption (strong adsorption, which involves bond weakening or breaking in the reactant). Then, interaction between the reactants on surface of the catalyst takes place. The last stage is the desorption of products from the catalyst surface so new molecules attach and react. Adsorption of reactants on the catalyst surface needs to be strong enough for reactants to react, although very strong adsorption leads to difficulty of product desorption from the catalyst surface. Heterogeneous catalysis has several advantages over homogenous catalysis, as shown in Table 1.1.

Table 1.1: Comparison between heterogeneous and homogeneous catalysts

Criterion	Heterogeneous	Homogeneous
Catalyst phase	Generally solid. Metal or metal oxide	Metal complex
Recyclability	Easy	Difficult
Selectivity	Variable	Usually high
Stability	Stable at high temperature	Decomposed
Solvent	Often not required	Required
Application	Wide	Limited

There are many industrial applications that use heterogeneous catalysis in chemical, pharmaceutical, food and petrochemical industries [6]; some of the industrial processes which use heterogeneous catalysis are described in Table 1.2.

Table 1.2: Processes based on heterogeneous catalysts [7]

Process	Catalyst
Ethylene epoxidation	Ag
Dehydrogenation of alkanes	V (oxide), Pt/Al_2O_3
Ammonia synthesis	Fe
Methanol synthesis	$Cu/ZnO/Al_2O_3$
Catalytic cracking of crude oil	Zeolites
Water-gas shift reaction	Fe (oxide), Cu-ZnO
Hydrogenation of vegetable oil	Ni
Reduction of NOx	Rh, V (oxide)

It has become important to develop environmentally friendly chemical processes over the past 25 years. In 1998, Warner and Anastas explained the concept of green chemistry in 12 principles [8, 9]. These principles are presented as follows:

1. Preventing the emergence of waste is less environmentally damaging than treating or disposing of waste (or a combination of the two) once it has already been produced.

2. Waste minimisation should be achieved by ensuring the maximisation of atom efficiency, thereby meaning that every reagents' atoms are integrated into the product.

3. The synthesis of environmentally toxic products (or the use of approaches which are in themselves hazardous) should not take place if there are less toxicity alternatives.

4. Design of a product which is fit for purpose should always be combined with the aim to minimise chemical and process hazardousness.

5. When practicable, the minimisation and, ideally, the elimination of solvent and auxiliary utilisation should be sought, and where impracticable, toxic and hazardous solvents and auxiliaries should not be used.

6. Environmental sustainability considerations should guide every practitioner's attempt to maximise process efficiency, with one implication of this being that ambient reaction conditions are unanimously preferable for minimising energy consumption.

7. Renewable raw materials should be used over non-renewable raw materials, with this consideration being even more pertinent when the non-renewable raw materials are not abundant.

8. Waste minimisation should be achieved by avoiding and, ideally, eliminating the transformation of intermediates into derivatives.

9. The process should utilise catalysis and eliminate the stoichiometric employment of reagents.

10. Product lifetimes should be minimised by the product design process after it has fulfilled its purpose to ensure the least impactful environmental effect.

11. Online monitoring and analysis of a system should be engaged in for the purpose of controlling undesirable and toxic waste and its release to the environment.

12. Risk minimisation considerations regarding toxic waste leakage, explosions, spillages, and fires should be incorporated into process design.

1.4. Carbon dioxide (CO_2)

The carbon cycle of carbon dioxide (CO_2) naturally occurs in aquatic and terrestrial environments in a dynamic exchange with the atmosphere. The main sources of CO_2 emissions are fossil fuels, natural gas, deforestation and coal, as well as some chemical processes [10]. These emissions of CO_2 are not balanced with the consumption of CO_2, therefore, the CO_2 concentration in the atmosphere has kept steadily increasing in the last 200 years [10]. This increase in CO_2 level, along with other greenhouse gases, directly affects the atmosphere and causes the increase in the planetary temperature that is associated with global climate change [11]. In recent years, there has been increasing interest in using CO_2 as a chemical starting material for conversion into valuable organic chemicals as it is abundant, non-toxic and low cost. A reduction in CO_2 emissions could be achieved through the reutilisation of CO_2. Around 110 Mton of carbon dioxide per year is utilised as a synthetic building block [11], 90 Mton of CO_2 per annum used for the synthesis of urea. Salicylic acid has been synthesised from phenol and CO_2 since 1890 as it is used in the production of aspirin. Furthermore, carbon dioxide can be incorporated into organic chemicals processes such as polycarbonates [12] and cyclic carbonates [13].

1.5. Cyclic carbonates (CCs)

Cyclic carbonates (CCs) such as ethylene and propylene carbonates are extensively used as intermediates in the synthesis of pharmaceuticals, raw materials for engineering plastics, aprotic polar solvents, electrolytes for lithium-ion batteries, monomers for synthesising polycarbonates and the use of CCs is one of the most effective routes for CO_2 fixation [14]. Cyclic carbonates are prepared *via* the cycloaddition of CO_2 with

epoxides as shown in Scheme 1.1. In this method CO_2 is used instead of toxic and hazardous reactants such as phosgene as the C_1-building block, as it is 100% atom economical, hence greatly desirable for transformation [14].

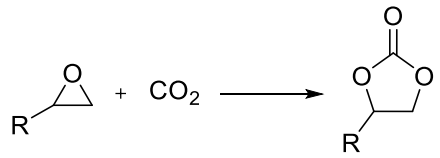

Scheme 1.1: Cycloaddition of CO_2 with epoxide.

Several studies have been developed for the synthesis of cyclic carbonates whether using homogeneous or heterogeneous catalysts. The following sections describe the developments in the area of catalysis of cyclic carbonate synthesis from CO_2 and epoxide.

1.5.1. Cyclic carbonate synthesis catalysed by quaternary ammonium salts

Quaternary ammonium salts are typically used as homogeneous catalysts for the synthesis of cyclic carbonate by the cycloaddition of carbon dioxide with the epoxide [15]. It was shown that a mixture of tetrabutylammonium bromide (Bu_4NBr) and tetrabutylammonium iodide (Bu_4NI) (1:1) can catalyse the cycloaddition of CO_2 (at atmospheric pressure) with styrene oxide to produce an 83% yield of styrene carbonate achievable at 120°C within 4 h [15]. Park and co-worker studied the effect of alkyl group length in ammonium salt in the synthesis of cyclic carbonate; they showed that the catalytic activity enhanced with increased length of the alkyl groups [16]. However, a decreased in the conversion was found with longer than C_8 alkyl group because it is too bulky to form an intermediate. Similar observations were found in previous studies described by Zhang and his group, which combined experimental and computational study for the conversion of ethylene oxide to ethylene carbonate [17]. In their work, they verified that reactions catalysed by tetraethylammonium chloride (Et_4NCl) and tetraethylammonium bromide (Et_4NBr) had a higher activation barrier (30.69 kcal mol^{-1}, 29.76 kcal mol^{-1} respectively) than those catalysed by Bu_4NBr (28.20 kcal mol^{-1}). The bulkiness of the tetrahedral ammonium ion $[NR_4]^+$ forces the Br anion away from the cation, which then results in a smaller amount of electrostatic interaction between Br^- and cation, which in turn results in more nucleophilicity of the anion. Regarding the effect of the anion in the quaternary ammonium salt, it was demonstrated that the order of activity was found to be $Bu_4NBr > Bu_4NI > Bu_4NCl$ [18]. In the case of Bu_4NI, when it was added into the reaction mixture of TBHP and styrene, the colour of the mixture changed to dark orange, which may indicate the formation of iodine by oxidation with TBHP [18].

Furthermore, a previous study showed that there was a synergistic effect of Lewis acid such as $ZnBr_2$ and the Lewis base on the catalytic synthesis of cyclic carbonate from CO_2 and epoxide [19]. Furthermore, they observed that the cycloaddition of CO_2 with epoxide using Lewis base and Lewis acid resulting to an increase in the reaction efficiency of up to 40 times comparing with the reaction carried out using only Lewis acid [19]. Furthermore, very low yield of cyclic carbonate (2.13%) was detected when using cyclooctene oxide as substrate [19]. Lewis acid enhances the activity of ammonium salt, as suggested by Kossev and his group [20]. It was found that Lewis acid promoted the reaction between carbon dioxide and different epoxides to synthesise cyclic carbonates using quaternary ammonium salts as catalysts. Different molar ratios were studied between ammonium salt and Lewis acid and found that the optimum molar ratio (Lewis base: Lewis acid) is 2:1 where a significant increase in the cyclic carbonate yield was obtained (96%). However, low cyclic carbonate yield was found (15%) when the molar ratio was 1:1 [20]. It was proposed that Lewis acid and the Lewis base are working together to open the epoxide ring, as suggested in the previous reported studies. The Lewis acid activates the epoxide, whereas the quaternary ammonium salt opens the ring of the epoxide [20]. Very efficient reaction can be achieved due to the cooperative between Zn complex and quaternary salts [18, 20]. Nevertheless, homogeneous catalysts such as Bu_4NBr are dissolved in a reaction mixture containing cyclic carbonates. Therefore, separating the catalysts from the reaction mixture may require more energy through a purification process.

1.5.2. Cycloaddition of CO_2 with the epoxide for cyclic carbonate synthesis using heterogeneous catalysts

Limited studies were carried out on the synthesis of cyclic carbonate using heterogeneous catalysts [21-29]. As shown previously, Bu_4NBr is the most active homogeneous catalyst for cycloaddition of CO_2 with epoxides. However, homogeneous catalysts are dissolved in the reaction mixture, which contains cyclic carbonate, therefore it is necessary to run a purification process to separate the catalysts from the products. Consequently, immobilising the quaternary ammonium salt by dispersing it on inorganic support would be a good solution in order to separate and recover the catalyst easily from the reaction mixture.

He and his group [22] investigated the synthesis of cyclic carbonates from terminal epoxides using silica-supported quaternary ammonium as a catalyst and CO_2 under supercritical conditions. They compared the activity of unsupported and silica-supported

tetrabutylammonium halide salts for cycloaddition of CO_2 with propylene oxide using 80 atmospheres pressure CO_2 with 1 mmol% catalyst for 10 h at 150°C. 97% and 96% cyclic carbonate yield were achieved when using the silica supported salts with the bromide and iodide respectively. The homogeneous Bu_4NBr provided a similar result. However, the fluoride salt gave only a 66% cyclic carbonate yield. However, fluoride salt showed a leaching after the fourth run, which results in decreased cyclic carbonate yield.

It is challenge to stabilise Bu_4NBr on the support and avoid the leaching of the active species. Other strategy is to find a material which can share the effectiveness of Bu_4NBr as well as stay insoluble in an organic solvent would be the perfect solution for the leaching of a catalyst in the liquid phase. It was reported that polydiallyldimethylammonium bromide supported on silica with $ZnBr_2$ can catalyse the cycloaddition of CO_2 with propylene oxide with 80% conversion and 96% selectivity for cyclic carbonate [23]. Furthermore, this catalyst could be recovered by a simple centrifugation after the reaction, and could then be reused 10 times without significant loss of activity [23]. More interestingly, this catalyst is non-toxic as it is used for drinking water pre-treatment [23].

Hydrotalcite and MgO were shown to be good catalysts for this reaction [24-26] due to their acidic and basic properties, which can help to adsorb CO_2 onto the surface. One study has used MgO for the cycloaddition of CO_2 with propylene and styrene oxides [24]; 41% and 47% yield of propylene and styrene carbonates being obtained respectively at 135°C using 20 atm CO_2 for 12 h using DMF as a solvent. Moreover, using hydrotalcite (Mg/Al=5) resulted in increasing the propylene carbonate yield to 88% using 3 atm CO_2 at 120°C for 24 h and DMF as a solvent, whereas only 38% yield of styrene carbonate was achieved under the same conditions [26]. Hydrotalcites and MgO catalysts usually required a polar organic solvent, high temperature and long reaction time in order to achieve good yield of cyclic carbonate [24-26].

Furthermore, the catalytic activity for imidazolium-based ionic liquids for cyclic carbonate synthesis was reported [27]. Miralda *et al.* prepared a zeolitic imidazole framework-8 catalyst for the synthesis of chloropropene carbonate by cycloaddition of carbon dioxide with epichlorohydrin and no co-catalysts or solvents were required during the reaction [27]. 98% epoxide conversion and only 33.4% selectivity for the cyclic carbonate was reported due to the formation of diol (selectivity 29.8%) and dimer (selectivity 36.8%) using 7 bar CO_2 at 100°C for 4 h. Another study showed that the imidazolium-based ionic liquids supported on silica (1.8 mmol%) can convert propylene

oxide to the corresponding cyclic carbonate (yield 99%) under solvent-free conditions using 8 MPa CO_2 at 160°C for 4 h [28]. This catalyst can be reused over four times with only a small decrease of its catalytic activity. Furthermore, under the same conditions, they studied the effect of MgO (1.8 mmol%) as a catalyst for this reaction and it was found that no cyclic carbonate was produced and only 2% conversion of the epoxide was observed [28]. Sankar and co-worker reported that a simple organic base can be anchored onto silica and used as a heterogeneous catalyst for cycloaddition of CO_2 with the epoxide [29]. They proposed that this catalyst has several advantages over the supported ionic liquid-based catalysts, which are effective in producing cyclic carbonate under solvent-free conditions, it is easy to synthesise, cost effective and can be reused several times without the addition of halide ions. 79% Conversion of styrene oxide and 97% selectivity for cyclic carbonate were obtained using imidazole supported silica using 0.6 MPa CO_2 at 130°C for 10 h [29]. However, using an expensive epoxide as raw materials would result in a decrease in the CCs production. Therefore, the direct synthesis of cyclic carbonates from low-priced olefins would be interesting to study.

1.5.3. Cyclic carbonate synthesis via oxidative addition of CO_2 with olefins

Cyclic carbonates can be produced by simpler and cheaper approaches directly from CO_2 and olefin instead of an expensive epoxide, which were shown to be remarkably economical methods because of the use of the low-priced olefins as starting materials as well as minimising the use of chemicals, the waste production and the processing time [18, 30, 31]. The oxidative carboxylation process (Scheme 1.2 a) consists of a combination of two sequential reactions; first, epoxidation of the olefin and then the cycloaddition of carbon dioxide with formed epoxide in a one-pot reaction to produce cyclic carbonate (Scheme 1.2 b).

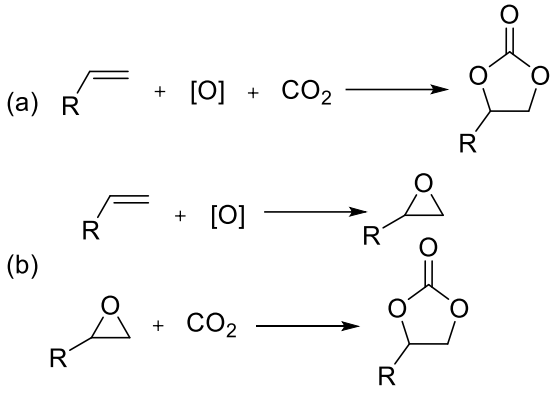

Scheme 1.2: The synthesis of cyclic carbonate from the oxidative carboxylation of olefins. Adapted from [18].

The one-pot synthesis of cyclic carbonate (simultaneous oxidation and carboxylation) from olefin involves the addition of CO_2 and a co-catalyst at the beginning of the reaction, with olefins, oxidants and catalysts required for the epoxidation step. In the one-pot multistep reaction (sequential oxidation and carboxylation), CO_2 and a co-catalyst are added to the same reactor after the epoxidation reaction is completed instead of being added at the beginning of the reaction (Scheme 1.3).

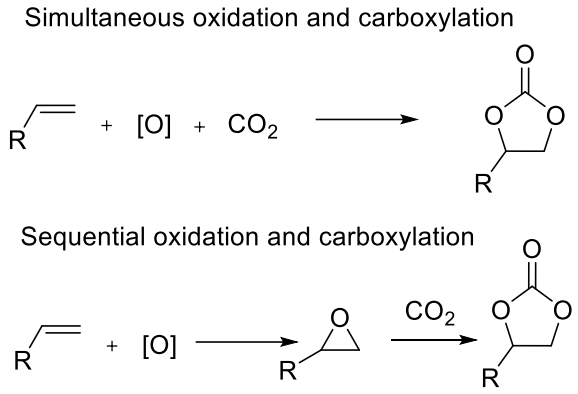

Scheme 1.3: Approaches for oxidative carboxylation of olefins. Adapted from [30].

In spite of the fact that the oxidative carboxylation of olefins has been known since 1962 [32], little attention was paid to this method compared with the route that employs epoxide as a starting material. Aresta and co-worker reported the direct synthesis of styrene carbonate using the $Nb_2O_5/NbCl_5$ catalyst [33]; the highest yield of styrene carbonate was only 11%, which attributed to the formation of by-products such as benzoic acid and benzaldehyde. Another study for the direct synthesis of cyclic carbonate done by Srivastava and co-worker using titaniosilicate catalysts. They first conducted the epoxidation of allylchloride or styrene (26.2 mmol) using titaniosilicate catalysts and H_2O_2 (14.7 mmol) as an oxidant at 60°C for 8 h in the presence of acetone as a solvent. After that, CO_2 (6.9 bar) and N,N-dimethylaminopyridine (DMAP; 0.0072 mmol) was added at 120°C and the reaction was conducted for a further 4 h. The results are shown in Table 1.3 [34]. 54.6% Allyl chloride conversion and 55.6% cyclic carbonate selectivity were obtained; it was detected amount of ring-hydrolysed products. A conversion of 50.4% and cyclic carbonate selectivity of 26% were obtained when styrene was the olefin.

Table 1.3: Synthesis of cyclic carbonates from olefins [34]

Catalyst (weight in mg)	Olefin	Stage 1 Olefin to epoxide		Stage 2 Epoxide to cyclic carbonate	
		Olefin conversion (%)	Epoxide selectivity (%)	Epoxide conv. (%)	Cyclic carbonate sel. (%)
TS-1 (400 mg)	Allylic chloride	54.6	100	92.5	55.6
TS-1 (400 mg)	Styrene	50.4	89	49.2	26

Another study by Aria and his group investigated the direct synthesis of cyclic carbonate from styrene [35]. Bu_4NBr (11.56 mmol%) was used as a catalyst for this reaction and TBHP (25.4 mmol) as an oxidant; The styrene carbonate yield could reach 38% at 80°C for 6 h under 1 MPa CO_2. Another investigations by the same group tested the performance of Bu_4NBr in the presence of zinc bromide for the cycloaddition of carbon dioxide with styrene oxide [18]. A short reaction time (1 h) was required for styrene carbonate to be produced (yield 100%) at 80°C when using Bu_4NBr and $ZnBr_2$ as catalysts and only 28% cyclic carbonate yield was obtained with Bu_4NBr. Furthermore, for the one-pot synthesis of cyclic carbonate, they combined $ZnBr_2$ and Bu_4NBr with Au/SiO_2, as they suggested that the latter is a good catalyst for the epoxidation reaction. A 42% yield of styrene carbonate was produced at 80°C for 4 h under solvent-free conditions [18]. They also observed that the addition of Bu_4NBr and $ZnBr_2$ did not have any decrease in the epoxide yield during the epoxidation reaction and supported gold catalyst has no activity for the cycloaddition of CO_2 with styrene oxide [18].

Yokoyama and co-worker [36] studied the synthesis of styrene carbonate, beginning with styrene in a one-pot multi-step synthesis (sequential oxidation and carboxylation). They used (MTO/UHP/$Zn[EMIm]_2Br_4$/($[BMIm]BF_4$) system, where methyltrioxorhenium (MTO) was used as the oxidation catalyst and urea hydrogen peroxide (UHP) was the oxidant; and the ionic liquids (BMIm = 1-butyl-3-methylimidazolium), (EMIm = 1-ethyl-3-methylimidazolium) as catalysts for cycloaadition of CO_2 with formed epoxide. An 83% yield of styrene carbonate was formed, using 30 atm of CO_2 at 110°C and only a 55% yield of cyclic carbonate was produced at 80°C using the same procedure. However, no cyclic carbonate was detected when they applied one-pot single step (simultaneous oxidation and carboxylation) and the reason may be that CO_2 play a

negative effect on oxidation step, which might come from its interaction with the oxidant UHP resulting to degrade the performance of the UHP [36].

This investigation is in agreement with another study [37], which demonstrated that the one-pot multistep synthetic protocol could efficiently promote oxidative carboxylation of 1-octene to yield 83% of cyclic carbonate. In contrast, the one-pot single step (simultaneous oxidation and carboxylation) of $MoO_2(acac)_2$/TBHP-Bu_4NBr system clearly stopped the epoxidation reaction and no 1-octene carbonate was produced as Bu_4NBr prevented the epoxidation reaction. This observation is in contrast to an earlier study [18], which observed that Bu_4NBr and $ZnBr_2$ have no effect on the epoxidation of styrene.

In fact, the combination of two reactions in a one-pot process usually needs compatibility between the reaction conditions such as temperature, pressure and the suitable catalysts for both reactions in the oxidative carboxylation process in one pot. Some of the catalysts exhibited low activity towards the epoxidation step, which resulted in a low yield of CCs; therefore, finding more active catalysts for the oxidation of olefins is important in one-pot synthetic reaction.

1.6. Catalysis by gold

Historically, gold (Au) was considered to be catalytically inactive (as the d-orbitals are filled) until the 1970s where Bond *et al.* [38] were the first to use a supported gold catalyst. They prepared Au/SiO_2 by the impregnation method and then dried and reduced in H_2 and was used in the hydrogenation of olefins. Significant attention had been placed on gold catalysis in chemistry after two important reports in the 1980s. These reports are as follows: Haruta and co-worker reported that gold nanoparticles supported on iron oxide are very active for CO oxidation at low temperatures [39]. Furthermore, Hutchings showed that gold was the most effective catalyst for the hydrochlorination of ethyne to vinyl chloride [40]. After these two highly important discoveries, the number of publications and patents using a gold catalyst have increased [41, 42]. There are many important industrial applications for using gold as a catalyst, such as CO oxidation at low temperatures [43, 44], synthesis of hydrogen peroxide under non-explosive conditions [45], oxidation of hydrocarbon, oxidation of alcohol and hydrogenation of alkynes [46-48].

Numerous studies have shown that Au particle size strongly influences their activity for many different reactions. The preparation method of the gold catalysts and the choice of

the support both have a large influence on the Au particle size [49-53]. Different preparation methods have been used for introduction of gold precursors on the support such as impregnation, deposition precipitation and sol-immobilisation. The impregnation is a simple method for preparing a gold supported catalyst. In this method, the gold precursor solution is stirred with the support, gold chloride ($AuCl_3$) and chloroauric acid ($HAuCl_4$) are frequently used as gold precursors. The gold particles prepared by this method are large (2-100 nm), these catalysts have been used for the direct synthesis of hydrogen peroxide [49] and alcohol oxidation [50] and have shown excellent activity. However, no activity has been found with CO oxidation. This observation leads to further development in the gold preparation method of supported gold catalysts of the deposition precipitation by Haruta [51]. The solution of the gold precursor is added to the mixture of deionised water with support with a simultaneous addition of sodium carbonate to increase the pH of the solution to a fixed value. In this method, a smaller particle size of gold catalysts has been produced but the nature of the formed catalyst depends on different factors, such as: the pH of the solution, the base used, time for the deposition to occur and heat treatment conditions [52]. In the sol-immobilisation method, the Au particles are immobilised on the support surface by adding the support to a colloidal suspension. Poly vinyl alcohol (PVA) is added (as a stabiliser) to protect the nanoparticles of gold catalyst from aggregation. As such, much smaller nanoparticle size distribution (2-5 nm) as well as a higher dispersion of gold have been found with the sol-immobilisation method [53].

1.6.1. Selective oxidation of alkenes by supported gold catalysts

Selective oxidation is a key process for commercial applications, especially for the synthesis of a chemical intermediate. Therefore, oxidation of hydrocarbons for generating compounds containing oxygen is an important industrial reaction [54]. Organic compounds which contain oxygen, such as epoxides, alcohols, aldehydes, ketones and acids, are used to produce plastics, detergents, paints, cosmetics and food additives. Aerobic epoxidation of terminal alkenes, containing allylic hydrogen are challenges in oxidation catalysis. Epoxide is one of the key intermediates in the manufacture of functionalised fine chemicals and pharmaceutics. Molecular oxygen from the air is the preferred oxidant in terms of green chemistry. Using molecular oxygen for epoxidation reactions in combination with an appropriate transition metal catalyst is the main target in heterogeneous catalysis [55].

Supported gold catalysts have a significant activity on oxidation of several types of alkenes [56-60]. Propene epoxidation is one of the most important topics in industrial processes. It can be used in the production of different products depending on the reaction conditions and the catalysts used [58]. Haruta established the earliest study of using supported gold catalysts for the epoxidation of alkenes [59]. He studied how the gold (prepared by deposition-precipitation) catalysed epoxidation of propene in the presence of hydrogen as a sacrificial reductant. 1% conversion of propene with 99% selectivity for propene oxide was obtained using 1% Au/TiO_2 [59]. Another study for the oxidation of propene by Haruta and his group used an Au/Ti-MCM-41 catalyst. They showed 2% conversion of propene and 95% selectivity for propene oxide at 100°C [60]. 1-Octene oxidation was also studied using Au/CeO_2 catalysts in the presence of 2,2-Azoisobutyronitrile (AIBN) as the radical initiator by Corma and his group [61]. They demonstrated that after 5 h of reaction in the absence of AIBN, very low conversion of 1-octene was detected, whereas in the presence of AIBN the conversion increased up to 5% and selectivity for the epoxide up to 45%. Different allylic products were produced from oxidation of 1-octene. Another study for the oxidation of 1-octene used graphite supported gold in the presence of *tert*-butyl hydroperoxide (TBHP) as a radical initiator using oxygen from the air under solvent-free conditions [62]. It was found that the activity of gold supported on different supports was as following: graphite > Al_2O_3 > SiC > MgO > SiO_2. Moreover, it was observed that the catalyst prepared using the sol-immobilisation method showed higher 1-octene conversion (3.7%) and selectivity for the epoxide (29.3%).

Solvent-free oxidation of 1-hexene with air by using supported gold catalysts with a small amount of TBHP as initiator was studied [63]. 1% Au/graphite catalysts were prepared using impregnation, deposition-precipitation or deposition-precipitation with urea, which leads to catalysts that display very similar activity (conversion 0.9% and epoxide selectivity 3.7-4.6%). However, a sol-immobilisation method gave higher conversion of 1-hexene to 2.4% and epoxide selectivity 11.8% and 77% selectivity for allylic products. Furthermore, supported gold catalysts have shown excellent activity in the epoxidation of cyclic alkenes [64-67]. It was shown previously that a supported gold catalyst can oxidise cyclohexene to the corresponding epoxide using O_2 and a small amount of *tert*-butyl hydroperoxide as a radical initiator in the presence of a solvent. It was found that the epoxide selectivity is strongly dependant on the type of solvent, C_6 products are produced in high yield when using non-polar solvents, whereas the presence of polar

solvents results in the formation of formic acid and CO_2 [64]. For instance, cyclohexene was almost converted with no C_6 products detected when water was used as a solvent, whereas a significant increase in the C_6 products selectivity of 76% (50% cyclohexane oxide and 26% 2-cyclohexen-1-one) and 30% conversion of cyclohexene when 1,2,3,5-tetramethylbenzene was used as the solvent. Moreover, it was established in this study that cyclooctene can be oxidised under solvent-free conditions using similar conditions with high selectivity for the epoxide.

Another study using gold nanoparticles supported on Si nanowires catalysts for oxidation of cycloalkenes was done by Lee and co-worker [68], they displayed that high conversion of cyclohexene (92%) and cyclooctene (38%) can be achieved. Moreover, more than 90% selectivity for cyclooctene oxide was detected whereas very low selectivity for cyclohexene (0.2%) was found and 2-cyclohexen-1-ol and 2-cyclohexen-1-one were the major final products after 24 h. Li and co-workers studied the oxidation of cyclooctene using gold supported on carbon nanotubes as the catalyst [69]. 54% conversion of cyclooctene and 44% selectivity for cyclooctene oxide could be obtained using TBHP and in the presence of CH_3CN as a solvent. Corma and his group [66] studied the oxidation of cyclohexene using 1.3% Au/CeO_2 catalyst and AIBN as a radical initiator. 20% cyclohexene oxide yield and 15% 2-cyclohexen-1-ol yield were obtained at 60°C using O_2 as an oxidant.

Another research on the oxidation of cyclooctene by Hutchings and co-worker [65, 67] used different types of supports for gold catalysts. They demonstrated that gold supported on graphite displayed the highest activity. Furthermore, they studied the influence of preparation method of supported gold catalysts on oxidation of cyclooctene, the sol-immobilisation method was found to produce more active catalysts for this reaction. It was demonstrated that the catalyst prepared by the sol-immobilisation method displayed small particle size (2-3 nm) and this may be the reason for the high activity. However, the 1% Au/graphite catalyst prepared by deposition-precipitation and wet-impregnation methods, which also exhibit a larger particle size distribution of 10-30 nm, gave 4-4.2% conversion and 71-78% epoxide selectivity as shown in Table 1.4.

Table 1.4: The effect of preparation methods on the epoxidation of cyclooctene [65]. Refer to Scheme 1.4

Preparation method	Cyclooctene conversion (%)	Epoxide selectivity (%)
Sol-immobilisation	7.7	81
Wet-impregnation	4.2	71
Deposition-precipitation	4	78

It was demonstrated that a small amount of the peroxide can be used as a reaction initiator for the oxidation of alkenes with supported gold catalysts [70, 71]. Hutchings and co-worker reported that TBHP can be used as a radical initiator for the oxidation of different cycloalkenes and in its absence no conversion was found [65]. Another investigation on the effect of radical initiators on oxidation of cyclooctene was studied [65]. They tested a range of radical initiators such as dibenzoyl peroxide (DBP), cumene hydroperoxide (CHP), *tert*-butyl hydroperoxide (TBHP) and azobisisobutyronitrile (AIBN) on the oxidation of cyclooctene with and without a supported gold catalyst. In the absence of the catalyst, very low activity was found with TBHP, whereas some activity was found with CHP, DBP and AIBN. Furthermore, the activity of oxidation of cyclooctene was increased when increasing the concentration of the initiator, regardless of the absence or presence of the supported gold catalyst. This is in agreement with the study by Liu *et al.* [72]; they noticed that with increasing the concentration of TBHP, the reaction activity of styrene oxidation also increased.

The proposed mechanism of oxidation of cyclooctene using supported gold catalyst and TBHP as a radical initiator was reported [65] as shown in Scheme 1.4. It was suggested that the concentration of TBHP has a notable influence on the pathway. TBHP decomposes to $(CH_3)COO^{\cdot}$ or $(CH_3)CO^{\cdot}$ in the presence of supported gold catalyst and these radicals abstract H atoms to produce allylic radicals (1) to give the oxygen adduct (2) and then produces cyclooctene hydroperoxide (3), which is the essential intermediate for the oxidation of cyclooctene on the gold surface. Then, cyclooctene hydroperoxide (3) transformed into cyclooctenelyloxy radical (4), which then abstracts one H atom to form intermediate radical (5), which rearranges to generate the epoxide and the allylic radical.

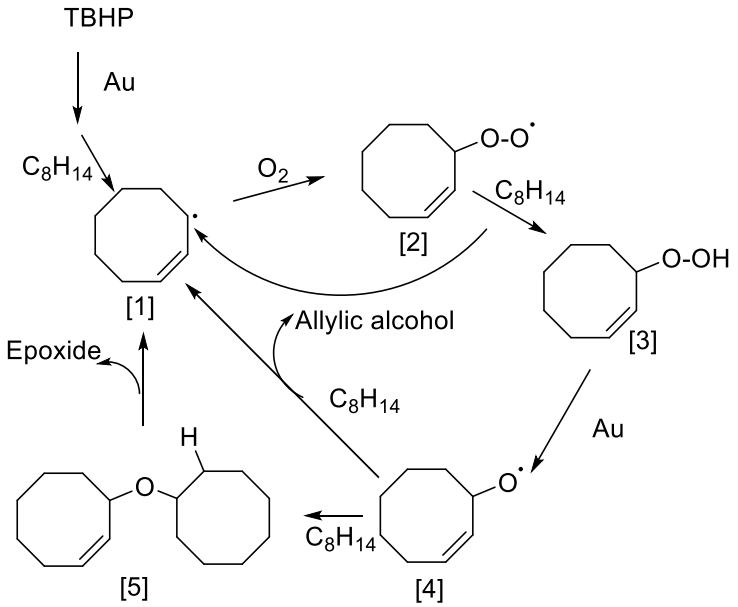

Scheme 1.4: Proposed mechanism for oxidation of *cis*-cyclooctene using 1% Au/graphite catalyst in presence of TBHP as a radical initiator. Adapted from reference [65].

An extension of this study was also carried out by Hutchings and his group on the oxidation of different ring size of cycloalkene using supported gold nanoparticles under solvent-free conditions using oxygen as the oxidant and a small amount of the radical initiator. They found that for the oxidation of cycloalkenes as the ring size decrease (sizes of C_7 or smaller) allylic oxidation was the dominant reaction pathway (cyclopentene oxide selectivity 10.9%, allylic products 77%), whereas with the larger ring sizes, epoxidation reaction pathway was preferred (selectivity for cyclooctene oxide 86%, allylic products 13%) [73]. Furthermore, they detected that the initiator was not necessary during the oxidation of cyclic alkenes and internal linear alkenes after removal of stabilisers (added by the manufacturers to prevent oxidation) from the alkenes [74]. In contrast, the epoxidation of terminal alkenes still required the presence of the radical initiator, which remains a challenge in selective oxidation catalysis. Terminal alkenes such as 1-hexene or 1-decene have shown competing pathways for oxidation [75], namely epoxidation and allylic oxidation. It was demonstrated that the epoxidation of 1-decene was achieved over gold supported on graphite prepared *via* an incipient-wetness impregnation method in the presence of a small amount of radical initiator (AIBN) using oxygen from air as the terminal oxidant at 90°C for 24 h (conversion 12.3% and epoxide selectivity 30.9%).

1.7. Selective oxidation of alkenes by different catalysts

Various studies observed that the heterogeneous epoxidation of alkenes, with the exception of ethene, is challenging [76, 77]. This may be due to the presence of labile allylic H atoms, whose facile abstraction results in production of allylic products instead of epoxidation of alkene. The improvement of low-priced heterogeneous catalysts toward the epoxidation of alkene has become a hot topic in recent chemical research.

Liang *et al.* applied iron-based heterogeneous catalysts with molecular oxygen for the epoxidation of cyclooctene in the absence of a sacrificial reductant [76] observing that the epoxidation of cyclooctene proceeded with conversion 40.2% and high selectivity (>96%) at 100°C for 24 h and 20 atm of O_2. Further research groups have studied the epoxidation of propylene over Ag-based catalyst mixed with 3d-transition metals using oxygen as an oxidant [77]. They observed that the highest yield of propylene oxide (0.68%) was produced by the addition of Ni to the Ag catalyst at 170°C. Another advantage is that the addition of a small amount of Ni decreased the required temperature of the reaction (from 230°C to 170°C) [77]. Another study has used porous nickel phosphate VSB-5 for the epoxidation of different cycloalkenes at 60°C for 7-8 h using H_2O_2 and acetonitrile as solvent. 84% and 49% conversion of cyclohexene and cyclooctene were obtained with 51% and 91% selectivity for their corresponding epoxides. However, low cyclododecene conversion (12%) and epoxide selectivity (7.1%) were obtained and the main product was the ketone [78]. They showed that the catalyst could be used many times without any structural degradation. Another group studied nickel catalysts deposited on non-porous carbon with O_2 and isobutyraldehyde [79]; they found that the different alkenes displayed different reactivity towards nickel-supported catalysts. Only a 27% conversion of 1-octene was seen, whereas 98% conversion of norbornene was observed. However, there was leaching of catalytic active species, which resulted in a loss of activity of the catalyst. Another investigation was performed into the epoxidation of styrene by TBHP using different supports for NiO, and showed the NiO/SiO_2 is the best choice for the epoxidation of styrene (selectivity for epoxide 77.7%) [80].

Cobalt-based catalysts were reported to be active in epoxidation reactions in both homogeneous [81, 82] as well as heterogeneous reactions [83-90]. It was shown that cobalt can successfully convert alkenes into the corresponding epoxides. Commercially available cobalt(II) perchlorate was investigated for epoxidation of terminal alkenes using 3-chloroperoxybenzoic acid as the oxidant and performed in CH_3CN at room temperature

in short time (10 min). 1-Hexene almost converted to give 86% yield of 1,2-epoxyhexane, 94% conversion of 1-octene and 92% of the 1,2-epoxyoctane was observed [81]. Another study investigated epoxidation of norbornene using [Co(2-hydroxy-1-naphthaldehyde)$_2$(DMF)$_2$] with TBHP as oxidant, 100% conversion and 100% selectivity was found within 6 h in CH_3CN [82]. Furthermore, the same group studied the immobilisation of [Co(2-hydroxy-1-naphthaldehyde)$_2$(DMF)$_2$] onto a modified iron oxide nanomagnet and used it for epoxidation of norbornene under the same conditions. 100% norbornene conversion and epoxide selectivity was observed similar to the homogenous one [82]. They also investigated the reusability of this catalyst and found that after five runs, there is a decrease in the norbornene conversion from 100% to 97% without any change in the epoxide selectivity.

Heterogeneous cobalt catalysts have been applied for the epoxidation of different alkenes, such as styrene and stilbene, to the corresponding epoxides using molecular oxygen as a primary oxidant in the presence of a polar solvent such as DMF [84-88]. Patil *et al*. studied the epoxidation of α-pinene using Co^{2+} ions-exchanged zeolite Y having various alkali and alkaline earth metal with O_2 as oxidant and using DMF as a solvent, 47% conversion and 61% epoxide selectivity was found [84].

Beier and co-worker also investigate the metal–organic framework STA-12(Co) catalyst to study the epoxidation of different alkenes in the presence of DMF as a solvent [87]. They found that the selectivity for styrene oxide was low due to oligomerisation, whereas high conversion of (*E*)-stilbene was observed with high selectivity for the epoxide 89%. They observed that STA-12(Co) catalyst was reusable with only a small loss of activity [87]. Baiker and co-worker demonstrated that DMF is not an inert solvent and should be considered a "sacrificial" solvent in the epoxidation of styrene with molecular oxygen. It is autoxidised with molecular oxygen to produce *N*-(hydroperoxymethyl)-*N*-methylformamide, which acting as an oxygen-transfer agent, which results in producing *N*-formyl-*N*-methylformamide [88]. Formation of *N*-Formyl-*N*-methylformamide ran parallel with the conversion of styrene and formation of styrene oxide. They proposed that the atom-efficiency of this reaction in the presence of DMF is poor and far from a "green" technology [88].

A cobalt(II) Schiff base complex has been immobilised onto the surface of Si-MCM-41 and has been reported to show catalytic activity for the aerobic epoxidation of different terminal alkenes in DMF. 47% 1-hexene conversion with 47% yield of the epoxide was observed, and 35% conversion of 1-octene with 30% yield of the epoxide was detected at

80°C and the flow rate of O_2: 3.0 cm^3 min^{-1} using DMF as a solvent. Furthermore, it was observed that this catalyst could be recovered and reused without any loss of activity [91].

1.8. Thesis overview

In the light of the above literature review, it was understood that the direct synthesis of cyclic carbonates from olefins and CO_2 consists of two sequential reactions of epoxidation of the olefin and the subsequent cycloaddition reaction of CO_2 with the epoxide formed in one pot. The main objective of the thesis is to consider the cyclic carbonate formation from the epoxide with a view to finding complementary reaction conditions to the alkene epoxidation step.

To obtain more information on the roles of catalyst components, epoxidation of 1-decene (first step) and cycloaddition of CO_2 with 1,2-epoxydecane (second step) are conducted individually. Three major studies have been carried out and are described in three results chapters:

1- Chapter 3 describes the use of supported cobalt catalysts for epoxidation of 1-decene with an investigation on the effect of different reaction parameters by identifying the blank conditions in which the 1-decene epoxidation can be performed, the effect of support and the effect of radical scavenger.

2- Chapter 4 demonstrates the use of a supported gold nanoparticulate catalyst for 1-decene epoxidation under green conditions and highlights the effects of different parameters, namely the effects of temperature, time, support, preparation method, reaction in the absence of oxygen and of radical scavenger.

3- Chapter 5 demonstrates suitable catalysts for the cycloaddition of CO_2 with different types of epoxides. Furthermore, this Chapter shows the effect of these catalysts on the epoxidation step and the effect of gold catalysts on the cycloaddition step. furthermore, this Chapter shows the direct synthesis of cyclic carbonate from 1-decene and demonstrates the challenge in oxidative carboxylation of cycloalkenes.

1.9. References

[1] M. Bowker, *The Basic and Application of Heterogeneous Catalysis*, Oxford chemistry primers, Oxford, 1998.

[2] G. Lemoine, *Ann. Chim. Phys.,* 1877, **12**, 145.

[3] M. Bowker, *The Basic and Application of Heterogeneous Catalysis*, Oxford chemistry primers, Oxford, 1998.

[4] G. C. Bond, *Heterogeneous catalysis: principle and applications*, Clarendon Press, Oxford, 1974.

[5] I. Chorkendorff and J. W. Niemantsverdriet, *Concepts of Modern Catalysis and Kinetics*, WILEY-VCH Verlag GmbH & Co., Weinheim, 2003.

[6] J. N. Armor, *Appl. Catal., A*, 2001, **222**, 407.

[7] I. Chorkendorff and J. W. Niemantsverdriet, *Concepts of Modern Catalysis and Kinetics*, WILEY-VCH Verlag GmbH & Co., Weinheim, 2003.

[8] P. T. Anastas and J. C. Warner, *Green Chemistry: Theory and Practice*, Oxford University Press, New York, 1998.

[9] R. A. Sheldon, I. Arends and U. Hanefeld, *Green Chemistry and Catalysis*, Wiley-VCH Verlag GmbH and Co., Weinheim, 2007.

[10] B. Clark and R. York, *Theory Soc.*, 2005, **34**, 391.

[11] M. Aresta and A. Dibenedetto, *Dalton Trans.*, 2007, 2975.

[12] H. Sugimoto and S. Inoue, *J. Polym. Sci. A Polym. Chem.*, 2004, **42**, 5561.

[13] A. A. G. Shaikh and S. Sivaram, *Chem. Rev.*, 1996, **96**, 951.

[14] D. Bai and H. Jing, *Green Chem.*, 2009, **12**, 39.

[15] V. Caló, A. Nacci, A. Monopoli and A. Fanizzi, *Org. Lett.*, 2002, **4**, 2561.

[16] H.-Y. Ju, M.-D. Manju, K.-H. Kim, S.-W. Park and D.-W. Park, *J. Ind. Eng. Chem.*, 2008, **14**, 157.

[17] J.-Q. Wang, K. Dong, W.-G. Cheng, J. Sun and S.-J. Zhang, *Catal. Sci. Technol.*, 2012, **2**, 1480.

[18] J. M. Sun, S. Fujita, F. Y. Zhao, M. Hasegawa and M. Arai, *J. Catal.*, 2005, **230**, 398.

[19] P. Ramidi, P. Munshi, Y. Gartia, S. Pulla, A. S. Biris, A. Paul and A. Ghosh, *Chem. Phys. Lett.*, 2011, **512**, 273.

[20] K. Kossev, N. Koseva and K. Troev, *J. Mol. Catal. A: Chem.*, 2003, **194**, 29.

[21] R. Srivastava, D. Srinivas and P. Ratnasamy, *Tetrahedron Lett.*, 2006, **47**, 4213.

[22] J.-Q. Wang, D.-L. Kong, J.-Y. Chen, F. Cai and L.-N. He, *J. Mol. Catal. A: Chem.*, 2006, **249**, 143.

[23] B. Song, L. Guo, R. Zhang, X. Zhao, H. Gan, C. Chen, J. Chen, W. Zhu and Z. Hou, *J. CO_2 Util.*, 2014, **6**, 62.

[24] T. Yano, H. Matsui, T. Koike, H. Ishiguro, H. Fujihara, M. Yoshihara and T. Maeshima, *Chem. Commun.*, 1997, 1129.

[25] B. M. Bhanage, S. I. Fujita, Y. Ikushima and M. Arai, *Appl. Catal., A*, 2001, **219**, 259.

[26] K. Yamaguchi, K. Ebitani, T. Yoshida, H. Yoshida, and K. Kaneda, *J. Am. Chem. Soc.*, 1999, **121**, 4526.

[27] C. M. Miralda, E. E. Macias, M. Zhu, P. Ratnasamy and M. A. Carreon, *ACS Catal.*, 2012, **2**, 180.

[28] J.-Q. Wang, X.-D. Yue, F. Cai and L.-N. He, *Catal. Commun.*, 2007, **8**, 167.

[29] M. Sankar, T. G. Ajithkumar, G. Sankar, P. Manikandan, *Catal. Commun.*, 2015, **59**, 201.

[30] A. A. Sathe, A. M. K. Nambiar and R. M. Rioux, *Catal. Sci. Technol.*, 2017, **7**, 84.

[31] M. Aresta, A. Dibenedetto and I. Tommasi, *Appl. Organomet. Chem.*, 2000, **14**, 799.

[32] J. A. Verdol, US Patent 3,025,305, Mar. 13, 1962.

[33] M. Aresta and A. Dibenedetto, *J. Mol. Catal. A: Chem.*, 2002., **182**, 399.

[34] R. Srivastava, D. Srinivas and P. Ratnasamy, *Catal. Lett.*, 2003, **91**, 133.

[35] J. Sun, S.-I. Fujita, B. M. Bhanage and M. Arai, *Catal. Today*, 2004, **93**, 383.

[36] F. Ono, K. Qiao, D. Tomida and C. Yokoyama, *Appl. Catal., A*, 2007, **333**, 107.

[37] F. Chen, T. Dong, T. Xu, X. Li and C. Hu, *Green Chem.*, 2011, **13**, 2518.

[38] G. C. Bond and P. A. Sermon, *Gold Bull*, 1973, **6**, 102.

[39] M. Haruta, T. Kobayashi, H. Sano and N. Yamada, *Chem. Lett.*, 1987, **16**, 405.

[40] G. J. Hutchings, *J. Catal.*, 1985, **96**, 292.

[41] G. J. Hutchings, *Chem. Commun.*, 2008, 1148.

[42] A. S. K. Hashmi and G. J. Hutchings, *Angew. Chem. Int. Ed.*, 2006, **45**, 7896.

[43] G. C. Bond and D. T. Thompson, *Catal. Rev.*, 1999, **41**, 319.

[44] M. Haruta, *Gold Bull.*, 2004, **37**, 27.

[45] J. K. Edwards, S. J. Freakley, R. J. Lewis, J. C. Pritchard and G. J. Hutchings, *Catal. Today*, 2015, **248**, 3.

[46] M. Santonastaso, S. J. Freakley, P. J. Miedziak, G. L. Brett, J. K. Edwards, G. J. Hutchings, *Org. Process Res. Dev.*, 2014, **18**, 1455.

[47] M. Juliusa, S. Robertsa, J. C. Q. Fletchera, *Gold Bull.*, 2010, **43**, 298.

[48] T. Hayashi, K. Tanaka and M. Haruta, *J. Catal.*, 1998, **178**, 566.

[49] J. K. Edwards, B. E. Solsona, P. Landon, A. F. Carley, A. Herzing, C. J. Kiely and G. J. Hutchings, *J. Catal.*, 2005, **236**, 69.

[50] D. I. Enache, J. K. Edwards, P. Landon, B. Solsona-Espriu, A. F. Carley, A. A. Herzing, M. Watanabe, C. J. Kiely, D. W. Knight and G. J. Hutchings, *Science*, 2006, **311**, 362.

[51] D. I. Enache, D. W. Knight and G. J. Hutchings, *Catal. Lett.*, 2005, **103**, 43.

[52] F. Moreau, G. C. Bond and A. O. Taylor, *J. Catal.*, 2005, **231**, 105.

[53] P. Miedziak, M. Sankar, N. Dimitratos, J. A. Lopez-Sanchez, A. F. Carley, D. W. Knight, S. H. Taylor, C. J. Kiely and G. J. Hutchings, *Catal. Today*, 2011, **164**, 315.

[54] M. Pagliaro, R. Ciriminna and S. Campestrini, *Chem. Soc. Rev.*, 2005. **34**, 837.

[55] A. Ansmann, R. Kawa and M. Neuss, US Patent 7,083,780 B2, Aug. 1, 2006.

[56] J. J. Bravo-Suárez, K. K. Bando, J. Lu, T. Fujitani and S. T. Oyama, *J. Catal.*, 2008, **255**, 114.

[57] J. Lu, X. Zhang, J. J. Bravo-Suárez, K. K. Bando, T. Fujitani and S. T. Oyama, *J. Catal.*, 2007, **250**, 350.

[58] C. L. Bracey, A. F. Carley, J. K. Edwards, P. R. Ellis and G. J. Hutchings, *Catal. Sci. Technol.*, 2011, **1**, 76.

[59] M. Haruta, *Catal. Today*, 1997, **36**, 153.

[60] A. K. Sinha, S. Seelan, S. Tsubota and M. Haruta, *Top. Catal.*, 2004, **29**, 95.

[61] C. Aprile, A. Corma, M. E. Domine, H. García and C. Mitchell, *J. Catal.*, 2009, **264**, 44.

[62] H. Alshammari, *Reac. Kinet. Mech. Cat.*, 2016, **119**, 149.

[63] H. Alshammari, P. J. Miedziak, S. Bawaked, D. W. Knight and G. J. Hutchings, *Chem. Cat. Chem.*, 2012, **4**, 1565.

[64] M. D. Hughes, Y.-J. Xu, P. Jenkins, P. McMorn, P. Landon, D. I. Enache, A. F. Carley, G. A. Attard, G. J. Hutchings, F. King, E. H. Stitt, P. Johnston, K. Griffin and C. J. Kiely, *Nature*, 2005, **437**,1132.

[65] S. Bawaked, N. F. Dummer, D. Bethell, D. W. Knight and G. J. Hutchings, *Green Chem.*, 2011, **13**, 127.

[66] M. Álvaro, C. Aprile, A. Corma, B. Ferrer and H. García, *J. Catal.*, 2007, **245**, 249.

[67] S. Bawaked, Q. He, N. F. Dummer, A. F. Carley, D. W. Knight, D. Bethell, C. J. Kiely and G. J. Hutchings, *Catal. Sci. Technol.*, 2011, **1**, 747.

[68] C. H. A. Tsang, Y. Liu, Z. Kang, D. D. D. Ma, N.-B. Wong and S.-T. Lee, *Chem. Commun.*, 2009, 5829.

[69] B. Li, P. He, G. Yi, H. Lin and Y. Yuan, *Catal. Lett.*, 2009, **133**, 33.

[70] D. Gajan, K. Guillois, P. Delichère, J.-M. Basset, J.-P. Candy, V. Caps, C. Coperet, A. Lesage and L. Emsley, *J. Am. Chem. Soc.*, 2009, **131**, 14667.

[71] P. Lignier, F. Morfin, L. Piccolo, J.-L. Rousset and V. Caps, *Catal. Today*, 2007, **122**, 284.

[72] J. Liu, F. Wang, T. Xu and Z. Gu, *Catal. Lett.*, 2010, **134**, 51.

[73] H. Alshammari, P. J. Miedziak, D. W. Knight, D. J. Willock and G. J. Hutchings, *Catal. Sci. Technol.*, 2013, **3**, 1531.

[74] H. Alshammari, P. J. Miedziak, T. E. Davies, D. J. Willock, D. W. Knight, and G. J. Hutchings, *Catal. Sci. Technol.*, 2014, **4**, 908.

[75] U. N. Gupta, N. F. Dummer, S. Pattisson, R. L. Jenkins, D. W. Knight, D. Bethell and G. J. Hutchings, *Catal. Lett.*, 2015, **145**, 689.

[76] J. Liang, Q. Zhang, H. Wu, G. Meng, Q. Tang and Y. Wang, *Catal. Commun.*, 2004, **5**, 665.

[77] A. Takahashi, N. Hamakawa, I. Nakamura and T. Fujitani, *Appl. Catal., A*, 2005, **294**, 34.

[78] S. H. Jhung, J. H. Lee, A. K. Cheetham, G. Férey and J. S. Chang, *J. Catal.*, 2006, **239**, 97.

[79] S. Y. Lim, M. Kang, J. Kim and I.-M. Lee, *Bull. Korean Chem. Soc.*, 2005, **26**, 887.

[80] V. R. Choudhary, R. Jha, and P. Jana, *Catal. Commun.*, 2008, **10**, 205.

[81] M. Y. Hyun, S. H. Kim, Y. J. Song, H. G. Lee, Y. D. Jo, J. H. Kim, I. H. Hwang, J. Y. Noh, J. Kang and C. Kim, *J. Org. Chem.*, 2012, **77**, 7307.

[82] Z. Asgharpour, F. Farzaneh and A. Abbasi, *RSC Adv.*, 2016, **6**, 95729.

[83] Q. Tang, Y. Wang, J. Liang, P. Wang, Q. Zhang and H. Wan, *Chem. Commun.*, 2004, 440.

[84] M. V. Patil, M. K. Yadav and R. V. Jasra, *J. Mol. Catal. A: Chem.*, 2007, **277**, 72.

[85] Q. Tang, Q. Zhang, H. Wu and Y. Wang, *J. Catal.*, 2005, **230**, 384.

[86] X.-Y. Quek, Q. Tang, S. Hu and Y. Yang, *Appl. Catal., A*, 2009, **361**, 130.

[87] M. J. Beier, W. Kleist, M. T. Wharmby, R. Kissner, B. Kimmerle, P. A. Wright, J.-D. Grunwaldt and A. Baiker, *J. Chem. Eur.*, 2012, **18**, 887.

[88] Z. Opre, T. Mallat and A. Baiker, *J. Catal.*, 2007, **245**, 482.

[89] K. M. Jinka, J. Sebastian and R. V. Jasra, *J. Mol. Catal. A: Chem.*, 2007, **274**, 33.

[90] M. L. Kantam, B. P. Rao, R. S. Reddy, N. S. Sekhar, B. Sreedhar and B. M. Choudary, *J. Mol. Catal. A: Chem.*, 2007, **272**, 1.

[91] S. Bhunia, S. Jana, D. Saha, B. Dutta and S. Koner, *Catal. Sci. Technol.*, 2014, **4**, 1820.

Chapter 2: Experimental

2.1. Chemicals

All chemicals used in this study were obtained from commercial sources. These chemicals were used without further purification. Details of these chemicals are shown in Table 2.1.

Table 2.1: List of chemicals used in the experiments

No.	Chemical	Chemical source, purity
1	1-Decene[a]	Sigma Aldrich, ≥ 94%
2	1,2-Epoxy decane	Aldrich, 98%
3	Graphite	Aldrich
4	Titania P25	Degussa
5	SiO_2	Aldrich
6	MgO	Aldrich
7	Hydrotalcite	Aldrich
8	Chloroauric acid, $HAuCl_4$	Johnson Matthey, 99.9%
9	Cobalt nitrate $Co(NO_3)_2 \cdot 6H_2O$	Aldrich, 99%
10	*Tert*-Butylhydroperoxide (TBHP)	Merck, 70% in H_2O
11	α,α-Azoisobutyronitrile (AIBN)	Aldrich, 97.5%
12	Cumene hydroperoxide (CHP)	Merck, 75%
13	Sodium borohydride ($NaBH_4$)	Aldrich, 99%
14	Polyvinyl alcohol (PVA)	Aldrich, + 99%
15	Tetrabutylammoniumbromide (Bu_4NBr)	Alfa Aesar, + 98%
16	Zinc bromide ($ZnBr_2$)	Alfa Aesar, 98%
17	Imidazole	Aldrich, + 99%
18	Polydiallydimethylammonium chloride	Aldrich, 20% in H_2O
19	Amberlite® IRA-400 chloride	Aldrich
20	Cyclopentene oxide	Aldrich, 98%
21	Cyclohexene oxide	Aldrich, 98%
22	Cyclooctene oxide	Aldrich, 99%
23	Cyclododecene oxide	Aldrich, 95%
24	Tetraethylammoniumbromide	Aldrich, 98%
25	Tetramethylammoniumbromide	Aldrich, 98%
26	Tetrapropylammoniumbromide	Aldrich, 98%

(a): Impurity of 1-decene: ≤ 2.0% 2-butyl-1-hexene and ≤ 2.0% 2-ethyl-1-octene as provided by the supplier.

2.2. Catalyst preparation

A number of methods were adopted in this study during catalyst preparation, using different catalysts supports namely: magnesium oxide, hydrotalcite, graphite, titanium dioxide and silica dioxide. All catalyst metal loading on the support are percentage metal by weight of the support.

2.2.1. Sol-immobilisation method

Supported Au catalysts (2 g) were prepared using sol-immobilisation method [1]. The preparation method was as follows: the required amount of $HAuCl_4$ solution (Johnson Matthey, 4.94 mg/mL) (4.048 mL) was added to 800 mL of deionised water under continuous stirring. Freshly prepared polyvinyl alcohol (1 wt% solution, MW = 10 000, 80% hydrolysed) was added (PVA/Au (by wt) = 0.65). The polyvinyl alcohol is added to protect and stabilise Au nanoparticles. The mixture was stirred for another 15 min; a freshly prepared $NaBH_4$ solution (solvent water, 0.2 M, $NaBH_4$/Au (mol/mol) = 5) was then added to form a dark-brown sol. The mixture was stirred for additional 30 min while the pH was adjusted to 2 by drop wise addition of H_2SO_4 (with graphite, TiO_2, SiO_2). About 1.98 g of the support was added to the colloid mixture and stirred for 2 hours. The catalyst was filtered, washed thoroughly using deionised water (2 L) and then dried at 110°C for 16 hours prior to use.

2.2.2. Wet-impregnation method

1 g of the specific catalyst was synthesised using required amount of cobalt nitrate [$Co(NO_3)_2 \cdot 6H_2O$] (0.0493 g for 2% Co/support), dissolved in deionised water or aqueous solutions of $HAuCl_4$ (Johnson Matthey, 4.94 mg/mL) (2.024 mL). The solution was mixed with the required amount of the support (MgO, graphite, TiO_2, SiO_2) under continuous stirring at 80°C to allow water evaporation. The resulting paste was dried at 110°C for 16 h, ground before calcination in static air at 400°C for 3 h at a heating rate of 20°C min^{-1} [1].

2.2.3. Incipient-wetness method

About 1 g of 1% Au/graphite catalyst was prepared using incipient-wetness method [2]. An aqueous solution of $HAuCl_4$ (Johnson Matthey, 4.94 mg/mL) (2.024 mL) was mixed with 1 mL of deionised water and added drop wise to fill the pores of the graphite support prior to air drying. The paste was dried at 110°C for 16 h prior to use.

2.2.4. Deposition-precipitation method

1% Au/graphite (1 g) was prepared by mixing 250 mL deionised water with graphite support (0.99 g) and stirred at 60°C. Sodium carbonate solution (0.53 g/100 mL) was added to the mixture drop wise to keep the pH around 8. $HAuCl_4$ solution (Johnson Matthey, 4.94 mg/mL) (2.024 mL) was then added to the mixture with a simultaneous addition of sodium carbonate to maintain pH of 8. The solution was mixed for 1.5 h, filtered and the catalyst washed using 1.5 L of deionised water. The catalyst was dried in an oven at 110°C for 16 h. The resulting powder was ground and calcined in static air at 400°C for 3 h at a ramp rate of 20°C min^{-1} [3].

2.2.5. Preparation of 15% Bu_4NBr supported catalysts for cycloaddition of CO_2 with 1,2-epoxydecane

The route for preparation of supported tetrabutylammonium bromide (15% Bu_4NBr/support) followed the methodology previously reported in the literature [4]. About 0.3 g of Bu_4NBr was added to 1.7 g of the support (magnesium oxide, hydrotalcite or silica-gel). The mixture was dissolved in methanol and the solvent was removed by evaporation. After evaporation of the solvent, the catalyst was dried in an oven at 110°C for 16 h.

2.2.6. Catalyst preparation of PDDA-Br/SiO_2

The preparation of polydiallyldimethylammonium bromide (PDDABr) was done by a simple ion-exchange procedure in water. About 20 g of Amberlite® IRA-400 chloride form was washed extensively with a high volume of water (1 L) [5]. NaBr aqueous solution (8.8 M, 14 mL) was then mixed with Amberlite three times to obtain the resin in bromide form. Afterwards, 5 g of an aqueous solution (20%) of polydiallyldimethylammonium chloride was mixed with 10 mL of deionised water. The resulting mixture was mixed with 6.7 g of resin and stirred at room temperature for 6 h. This mixture was filtered, and the solution was subjected to another ion-exchange process with fresh resin in bromide form. This process was repeated three times. The PDDA-Br solution was dried under vacuum at 80°C to produce yellow solid. The PDDA-Br/SiO_2 was prepared by mixing 5 mL of deionised water with 0.1 g PDDA-Br, prior to mixing of the solution with 0.5 g silica-gel. The mixture was stirred at 80°C for 6 h to remove water via evaporation, and the remaining H_2O was removed under vacuum at 80°C for 1.5 h to obtain PDDA-Br/SiO_2 (colourless powder, 20% PDDA-Br/SiO_2).

2.2.7. Catalyst preparation of supported imidazolium catalyst (Imid/SiO_2)

The route for preparation of supported imidazolium catalyst (Imid/SiO_2) followed the methodology previously reported by Sankar and co-worker [6]. Silica (5 g), 3-triethoxychloropropylsilane (2.23 g) and imidazole (0.63 g) were mixed with 175 mL of dry toluene and the resultant solution was refluxed for 24 h. The catalyst was filtered and washed with toluene (200 mL) and propylene oxide (50 mL) to yield a colourless powder.

2.3. Catalytic testing for epoxidation of 1-decene

2.3.1. Glass reactor

Epoxidation reactions were carried out in a magnetically stirred, round-bottomed glass flask reactor (50 cm^3 capacity) fitted with a reflux condenser (Figure 2.1). Reaction mixtures were heated between 60-90°C using a hot-plate. In a standard reaction, the required amount of a catalyst (0.05-0.2 g), 10 mL of 1-decene (53 mmol) and a small amount of radical initiator (TBHP 0.01 mL, AIBN 6 mg, CHP 0.01 mL) were used. After the required reaction time, the mixture was cooled down to room temperature, filtered and analysed by gas chromatography (GC) (Section 2.7.1).

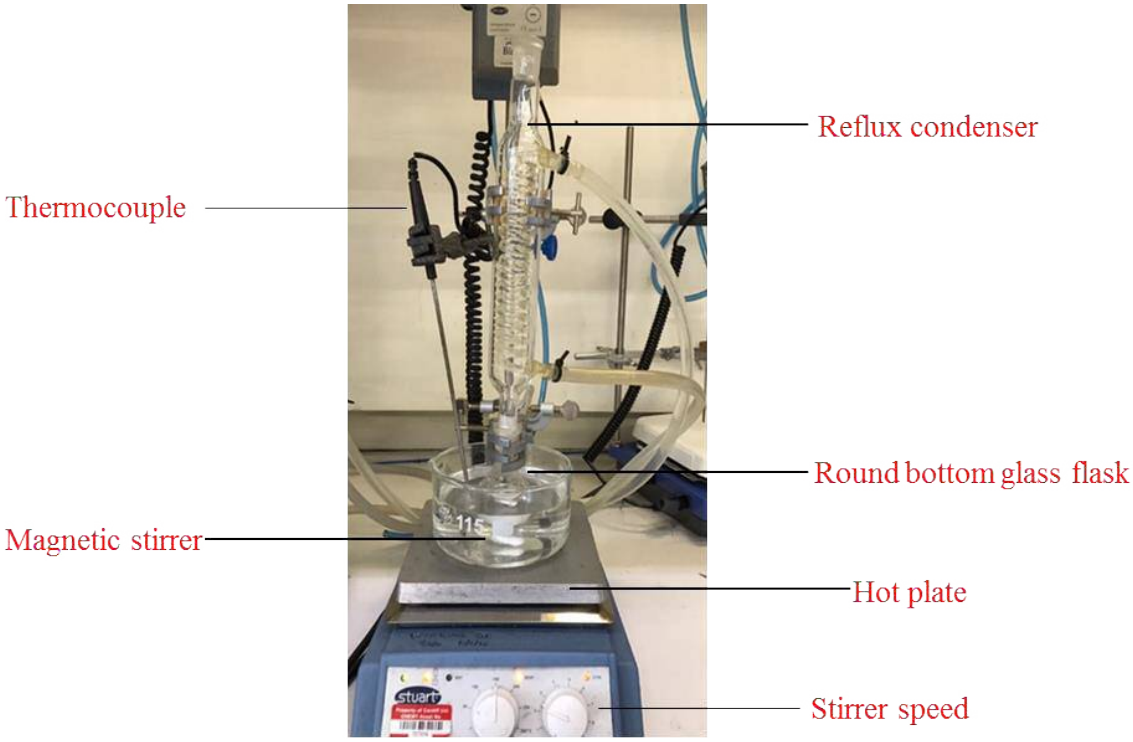

Figure 2.1: Glass reactor for epoxidation of 1-decene.

2.3.2. Autoclave

Epoxidation reactions were performed in a 50 cm^3 Parr stainless steel autoclave reactor, with an inner lining of Teflon. 1-Decene (53 mmol, 10 mL), the required amount of a catalyst (0.1 g) and a small amount of radical initiator (AIBN, 6 mg) were placed into the reactor. Before starting the reaction, the autoclave was purged three times with N_2, then pressurised with oxygen to the required pressure (5-15 bar). The entire setting was heated to the required temperature (90°C) under continuous stirring (Figure 2.2) to the required reaction time. The reactor was cooled down in an ice water bath and the products were analysed using GC.

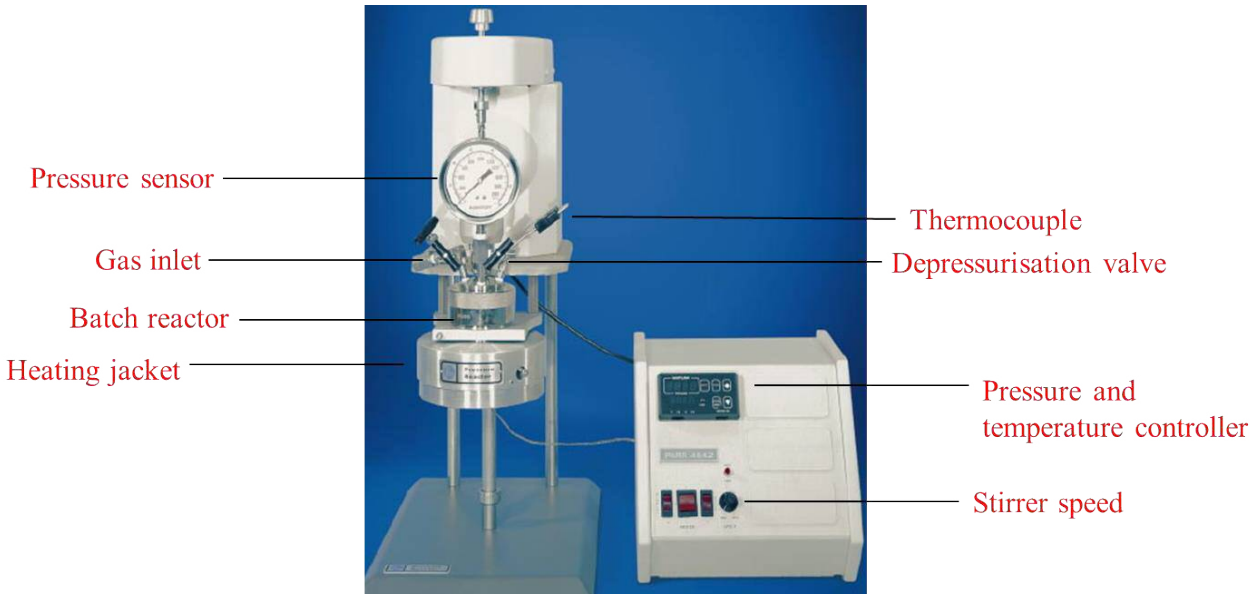

Figure 2.2: Parr autoclave and controller.

2.4. Catalyst testing for cycloaddition of CO_2 with epoxide

Catalytic experiments were performed in a 50 cm^3 Parr stainless steel autoclave reactor, with an inner lining of Teflon. The required amount of a catalyst and the epoxide (5 mL, cyclooctene oxide 5 g) were added into the autoclave. The reactor was purged with CO_2 three times and then charged with CO_2 to the desired pressure (10-20 bar). Then the autoclave was heated to a temperature (60-150°C) under continuous stirring for a required reaction time (2-48 h). When the reaction was completed, the reactor was cooled in an ice water bath. Products were analysed using gas chromatography, gas chromatography coupled with mass spectrometry (GC-MS) and nuclear magnetic resonance spectroscopy (NMR).

2.5. Catalyst testing for one-pot synthesis of cyclic carbonate

One-pot synthesis of cyclic carbonate (simultaneous oxidation and carboxylation) was performed in a 50 cm^3 stainless steel autoclave reactor, with an inner lining of Teflon. The reactor was charged with the required amount of 1% Au/support (0.1 g), Bu_4NBr (0.2-0.4 g), $ZnBr_2$ (0.08-0.16 g), 1-decene (53 mmol, 10 mL), and AIBN (6 mg). The autoclave was purged three times with O_2, and then pressurised with O_2 and CO_2 at required pressure before heated to a required temperature (80-90°C) under continuous stirring. On completion of the reaction, the reactor was cooled in an ice water bath and depressurised. The catalyst was separated from the reaction mixture by filtration, and products and residual 1-decene were analysed by GC.

For one-pot multistep synthesis of the cyclic carbonate (sequential oxidation and carboxylation), first the epoxidation reaction was carried out as described in 2.3.1 and 2.3.2. After the completion of the epoxidation step, the reactor was cooled in an ice water bath and depressurised. When the epoxidation step was completed in the glass reactor, the reaction mixture transferred to the autoclave. Then co-catalysts Bu_4NBr (0.4 g) and $ZnBr_2$ (0.16 g) were added to the reaction vessel. The reactor was closed and pressurised with CO_2 (20 bar) until complete cycloaddition of CO_2 with epoxide step is achieved (4 h). The reactor was cooled in an ice water bath and depressurised, while the catalyst was separated from the reaction mixture by filtration. Subsequently, the reaction products and residual 1-decene were analysed by GC.

2.6. Determination of 1-decene hydroperoxide

The amount of 1-decene hydroperoxides was determined using the method described here, as these products are not distinguished by GC analysis. Standard reaction was carried out as described in 2.3.1 and the reaction mixture was filtered and divided into two aliquots; the first aliquot was stirred for 1 h in air at room temperature with 0.15 g of triphenylphosphine (PPh_3), while the second aliquot was analysed directly using GC.

2.7. Quantitative analysis techniques

Quantitative analysis of the reaction mixtures was performed using GC, GC-MS and NMR techniques. These techniques are described in the following section.

2.7.1. Gas chromatography (GC)

Gas chromatography (GC) is a type of chromatography widely used for separation, identification and analysis of chemical compounds. The basic components of a GC

consist of an injector, a column housed within an oven and detector as shown in Figure 2.3.

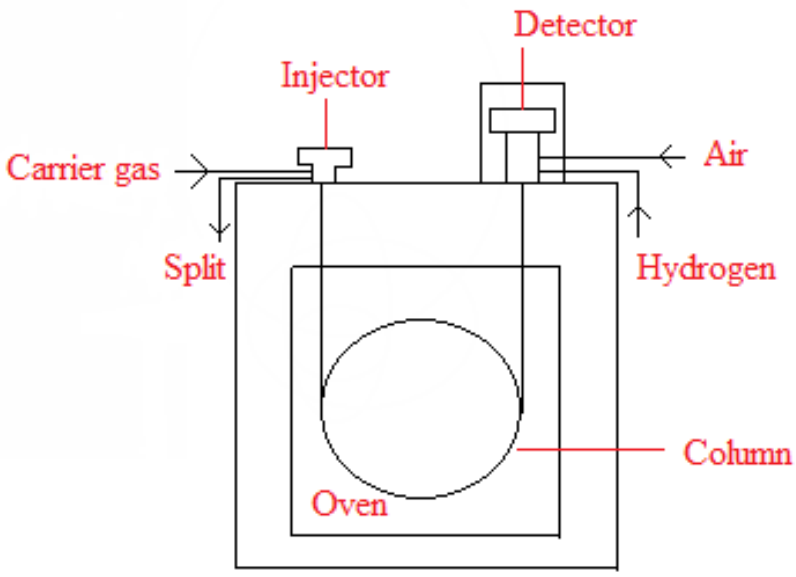

Figure 2.3: The basic components of a GC.

On injection, the sample is vaporised and then mixed up with a carrier gas (usually helium or nitrogen) which flows through the column. There are two general types of a column: capillary and packed columns. The capillary column is the most commonly used column in GC as it has great sensitivity and high resolution [7]. The compounds leaving the column are exposed to a detector. The flame ionisation detector (FID) is the most commonly used GC detector.

Products from the reaction mixture were analysed using a gas chromatograph (Varian star 3400 CX) with a CP-wax 52 column (capillary column, 25 m, 0.35 mm ID, 0.2 micron) coupled with FID detector. A sample (0.02 µl) was automatically injected into the GC using a micro syringe. The GC was operated under standard conditions; a constant injector and detector temperature of 250°C, an initial column temperature of 60°C with a ramp of 10°C/min. Products of 1-decene epoxidation were identified previously in our group [2] using GC-MS by comparing mass spectra and retention times with commercial standards. For all reactions studied the 1,2-epoxydecane was formed. As a 2,3-epoxydecane standard was unavailable, GC-MS was compared to a 2,3-epoxydecane simulated spectrum from the NIST database [2], which confirm no 2,3-epoxide was observed in the reaction. Response factors (RF) for known products were determined using commercial standards, and these response factors were used to determine conversion and selectivity of the products. Three different solutions were prepared for calibration with the known products. The first solution for calibration contained 10 g of

1-decene and 20 mg of each known product. The second and third solutions contained 30 and 50 mg of each product respectively in addition to 10 g of 1-decene. RF used was an average of the three different calibration solutions using the equation below:

Equation 2.1

Table 2.2 below displays the RF for oxidation of 1-decene products.

Table 2.2: Response factors (RF) for the different products in the oxidation of 1-decene

Compound	RF
1-Decene	1
Octanal	0.75
3-Nonanone	0.69
Nonanal	0.5
1-Heptanol	0.8
1,2-Epoxydecane	0.80
1-Decen-3-one	0.71
1-Octanol	0.8
2-Decenal	0.76
1-Decen-3-ol	0.82
2-Decen-1-ol	0.69
Heptanoic acid	0.71
Octanoic acid	0.5
2-Decenoic acid	0.81
Nonanoic acid	0.7
3-Nonen-1-ol	0.80
1,2-Decanediol	0.71

The calculated response factors were used to determine 1-decene conversion, selectivity and the yield of products. Conversion was calculated using GC counts (corrected area: GC count/RF) according to the formula in Equation 2.2:

Conversion (%) = Equation 2.2

Product selectivity was calculated according to the formula Equation 2.3:

Selectivity = Equation 2.3

Product yield was calculated according to the formula in Equation 2.4:

$$\text{Yield (\%)} = \frac{\text{Selectivity} \times \text{Conversion}}{100}$$ Equation 2.4

2.7.2. Gas chromatography-mass spectrometry

GC-MS is an effective analytical instrument with numerous applications in the chemical industry. It consists of GC, interface, mass spectrometer and data–control system interconnected together. Owing to the integration of the two components, GC-MS cannot only divide mixtures into distinct components, but can also characterise each component qualitatively and quantitatively in terms of volume and chemical structure of each separated compound. The analysis process involves an injection of the volatile sample into a heated inlet port ensuring that it is all in the gas phase, which is carried through the column by a mobile phase (helium). The analytes in the sample mixture interact with the station phase of the column leading to separation of the analytes. The compounds as they come off the column are then ionised (electron ionisation for our GCT Premier) in the mass spectrometer source under vacuum. The ion beam produced is then passed through to the TOF (time of flight) tube where separation of ions takes place (low mass ions move faster than higher mass ones) through to the detector (mass analyser) producing our mass spectra [8]. All GC-MS was conducted by the Cardiff university GC-MS service and analysed by Dr. Simon Waller. The GC-MS used in this study is a Walters GCT Premier GC coupled with a HP 6890N mass spectrometer for identification of products for the cycloaddition of CO_2 with different epoxides.

2.7.3. Nuclear magnetic resonance spectroscopy

NMR is another form of spectroscopy, most frequent used as a technique in analytical chemistry. This technique requires samples containing nuclei possessing spin. Due to the difference in the nuclei spins, NMR experiments can be sensitive for only one particular isotope of one particular element. Moreover, chemical environment of ^{1}H and ^{13}C nuclei has been subjugated by organic chemists, since they provide valuable information that can be used to deduce the structure of organic compounds. Thus, chemists and biochemists can apply NMR spectroscopy to analyse molecular conformation in solution and analysing the physical features at the molecular level such as solubility and conformational exchange [9].

For this work, a Bruker ‘Avance’400MHz DPX spectrometer was used to record the ^{1}H NMR spectra with a silicon graphics workstation running on an X win 1.3 software. The results obtained were presented in ppm with the corresponding number of protons, multiplicity and assignment. Chemical shifts within the ^{1}H NMR spectrum were measured in either deuterated chloroform or deuterated dimethyl sulfoxide.

2.8. Catalyst characterisation techniques

2.8.1. Thermal gravimetric analysis (TGA)

Thermal gravimetric analysis (TGA) is a method of thermal analysis which describes the changes of the chemical and physical properties of a sample as a function of increasing temperature (constant heating rate) or isothermally as a function of time. Thermal gravimetric analysis is frequently used to determine either loss or gain of the sample mass and that may be due to decomposition or oxidation of the material.

Thermal gravimetric analysis consists of three essential parts:

(a) An automatic magnetic re-equilibrating balance with a signal-recording device, capable of detecting weight change even in small amount (0.1 μg).

(b) A furnace that generates the required temperatures ranging from room temperature to 1000°C. TGA must use high-temperature inert sample holders such as quartz, ceramic material and platinum.

(c) A gas flow controlled using a switch valve, which enable operation in either an inert atmosphere (N_2, He) or a reactive atmosphere (O_2, H_2).

The TGA was performed using a Perkin Elmer, thermo gravimetric analyzer, TGA 4000. The catalyst (6.55 mg) was heated from 25-600°C under atmospheric air at a heating rate of 5°C min^{-1}.

2.8.2. Scanning electron microscopy (SEM)

Scanning electron microscopy (SEM) involves a microscope that uses electrons as an alternative to light to build a three–dimensional image at higher magnification. SEM can provide a better depth of focus for the image comparing to optical microscopy. In a typical scanning electron microscopy (Figure 2.4), the electron beam is produced from an electron gun. The electron beam passes through the column of the microscope and makes its way through electromagnetic lenses that are able to focus and direct the beam toward the sample [10].

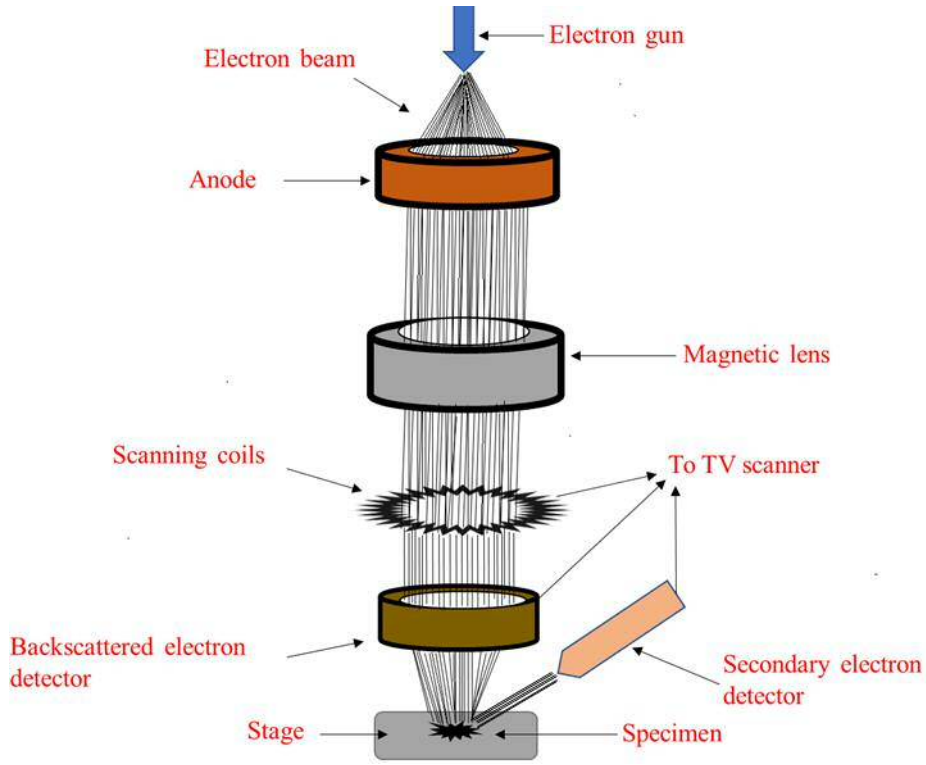

Figure 2.4: Schematic diagram of SEM. Adapted from [10].

When the electron beam interacts with the sample, two types of electrons are generated, namely secondary electrons and backscatter electrons [10]. The secondary electrons are produced when the high-energy electron beam is displacing loosely held surface electrons that are recorded using a secondary electron detector to produce an image of the surface. The principle of secondary electrons relied on the surface area in the specific area of intersection of the beam and therefore relate to topographic features. Backscatter electrons consist of high-energy electrons from the electron beam that are scattered back out of the sample by the atomic nuclei. The intensity of the signal is dependent on the atomic number of the area of interaction. The backscatter image displays the contrast in chemical composition, and these electrons can provide information about the scanned area, such as the topography of the surface and the average atomic number in this area. Secondary and backscatter electrons are collected by the detector that converted them to a signal which then sent to a viewing screen to create the image of the sample.

In this study, the analysis was carried out using an EVO40VP model Carl Zeiss scanning electron microscope. The sample (0.2 g) was ground before sprinkled over a carbon disc stuck onto an aluminium stub and the excess sample were tapped off the disc prior to attaching to the sample holder. The entire SEM column was pumped to attain a good vacuum ($<10^{-6}$ Torr) required for proper functioning of the SEM. The sample stage was

placed at a working distance between 8-10 mm. The electron gun emits an electron beam within a voltage range of 5-25 kV at an I-probe current of 1000 pA (1.0 nA), the generated secondary electron was utilised for topographic analysis.

2.8.3. Transmission electron microscopy (TEM)

Electron microscopy technique can provide information about the shape, size and compositions of supported particles. As mentioned for scanning electron microscopy, transmission electron microscopy (TEM) is another type of electron microscopy technique which operates on the same basic principle as the light microscope. It uses electrons instead of light as a source to image the target [11]. As the metal has a higher density than support, it becomes darker in the TEM image (Figure 2.5). Despite the enormous applications and higher resolution of TEM compare to SEM, TEM analysis is time consuming during the extensive sample preparation to produce a thin enough layer to be electron transparent. In spite of this limitation, TEM is a valuable tool in different fields such as medical, biological, materials and characterisation of heterogeneous catalysts because of its high resolution. The instrument used for TEM analysis was a JEOL 2000FX TEM operating at 200 kV and analysed by Dr. Peter Miedziak. Sample preparation was as follows: the catalyst powder was dispersed in high purity ethanol, then a drop of the suspension was allowed to evaporate on a holey carbon film supported on a TEM grid. Images were acquired in transmission mode and particle size distributions were calculated using Image J software.

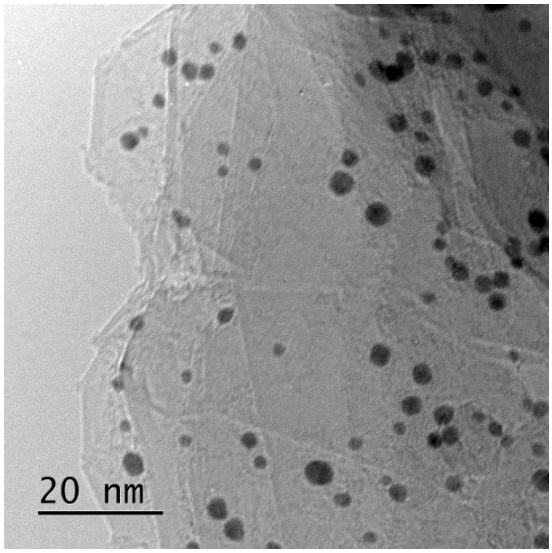

Figure 2.5: TEM image of 1% Au/G.

2.8.4. X-ray powder diffraction (XRD)

XRD is a common analytical technique used for identification of the bulk phase of crystalline compounds and providing information about the unit cell dimensions [12]. When a focused X-ray beam strikes crystalline sample, they are scattered and hence constructive interference will occur when scattered X-rays are in-phase with one another (Figure 2.6) and a diffraction pattern will be obtained.

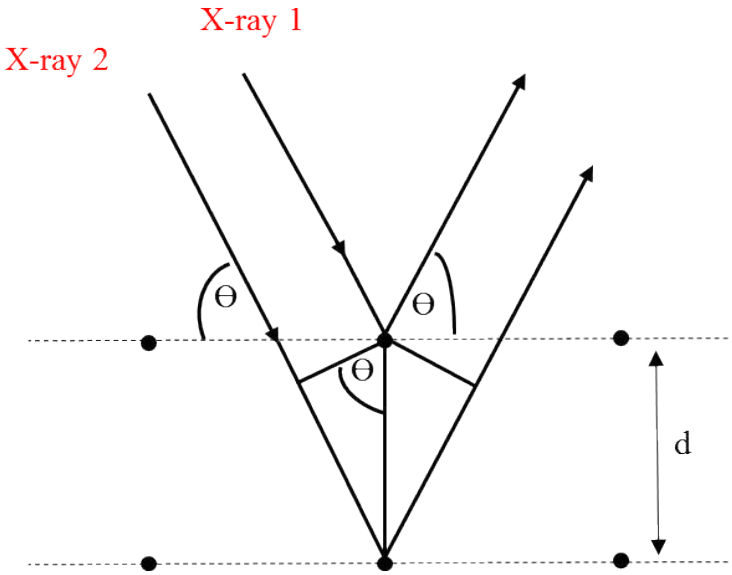

Figure 2.6: Interaction of X-rays within a crystalline surface. Adapted from [12].

The distances between the planes can be measured using the Bragg's equation [12], which is shown in Equation 2.5:

$$n\lambda = 2d\sin\theta \qquad \text{Equation 2.5}$$

n = an integer

λ = the X-rays wavelength.

d = distance between two lattice planes.

θ = the scattering angle.

XRD pattern of a pure powder sample is a fingerprint of the morphology of the substance, and each material has its own characteristic diffraction pattern. The X-ray instrument consist of an X-ray source, a rotating sample stage and a detector, which collects the diffracted X-ray as shown in Figure 2.7.

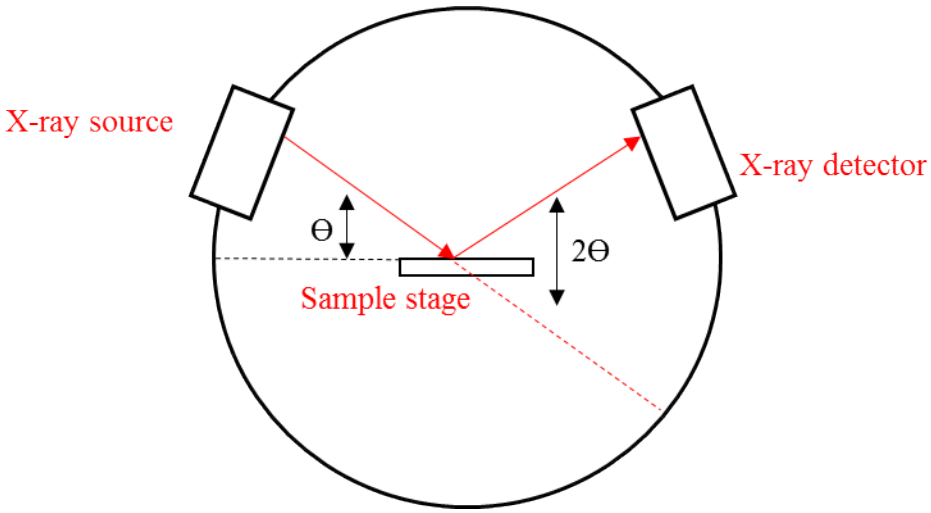

Figure 2.7: Basic set up of an X-ray diffractometer.

XRD analysis was performed using a PANalytical X'Pert PRO MPD instrument with a Cu Kα X-ray source. The catalyst sample (0.5 g) were ground, placed and flatten on a sample disc. The discs were placed onto a sample holder before placed into the XRD instrument. A typical scan was performed at diffraction angle (2θ) of 10 to 80 ° at 40 kV and 40 mA using an X'Celerator detector.

2.8.5. Nitrogen physisorption analysis of the surface area using Brunauer, Emmett and Teller (BET) method

The measurement of the surface area is an important characterisation technique for catalytic materials. The BET method [13] is one of the most commonly used techniques to determine the surface area of a catalyst. The theory is based on the BET equation (Equation 2.6):

Equation 2.6

Where:

C = the BET constant.

V = the volume of the adsorbed gas.

V_m = the volume of the monolayer of adsorbed gas.

P = the equilibrium pressure.

P^o = the saturation pressure of adsorbates at the temperature of adsorption.

Moreover, plotting ——— against — to give a gradient of — and intercept — and surface area can be calculated using equation 2.7:

$$S = (V_m).(N_a).(A) \qquad \text{Equation 2.7}$$

Where:

S= specific surface area.

N_a = Avogadro's number.

A= cross sectional area of adsorbent gas.

The principle BET method is to determine or estimate the surface area based on the amount of gas adsorbed. N_2 is typically the adsorptive gas used in BET surface area determination at a constant temperature (77 K). At a given pressure, the total amount of gas adsorbed can be used for calculating the amount of adsorbed gas molecules that would generate a monolayer on the surface for this sample. Depending on the size of the N_2 molecules adsorbed, the surface area can be simply calculated. The nitrogen physisorption analysis was performed using a Micromeritics Gemini 2360 Analyser. About 1 g of catalyst samples placed in a sample tube was degassed for 50 minutes at 120°C to remove moisture and other surface impurities. The tube was allowed to cool at room temperature before connecting to a gas inlet (liquid N_2 at -196°C) which was parallel to an empty reference tube. Both tubes were immersed into a Dewar containing liquid nitrogen. The setting was initially ran without any sample, before a subsequent run containing the sample for nitrogen physisorption analysis. Usually, five-point analysis was used and the surface area was calculated using BET equation.

2.8.6. X-ray photoelectron spectroscopy (XPS)

XPS, which is also called electron spectroscopy for chemical analysis (ESCA), is the most extensively used surface analysis technique (at depth of 10 nm) due to its relative simplicity and revealing of different oxidation state of a sample species under investigation. Moreover, it can be used for studying the dispersion of supported catalysts [14, 15]. The photoelectronic effect is the basic principle of this technique. When X-ray photons ($E = h\nu$) hit the sample, it interacts with the inner shell electrons and ionises the atom to generate an ejected free photoelectron as presented in Figure 2.8.

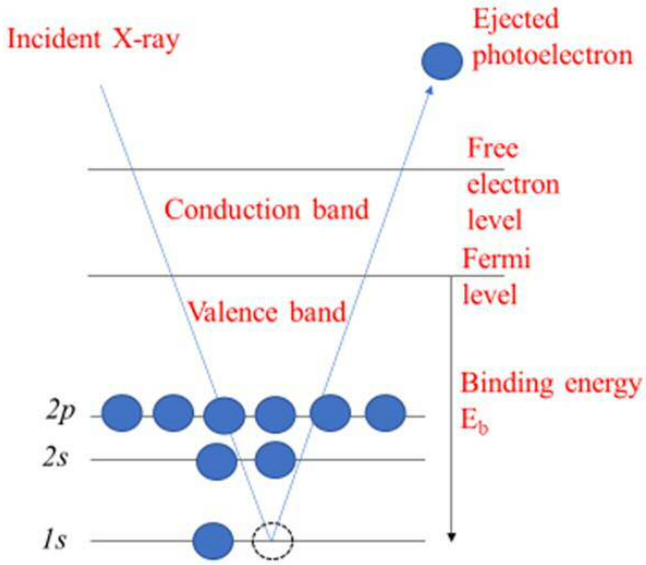

Figure 2.8: Ejected electron by x-ray photon. Adapted from [14].

The kinetic energy of the emitted photoelectrons can be determined from the energy of the photon and the binding energy of the electron using the equation below:

$$E_k = h\nu - E_b - \Phi \qquad \text{Equation 2.8}$$

Where:

h = Planck's constant

ν = frequency of radiation

E_b = electron binding energy

Φ = the work function of the material

The electron binding energy (E_b) is dependent on the chemical bonding of the atom, which makes XPS valuable to identify the oxidation state for an atom. Every element has characteristic binding energy, which is associated with all core atomic orbitals, and the concentration of the element is relative to the intensity of the peaks.

XPS instruments consist of:

1- X-ray source
2- Sample stage
3- Energy analyser for the photoelectrons
4- Electron detector

All XPS was carried out by Dr David Morgan using Kratos Axis Ultra DLD system, which was utilised for collection of XPS spectra using monochromatic Al $K\alpha$ X-ray source, operating at 120 W. Data were collected in the Hybrid mode of operation, using a combination of electrostatic and magnetic lenses, and at pass energies of 40 and 160 eV for high resolution and survey spectra respectively. All spectra were collected at 90° take off angle, using a base pressure of $\sim 1\times10^{-9}$ Torr, which was maintained during collection of the spectra. The resulting spectra were calibrated to the C(1s) line at 284.8 eV.

2.8.7. Temperature-programmed reduction (TPR)

Temperature-programmed reduction (TPR) is a technique used for the characterisation of solid materials, frequently utilised in the field of heterogeneous catalysis, where most efficient reduction conditions are ascertained. In this procedure, a catalyst is subjected to a predetermined incremental rise in temperature while a reducing gas is flown across it. A typically U–tube sample holder containing a catalyst and a thermocouple is inserted into it, which measures the temperature of the sample. The entire set up is placed into a furnace with temperature control equipment. Air present within the container is expelled using inert gases such as N_2 or Ar. 10 Vol-% H_2 in N_2 is passed through the line via flow controllers to provide supplementary hydrogen. The resultant gaseous mixture is measured at the exit of the sample container attached to a thermal conductivity detector. The sample is then subjected to incremental rise in temperature within the oven. If a reduction takes place at certain temperature, the consumption of hydrogen will be an indicator, which is detected by the measuring instruments [16].

TPR analysis was carried out on a Thermo TPD/R/O 1100 series instrument equipped with a thermal conductivity detector (TCD). About 50 mg of the catalyst was placed in the U–tube sample holder and then heated up to 800°C under the flow of 10% H_2/Ar at a heating rate of 5°C min^{-1}.

2.8.8. Inductively coupled plasma-mass spectrometry (ICP-MS)

ICP-MS, or inductively coupled plasma-mass spectrometry is highly effective in the analysis of metal concentrations within the solution, which also is highly sensitive to a number of elements. Curves resulting from linear calibrations are evident over several orders of intensity for the ionisation procedure, which is outline as follows; specimen introduction, ICP torch, interfaces and mass spectrometry [17]. ICP-MS was conducted by the Cardiff university ICP-MS service and analysed by Dr. Simon Waller. Analysis was conducted using the Agilent 7900 ICP-MS. A five-point calibration was made using

certified standards. The run consists of a blank to ensure no contamination at the start of the run, followed by the calibration standards lowest to highest concentration, then two or more blank runs to ensure no carry over from the highest standard follows. Afterwards, the sample was run in duplicate separated by a carry over blank to ensure no samples carry over into subsequent ones. Each sample itself is a minimum of a triplicate measurement. When the run is complete, the internal standard response is linear throughout the run.

2.8.9. Fourier transform infrared spectroscopy (FT-IR)

Fourier transform infrared spectroscopy is often used to obtain an infrared spectrum of emission or absorption of different materials. Firstly, infrared radiation permeates a specimen, some of which is transmitted or absorbed. The resultant spectrum denotes molecular rates of transmission and absorption, essentially formulating a molecular fingerprint of the specimen. IR spectroscopy thus leads to efficient positive identification via qualitative analysis for all substances and materials. Furthermore, the peak sizes across a spectrum relate directly to the quantity of materials present.

Fourier transform infrared spectroscopy is a superior approach for a number of reasons, as it is highly accurate in taking immediate readings that do not depend on prior calibration as well as it is able to speed up the process, taking one measurement per second. Furthermore, it is a non-destructive technique and capable of a more refined optical throughput. Moreover, it is basic in its physical mechanism, bestowing one moving part only.

FTIR consist of five main parts:

1. IR source.

2. Interferometer.

3. Sample.

4. Detector.

5. Computer.

Due to the requirement for a relative scale in absorption intensity, background spectra must be taken into account in such procedures; this is typically a measurement with no sample in the beam [18]. Infrared spectra analysis was carried out using a FT/IR-660 Plus

fourier transform infrared spectrometer (JASCO). The sample holder was cleaned with ethanol; then the sample was placed in the sample holder and the measurement taken. Scans were conducted between 400 and 4000 cm^{-1}.

2.9. References

[1] H. Alshammari, P. J. Miedziak, D. J. Morgan, D. W. Knight and G. J. Hutchings, *Green Chem.*, 2013, **15**, 1244.

[2] U. N. Gupta, N. F. Dummer, S. Pattisson, R. L. Jenkins, D. W. Knight, D. Bethell and G. J. Hutchings, *Catal. Lett.*, 2015, **145**, 689.

[3] S. Bawaked, N. F. Dummer, N. Dimitratos, D. Bethell, Q. He, C. J. Kiely and G. J. Hutchings, *Green Chem.*, 2009, **11**, 1037.

[4] P. Tundo and M. Selva, *Green Chem.*, 2005, **7**, 464.

[5] B. Song, L. Guo, R. Zhang, X. Zhao, H. Gan, C. Chen, J. Chen, W. Zhu and Z. Hou, *J. CO_2 Util.*, 2014, **6**, 62.

[6] M. Sankar, T. G. Ajithkumar, G. Sankar and P. Manikandan, *Cat. Commun.*, 2015, **59**, 201.

[7] F. Rouessac, A. Rouessac, *Chemical Analysis: Modern Instrumentation Methods and Techniques* (2nd Edition), John Wiley & Sons, England, 2007.

[8] M. C. McMaster, *GC/MS: A Practical User's Guide* (2nd Edition), John Wiley&Son, Inc, New Jersy, 2007.

[9] H. Frieblin, *Basic One and Two Dimensional NMR Spectroscopy* (5th Edition), WILEY-VCH Verlag GmbH & Co. KGaA, Weinheim, 2010.

[10] Scanning Electron Microscope. Retrieved from https://www.purdue.edu/ehps/rem/rs/sem.htm. (date accessed 02/03/2017).

[11] I. Chorkendorff and J. W. Niemantsverdriet, *Concepts of Modern Catalysis and Kinetics*, WILEY-VCH Verlag GmbH & Co., Weinheim, 2003.

[12] I. Chorkendorff and J. W. Niemantsverdriet, *Concepts of Modern Catalysis and Kinetics*, WILEY-VCH Verlag GmbH & Co., Weinheim, 2003.

[13] S. Braunauer, P. H. Emmett and E. Teller, *J. Am. Chem. Soc.*, 1938, **60**, 309.

[14] X-ray photoelectron spectroscopy. Retrieved from https://www.slideshare.net/uljansinani1/clipboards/my-clips (date accessed 08/03/2017)

[15] I. Chorkendorff and J. W. Niemantsverdriet, *Concepts of Modern Catalysis and Kinetics*, WILEY-VCH Verlag GmbH & Co., Weinheim, 2003.

[16] I. Chorkendorff and J. W. Niemantsverdriet, *Concepts of Modern Catalysis and Kinetics*, WILEY-VCH Verlag GmbH & Co., Weinheim, 2003.

[17] A. Bazilio and J. Weinrich, *The Easy Guide to: Inductively Coupled Plasma-Mass Spectrometry (ICP-MS)*, (December 2012), Retrieved from http://www.ecs.umass.edu/eve/facilities/equipment/ICPMS/ICPMS%20quick%20guide.pdf (date accessed 03/03/2017)

[18] J. W. Niemantsverdriet, *Spectroscopy in catalysis*, Wiley-VCH, Weinheim, 2007, **3**, 217.

Chapter 3: Solvent-free aerobic epoxidation of 1-decene using supported cobalt catalysts

3.1. Introduction

Selective oxidation is a key process for commercial applications especially for the synthesis of chemical intermediates. Therefore, oxidation of hydrocarbons for generating compounds containing oxygen is an important industrial reaction [1, 2]. Epoxides are considered to be one of the key intermediates in the manufacture of functionalised fine chemicals, pharmaceutics, and cosmetics; they facilitate the mixing of lipid soluble acids in creams and lotions [3]. The epoxidation of ethene to ethylene oxide is catalysed using silver supported on α-alumina catalyst. High selectivity for the epoxide (up to 90%) was found. This is due to the absence of an allylic hydrogen [4]. The epoxidation of the olefins with longer chains is less facile than ethene due to the presence of this allylic hydrogen. The oxidation of propene proceeded through the chlorohydrin process using chlorinated reagents and there was a formation of unwanted by-products [5]. The oxidation of propene over a titanium silicalite (TS-1) catalyst was also studied. However, this method used stoichiometric amounts of hydrogen peroxide [6]. Molecular oxygen is the preferred oxidant; hence, using molecular oxygen for epoxidation reactions in combination with an appropriate transition metal catalyst is the main target of a heterogeneous catalysis. Various studies using different types of heterogeneous catalysts have observed that the electrophilic addition of oxygen to alkenes to form epoxide is challenging [7-10]. Well-known epoxidation catalysts, such as supported gold catalysts, were previously reported as highly selective in the epoxidation of different olefins, such as propene, 1-octene and cyclooctene [11-16]. However, the application of cost-effective transition metals in epoxidation reactions would be more desirable from an economical point of view.

Cobalt-based catalysts were reported as active in epoxidation reactions in both homogeneous [17, 18] as well as heterogeneous reactions [19-26] as mentioned in Section 1.7. Heterogeneous cobalt catalysts have been applied for the epoxidation of different alkenes such as styrene and stilbene to the corresponding epoxides. However, most of these studies used solvents such as dimethylformamide (DMF), which is not an inert solvent in the epoxidation of alkenes and is proposed to act as an oxygen-transfer agent as well as leading to considerable amount of waste [24]. Therefore, there is still scope to

improve the epoxidation of alkene under solvent-free conditions using supported cobalt catalyst.

Herein, simple, selective supported cobalt catalysts have been used for the epoxidation of 1-decene under solvent-free conditions using oxygen from air as the primary oxidant at atmospheric pressure. A range of radical initiators have been studied at different temperatures in the absence of the catalyst as it was previously observed that the nature of the radical initiator present in the reaction mixture affect products selectivity [27].

3.2. Results and discussion

3.2.1. Reactions in the absence of catalyst and radical initiator

Temperature is one of the most important factors affecting reaction conversion [28]. It is important to establish the reaction conditions such as reaction temperature in the absence of the radical initiator and the catalyst. To study the effect of temperature on 1-decene conversion, the substrate was heated to different temperatures (60-110°C) for 24 h. Table 3.1 shows that the oxidation of 1-decene does not start below 100°C, whereas at 110°C the reaction starts spontaneously, reaching a conversion of 8%. Therefore, in order to avoid 1-decene autoxidation, temperatures below 100°C (60-90°C) have been used for the epoxidation of 1-decene.

Table 3.1: Epoxidation of 1-decene at different temperature

T (°C)	Conversion (%)	Epoxide selectivity (%)
60	0	0
70	0	0
80	0	0
90	0	0
100	1	0
110	8	23

Reaction conditions: 1-decene (53 mmol, 10 mL), atmospheric pressure air, reaction time 24 h, rate of stirring 800 rpm.

3.2.2. Influence of radical initiators on 1-decene epoxidation

As molecular oxygen is a diradical in its ground state, this may lead to the contribution of radical reactions, especially in the presence of a radical initiator [7-10]. The presence of a radical initiator in the oxidation of alkenes is the key component in increasing the selectivity for the epoxide [15, 16]. In addition, very small amounts of radical initiators can facilitate the oxidation of 1-decene at lower temperatures (below 100°C). It is important to determine the radical reactions in the absence of catalyst in order to fully

understand the role of the catalytic material. In this study, oxidation of 1-decene was performed with the addition of three different radical initiators namely: *tert*-butylhydroperoxide (TBHP), cumenehydroperoxide (CHP) as hydroperoxide radical initiators and azobisisobutyronitrile (AIBN) as azoradical initiator (Figure 3.1) at different temperatures (60-90°C) in the presence of air and in the absence of the catalyst.

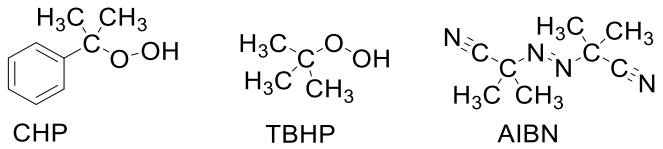

Figure 3.1: Structures of radical initiators.

As can be seen in Table 3.2, no reaction was observed over the range of temperatures (60-90°C) in the absence of both an initiator and a catalyst as discussed previously. Furthermore, there was a gradual increase in the activity with an increase in the temperature with all initiators in the absence of a catalyst. TBHP exhibited very low activity at low temperatures, AIBN and CHP displayed higher activity than TBHP. The selectivity for the epoxide increased from 1.4%, 1.3% and 0.2% at 60°C to be 17.2%, 13.3% and 13.3% at 90°C when using AIBN, CHP and TBHP respectively as radical initiators for this reaction. AIBN became more active and selective toward the epoxide compared to other initiators even at lower temperatures. Many other by-products were detected during the reaction. Significant quantities of allylic products such as 1-decen-3-one, 1-decen-3-ol, 2-decenal, 2-decen-1-ol are formed during the reaction. Furthermore, C-C cleavage reactions occurred forming different C_7+C_8+C_9 products, which will be explained in more details in Section 3.2.3.1.

Table 3.2: Effect of temperature on 1-decene epoxidation using different radical initiators

Initiator	T= 60°C		T= 70°C		T= 80°C		T= 90°C	
	Conversion (%)	Selectivity (%)*	Conv. (%)	Sel. (%)	Conv. (%)	Sel. (%)	Conv. (%)	Sel. (%)
-	0	0	0	0	0	0	0	0
AIBN	1.3	1.4	1.6	3.7	3.4	14.2	6.4	17.2
CHP	1.3	1.3	1.2	3.1	3	4.2	5.5	13.3
TBHP	0.5	0.2	0.7	0.7	1.5	3.5	2.3	13.3

Reaction conditions: 1-decene (53 mmol, 10 mL), TBHP (0.064 mmol, 0.01 mL), AIBN (0.036 mmol, 6 mg), CHP (0.028 mmol, 0.01 mL), atmospheric pressure air, reaction time 24 h, rate of stirring 800 rpm. *Selectivity for epoxide.

The relatively high activity of AIBN can be explained by its stronger nucleophilic nature compared to other radical initiators or there may be low stability and quicker formation of radicals in the reaction compared to TBHP (temperatures for 10 h half-lives of radical initiators: TBHP 170°C, CHP 135°C, AIBN 65°C) [29] as shown in Figure 3.2.

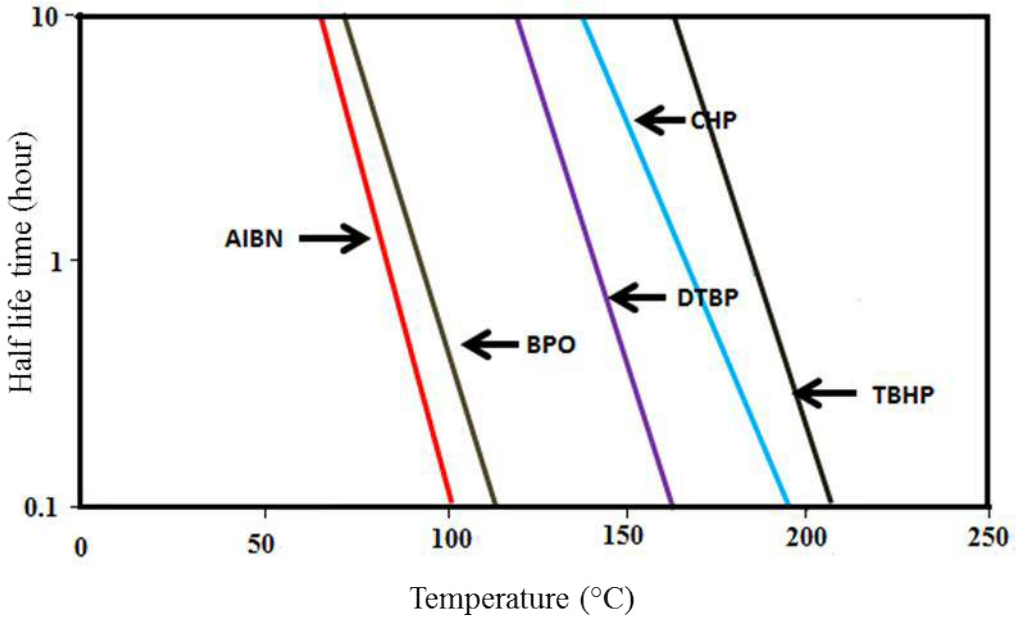

Figure 3.2: Half-life times of various initiators as function of temperature. Adapted from [29]. BPO: Benzoyl peroxide, DTBP: Di-*tert*-butyl peroxide.

Furthermore, AIBN produces different types of a radical to TBHP. AIBN decomposes to produce nitrogen and 1-cyano-1-methylethyl radical as shown in Scheme 3.1. This radical interacts with oxygen to generate ROO˙ (R˙= 1-cyano-1-methylethyl radical), which therefore enhances the oxidation of 1-decene in the absence of the catalyst.

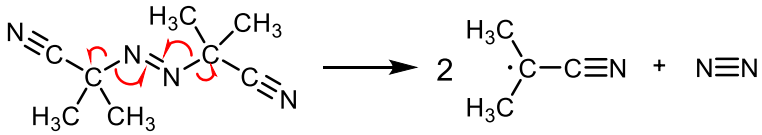

Scheme 3.1: Decomposition of AIBN.

TBHP usually decomposes to yield an RO˙ radical ($Me_3CO^{\cdot}$). This is because the dissociation energy for the O-H bond is higher than the dissociation energy for the O-O bond [30], which may be the reason for the low concentration of ROO˙. In the presence of the catalyst surface, the O-H homolysis can also facilitate producing $Me_3COO^{\cdot}$, which is active in abstracting the hydrogen from the allylic position in 1-decene, which may explain the activity and selectivity for the epoxide with TBHP in the presence of a catalyst. The range of radicals produced during the thermal decomposition of TBHP are shown in Scheme 3.2.

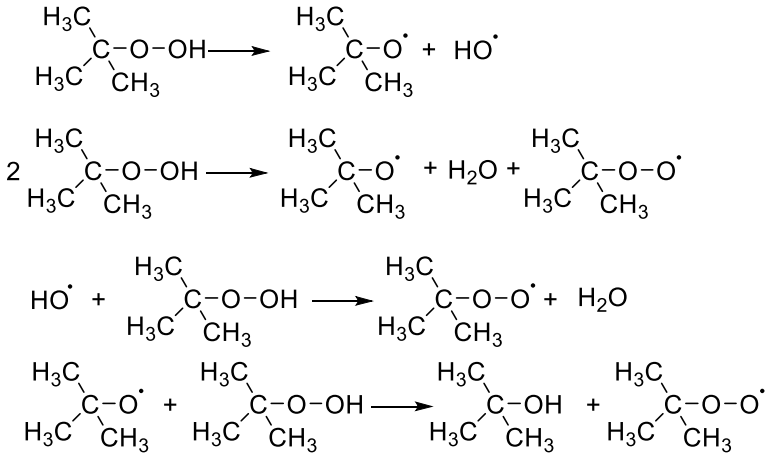

Scheme 3.2: Thermal decomposition of TBHP [30].

Based on all of these previously mentioned data, as TBHP exhibits the lowest activity at 80°C when compared to other radical initiators in the absence of the cobalt catalyst (Table 3.2), it was decided to perform further studies with supported cobalt catalysts using this particular initiator.

3.2.3. Cobalt catalysed reactions

3.2.3.1. Effect of metal loading

After investigating the oxidation of 1-decene in the absence of catalyst, further experiments were carried out in the presence of supported cobalt catalysts. MgO was chosen for the preliminary studies as it is shown in the literature that MgO is an effective catalyst for the cycloaddition of CO_2 with the epoxide [31, 32], an attempt was made to combine the active catalysts for both steps of the oxidative carboxylation of alkene. First, MgO support alone was tested, and this showed low activity in the epoxidation reaction (2% conversion and 4% epoxide selectivity) as shown in Figure 3.3. A number of catalysts with cobalt loading from 0.5 to10% (percentage metal by weight of the support) were prepared by wet-impregnation and screened for activity in the epoxidation of 1-decene. Conversion of 1-decene, epoxide selectivity and epoxide yield (yield obtained by using GC analysis) are shown in Figure 3.3. It can be seen that the cobalt loading had an important effect on the catalytic properties. As the cobalt loading increased, both the 1-decene conversion and the selectivity for 1,2-epoxydecane increased significantly. 2% Co/MgO produced the highest epoxide yield. A further increase in the cobalt loading led to a decrease in the activity, which may be attributed to the growth of catalyst particles caused by agglomeration and sintering during the heat treatment and this may result in the reduction of the active sites. Based on the data in Figure 3.3, 2% Co/MgO was chosen for further investigation.

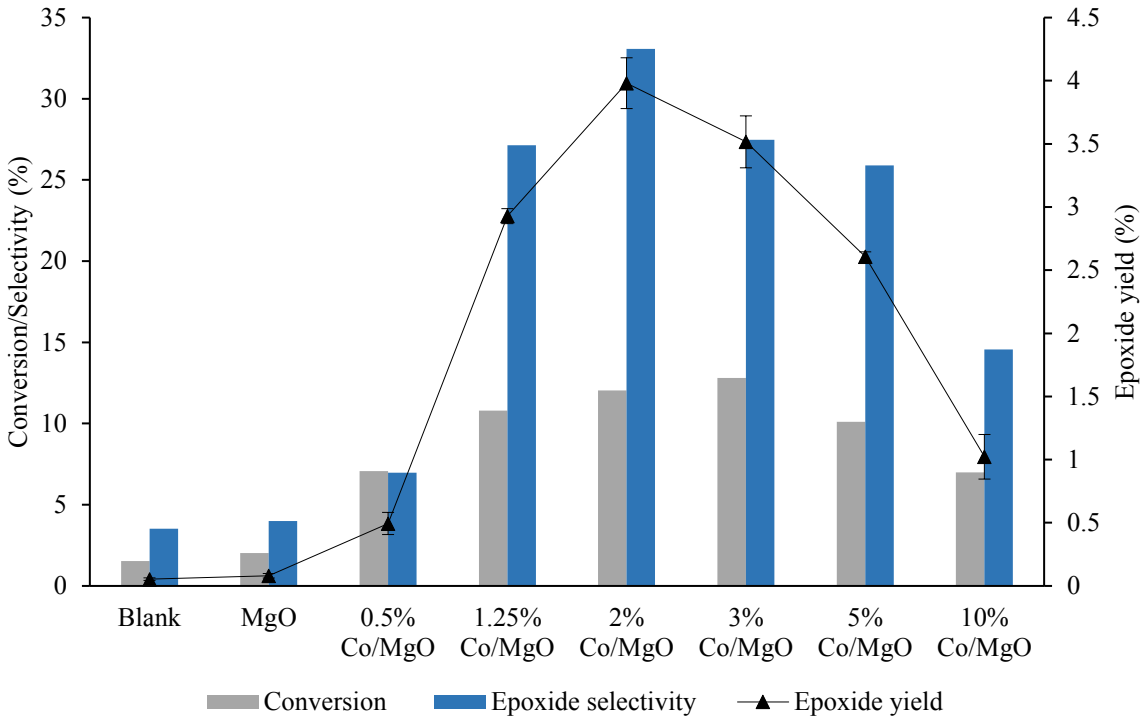

Figure 3.3: Effect of metal loading upon epoxidation of 1-decene. Reaction conditions: catalyst (0.1 g), 1-decene (53 mmol, 10 mL), TBHP (0.064 mmol, 0.01 mL), 80°C, atmospheric pressure air, reaction time 24 h, rate of stirring 800 rpm. Error bars indicate range of data based on three repeat experiments.

Obtaining a high selectivity for the epoxide in epoxidation reactions remains a challenge. As expected, a number of other by-products were detected and quantified. These products were identified previously by our group [16] using GC-MS by comparing retention times and mass spectra with commercial standards as previously mentioned in Section 2.7.1. The full list of products formed during the reaction with associated selectivities are presented in Table 3.3. Significant quantities of allylic products were formed during the reaction after 24 h. Furthermore, C-C cleavage reactions occurred, forming different C_7+C_8+C_9 products. A similar observation was found previously with the oxidation of 1-octene and 1-decene using supported gold catalyst [13, 16]. Corma and co-workers observed that allylic products were produced during the oxidation of 1-octene under solvent-free conditions and using oxygen as an oxidant [13].

Table 3.3: Product selectivity for 1-decene epoxidation at 12% conversion

Product	Selectivity (%)
1,2-Epoxydecane	33
1-Decen-3-one	4.5
1-Decen-3-ol	5
2-Decenal	6.5
2-Decen-1-ol	8
1,2-Decanediol	2
2-Decenoic acid	2.3
Octanal	2.1
Nonanal	2.8
1-Heptanol	1.1
1-Octanol	1.8
Heptanoic acid	1.6
Octanoic acid	3.3
Nonanoic acid	7.1
3-Nonen-1-ol	1.0
3-Nonanone	2.7
Cyclododecane	1.2
Unknown products	12.5

Reaction conditions: 2% Co/MgO (0.1 g), 1-decene (53 mmol, 10 mL), TBHP (0.064 mmol, 0.01 mL), 80°C, atmospheric pressure air, reaction time 24 h, rate of stirring 800 rpm.

3.2.3.2. Time online studies for 1-decene epoxidation over a 2% Co/MgO catalyst

It is desirable to analyse the product profiles during the course of the reaction, as some products may be formed from the sequential oxidation of others. In order to understand the detailed reaction profile of 1-decene epoxidation over the 2% Co/MgO catalyst, time online studies (effect of reaction time on conversion and selectivity) were carried out for 96 h as shown in Figure 3.4. It is clear that with increasing reaction time, the conversion of 1-decene significantly increases from 1.5% at 4 h to 34% at 96 h. In addition to that, it can be seen that the products of allylic oxidation such as 1-decen-3-one, 1-decen-3-ol, 2-decenal and 2-decen-1-ol were the predominant products at the beginning of the reaction. A further increase in the reaction time resulted in a drop of the selectivity for these products, accompanied with a gradual increase in the epoxide selectivity to be the maximum at 48 h at a conversion of 23%. Interestingly, a further increase in the reaction time (over 48 h) resulted in a steady decrease in the epoxide selectivity to a value of 28% at 96 h. Furthermore, the selectivity for the diol increased with increasing the reaction time. This is believed to be a result of opening the epoxide ring. This was caused by the reaction between the epoxide and *in-situ* formed water, which may come from condensation reactions or may *via* the breakdown of the hydroperoxy intermediate to form water and ketone or aldehyde. Once this water has formed, the epoxide is easily

hydrolysed to the diol. In addition to that, an increase in selectivity to cracked acids (heptanoic, octanoic, nonanoic acids) was also noted; this may be due to the oxidation of C_7, C_8 and C_9 alcohols and aldehydes. A similar observation was reported by Gupta *et. al* [16].

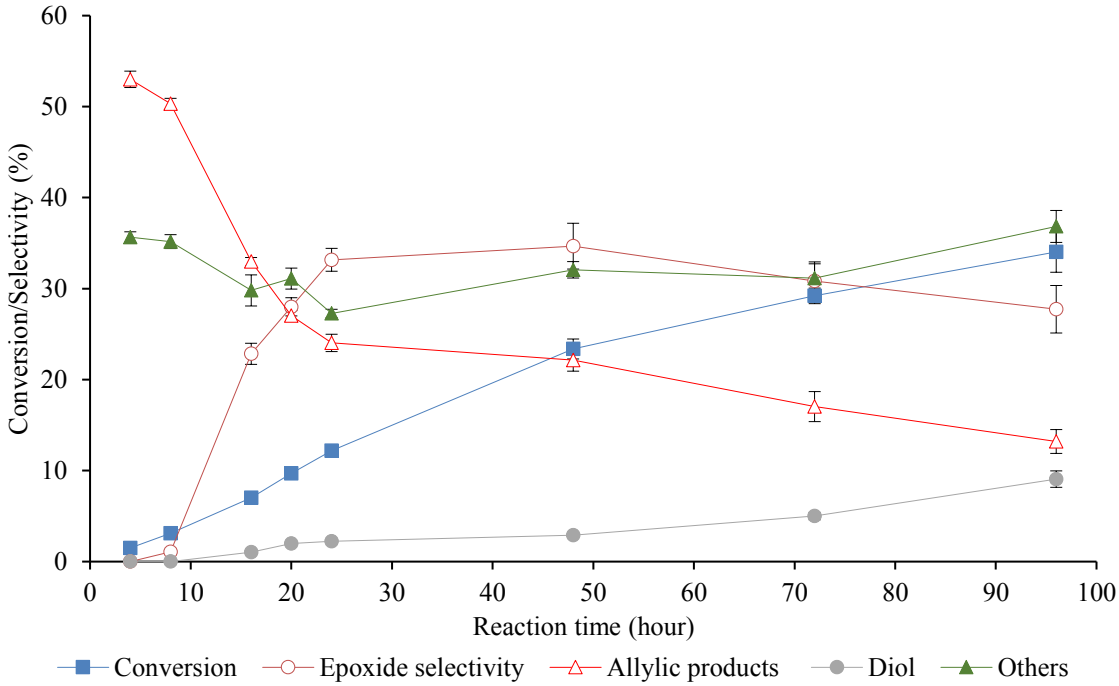

Figure 3.4: Effect of reaction time on conversion and selectivity. Reaction conditions: 2% Co/MgO (0.1 g), 1-decene (53 mmol, 10 mL), TBHP (0.064 mmol, 0.01 mL), 80°C, atmospheric pressure air, rate of stirring 800 rpm. Allylic products=∑ (1-decen-3-one, 1-decen-3-ol, 2-decenal, 2-decen-1-ol). Others=∑ (C_7+C_8+C_9 acids, C_8+C_9 aldehyde, C_7+C_8 alcohols, 3-nonen-1-ol, 3-nonanone, cyclododecane, 2-decenoic acid). Error bars indicate range of data based on three repeat experiments.

3.2.3.3. Evidence for a free radical mechanism

From Table 3.4 it can be seen that the absence of the radical initiator (carrying out the reaction without TBHP) resulted in negligible conversion after 24 h reaction, which suggests a free radical mechanism for the epoxidation of 1-decene. This observation is in agreement with previously reported studies [16, 33]. A diagnostic experiment to confirm the radical mechanism for 1-decene epoxidation involved the reaction in the presence of a radical scavenger, which should scavenge the radical chain reaction. The results shown in Table 3.4 suggest that using 2,6-di-*tert*-butyl-4-methylphenol (BHT) as a radical scavenger leads to termination of the reaction. Therefore, radical chemistry is involved in the present reaction medium. As a result, oxygen from the air seems to be being activated *via* a free-radical species.

Table 3.4: Effect of radical scavenger on epoxidation of 1-decene

Catalyst	Radical initiator	Radical scavenger	Conversion (%)	Epoxide selectivity (%)
2% Co/MgO	-	-	1	0
-	TBHP	-	1.5	3.5
2% Co/MgO	TBHP	-	12	33
2% Co/MgO	TBHP	BHT	0	0

Reaction conditions: 2% Co/MgO (0.1 g), 1-decene (53 mmol, 10 mL), TBHP (0.064 mmol, 0.01 mL), BHT (0.064 mmol, 0.014 g), 80°C, atmospheric pressure air, reaction time 24 h, rate of stirring 800 rpm.

3.2.3.4. Catalyst stability, effect of the support and leaching study

Although a comparatively high activity with the Co/MgO catalyst was observed, the leaching of the active component into the solution is a major problem facing heterogeneous catalysts especially in the liquid phase. In the case of 2% Co/MgO catalyst, ICP analysis showed leaching of the cobalt on the level of 45 ppm, corresponding to approximately 22% of the cobalt present in the catalyst. Furthermore, XPS analysis for both the fresh and the reused supported cobalt catalysts are displayed in Table 3.5. For the MgO supported cobalt samples, the cobalt signal was very weak for the fresh catalyst, but the binding energy ascertained from the peak maxima is in agreement with that of the nature of another supported catalyst (2% Co/TiO_2), which was found to have a binding energy of 781 eV, characteristic of Co^{2+}. The reused 2% Co/MgO catalyst, however, showed no cobalt, which again would indicate leaching or sintering of the cobalt to larger particles (Table 3.5).

Table 3.5: XPS derived molar concentrations (at%) for 2% Co catalysts supported on MgO andTiO_2

	Concentration (at%)[a]				
Sample identifier	**Co**	**Ti**	**Mg**	**O**	**C**
2% Co/MgO Fresh	0.4	--	21.8	39.8	38.0[b]
2% Co/MgO Reused	--	--	22.4	39.3	38.3
2% Co/TiO_2 Fresh	2.0	22.5	--	54.1	21.4[b]
2% Co/TiO_2 Reused	0.9	16.2	--	41.7	41.2

Note: (a): (at%) is the atomic concentration of the elements in the analysed area. It is the molar ratio of the elements. (b): carbon in the fresh sample may come from the atmosphere, solvent or from the tape that used to stick samples down or contamination from x-rays.

Cobalt leaching has to be given great attention since the homogeneous cobalt catalysts such as cobalt (II) perchlorate (2.86 mmol%, amount of cobalt in relation to the alkene amount) were found to be highly active for the epoxidation of different terminal alkenes [17]. It was observed that different terminal alkenes, such as 1-octene and 1-hexene almost converted to give 86-94% yield of the corresponding epoxide using 3-chloroperoxybenzoic acid as the oxidant and performed in CH_3CN at room temperature [17]. However, in the current study, the leached cobalt (0.011 mmol%) is much less than the cobalt amount used in the previous study. Furthermore, in our study oxygen from air was used as an oxidant under solvent-free conditions. Therefore, it is difficult to compare the catalysts activity under different reaction conditions.

It is important to increase the metal-support interaction in order to reduce the leaching of the active species. Reducible supports such as TiO_2 can diffuse onto the metal, which results in a marked effect on the catalytic activity known as strong metal support interactions (SMSIs) [34]. Furthermore, TiO_2 is well known to be an appropriate material for oxidation reactions and has good interaction with the metal when used as a support [35, 36]. Therefore, further studies were conducted using TiO_2.

For the next experiments, the same conditions were applied as for the studies with MgO. From Figure 3.5 it can be seen that 4% conversion of 1-decene and 16% selectivity for 1,2-epoxydecane was found when using TiO_2 support alone. In the presence of 2% Co/TiO_2 catalysts, the conversion of 1-decene and selectivity for the epoxide was greatly enhanced to be 14% and 34% respectively.

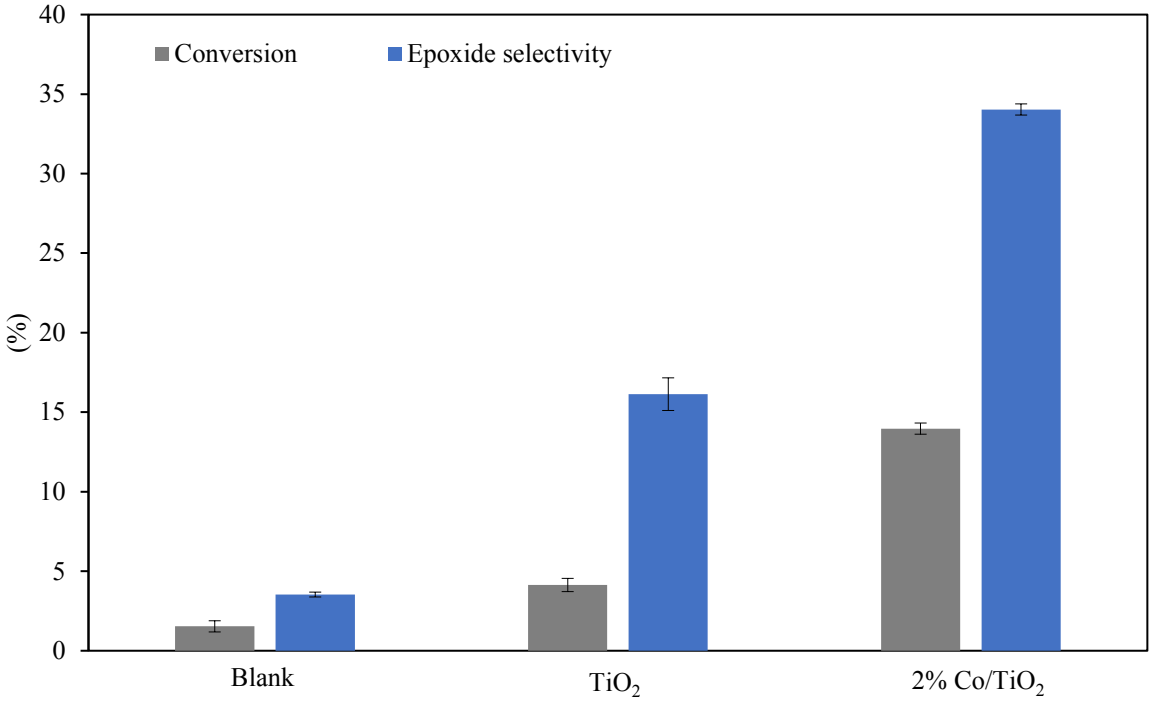

Figure 3.5: Effect of TiO_2 and 2% Co/TiO_2 on 1-decene epoxidation. Reaction conditions: catalyst (0.1 g), 1-decene (53 mmol, 10 mL), TBHP (0.064 mmol, 0.01 mL), 80°C, atmospheric pressure air, reaction time 24 h, rate of stirring 800 rpm. Error bars indicate range of data based on three repeat experiments.

By comparing the activity of the 2% Co/TiO_2 catalyst to the previously reported heterogeneous cobalt catalyst for the epoxidation of terminal alkenes [37], it was found that the 2% Co/TiO_2 catalyst (0.06 mmol%) became less active and selective for the epoxide. A cobalt(II) Schiff base complex immobilised onto the surface of Si–MCM-41 (0.07 mmol%) can convert different terminal alkenes, such as 1-hexene and 1-octene with 35-47% conversion and 30-47% yield of the epoxide at 80°C for 24 h. [37]. However, this later study was carried out in the presence of DMF (8 mL), which is not an inert solvent in the epoxidation reaction with molecular oxygen, as mentioned in Section 1.7 [24]. This reaction condition is against the concept of our study for the epoxidation of 1-decene under solvent-free conditions.

When TiO_2 was used as support for cobalt, the quantity of cobalt leached from the catalyst decreased to 12 ppm, accounting for 6% of total cobalt loading. It has been reported that alcohols and acids tend to cause leaching of the active components in liquid phase oxidations [38]. This was particularly observed in the epoxidation of 1-decene, where many products with alcohol and acid functional groups were formed.

Hot filtration experiments may help to draw conclusions about the nature of active species in this reaction. Table 3.6 compares the normal epoxidation of 1-decene at 8 h and 24 h

as well as a hot filtration reaction where the catalyst was filtered off after 8 h reaction time and then the reaction was run for another 16 h. As can be seen in Table 3.6, the reaction proceeded after catalyst removal, but with a significantly reduction in 1-decene conversion from 14 to 4% and in the epoxide selectivity from 34% to 14%. Therefore, this experiment helps to draw conclusion that the main catalytic route is heterogeneous with a minor contribution from homogeneous catalysis.

Table 3.6: Heterogeneous versus homogeneous cobalt catalysis

Reaction time (hour)	Conversion (%)	Epoxide selectivity (%)
8	3.4	10
24	14	34
HF[a]	4	14

Reaction conditions: 2% Co/TiO_2 (0.1 g), 1-decene (53 mmol, 10 mL), TBHP (0.064 mmol, 0.01 mL), 80°C, atmospheric pressure air, rate of stirring 800 rpm. (a): hot filtration, the catalyst was filtered off after 8 h reaction time and then the reaction was run for another 16 h.

3.2.3.5. Effect of the catalyst mass of the 2% Co/TiO_2

The effect of the amount of 2% Co/TiO_2 catalyst used in the oxidation of 1-decene was studied at 80°C using TBHP as radical initiator with a reaction time of 24 h. As can be seen in Table 3.7 the conversion of 1-decene increases with increasing the amount of catalyst, as does the selectivity for 1,2-epoxydecane. In contrast, the selectivity for allylic products decreases with increasing the catalyst mass. When doubling the catalyst mass from 0.05 to 0.1 g, the conversion increased from 7% to 14% respectively. However, increasing the mass from 0.1 to 0.2 g resulted in a 2% only increase in the conversion, which may indicate that there is a mass transport limitation in this range. Furthermore, when reactions were performed with 0.05 g of 2% Co/TiO_2 catalyst, the allylic products distribution was similar to the reaction performed without catalyst (selectivity 42-45%), whereas there was a significant reduction in the selectivity for these products when the catalyst mass increased to 0.1 g. Therefore, the optimum amount of catalyst to be used in the reaction was 0.1 g (0.06 mmol%, amount of cobalt in relation to the 1-decene amount). Amounts below this led to a decrease in the conversion and in the epoxide selectivity and only minor gains in the conversion and the epoxide selectivity were observed when doubling this amount.

Table 3.7: Effect of the catalyst mass of the 2% Co/TiO_2 on 1-decene oxidation

Catalyst	Conversion (%)	Epoxide selectivity (%)	Allylic products selectivity (%)	Others selectivity (%)
None (blank)	2	4	45	37
0.05 g	7	18	40	27
0.1 g	14	34	24	30
0.15 g	15	34	24	27
0.2 g	16	36	22	28

Reaction conditions:1-decene (53 mmol, 10 mL), TBHP (0.064 mmol, 0.01 mL), 80°C, atmospheric pressure air, reaction time 24 h, rate of stirring 800 rpm. Allylic products=∑ (1-decen-3-one, 1-decen-3-ol, 2-decenal, 2-decen-1-ol). Others=∑ (C_7+C_8+C_9 acids, C_8+C_9 aldehyde, C_7+C_8 alcohols, 3-nonen-1-ol, 3-nonanone, cyclododecane, 2-decenoic acid, 1,2-decanediol).

3.2.3.6. Presence of 1-decene hydroperoxide in the reaction

It was proposed that the hydroperoxide is the intermediate to produce epoxide and the allylic products [13, 16]. This intermediate cannot be easily identified using gas chromatography, as it decomposes in the injector due to the high temperatures [23, 39]. As a result, another way of product determination needs to be found. It is possible to reduce hydroperoxide into corresponding products such as alcohols using triphenylphosphine (PPh_3), which is frequently used to scavenge thermally unstable peroxides in GC analysis [23, 39]. A standard reaction was performed for 24 h at 80°C in the presence of TBHP and a 2% Co/TiO_2 catalyst. After filtration, the reaction mixture was divided into two solutions, then PPh_3 was added to one of them and stirred for 1 hour at room temperature. Reaction mixtures before and after PPh_3 treatment were analysed by GC. After analysis, it was noticed that there was a small increase in the selectivity for allylic products such as 2-decen-1-ol from 6.7% to 8.9% and 2-decenal from 3.4% to 6.2%. The increase in the aldehyde selectivity may be due to the loss of water from the hydroperoxide intermediate by breaking the O-O bond (probably a radical mechanism); the formed OH radical could pick off a hydride from the adjacent and very close CH_2 group, which then gives the aldehyde and water [40]. Alternatively, it may be due to the oxidation of the allylic alcohol to give the aldehyde. A similar observation was found in the previous study using supported gold catalyst for epoxidation of 1-decene [16]. After the addition of PPh_3, an increase in the selectivity for allylic products such as 2-decen-1-ol, 1-decen-3-one and 2-decenal was found.

3.3. Proposed mechanism for epoxidation of 1-decene

1,2-Epoxydecane was found to be the epoxide product of the reaction of TBHP with 1-decene in the absence of the catalyst; a similar observation by our group was found in a previous study for 1-decene oxidation [16]. This is an interesting finding because initial

radical abstraction of H would be anticipated at the 3-(allylic) position of 1-decene, and this is where an initial oxygen attack would be expected to take place to generate C_7H_{15}-CH(O-O.)-CH=CH_2. This route might potentially generate the 2,3-epoxydecane, which was not observed even in trace amounts as mentioned in Section 2.7.1. Oxygen attachment could be at the 1-position in the delocalised allylic radical to give the primary allylic hydroperoxide, followed by dehydration. This could generate C_7H_{15}-CH=CH-CHO, which may facilitate epoxidation by conversion into the corresponding peracid C_7H_{15}-CH=CH-CO-OOH, which was noted previously by Mukaiyama and co-workers [41]. The product of peracid epoxidation would selectively be the 1,2-epoxydecane along with an equivalent quantity of 2-decenoic acid [16]. Table 3.3 indicates that, in the presence of the catalyst, the allylic products and 2-decenoic acid were observed, but in minor quantities relative to 1,2-epoxydecane. Therefore, the involvement of the cobalt surface is critical in controlling this free radical chemistry and increasing the epoxide selectivity. A reaction mechanism for the epoxidation of 1-decene was previously proposed by our research group using a supported gold catalyst [16]. As shown in Scheme 3.3, over supported cobalt catalysts in the presence of TBHP as radical initiator, TBHP decomposes to create the radical. The radical produced abstracts an allylic hydrogen atom from the 1-decene molecule and produces allylic radical which further interacts with oxygen to produce a peroxy radical, which is the epoxidising species. This peroxy species reacts with a 1-decene molecule to produce the hydroperoxide and one mole of 1-decene radical which forms a cycle to generate a peroxy-radical again. In the absence of the supported cobalt catalyst, low conversion was observed and the decene hydroperoxide intermediate accumulated in the reaction mixture and hence more allylic products were observed as shown in Table 3.7. However, when the supported cobalt catalyst was present in the reaction mixture, the hydroperoxide so formed completed the reaction to produce 1,2-epoxydecane and the allylic products. This involves a complex sequence in which the hydroperoxide reacts on the surface of cobalt to generate a 3-dec-1-enyloxy radical. This radical interacts with the second 1-decene and subsequent fragmentation results in the formation of the epoxide and 3-decen-1-yl radical (Scheme 3.3). It is possible to envisage a similar process which would generate epoxide in addition to a decenyloxy radical. This process would involve the attachment of a peroxy radical to the terminal carbon of 1-decene, after which fragmentation (O-O cleavage) takes place. Since the cobalt surface directs the selectivity towards the epoxide rather than the allylic products, the presence of the cobalt surface throughout these processes is indispensable (Scheme 3.3).

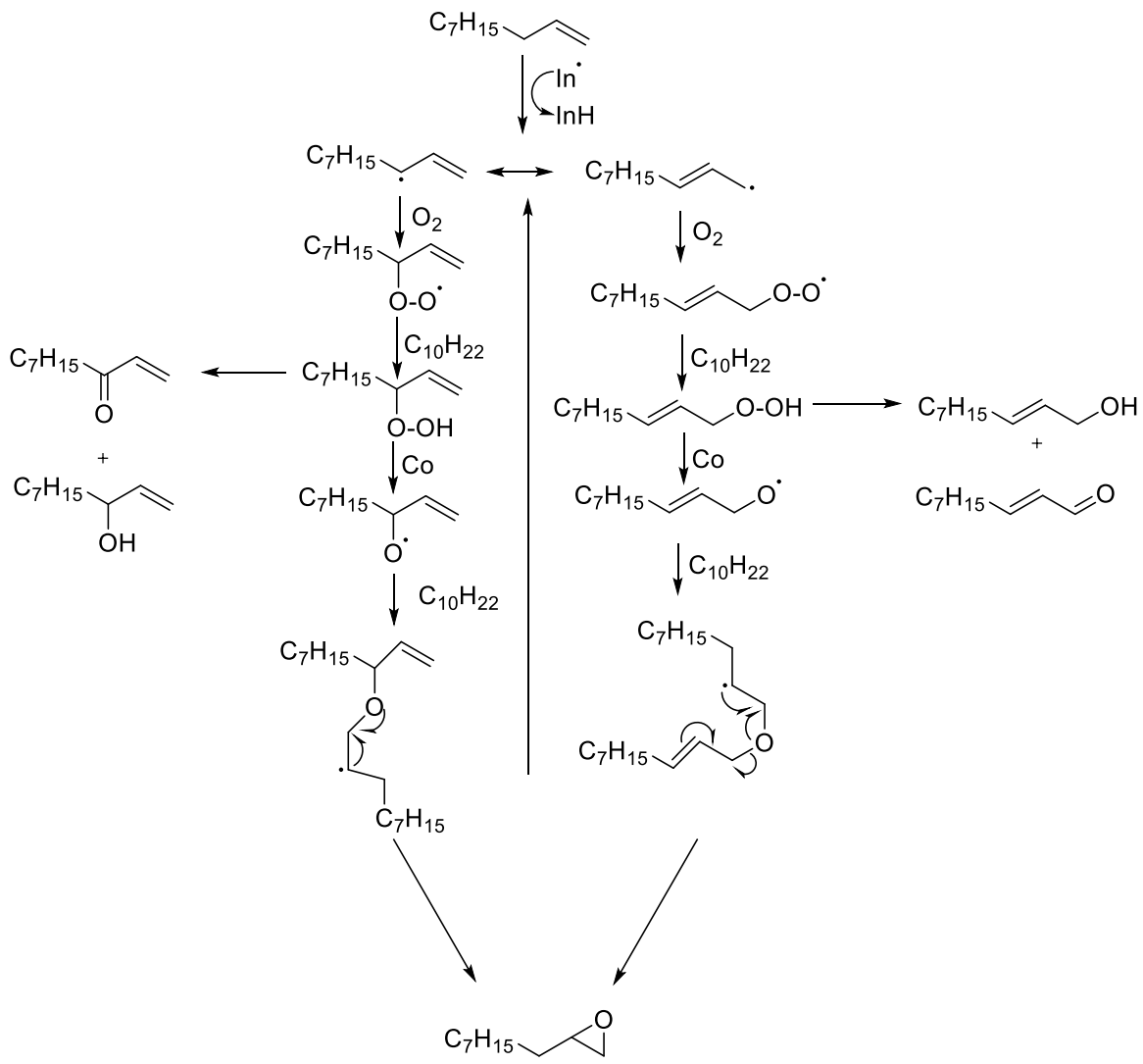

Scheme 3.3: Proposed mechanism of 1-decene epoxidation based on proposed mechanism by gold catalyst. Adapted from [16]. In: Radical initiator.

In the absence of supported cobalt catalyst, the reaction gave rise to more allylic oxidation products, rather than the 1,2-epoxydecane, as shown previously in Table 3.7. This may be explained by a Russell termination mechanism, as shown in Scheme 3.4 for the 3-dec-1-enylperoxy radical. Interaction of an oxygen molecule with the radical from 1-decene, which contains an α-hydrogen atom, leads to the peroxy radical, which can undergo Russell termination to give an alcohol and a ketone [42, 43]. Thus, the presence of the cobalt surface is essential to direct the reaction towards the formation of the 1,2-epoxydecane.

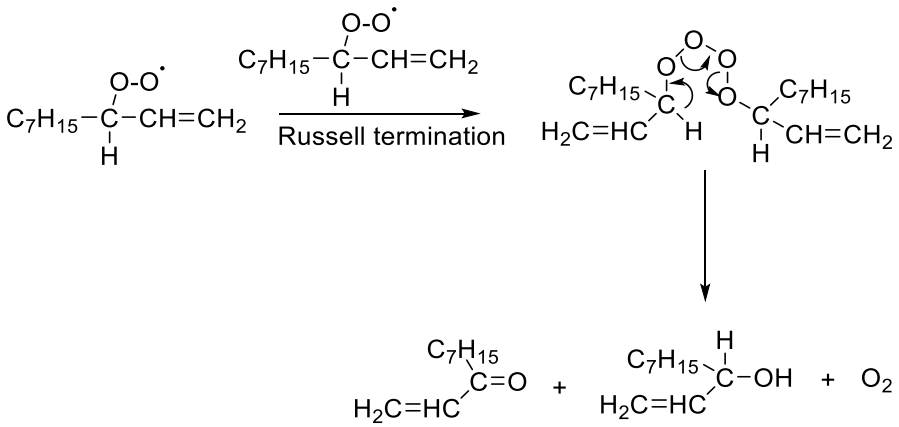

Scheme 3.4: Russell termination and formation of allylic products. Adapted from [16].

3.4. Catalyst reusability

After a standard reaction, the reuse of the catalysts was investigated. The reused 2% Co/TiO_2 catalysts were filtered off and either dried in the oven at 110°C for 16 h without a washing step, or washed with acetone (1 L) and then dried in the oven at 110°C for 16 h. The epoxidation of 1-decene over fresh and reused 2% Co/TiO_2 catalysts is summarised in Table 3.8. When the fresh 2% Co/TiO_2 catalyst was used in the reaction, the conversion of 1-decene reached 14% with an epoxide selectivity of 34%. The reused cobalt catalysts (dried only without a washing step) did not enable effective reuse and exhibited lower activity compared to the fresh one. This may be ascribed to the adsorption of products, which results in the deactivation of the 2% Co/TiO_2 catalyst. FTIR analysis of the reused catalyst confirmed the presence of additional species. Strong stretching in the region 2900-2970 cm^{-1} can be assigned to CH stretching modes (Figure 3.6), which may indicate the adsorption of products on the surface of the spent catalyst. When the catalyst was washed with acetone, the FTIR characteristic bands (Figure 3.6) reduced in size, suggesting that some of the adsorbed products were removed and the catalytic activity was slightly restored (conversion 11% (Table 3.8)). XPS analysis (Table 3.5) is in agreement with FTIR analysis, which indicates that the quantity of carbon (C) on the spent cobalt catalyst increased when compared to that on the fresh catalyst (from *ca.* 21.4% to *ca.* 41.2%). This resulted in a decrease in activity, which was probably due to the C blocking the active sites of the cobalt catalysts.

Table 3.8: Catalyst reusability study for epoxidation of 1-decene: 2% Co/TiO_2

Washing conditions	Conversion (%)	Epoxide selectivity (%)
Fresh catalyst	14	34
Reused without washing, dried static air at 110°C for 16 h	7	19
Reused and washed with acetone (1 L), dried static air at 110°C for 16 h	11	22

Reaction conditions: 2% Co/TiO_2 (0.1 g), 1-decene (53 mmol, 10 mL), TBHP (0.064 mmol, 0.01 mL), 80°C, atmospheric pressure air, reaction time 24 h, rate of stirring 800 rpm.

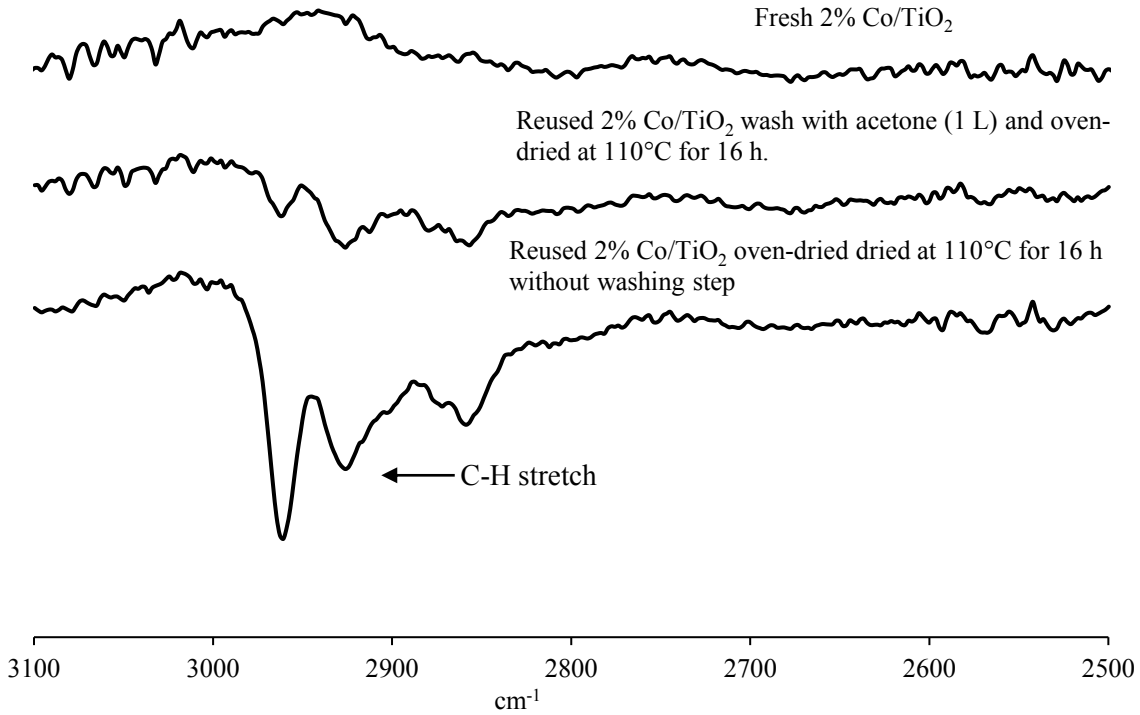

Figure 3.6: FTIR for the fresh and the reused 2% Co/TiO_2 catalysts.

3.5. Catalysts characterisations

In addition to the previously mentioned techniques (XPS and FTIR), the techniques of TGA, XRD, SEM, BET and TPR were used to characterise the supported cobalt catalysts.

Thermal gravimetric analysis (TGA) was used to detect the desired calcination temperature for the catalysts. It is suggested that 400°C is the suitable temperature for calcination in order to complete the decomposition of the precursor and the formation of the cobalt oxide as shown in Figure 3.7.

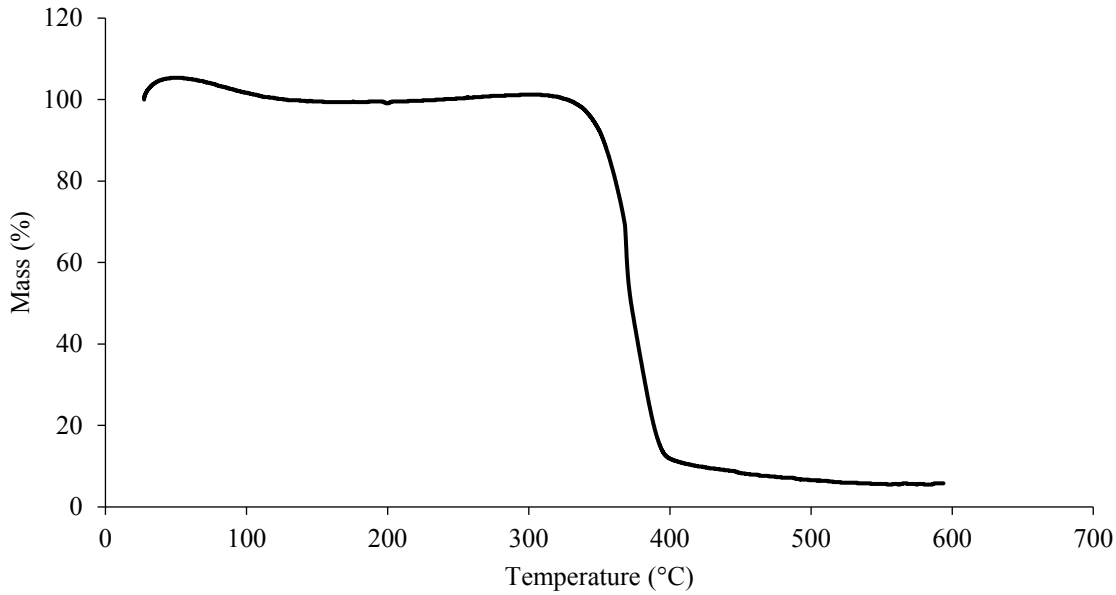

Figure 3.7: TGA of a cobalt catalyst (6.5 mg, dried only) prepared by wet-impregnation.

As the 2% Co/MgO and 2% Co/TiO_2 catalysts are the chosen catalysts for this study, XRD analysis of the supports and corresponding cobalt catalysts was carried out (Figure 3.8 and Figure 3.9). The reflections from the cobalt oxide would be expected to be 2θ= 19.0°, 31.3°, 37.0°, 38.6°, 44.9°, 55.8°, 59.4° and 65.4° [44]. The cobalt catalyst did not exhibit strong diffraction peaks as a number of reflections would overlap with the reflection patterns of the MgO, and the main reflection patterns can be assigned to the MgO, which can then hardly be distinguished. A broad reflection peak of the cobalt oxide at 59.4° was observed (Figure 3.8). A similar observation was found in a previous study [45]; it was demonstrated that the basic sites on the MgO surface could promote the dispersion of the cobalt during the impregnation, and thus no strong diffraction patterns can be observed for Co/MgO [45].

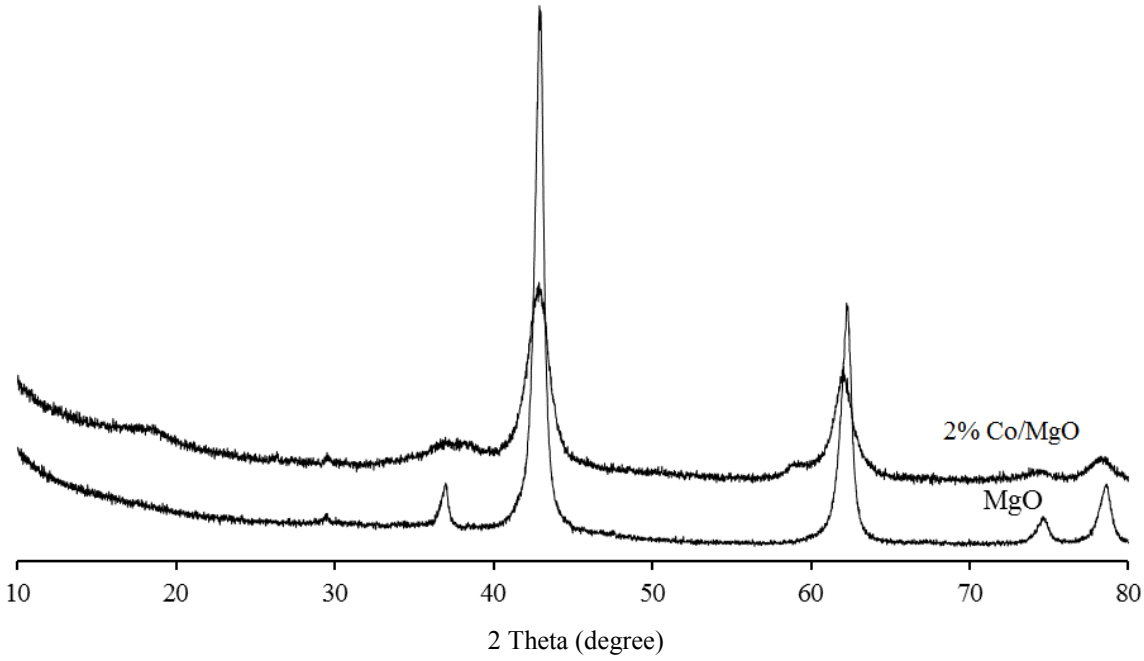

Figure 3.8: X-ray diffraction patterns for: MgO and 2% Co/MgO.

When the 2% Co/TiO_2 catalyst was analysed using XRD, a slight shift of the signals was noted for the fresh and reused 2% Co/TiO_2 towards smaller 2θ angles, compared with the TiO_2 support alone (Figure 3.9). This may indicate the incorporation of the cobalt into the lattice. Furthermore, it can be seen that the XRD reflections of the fresh and reused 2% Co/TiO_2 did not display enough distinguishable differences in their reflections. The characteristic XRD reflections of cobalt ion were not observed, indicating that cobalt was uniformly dispersed among the TiO_2 support. A similar observation was found in a previous study, where the authors could not detect cobalt in loading as high as 10% Co/TiO_2 by XRD [46].

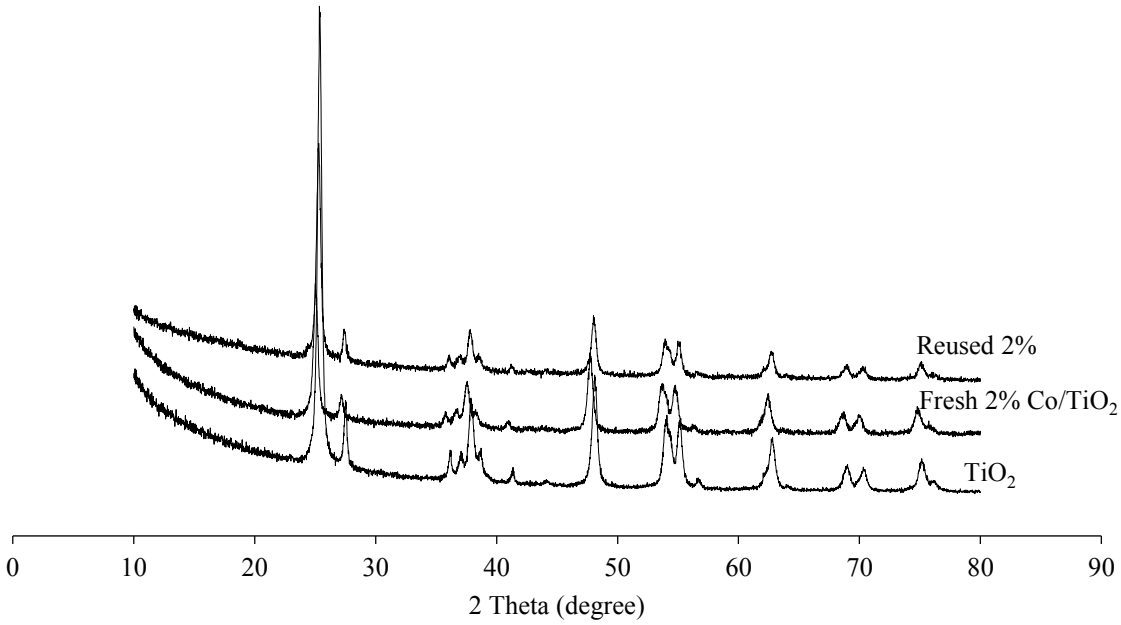

Figure 3.9: X-ray diffraction patterns for: TiO_2, the fresh and reused 2% Co/TiO_2.

The surface morphology for all the undoped supports and supported cobalt catalysts are shown in Figure 3.10, Figure 3.11 and Figure 3.12. It can be seen from the SEM images that the difference in morphology between the fresh and reused 2% Co/TiO_2 catalyst is negligible.

(1)

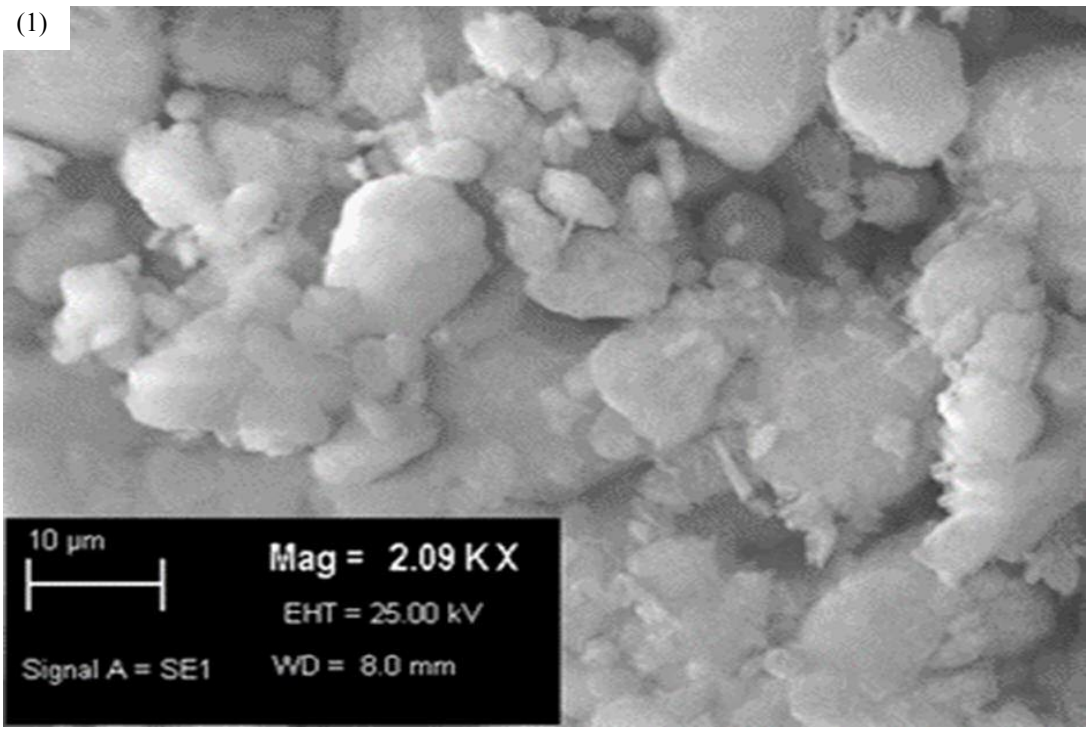

(2)

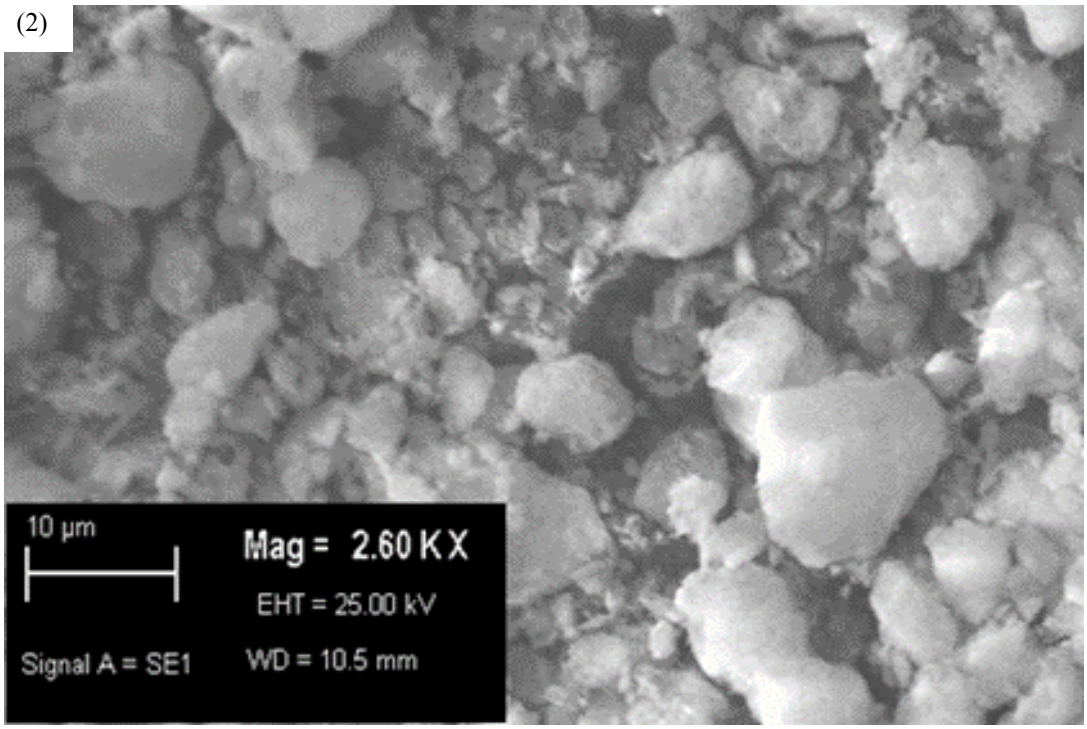

Figure 3.10: SEM image for: (1) MgO and (2) 2 % Co/MgO.

(1)

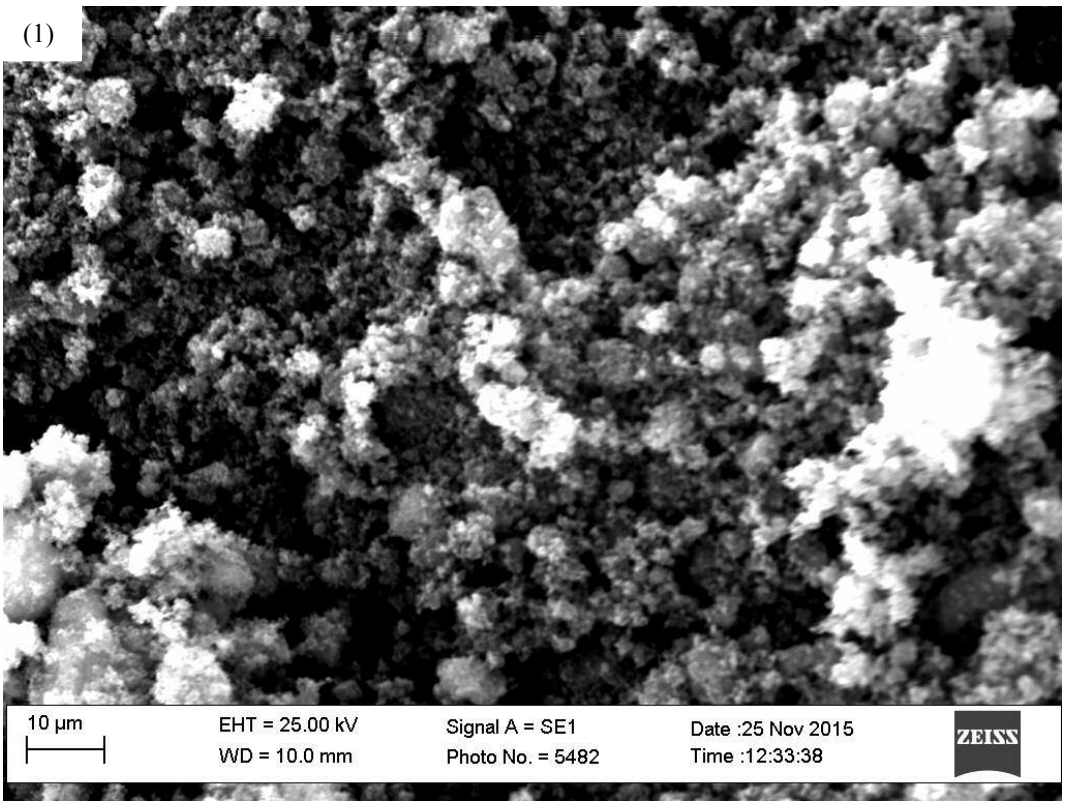

(2)

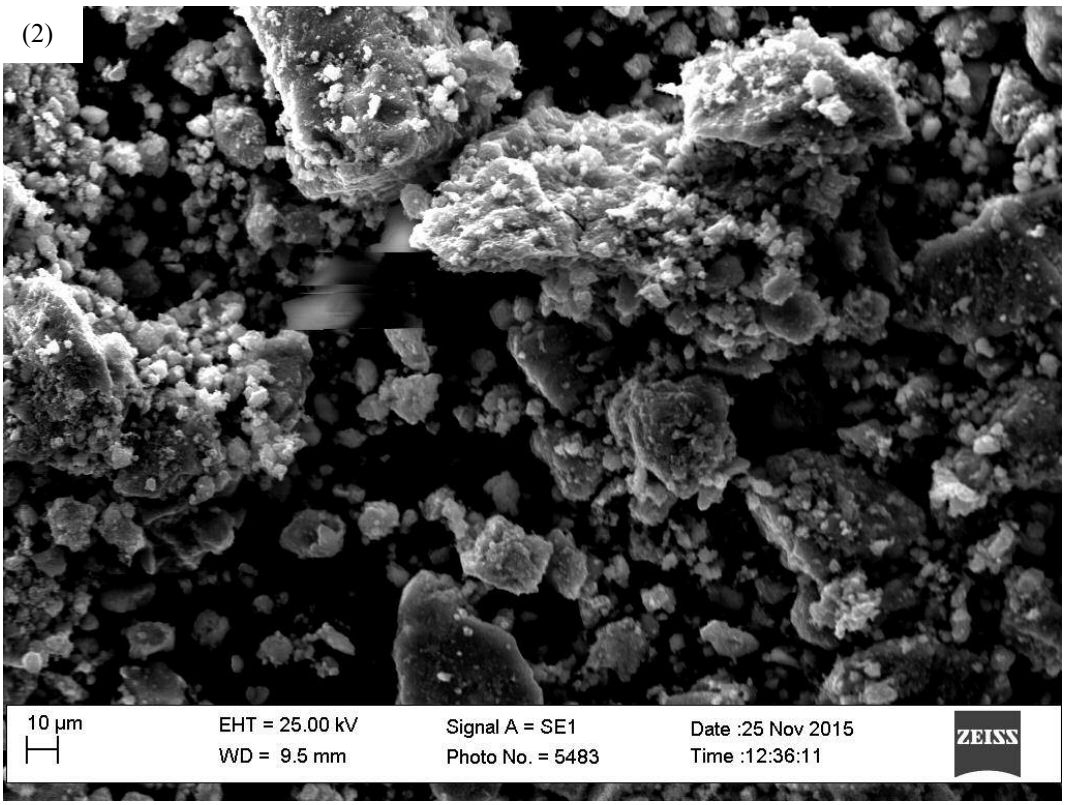

Figure 3.11: SEM image for: (1) TiO_2 and (2) fresh 2% Co/TiO_2.

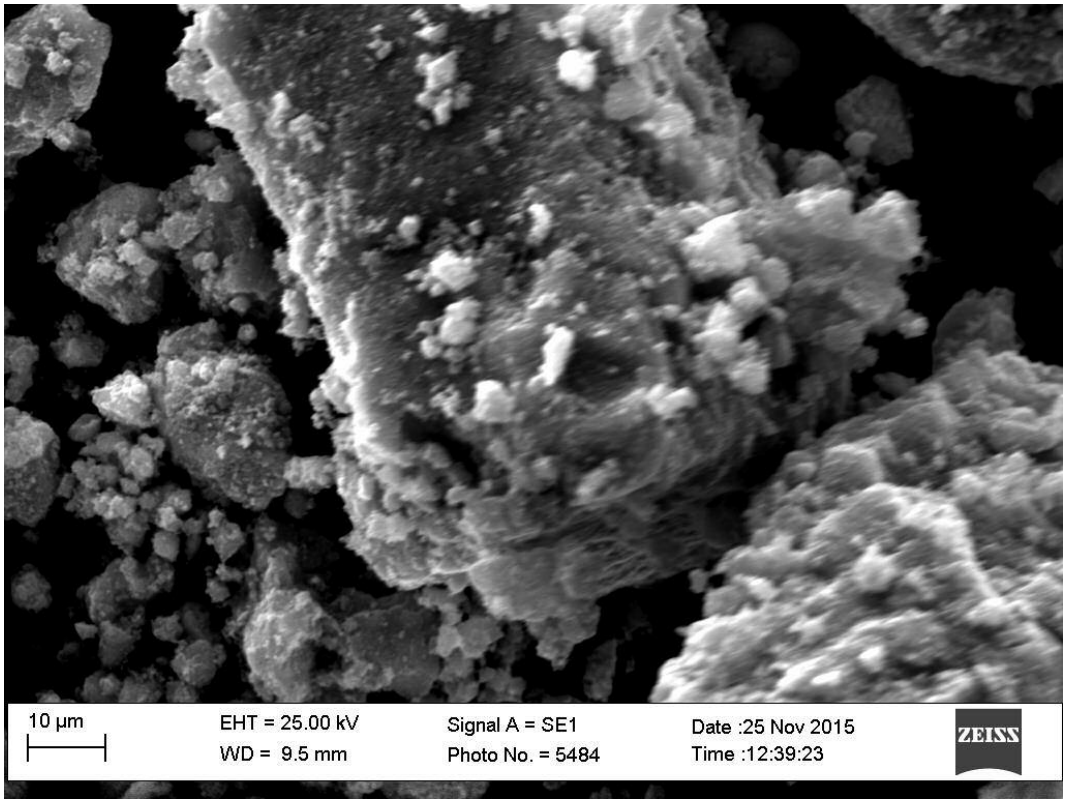

Figure 3.12: SEM image for reused 2% Co/TiO_2.

From the N_2 adsorption analysis, the surface areas of different supports and supported cobalt catalysts were calculated and listed in Table 3.9. There was a reduction in the surface area of the 2% Co/support catalysts compared to the undoped supports, which may indicate the incorporation of the cobalt in the support pores. There was a slight decrease in the surface area of the reused 2% Co/TiO_2 from 47 to 45 m^2 g^{-1}, which may be a result of the adsorption of some products and remaining substrate on the surface. The analysis was carried out twice and error in the analysis was no more than 1 m^2 g^{-1}.

Table 3.9: Nitrogen physisorption analysis of the surface area using BET method of different supports and supported cobalt catalysts

Catalyst	Surface area (m^2 g^{-1})
MgO	55
2% Co/MgO	49
TiO_2	51
2% Co/TiO_2	47
Reused 2% Co/TiO_2	45

The H_2-TPR profiles of the Co_3O_4 and 2% Co/TiO_2 catalysts are shown in Figure 3.13. The results show that the reduction peaks of the 2% Co/TiO_2 exhibit two hydrogen consumption peaks attributed to two-step reduction. The first reduction peak is observed between ~320-390°C and mainly resulted from the reduction of Co_3O_4 to CoO, which is in agreement with the reduction peak of unsupported Co_3O_4 in this temperature range. TPR analysis agrees with previously mentioned XPS analysis, which is that the cobalt is found to be Co^{2+}. The second set of peaks of the reduction of 2% Co/TiO_2 at 400-600°C may be attributed to the reduction of CoO to metallic Co. This is in agreement with previous studies reported for Co_3O_4/TiO_2 [46-48].

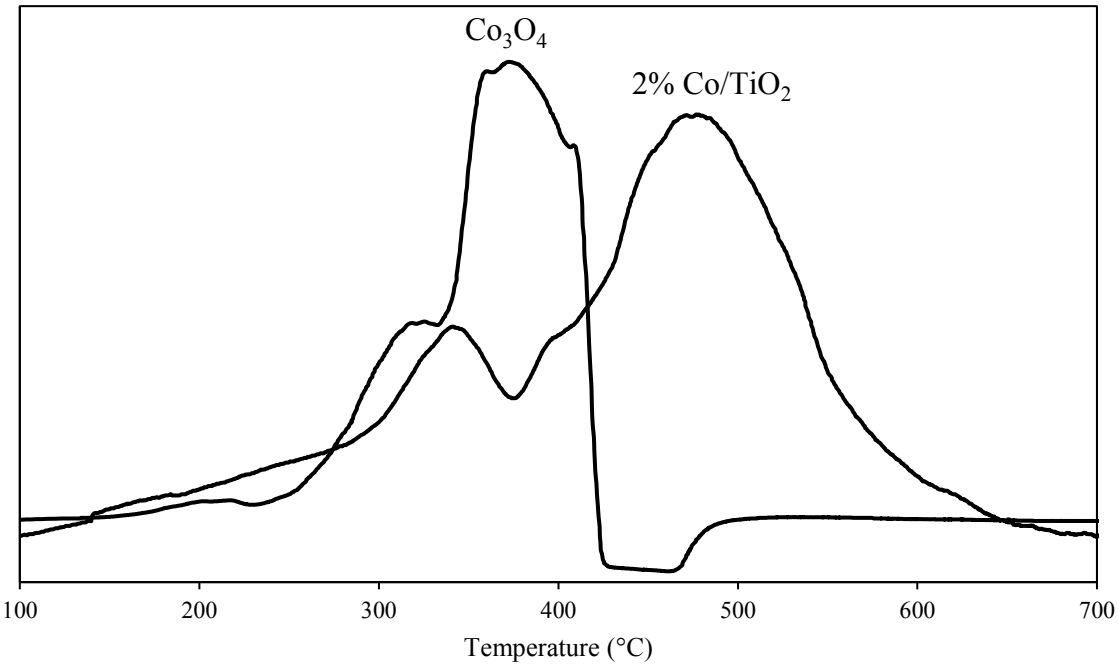

Figure 3.13: TPR for Co_3O_4 and 2% Co/TiO_2.

3.6. Conclusions

It has been shown that supported cobalt catalysts are active in the epoxidation of 1-decene under solvent free conditions in the presence of a very small of a radical initiator and oxygen from air as a primary oxidant at 80°C. The influence of the reaction temperature in the absence of a radical initiator and catalyst was investigated and it was found that the oxidation of 1-decene does not start below 100°C, whereas at 110°C the reaction starts spontaneously (as shown in Table 3.1). The presence of a very small amount of radical initiators allows for the use of atmospheric oxygen as an oxidant in place of expensive and environmentally hazardous oxidants. Different radical initiators were investigated, namely *tert*-butylhydroperoxide (TBHP), cumene hydroperoxide (CHP) and

azobisisobutyronitrile (AIBN). TBHP was identified as suitable as it exhibited the lowest activity (conversion 1.5% and epoxide selectivity 3.5%) at 80°C when compared to other radical initiators in the absence of the cobalt catalyst (as illustrated in Table 3.2). The combination of TBHP and 2% Co/MgO catalyst resulted in high conversion of 1-decene (12%). In the absence of TBHP and the presence of the 2% Co/MgO catalyst, traces of the conversion were observed, which indicates the importance of the radical initiator in this reaction. Using 2,6-di-*tert*-butyl-4-methylphenol (BHT) as a radical scavenger led to the termination of the reaction. This suggests free radicals are involved in the catalytic cycle in the liquid phase epoxidation of 1-decene (as shown in Table 3.4). When TiO_2 was used as a support for cobalt, the quantity of cobalt leached from the catalyst significantly decreased. It was also shown that there was a significant drop in the conversion with the reused catalysts without a washing step with acetone (from 14% to 7%), which may be due to the adsorption of the products and blocking of the active sites. After the washing step, the catalyst reusability slightly increased (conversion 11%) as illustrated in Table 3.8, suggesting that some of the adsorbed products were removed and the catalytic activity was slightly restored. FTIR and XPS indicated the adsorption of products and remaining substrate on the reused catalyst surface, resulting in a decrease in the catalyst activity.

3.7. References

[1] A. K. Suresh, M. M. Sharma and T. Sridhar, *Ind. Eng. Chem. Res*., 2000, **39**, 3958.

[2] J. H. Clark and D. J. Macquarrie, *Org. Process Res. Dev.*, 1997, **1**, 149.

[3] A. Ansmann, R. Kawa and M. Neuss, US Patent 7,083,780 B2, August 1, 2006, assigned to Cognis Deutschland.

[4] H. Pines, D. D. Eley and P. B. Weisz, *Advances in Catalysis*, Academic Press, New York, 1987.

[5] T. A. Nijhuis, M. Makkee, J. A. Moulijn and B. M. Weckhuysen, *Ind. Eng. Chem. Res.*, 2006, **45**, 3447.

[6] B. Notari, *Catal. Today*, 1993, **18**, 163.

[7] P. Lignier, F. Morfin, S. Mangematin, L. Massin, J-L Rousset and V. Caps, *Chem. Commun.*, 2007, 186.

[8] A. Takahashi, N. Hamakawa, I. Nakamura and T. Fujitani, *Appl. Catal. A: Gen*., 2005, **294**, 34.

[9] J. Liang, Q. Zhang, H. Wu, G. Meng, Q. Tang and Y. Wang, *Catal. Commun.*, 2004, **5**, 665.

[10] S. Y. Lim, M. Kang, J. Kim and I. M. Lee, *Bull. Korean Chem. Soc*., 2005, **26**, 887.

[11] T. Hayashi, K. Tanaka and M. Haruta, *J. Catal*., 1998, **178**, 566.

[12] M. D. Hughes, Y. X. Xu, P. Jenkins, P. McMorn, P. London, D. I. Enache, A. F. Carley, G. A. Attard, G. J. Hutchings, F. King, E. H. Stitt, P. Johnston, K. Griffin and C. J. Kiely, *Nature*, 2005, **437**, 1132.

[13] C. Aprile, A. Corma, M. Domine, H. Garcia, C. Mitchell and A. Cascade, *J. Catal*., 2009, **264**, 44.

[14] M. Haruta and M. Date, *Appl. Catal.: A*, 2001, **222**, 427.

[15] H. Alshammari, P. J. Miedziak, T. E. Davies, D. J. Willock, D. W. Knight and G. J. Hutchings, *Catal. Sci. Technol*., 2014, **4**, 908.

[16] U. N. Gupta, N. F. Dummer, S. Pattisson, R. L. Jenkins, D. W. Knight, D. Bethell and G. J. Hutchings, *Catal. Lett.*, 2015, **145**, 689.

[17] M. Y. Hyun, S. H. Kim, Y. J. Song, H. G. Lee, Y. D. Jo, J. H. Kim, I. H. Hwang, J. Y. Noh, J. Kang and C. Kim, *J. Org. Chem.*, 2012, **77**, 7307.

[18] Z. Asgharpour, F. Farzaneh and A. Abbasib, *RSC Adv.*, 2016, **6**, 95729.

[19] Q. Tang, Y. Wang, J. Liang, P. Wang, Q. Zhang and H. Wan, *Chem. Commun.*, 2004, 440.

[20] M. V. Patil, M. K. Yaday and R. V. Jasra, *J. Mol. Catal. A: Chem.*, 2007, **277**, 72.

[21] Q. Tang, Q. Zhang, H. Wu and Y. Wang, *J. Catal.*, 2005, **230**, 384.

[22] X.-Y. Quek, Q. Tang, S. Hu and Y. Yang, *Appl. Catal. A: Gen.*, 2009, **361**, 130.

[23] M. J. Beier, W. Kleist, M. T. Wharmby, R. Kissner, B. Kimmerle, P. A. Wright, W. Grunwaldt, J. Dierk and A. Baiker, *J. Chem. Eur.*, 2012, **18**, 887.

[24] Z. Opre, T. Mallat and A. Baiker, *J. Catal.*, 2007, **245**, 482.

[25] K. M. Jinka, J. Sebastian and R. V. Jasra, *J. Mol. Catal. A: Chem.*, 2007, **274**, 33.

[26] M. L. Kantam, B. P. Rao, R. S. Reddy, N. S. Sekhar, B. Sreedhar and B. M. Choudary, *J. Mol. Catal. A: Chem.*, 2007, **272**, 1.

[27] P. Lignier, S. Mangematin, F. Morfin, J-L Rousset and V. Caps, *Catal. Today*, 2008, **138**, 50.

[28] W. H. Brown, C. S. Foote, B. L. Iverson and E. V. Anslyn, *Organic Chemistry* (5th Ed) Brooks/Cole Cengage Learning, Belmont, 2009.

[29] J. Meijer and A. Hogt, *Acros Org. Rev*, 2006, **16**, 1.

[30] E. T. Denisov, T. G. Denisova and T. S. Pokidova, *Handbook of Free Radical Initiators,* John Wiley and Sons Ltd., New York, 2003.

[31] K. Yamaguchi, K. Ebitani, T. Yoshida, H. Yoshida and K. Kaneda, *J. Am. Chem. Soc.*, 1999, **121**, 4526.

[32] B. M. Bhanage, S. I. Fujita, Y. Ikushima and M. Arai, *Appl. Catal. A: Gen.*, 2001, **219**, 259.

[33] I. W. C. E. Arends and R. A. Sheldon, *Appl. Catal. A: Gen.*, 2001, **212**, 175.

[34] M. Bowker, *The Basic and Application of Heterogeneous Catalysis*, Oxford chemistry primers, Oxford, 1998.

[35] E. E. Stangland, K. B. Stavens, R. P. Andres and W. N. Delgass, *J. Catal.*, 2000, **191**, 332.

[36] C. Sivadinarayana, T. V. Choudhary, L. L. Daemen, J. Eckert and D. W. Goodman, *J. Am. Chem. Soc.*, 2004, **126**, 38.

[37] S. Bhunia, S. Jana, D. Saha, B. Dutta and S. Koner, *Catal. Sci. Technol*., 2014, **4**, 1820.

[38] G. Shul'pin, G. Nizova and Y. Kozlov, *New J. chem.*, 1996, **20**, 1243.

[39] A. E. Shilov and G. B. Shul'pin, *Chem. Rev.*, 1997, **97**, 2879.

[40] D. J. Hucknall, *Chemistry of Hydrocarbon Combustion*, Chapman and Hall Ltd., New York, 1985.

[41] T. Yamada, K. Takahashi, T. Kato, T. Takai, S. Inoki, T. Mukaiyama, *Chem. Lett.,* 1991*,* **20**, 641.

[42] G. A. Russell, *J. Am. Soc.*, 1957, **79**, 3871.

[43] R. A. Sheldon, J. K. Kochi, *Metal-catalysed oxidation of organic compounds*, Academic Press, New York, 1981.

[44] H. Wu, G. Pantaleo, G. Di Carlo, S. Guo, G. Marcì, P. Concepción, A. M. Veneziaa and L. F. Liotta, *Catal. Sci. Technol.*, 2015, **5**, 1888.

[45] W. Zhang, H. L. Tay, S. S. Lim, Y. Wang, Z. Zhong and R. Xu, *Appl. Catal., B*, 2010, **95**, 93.

[46] D. G. Castner, P. R. Watson and I. Y. Chan, *J. Phys. Chem.*, 1990, **94**, 819.

[47] A. Y. Khodakov, A. Griboval-Constant, R. Bechara and F. Villain, *J. Phys. Chem. B*, 2001, **105**, 9805.

[48] D. Shanke, S. Vada, E. A. Blekkan, A. M. Hilmen, A. Hoff and A. Holmen, *J. Catal.*, 1995, **156**, 85.

Chapter 4: Oxidation of 1-decene using supported gold catalysts

4.1. Introduction

Selective oxidation is a key process in chemical technology, especially for the synthesis of chemical intermediates. Using oxygen as a primary oxidant is an attractive concept to reduce waste and create green chemical routes [1, 2]. Many studies have been carried out with the use of supported gold catalysts for the oxidation of alkenes [3-7]. Nevertheless, the aerobic epoxidation of α-alkenes, containing allylic hydrogens, remains a challenge in oxidation catalysis. Earlier investigations by Hutchings and co-workers showed that supported gold nanoparticles are active for the oxidation of a range of alkenes under solvent-free conditions using oxygen as an oxidant and a very small amount of a radical initiator [3, 4, 8]. Furthermore, the same group studied the oxidation of cycloalkenes and showed that as the ring size of a cycloalkene decrease (sizes of C_7 or smaller), allylic oxidation was the dominant reaction pathway [9]. However, with larger ring sizes, an epoxidation reaction pathway was preferred. Hutchings and his group also demonstrated that an initiator was not needed during the oxidation of cyclic and internal linear alkenes after the removal of stabilisers (added to prevent oxidation) [10]. In contrast, the epoxidation of terminal alkenes still required the presence of a radical initiator [10]. In a previous report on the oxidation of 1-decene, 1% Au/graphite prepared by incipient wetness was found to be an effective catalyst [11].

In Chapter 3, supported cobalt catalysts were observed to have good activity for epoxidation of 1-decene under solvent-free conditions. However, the leaching of the active species took place, especially when using MgO as support (Co leached 22%); whereas there was a significant reduction in the leaching (6%) when using TiO_2 as a support. Therefore, it is preferable to use a non-leaching and more stable catalyst. Thus, the focus of this Chapter is on continuing and extending the investigation on the oxidation of 1-decene with the use of more stable and leaching resistant supported gold catalysts prepared by different methods and oxygen from air, or low-pressure molecular oxygen as an oxidant. The identification of background reactions in the absence of the supported gold catalysts will also be discussed. Previously, gold nanoparticles supported on oxides were suggested to be active for the epoxidation of different alkenes [3]. Therefore, three metal oxide supports: namely, TiO_2, SiO_2 and MgO, in addition to graphite, were used in the experiments. Finally, the optimisation of the reaction conditions such as the reaction time and O_2 pressure were examined.

4.2. Results and discussion

4.2.1. Reaction in the absence of catalyst

Initially, a range of blank reactions were carried out (in the absence of a catalyst) for the epoxidation of 1-decene with the use of oxygen from the air as the primary oxidant at atmospheric pressure. AIBN was chosen as the radical initiator for this reaction to continue and extend the previous investigation on 1-decene oxidation using supported gold catalysts [11]. Our group showed earlier that the presence of a radical initiator is essential for the oxidation of linear terminal alkenes (in contrast to internal alkenes) [10, 11]. Chapter 3 showed that without the presence of the catalyst and radical initiator, no reaction was recorded below 100°C, whereas at 110°C, 8% conversion and 23% selectivity for epoxide were observed after a 24 h reaction time. Consequently, all further reactions were performed in the temperature range of 60°C to 90°C. In the presence of AIBN, low conversion of 1-decene was observed over the studied temperature ranges 60-90°C, with a maximum conversion of 6% and an epoxide selectivity of 17% at 90°C (Table 4.1). A reaction temperature of 90°C was chosen for further catalyst screening to continue and extend the previous investigation on 1-decene oxidation [11].

Table 4.1: Effect of temperature on 1-decene epoxidation in the absence of the catalyst

Initiator	T= 60°C		T= 70°C		T= 80°C		T= 90°C	
	Conv.[(a)] (%)	Sel.[(b)] (%)	Conv. (%)	Sel. (%)	Conv. (%)	Sel. (%)	Conv. (%)	Sel. (%)
No initiator	0	0	0	0	0	0	0	0
AIBN	1	1	2	4	3	14	6	17

Reaction conditions: 1-decene (53 mmol, 10 mL), AIBN (0.036 mmol, 6 mg), atmospheric pressure air, reaction time 24 h, rate of stirring 800 rpm. (a) Conv.= Conversion, (b) Sel.= Selectivity for epoxide.

4.2.2. Graphite supported catalysts in epoxidation of 1-decene

4.2.2.1. Effect of the catalyst preparation method

An important factor that can affect the activity of a catalyst is the preparation method [12]. Initial studies on 1-decene epoxidation (90°C, AIBN as a radical initiator, atmospheric pressure of air) showed that 1% Au/graphite (1% Au/G) prepared by incipient wetness is an effective catalyst for this reaction [11]. The following three preparation methods of 1% Au/G were studied: sol-immobilisation, wet-impregnation and incipient wetness (as explained in Sections 2.2.1, 2.2.2 and 2.2.3). The results shown in Figure 4.1 demonstrate that 1% Au/G prepared by the sol-immobilisation method

resulted in the highest epoxide yield (yield obtained by using GC analysis). The conversion and epoxide selectivity were 11% and 28% respectively, which observed higher activity and epoxide selectivity than catalysts prepared using the wet-impregnation and the incipient-wetness methods. These results are in agreement with previous observations on the oxidation of different alkenes. It was found that the preparation of supported gold catalysts using the sol-immobilisation method significantly enhanced catalyst activity in the oxidation of cyclooctene, whereas lower activity was found with wet impregnation and deposition precipitation methods, as mentioned previously in Section 1.6.1 [3, 8-10, 13]. Furthermore, a similar observation was made with the oxidation of 1-hexene with air using supported gold catalysts with a very small amount of TBHP [14]. The sol-immobilisation method gave a higher conversion of 1-hexene and epoxide selectivity comparing to the wet-impregnation and deposition precipitation methods, which displayed similar activity. Moreover, the 1% Au/G catalyst prepared using sol-immobilisation method was observed to show higher 1-octene conversion and epoxide selectivity than that prepared with the other methods under solvent-free conditions [15].

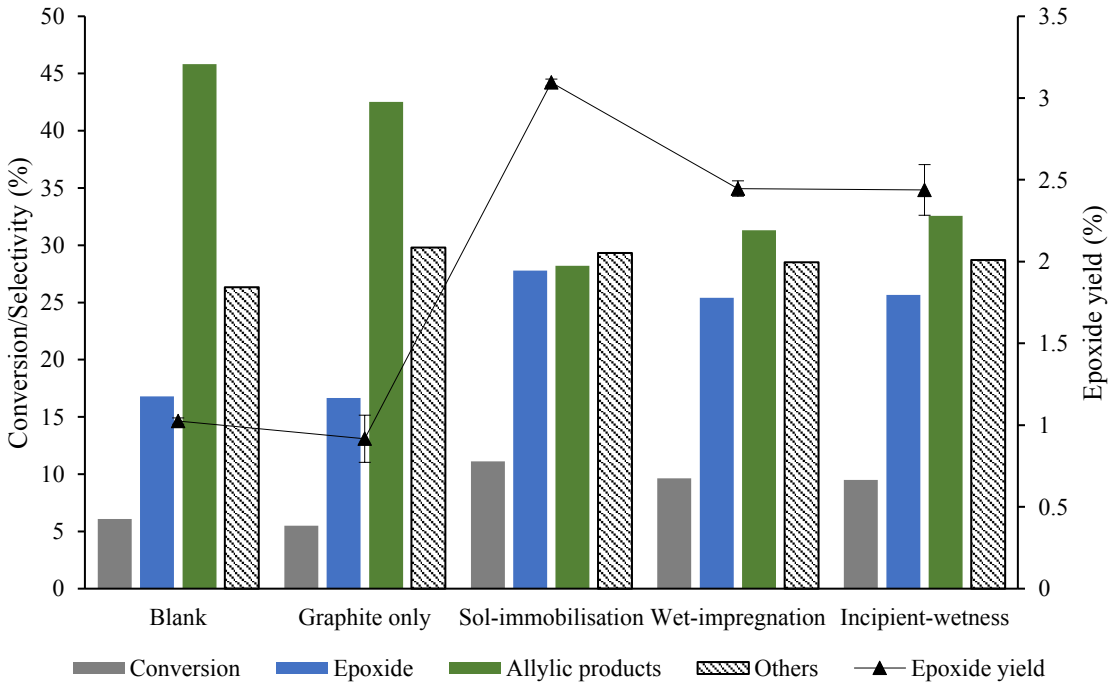

Figure 4.1: Effect of the catalyst preparation method on 1-decene oxidation. Reaction conditions: catalyst (0.1 g), 1-decene (53 mmol, 10 mL), AIBN (0.036 mmol, 6 mg), 90°C, atmospheric pressure air, reaction time 24 h, rate of stirring 800 rpm. Allylic products=∑ (1-decen-3-one, 1-decen-3-ol, 2-decenal, 2-decen-1-ol). Others=∑ (C_7+C_8+C_9 acids, C_8+C_9 aldehyde, C_7+C_8 alcohols, 3-nonen-1-ol, 3-nonanone, cyclododecane, 2-decenoic acid, 1,2-decanediol). Error bars indicate range of data based on three repeat experiments.

In a previous study, the metal particle size prepared by the impregnation method was found to be in the range 10-30 nm [3]. In contrast, much smaller particle sizes (2-3 nm) with a small distribution range (1-10 nm) were reported for catalysts prepared by sol-immobilisation [3]. Therefore, the 1% Au/G catalyst prepared using sol-immobilisation, which is the most active one in this study, has been characterised using TEM and XRD. The TEM data analysis and particle size distribution (PSD) are presented in Figure 4.2. Gold particles can be seen as dark contrasts on the surface of the graphite particles. PSD data has been determined from bright field TEM micrographs and measured diameter of at least 100 particles. For the 1% Au/G catalyst prepared using the sol-immobilisation method, the PSD showed that this catalyst contained much smaller particles, with most particles being 3-4 nm with a small distribution range 1-7 nm in diameter (Figure 4.2). Therefore, a possible explanation for the improved activity of the sol-immobilisation catalyst is the higher dispersion of Au through a smaller particle size.

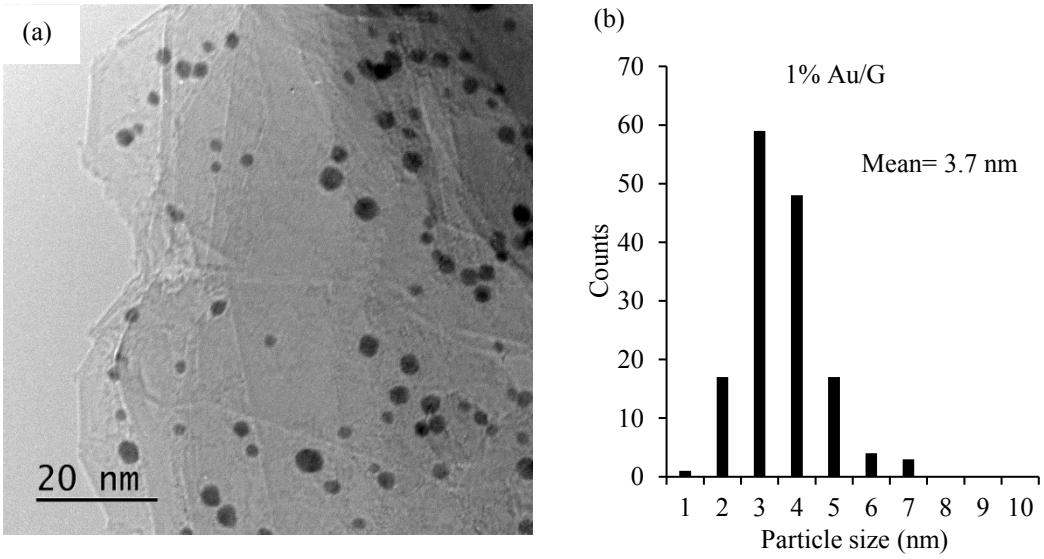

Figure 4.2: (a) TEM and (b) PSD for 1% Au/G prepared by sol-immobilisation method. Counts: number of occurrences of particles of indicated diameter within the sample assessed.

XRD reflections are shown in Figure 4.3 for the graphite and the 1% Au/G catalysts prepared by wet-impregnation and sol-immobilisation. A comparison with pure graphite reveals that most of the reflections come from the support. The main reflections of gold are expected at 38.5 °, 45.2° and 65.2°. The XRD pattern of the graphite and the 1% Au/G catalyst prepared by sol-immobilisation did not show distinguishable differences in their reflections, and no obvious gold peak was found. This result indicates higher dispersion of Au through a smaller particle size, which is in agreement with previous TEM data. In contrast, the presence of crystalline Au was observed for the catalyst prepared by wet-impregnation, and the Au nanoparticles size calculated from XRD is 18 nm, which

is much larger than that produced by the sol-immobilisation method. Therefore, the sol-immobilization method is a suitable technique for preparing 1% Au/G catalyst as it exhibits excellent control over the particle size. Smaller particles are more reactive because of the good dispersion of Au on the support surface; this resulted in generating more active sites, which, in turn, increase the activity and epoxide selectivity.

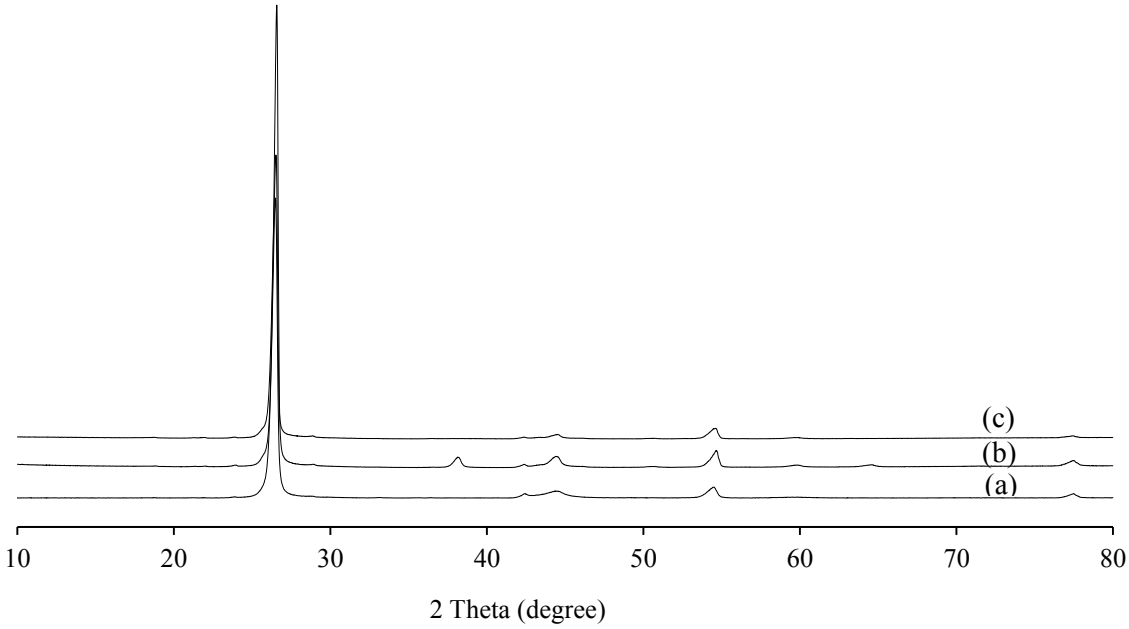

Figure 4.3: XRD diffraction patterns for : (a) graphite (b) 1% Au/G (wet-impregnation) (c) 1% Au/G (sol-immobilisation).

4.2.2.2. Time online study for epoxidation of 1-decene using 1% Au/G

To understand the detailed reaction profile of 1-decene oxidation over the 1% Au/G catalyst prepared using sol-immobilisation method, time online studies were carried out at a temperature of 90°C. The effect of reaction time for the reactivity of 1% Au/G prepared by the sol-immobilisation method was compared with the reactivity of the graphite support and the blank reaction as shown in Figure 4.4. The reaction profile with respect to the 1,2-epoxydecane yield (yield obtained by using GC analysis) was comparable between the blank reaction, the reaction with graphite and with the 1% Au/G catalyst. In all the reactions, an induction period of *ca.* 10 h was observed before the formation of any epoxide. After this induction period, the epoxide yield increased at different rates for the three reactions, with the rate of epoxide formation following the trend of 1% Au/G catalyst > graphite > blank. After the 24 h reaction time, a significant improvement in the epoxide yield (yield obtained by using GC analysis) was observed when the 1% Au/G catalyst was used. The presence of the supported gold catalyst,

therefore, directed the reaction preferentially towards the epoxide with a higher epoxide yield than the uncatalysed reaction.

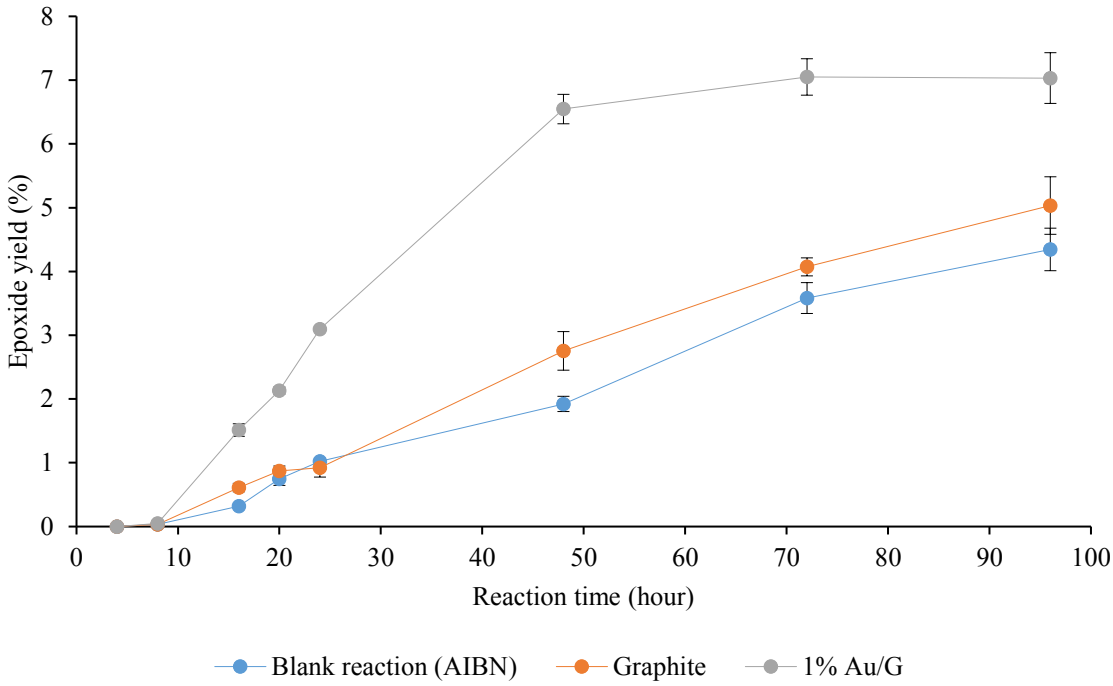

Figure 4.4: Epoxidation of 1-decene: time online study. Reaction conditions: catalyst (0.1 g), 1-decene (53 mmol, 10 mL), AIBN (0.036 mmol, 6 mg), 90°C, atmospheric pressure air, rate of stirring 800 rpm. Error bars indicate range of data based on three repeat experiments.

A better understanding of the evolution of the reaction pathways with respect to the reaction time can be found from the interpretation of 1-decene conversion and the selectivities for specific products. Figure 4.5 shows that with an increasing reaction time, the conversion of 1-decene gradually increased over the reaction time from 1% at 4 h to 33% at 96 h with a shorter induction period. This result may suggest that with longer reaction runs, a greater degree of conversion of 1-decene should be observed. Furthermore, the selectivity data shows that allylic products, such as 1-decen-3-one, 1-decen-3-ol, 2-decenal and 2-decen-1-ol, were the predominant products at the beginning of the reaction, and a lower selectivity for the epoxide was detected. Epoxide selectivity steadily increased with increasing the reaction time to be the maximum at 48 h. After 48 h, the selectivity for the epoxide was found to drop to a value of 9% after 96 h. furthermore, the selectivity for the diol increases with increasing the reaction time. This perhaps is the result of the opening of the epoxide ring, as discussed in Chapter 3. A similar observation was found with different terminal alkenes (1-hexene, 1-octene, 1-decene) [11, 14, 15], as the reaction time increased, there was an increase in the alkene conversion and epoxide selectivity.

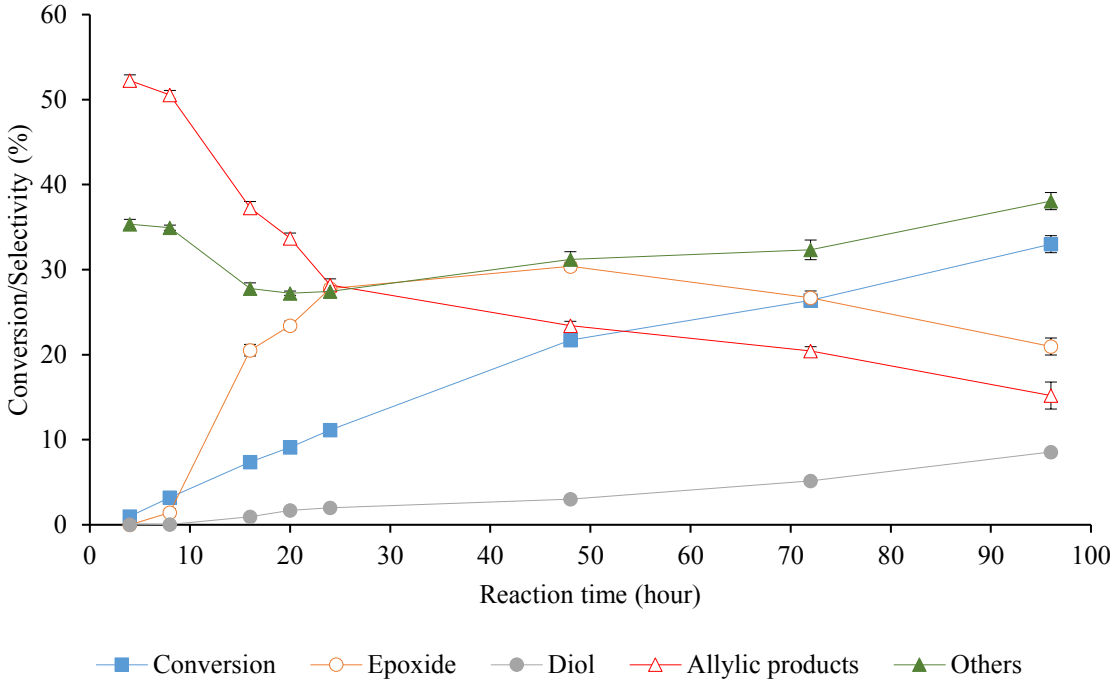

Figure 4.5: Effect of reaction time on conversion and selectivity. Reaction conditions: 1% Au/G (0.1 g), 1-decene (53 mmol, 10 mL), AIBN (0.036 mmol, 6 mg), 90°C, atmospheric pressure air, rate of stirring 800 rpm. Allylic products=∑ (1-decen-3-one, 1-decen-3-ol, 2-decenal, 2-decen-1-ol). Others=∑ (C_7+C_8+C_9 acids, C_8+C_9 aldehyde, C_7+C_8 alcohols, 3-nonen-1-ol, 3-nonanone, cyclododecane, 2-decenoic acid). Error bars indicate range of data based on three repeat experiments.

Table 4.2 shows the detailed selectivity profile for all the products for this catalysed reaction. Under these conditions, the selectivity for 1,2-epoxydecane was *ca.* 28% whereas the total selectivity for the products of C_{10} oxidation was more than 33%, which amounts to over 60% of the total products produced. Furthermore, C-C cleavage reactions occurred, forming different C_7+C_8+C_9 products. These results are in agreement with previous studies for oxidation of terminal alkenes where different allylic products were produced and C-C cleavage reactions occurred [11, 14, 15].

Table 4.2: Full list of products observed and quantified in the epoxidation of 1-decene using 1% Au/G

Conversion (%)	11
Product	**Selectivity (%)**
1,2-Epoxydecane	28
1-Decen-3-one	5.8
1-Decen-3-ol	7.3
2-Decenal	7.2
2-Decen-1-ol	8
1,2-Decanediol	2
2-Decenoic acid	2.3
Octanal	1.8
Nonanal	3.8
1-Heptanol	1.4
1-Octanol	1.1
Heptanoic acid	1.4
Octanoic acid	3.8
Nonanoic acid	8.5
3-Nonen-1-ol	1
3-Nonanone	2.5
Cyclododecane	1.2
Unknown products	10

Reaction conditions: 1% Au/G (0.1 g), 1-decene (53 mmol, 10 mL), AIBN (0.036 mmol, 6 mg), 90°C, atmospheric pressure air, reaction time 24 h, rate of stirring 800 rpm.

4.2.2.3. Effect of O_2 pressure

The previously mentioned reactions were carried out under atmospheric pressure of air. In the current study, we examined the effect of the O_2 pressure on the epoxidation of 1-decene by using 1% Au/G (sol-immobilisation). The conversion of 1-decene was found to increase when increasing the O_2 pressure from 3% at 0.2 bar to 24% at 15 bar of O_2 as shown in Figure 4.6. This increase in the conversion appears to be linear with the O_2 pressure. However, no significant change in 1,2-epoxydecane selectivity was observed with an increase in the O_2 pressure as shown in Figure 4.6. Furthermore, a slight decrease was found in the selectivity for the allylic products during the increase in the O_2 pressure from 5 to 10 bar, whereas some increases in the selectivity of C_8 and C_9 products were detected with increase the O_2 pressure. Similar observations were made for the epoxidation of different alkenes (styrene, cyclohexene, cyclooctene) using different catalysts [16, 17]. It was found that as the oxygen pressure increased, the conversion increased without any change in the epoxide selectivity [16, 17]. Therefore, the major effect of an increase in oxygen pressure is an increase in the 1-decene conversion to reach 24%, which is much higher than the conversion under the atmospheric pressure of air (11%).

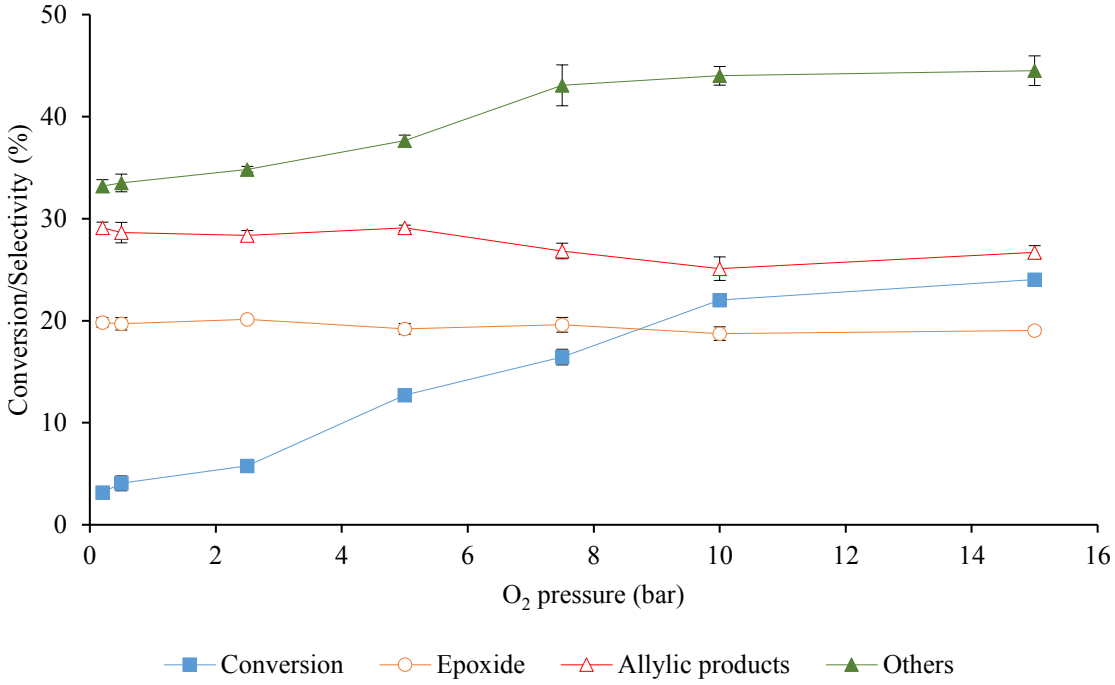

Figure 4.6: Effect of O_2 pressure of epoxidation of 1-decene using 1% Au/G. Reaction conditions: 1% Au/G (0.1 g), 1-decene (53 mmol, 10 mL), AIBN (0.036 mmol, 6 mg), 90°C, reaction time 24 h, rate of stirring 800 rpm. Allylic products=∑ (1-decen-3-one, 1-decen-3-ol, 2-decenal, 2-decen-1-ol). Others=∑ (C_7+C_8+C_9 acids, C_8+C_9 aldehyde, C_7+C_8 alcohols, 3-nonen-1-ol, 3-nonanone, cyclododecane, 2-decenoic acid, 1,2-decanediol). Error bars indicate range of data based on three repeat experiments.

To understand the role of increase in the O_2 pressure and the reaction profile, time online studies were carried for epoxidation of 1-decene under 15 bar of O_2 using 1% Au/G. Similar to the results obtained under the atmospheric pressure of air, with increasing reaction time, the conversion of 1-decene significantly increases from 4% at 4 h to 24% at 24 h. In addition to that, allylic products such as 1-decen-3-one, 1-decen-3-ol, 2-decenal, 2-decen-1-ol are the predominant products at the beginning of the reaction. A further increase in the reaction time resulted in a drop in the selectivity for these products, accompanied with an increase in the epoxide selectivity for a maximum of 19% after 24 h of reaction, as shown in Figure 4.7.

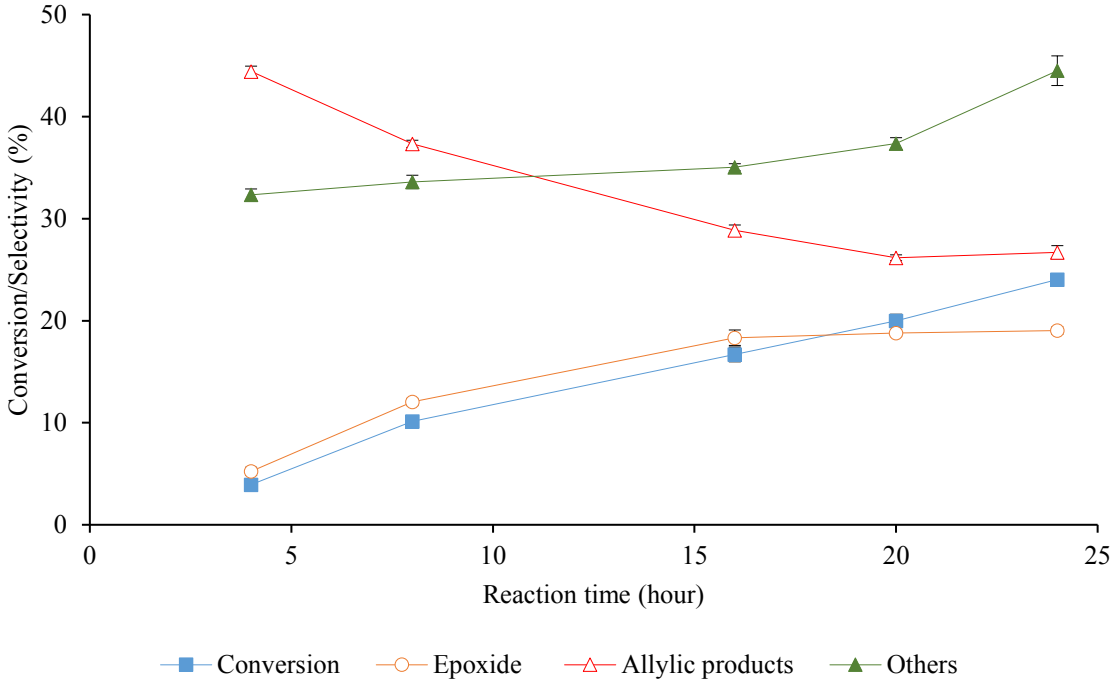

Figure 4.7: Time online study for epoxidation of 1-decene using 1% Au/G under O_2 pressure. Reaction conditions: 1% Au/G (0.1 g), 1-decene (53 mmol, 10 mL), AIBN (0.036 mmol, 6 mg), 90°C, 15 bar O_2, rate of stirring 800 rpm. Allylic products=∑ (1-decen-3-one, 1-decen-3-ol, 2-decenal, 2-decen-1-ol). Others=∑ (C_7+C_8+C_9 acids, C_8+C_9 aldehyde, C_7+C_8 alcohols, 3-nonen-1-ol, 3-nonanone, cyclododecane, 2-decenoic acid, 1,2-decanediol).

The epoxide selectivity was higher when the reaction was carried out under atmospheric pressure of air in the glass reactor. Therefore, further investigation was performed under atmospheric pressure of air.

4.2.3. Metal oxides as supports in the epoxidation of 1-decene

Supports are well known to play an important role in catalyst activity [8, 18]. Metal oxides are widely used as supports in heterogeneous catalysts because they highly influence catalysts activity [19]. The properties of these supports have been reported to play a predominant role in the adsorption of gold nanoparticles [19, 20, 21], which, in turn, influences catalytic activity. As metal oxides have shown good activity for alkene epoxidation [8, 22-27], three different metal oxides have been investigated for 1-decene oxidation. These supports have been classified into reducible (TiO_2) and non-reducible supports (SiO_2, MgO).

From the nitrogen physisorption analysis, the surface area of different supported gold catalysts is listed in Table 4.3. A reduction in the surface area of the 1% Au/support catalysts was observed compared with the undoped supports, which may indicate the incorporation of Au in the support pores. The analysis was carried out twice and error in the analysis was no more than 1 m^2 g^{-1}.

Table 4.3: Nitrogen physisorption analysis of the surface area using BET method of different supports and supported gold catalysts

Catalyst	Surface area $m^2 g^{-1}$
Graphite	9
1% Au/G	8
SiO_2	989
1% Au/SiO_2	970
MgO	55
1% Au/MgO	49
TiO_2	51
1% Au/TiO_2	47

From Figure 4.8 it can be seen that the XRD patterns of the TiO_2 and the 1% Au/TiO_2 did not display enough distinguishable differences in their reflections. This is due to the overlapping between TiO_2 phases and the Au reflections.

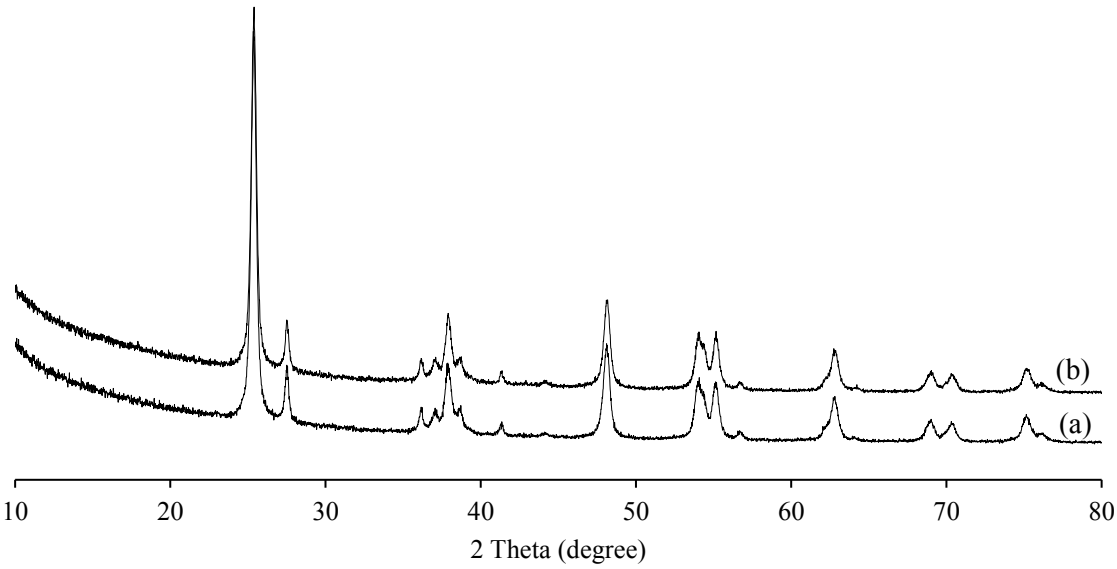

Figure 4.8: X-ray diffraction patterns for: (a) TiO_2 and (b) 1% Au/TiO_2.

The XRD patterns are shown in Figure 4.9 for the SiO_2 and the 1% Au/SiO_2. A broad reflection peak of Au at 38.5° was observed. Small Au particles with a range of 2-8 nm produced broader reflection peak.

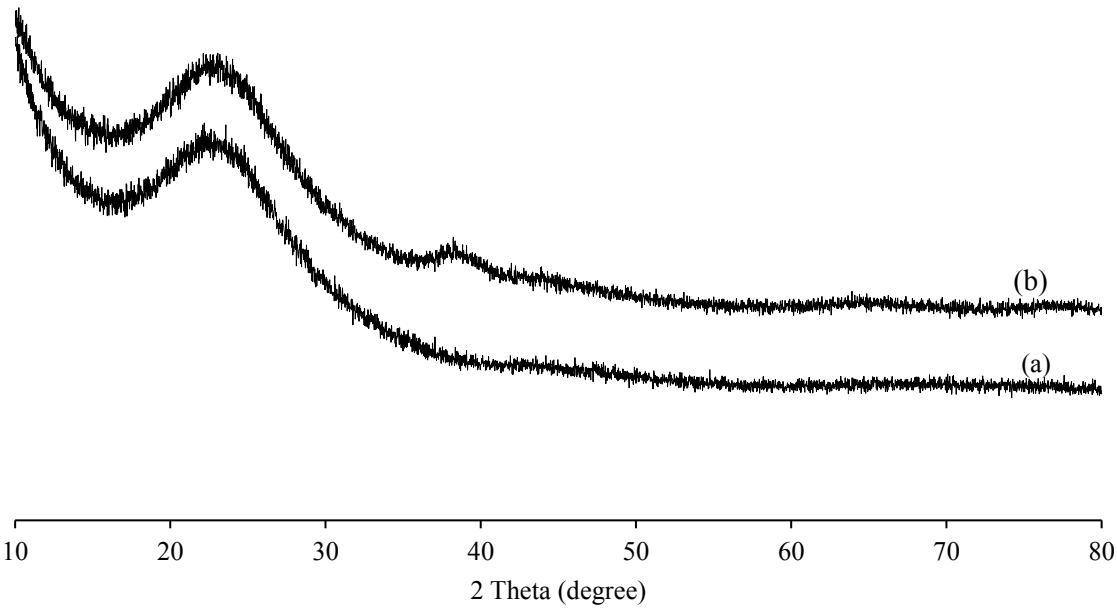

Figure 4.9: X-ray diffraction patterns for: (a) SiO_2 and (b) 1% Au/SiO_2.

Table 4.4 shows that the supports alone showed limited activity in the absence of gold. Some activity was observed when TiO_2 was used compared with the other supports. This observation may be due to the ability of TiO_2 to adsorb oxygen [28]. The addition of gold to the supports, using the three methodologies (wet-impregnation, deposition precipitation and sol-immobilisation), resulted in an increase in activity and selectivity for 1,2-epoxydecane in all cases. The supported gold catalysts prepared by the sol-immobilisation method exhibited the highest activity for each of the metal oxide supports. This result could be attributed to the formation of small Au particles, as the sol-immobilisation method leads to the formation of such particles. The SiO_2 and TiO_2 supported gold catalysts showed higher activity and epoxide selectivity than that of the MgO and graphite supported catalysts. This observation is in agreement with that of previous studies on propene epoxidation with 1% Au/TiO_2. It was suggested that a peroxide species is produced by gold and then epoxidised propene over titania sites [22-27]. Furthermore, TiO_2 can diffuse onto the metal, which can enhance catalytic activity [29]. The shape of the gold particles appears to be affected by the interaction with the support material during the adsorption of the gold colloids on the support surface in the sol-immobilisation method. It has been suggested that various geometries of the gold

particles can occur on each of the support, giving rise to different faceting and creation of defect sites, which would influence the catalytic properties of the supported gold particles [30]. Therefore, the choice of support affected the activity of gold catalysts and epoxide selectivity, providing clear evidence that the chemical nature of the support is important.

Table 4.4: Epoxidation of 1-decene using 1% Au/support prepared by different methods

Catalyst	Preparation method	Conversion (%)	Selectivity (%)			
			Epoxide	Allylic products	Diol	Others
Blank	-	6	17	45	1	25
SiO_2	-	5	25	38	1	22
1% Au/SiO_2	Wet-impregnation	8	25	33	2	30
	Dep-precipitation [a]	11	26	30	3	35
	Sol-immobilisation	13	34	28	1	27
TiO_2	-	9	27	33	1	25
1% Au/TiO_2	Wet-impregnation	11	27	32	2	30
	Sol-immobilisation	13	34	30	2	24
	Dep-precipitation [a]	11	28	33	2	30
MgO	-	5	18	35	1	26
1% Au/MgO	Wet-impregnation	8	24	32	1	33
	Sol-immobilisation	12	27	30	2	31
G	-	6	17	42	1	28
1% Au/G	Incipient-wetness	9.5	25.6	33	2	27
	Wet-impregnation	9.6	25.4	31	1	27
	Sol-immobilisation	11	28	28.3	2	27

Reaction conditions: Catalyst (0.1 g), 1-decene (53 mmol, 10 mL), AIBN (0.036 mmol, 6 mg), 90°C, atmospheric pressure air, reaction time 24 h, rate of stirring 800 rpm. Allylic products=∑ (1-decen-3-one, 1-decen-3-ol, 2-decenal, 2-decen-1-ol). Others=∑ (C_7+C_8+C_9 acids, C_8+C_9 aldehyde, C_7+C_8 alcohols, 3-nonen-1-ol, 3-nonanone, cyclododecane, 2-decenoic acid). (a): Deposition-precipitation.

TEM analysis for supported gold catalysts was performed and the images are presented in Figure 4.10 and the PSD in Figure 4.11. Similar to 1% Au/G, the sol-immobilisation method produced a small particle size of the supported gold catalysts. The size distribution of the Au particles for 1% Au/TiO_2, 1% Au/SiO_2, 1% Au/MgO and 1% Au/G, determined from bright field TEM micrographs are shown in Figure 4.11. Our group previously found the similarity of PSDs for the deposition-precipitation and impregnation methods, with most Au nanoparticles to be in the 10-30 nm size range [3]. In contrast, in this work, the 1% Au/support catalysts prepared using the sol-immobilisation method showed much smaller particles, with most particles being 3-5 nm in diameter (Figure 4.11). Interestingly, this result is in agreement with the activities of the 1% Au/support catalysts shown in Table 4.4, which confirms that the catalysts prepared using the sol-immobilisation method produced a much smaller Au particle size, which resulted in the higher activity of the catalysts. Smaller particles are more reactive because of the good dispersion of Au on the support surface; this results in generating more active sites, which, in turn, increases the activity.

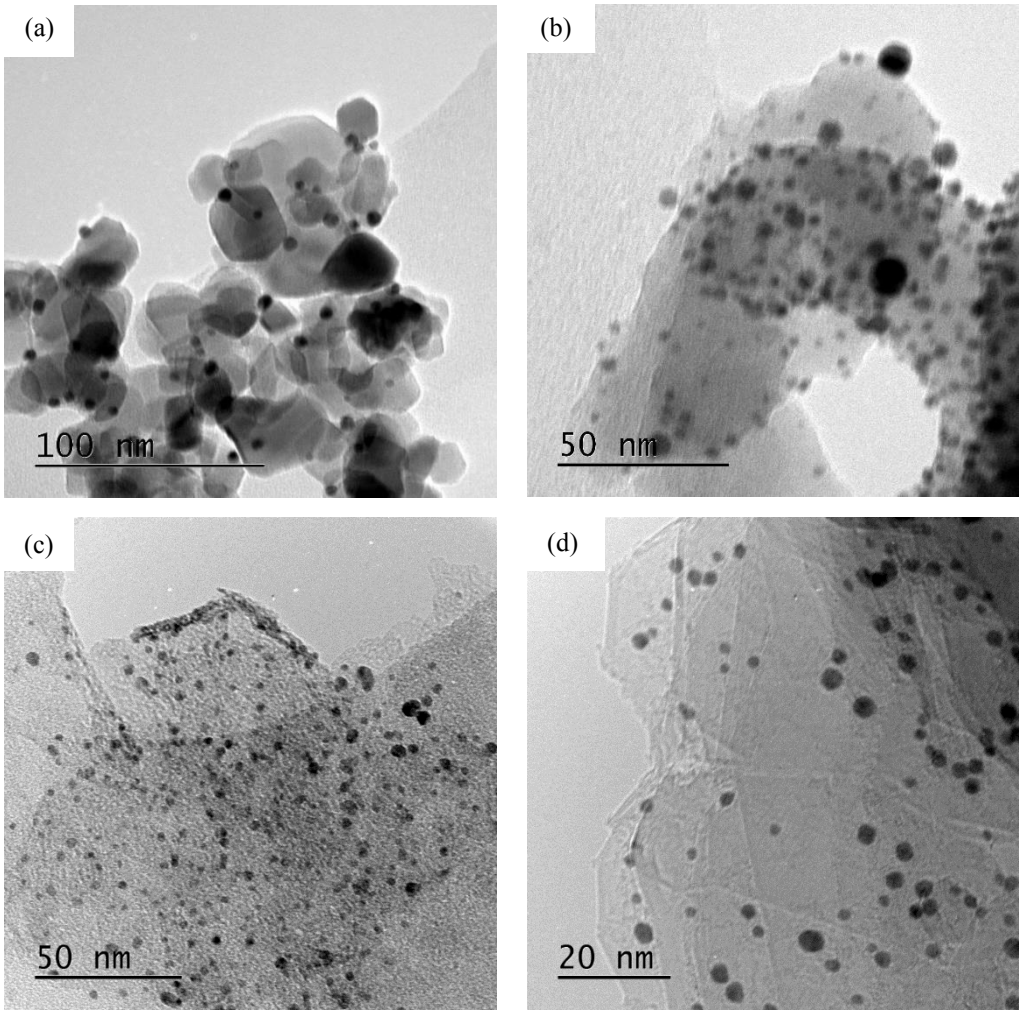

Figure 4.10: TEM for (a) 1% Au/TiO_2 (b) 1% Au/SiO_2 (c) 1% Au/MgO (d) 1% Au/G. Catalysts prepared using sol-immobilisation method.

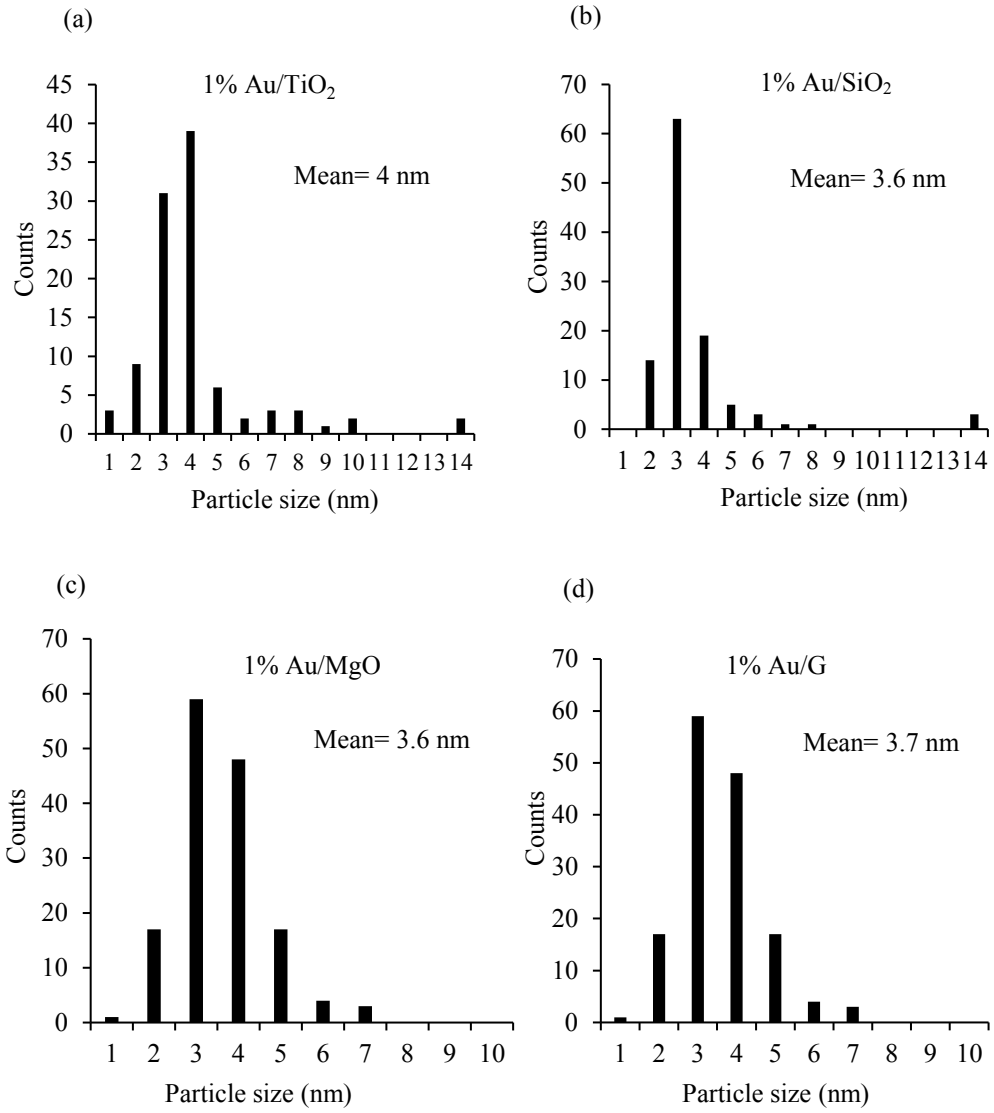

Figure 4.11: PSD for: (a) 1% Au/TiO_2 (b) 1% Au/SiO_2 (c) 1% Au/MgO (d) 1% Au/G. Catalysts prepared using sol-immobilisation method.

4.2.4. Effect of the catalyst mass of the 1% Au/TiO_2

Further we studied the effect of catalyst mass on epoxidation of 1-decene using 1% Au/TiO_2. The amount of 1% Au/TiO_2 varied in the range 0.05-0.2 g. Table 4.5 shows that the conversion of 1-decene increased from 8% to 16% with increasing catalyst mass from 0.05 g to 0.2 g, the selectivity for the epoxide also increased from 22% to 36% respectively. In contrast, the selectivity for allylic products decreased with increasing catalyst mass, which indicates the importance of the Au surface for directing the selectivity toward 1,2-epoxydecane. When doubling the catalyst mass from 0.05 to 0.1 g, the conversion increased from 8% to 13% respectively. However, increasing the mass from 0.1 to 0.2 g resulted in only a 3% increase in the conversion, which may indicate the mass transport limitation in this range. Therefore, 0.1 g (0.0094 mmol%, amount of Au in relation to the 1-decene amount) is the desired amount of 1% Au/TiO_2 catalyst for the epoxidation of 1-decene under these conditions.

Table 4.5: Effect of the catalyst mass of the 1% Au/TiO_2 on 1-decene oxidation

Catalyst	Conversion (%)	Epoxide selectivity (%)	Allylic products selectivity (%)	Others selectivity (%)
None (blank)	6	17	42	27
0.05 g	8	22	36	28
0.1 g	13	34	30	26
0.15 g	14	35	22	28
0.2 g	16	36	21	27

Reaction conditions: 1-decene (53 mmol, 10 mL), AIBN (0.036 mmol, 6 mg), 90°C, atmospheric pressure air, reaction time 24 h, rate of stirring 800 rpm. Allylic products=∑ (1-decen-3-one, 1-decen-3-ol, 2-decenal, 2-decen-1-ol). Others=∑ (C_7+C_8+C_9 acids, C_8+C_9 aldehyde, C_7+C_8 alcohols, 3-nonen-1-ol, 3-nonanone, cyclododecane, 2-decenoic acid, 1,2-decanediol).

4.2.5. Evidence of radical initiated 1-decene oxidation

In the absence of AIBN, the epoxidation of 1-decene did not occur even in the presence of the 1% Au/TiO_2 where the conversion was only 1% and no epoxide was produced. In the presence of AIBN only, low conversion and selectivity for the epoxide was detected. However, when 1% Au/TiO_2 catalyst was present with AIBN, significant improvement in the catalytic activity was seen in the epoxidation of 1-decene. A radical scavenger was used in this study in order to establish the role of the small amount of AIBN for the oxygen activation in the presence of 1% Au/TiO_2. Therefore, addition of the radical scavenger 2,6-di-*tert*-butyl-4-methylphenol (BHT) resulted in interaction with radicals and terminated the propagation of the radical mechanism (Table 4.6), which shows that radical chemistry is involved in the reaction. Therefore, oxygen from air seems to be activated via free-radical species. Another diagnostic experiment that indicated the involvement of oxygen in this reaction involved carrying out the reaction under N_2 atmosphere instead of air. It was observed that no epoxide was detected, which indicates that molecular oxygen from the air is involved in the oxidation route. Similar observations were detected previously when using oxygen from air as the primary oxidant [11, 14]. This demonstrates that the addition of radical scavenger resulted in inhibiting the oxidation of alkenes (1-decene, 1-hexene) [11, 14].

Table 4.6: Effect of radical scavenger on epoxidation of 1-decene

Catalyst	Radical initiator	Radical scavenger	Conversion (%)	Epoxide selectivity (%)
1% Au/TiO_2	-	-	1	0
-	AIBN	-	6	17
1% Au/TiO_2	AIBN	-	13	34
1% Au/TiO_2	AIBN	BHT	Trace	0
1% Au/TiO_2 under N_2	AIBN	-	1	0

Reaction conditions: 1% Au/TiO_2 (0.1 g), 1-decene (53 mmol, 10 mL), AIBN (0.036 mmol, 6 mg), BHT (0.036 mmol, 7.93 mg), 90°C, atmospheric pressure air, reaction time 24 h, rate of stirring 800 rpm.

Table 4.7 shows the detailed selectivity profile for all the products for this catalysed reaction. Similar observations to what was found with 1% Au/G. The selectivity for 1,2-epoxydecane is *ca.* 34% whereas the total selectivity for the products of C_{10} oxidation is more than 30%. Furthermore, C-C cleavage reactions occurred, forming different C_7+C_8+C_9 products.

Table 4.7: Products observed for the epoxidation of 1-decene using 1% Au/TiO_2

Conversion (%)	13
Product	**Selectivity (%)**
1,2-Epoxydecane	34
1-Decen-3-one	6
1-Decen-3-ol	7
2-Decenal	7.5
2-Decen-1-ol	9.5
1,2-Decanediol	2
2-Decenoic acid	2
Octanal	1.3
Nonanal	1.7
1-Heptanol	1.2
1-Octanol	1.9
Heptanoic acid	1.6
Octanoic acid	3.3
Nonanoic acid	7.3
3-Nonen-1-ol	1
3-Nonanone	2.7
Cyclododecane	1.5
Unknown products	7.7

Reaction conditions: 1% Au/TiO_2 (0.1 g), 1-decene (53 mmol, 10 mL), AIBN (0.036 mmol, 6 mg), 90°C, atmospheric pressure air, reaction time 24 h, rate of stirring 800 rpm.

4.2.6. Reusability and stability of supported gold catalysts

One of the key advantages of heterogeneous catalysts is their ability to be readily recovered by filtration for re-use. Therefore, 1% Au/TiO_2 prepared by sol-immobilisation was investigated. The 1-decene epoxidation reaction was carried out under standard conditions for 24 h, followed by recovery of the catalyst by filtration; washing the catalyst with acetone, and then drying it before it was re-introduced to the reactor for the second test. The epoxidation of 1-decene over fresh and reused 1% Au/TiO_2 catalysts is summarised in Table 4.8.

As mentioned previously, the fresh 1% Au/TiO_2 was found to have 13% conversion with an epoxide selectivity of 34%. The activity of the reused 1% Au/TiO_2, which was oven dried without the washing step, had a much lower conversion of only 4% over 24 h. This may be due to the adsorbed materials resulting in the deactivation of the catalyst. When the reused catalyst was washed with acetone, it was found to be more active than the dry one, providing evidence of products inhibition. However, epoxide selectivity was noted to be reduced for all the reused catalysts.

Table 4.8: Catalyst reusability study for epoxidation of 1-decene: 1% Au/TiO_2

Washing conditions	Conversion (%)	Epoxide selectivity (%)
Fresh catalyst	13	34
Reused, without washing, dried static air, 110°C, 16 h	4	20
Reused, washed with acetone (1 L), dried static air, 110°C, 16 h	10	24

Reaction conditions: 1% Au/TiO_2 (0.1 g), 1-decene (53 mmol, 10 mL), AIBN (0.036 mmol, 6 mg), 90°C, atmospheric pressure air, reaction time 24 h, rate of stirring 800 rpm.

TEM analysis of the reused 1% Au/TiO_2 catalyst was conducted to compare between the fresh and reused catalysts. The PSDs showed that the fresh 1% Au/TiO_2 catalyst contained smaller particles, with most particles being 2-5 nm. In contrast, the reused 1% Au/TiO_2 catalyst showed some large particles in the range of (2-17 nm), which may also have resulted in reducing the activity of the reused catalyst, as shown in Figure 4.12. The increase in the particle size may indicate sintering and growth of the Au nanoparticles, probably resulting from disruption of the protective ligand shell (PVA) during drying the catalyst. PVA was added during preparing of the catalyst to protect the nanoparticles, as mentioned previously in Section 2.2.1.

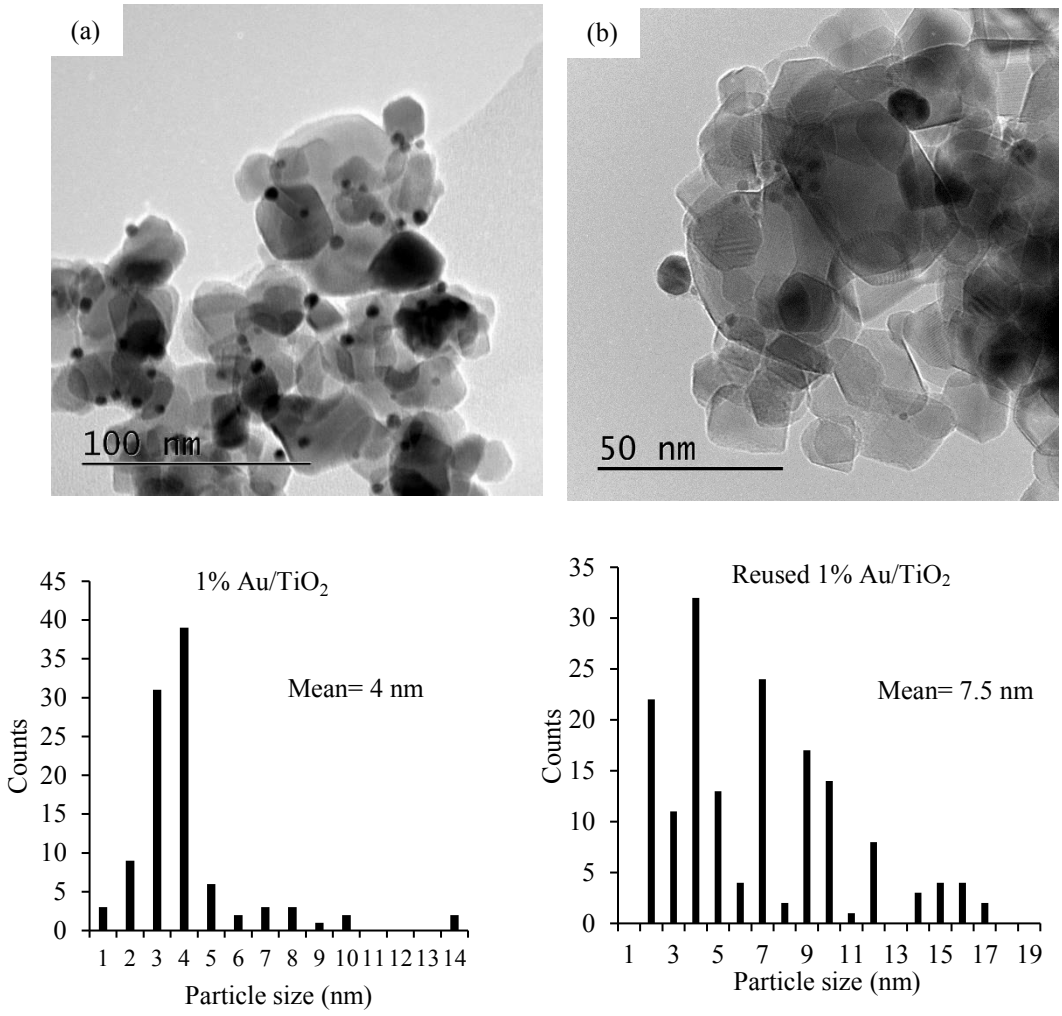

e 4.12: TEM for: (a) fresh 1% Au/Ti[illegible], reused 1% Au/TiO₂ and PSD for: (c) fresh 1% Au/TiO₂ (d) reused 1% Au/TiO₂ prepared by sol-immobilisation method.

4.3. Conclusions

1-Decene epoxidation was performed over supported gold catalysts in the presence of a small amount of radical initiator (AIBN, 6 mg) under mild, solvent-free conditions using oxygen as the oxidant. In the absence of the radical initiator, no oxidation reaction was observed. The optimal reaction temperature range is 60-90°C (as mentioned in Table 4.1), as above 100°C the reaction proceeded spontaneously without the addition of AIBN or the catalyst. Various preparation methods of the gold catalyst were attempted; sol-immobilisation is the optimum procedure for preparation of the active supported gold catalysts for epoxidation of 1-decene and the particle size distribution for these catalysts showed much smaller particles, with most particles being 3-5 nm in diameter. When increasing the reaction time, the conversion of 1-decene increased. In addition to that, it can be seen that allylic products were the predominant products at the initial stage of the reaction. A further increase in the reaction time resulted in a drop of selectivity for these

products, accompanied by a slight increase in the epoxide selectivity. A further increase in the reaction time (over 48 h) resulted in a steady decrease in the epoxide selectivity and an increase in the diol selectivity, which is believed to be a result of the epoxide ring opening resulting in the diol formation (as shown in Figure 4.5). When epoxidation of 1-decene was performed under O_2 pressure, it was found that as the O_2 pressure increased, conversion of 1-decene was observed to increase correspondingly, but no effect was detected on 1,2-epoxydecane selectivity (as explained in Figure 4.6). Gold nanoparticles were supported on graphite, TiO_2, SiO_2 and MgO; TiO_2 and SiO_2 showed the highest activity. Reactions with a radical scavenger have confirmed that a very small amount of radical initiator (AIBN, 6 mg) was necessary to initiate epoxidation of 1-decene (as illustrated in Table 4.6). No epoxide was detected when carrying out the reaction under N_2 atmosphere, which indicates that molecular oxygen from the air was involved in the oxidation route. Increasing the 1% Au/TiO_2 catalyst mass resulted in increasing the conversion and epoxide selectivity. 0.1 g was the desired amount of 1% Au/TiO_2 catalyst for epoxidation of 1-decene under these conditions (as mentioned in Table 4.5). Supported gold catalysts are a promising catalyst for 1-decene oxidation, with the addition of a very small amount of AIBN.

4.4. References

[1] R. A. Sheldon, *Stud. Surf. Sci. Catal*., 1991, **66**, 573.

[2] P. Gallezot, *Catal. Today*, 1997, **37**, 405.

[3] S. Bawaked, N. F. Dummer, N. Dimitratos, D. Bethell, Q. He, C. J. Kiely and G. J. Hutchings, *Green Chem*., 2009, **11**, 1037.

[4] M. D. Hughes, Y.-J. Xu, P. Jenkins, P. McMorn, P. Landon, D. I. Enache, A. F. Carley, G. A. Attard, G. J. Hutchings, F. King, E. H. Stitt, P. Johnston, K. Griffin and C. J. Kiely, *Nature*, 2005, **437**, 1132.

[5] T. Hayashi, K. Tanaka and M. Haruta, *J. Catal*., 1998, **178**, 566.

[6] M. Haruta and M. Daté, *Appl. Catal. A: Gen*., 2001, **222**, 427.

[7] G. Mul, A. Zwijnenburg, B. Linden, M. Makkee and J. A. Moulijn, *J. Catal*., 2001, **201**, 128.

[8] S. Bawaked, N. F. Dummer, D. Bethell, D. W. Knight and G. J. Hutchings, *Green Chem*., 2011, **13**, 127.

[9] H. Alshammari, P. J. Miedziak, D. W. Knight, D. J. Willock and G. J. Hutchings, *Catal. Sci. Technol*., 2013, **3**, 1531.

[10] H. Alshammari, P. J. Miedziak, T. E. Davies, D. J. Willock, D. W. Knight and G. J. Hutchings, *Catal. Sci. Technol*., 2014, **4**, 908.

[11] U. N. Gupta, N. F. Dummer, S. Pattisson, R. L. Jenkins, D. W. Knight, D. Bethell and G. J. Hutchings, *Catal. Lett*., 2015, **145**, 689.

[12] P. Miedziak, M. Sankar, N. Dimitratos, J. A. Lopez-Sanchez, A. F. Carley, D. W. Knight, S. H. Taylor, C. J. Kiely and G. J. Hutchings, *Catal. Today*, 2011, **164**, 315.

[13] J. A. Lopez-Sanchez, N. Dimitratos, P. Miedziak, E. Ntainjua, J. K. Edwards, D. Morgan, A. F. Carley, R. Tiruvalam, C. J. Kiely and G. J. Hutchings, *Phys. Chem. Chem. Phys*., 2008, **10**, 1921.

[14] H. Alshammari, P. J. Miedziak, S. Bawaked, D. W. Knight and G. J. Hutchings, *Chem. Cat. Chem*., 2012, **4**, 1565.

[15] H. Alshammari, *Reac. Kinet. Mech. Cat*., 2016, **119**, 149.

[16] K. M. Jinka, J. Sebastian and R. V. Jasra, *J. Mol. Catal. A: Chem*., 2007, **274**, 33.

[17] Q. Tang, Q. Zhang, H. Wu and Y. Wang, *J. Catal*., 2005, **230**, 384.

[18] A. Wolf and F. Schüth, *Appl. Catal. A: Gen.*, 2002, **226**, 1.

[19] M. Comotti, W. Li, B. Spliethoff and F. Schüth, *J. Am. Chem. Soc*., 2006. **128**, 917.

[20] N. S. Patil, B. S. Uphade, D. G. McCulloh, S. K. Bhargava and V. R. Choudhary, *Catal. Commun*., 2004, **5**, 681.

[21] C. D. Evans, S. A. Kondrat, P. J. Smith, T. D. Manning, P. J. Miedziak, G. L. Brett, R. D. Armstrong, J. K. Bartley, S. H. Taylor, M. J. Rosseinsky, and G. J. Hutchings, *Faraday Discuss*., 2016, **188**, 427.

[22] T. A. Nijhuis, T. Visser and B. M. Weckhuysen, *J. Phys. Chem. B*, 2005, **109**, 19309.

[23] B. S. Uphade, S. Tsubota, T. Hayashi and M. Haruta, *Chem. Lett*., 1998, **27**, 1277.

[24] T. A. Nijhuis, T. Q. Gardner and B. M. Weckhuysen, *J. Catal*., 2005, **236**, 153.

[25] N. Yap, R. P. Andres and W. N. Delgass, *J. Catal*., 2004. **226**, 156.

[26] C. Qi, T. Akita, M. Okumura, K. Kuraoka and M. Haruta, *Appl.Catal. A*, 2003, **253**, 75.

[27] B. Taylor, J. Lauterbach and W. N. Delgass, *Appl. Catal. A*, 2005, **291**, 188.

[28] P. Lignier, F. Morfin, L. Piccolo, J.-L. Rousset and V. Caps, *Catal. Today*, 2007, **122**, 284.

[29] M. Bowker, *The Basic and Application of Heterogeneous Catalysis*, Oxford University Press, Oxford, 1998.

[30] M. S. Chen, and D. W. Goodman, *Catal. Today*, 2006, **111**, 22.

Chapter 5: Synthesis of cyclic carbonates

5.1. Introduction

The main sources of anthropogenic CO_2 emissions are from the use of fossil fuels such as natural gas, oil and coal. These emissions lead to an increase in the concentration of carbon dioxide in the atmosphere. Carbon dioxide utilisation technology can contribute to reducing the CO_2 level by using carbon dioxide as a starting material and transforming it into valuable chemicals such as cyclic carbonates [1]. There is a wide range of applications of cyclic carbonates; they are extensively used as intermediates in the synthesis of pharmaceuticals, raw materials for engineering plastics, aprotic polar solvents and electrolytes for lithium-ion batteries [2-6]. The use of cyclic carbonates (CCs) is one of the most effective routes for carbon dioxide fixation. Cyclic carbonates are usually prepared *via* the cycloaddition of carbon dioxide with epoxides to form a five-membered ring [3,7-11]. In the production of cyclic carbonate, carbon dioxide is a C1 building block with 100% atom economy and thus, a better alternative to toxic and hazardous reagents such as phosgene [12]. Different catalysts were reported for this transformation such as quaternary ammonium salts [7-10], phthalocyanine and salen complexes [13-15], ionic liquids [16-18], metal oxides [19-22] and immobilised catalysts [23-27].

To realise cyclic carbonate production on a large scale, epoxides themselves will have to be synthesised by the oxidation of alkenes [28]. The direct synthesis of cyclic carbonates from low-price olefins, avoiding additional work-up procedures, would be an interesting and economically feasible route. The oxidative carboxylation process (Scheme 5.1 b) consists of a combination of two sequential reactions: first epoxidation of the olefin, and then the cycloaddition reaction of CO_2 with formed epoxide in an one-pot reaction to produce cyclic carbonate (Scheme 5.1 a).

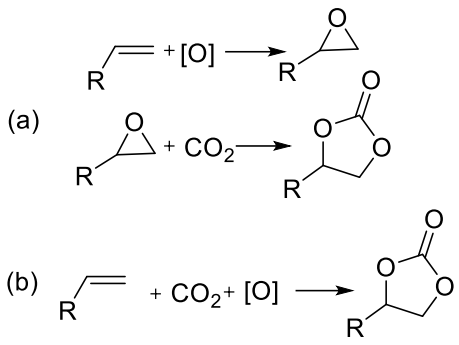

Scheme 5.1: The synthesis of cyclic carbonate from the oxidative carboxylation of olefins [29].

A previous study observed that cyclic carbonates can be produced directly from CO_2 and styrene using a supported gold catalyst and TBHP as an oxidant to form the epoxide with zinc bromide ($ZnBr_2$) and tetrabutylammonium bromide (Bu_4NBr) as catalysts for the cycloaddition of CO_2 with the formed epoxide, in one-pot (simultaneous oxidation and carboxylation) [29]. In contrast, another study found that in the one-pot reaction, Bu_4NBr prevented the epoxidation reaction and the expected cyclic carbonate was not obtained, whereas a very high yield of cyclic carbonate could be achieved by changing the one pot reaction to a multistep protocol (sequential oxidation and carboxylation) [30]. In spite of the fact that the oxidative carboxylation of olefins has been known since 1962 [31], little attention has been paid to this method compared with the route that employs epoxide as a starting material. The combination of two reactions in an one-pot process usually needs compatibility between reaction conditions. Therefore, it is important to investigate the suitable reaction conditions such as temperature, pressure and suitable catalysts for both reactions before coupling them in one-pot reaction.

To obtain more information on the roles of catalyst components, the epoxidation of 1-decene (first step) and the cycloaddition of CO_2 with 1,2-epoxydecane (second step) were conducted individually. Chapter 4 provides a more detailed explanation about the epoxidation of 1-decene using supported gold catalysts. 1% Au/SiO_2 and 1% Au/TiO_2 prepared by the sol-immobilisation gave the highest yield of 1,2-epoxydecane at 90°C for 24 h under solvent-free conditions. In this Chapter, firstly, the reaction of the cycloaddition of CO_2 with epoxide is investigated, using either a homogeneous catalyst such as quaternary ammonium salt or a heterogeneous catalyst such as polydiallydimethylammonium bromide supported on silica ($PDDABr/SiO_2$) or imidazole supported on silica ($Imid/SiO_2$). In this study, the reactions were carried out under solvent-free conditions. Furthermore, it is important to study the compatibility between these two catalysts for the two different steps before coupling them in one-pot reaction. Therefore, the epoxidation reaction was conducted in the presence of Bu_4NBr or 40% $PDDABr/SiO_2$ or $Imid/SiO_2$ to detect the effect of these catalysts in the epoxide yield. Furthermore, supported gold catalysts were added to the cycloaddition reaction to study their effect on this reaction. Then, the final aim of this study was the combination of the epoxidation of 1-decene and cycloaddition of CO_2 with the epoxide in one-pot (simultaneous oxidation and carboxylation), and one-pot multistep protocols (sequential oxidation and carboxylation). Furthermore, cycloaddition of CO_2 with different cycloalkene oxides was studied using Bu_4NBr and $ZnBr_2$ catalysts.

5.2. Synthesis of cyclic carbonate

5.2.1. Cycloaddition of CO_2 with 1,2-epoxydecane using quaternary ammonium salts catalysts

Quaternary ammonium salts are typically used as homogeneous catalysts for the synthesis of CCs through the cycloaddition of carbon dioxide with the epoxide [32, 33]. In a previous study, it was shown that there is a synergistic effect of Lewis acids, such as $ZnBr_2$, and Lewis bases on the catalytic synthesis of CCs from CO_2 and epoxides [34]. Lewis acids enhance the activity of the ammonium salts, as suggested by Kossev and co-worker [35], who detected that Lewis acids promote the reaction between carbon dioxide and different epoxides to synthesise CCs using quaternary ammonium salts as catalysts. The principle of Lewis acid is to activate the epoxide, whereas the quaternary ammonium salt opens the ring of the epoxide [35]. Furthermore, they have studied different molar ratios between ammonium salt and Lewis acid and found that the optimum molar ratio (Lewis base: Lewis acid) is 2:1 as mentioned in Section 1.5.1. Another study conducted by Arai and co-worker [36] also found that a catalyst system consisting of Bu_4NBr and $ZnBr_2$ is active for CO_2 cycloaddition, as styrene carbonate could be produced from styrene oxide at 80°C for 1 h. Although $ZnBr_2$ alone does not show significant activity in this reaction, it is proposed that $ZnBr_2$ and the Lewis base work together to open the epoxide ring and activate CO_2, as suggested in previously reported studies [19, 35]. Four different types of quaternary ammonium salts were tested for cycloaddition of CO_2 with 1,2-epoxydecane. Table 5.1 shows that the catalytic activity among quaternary ammonium salts depends on the alkyl group chain lengths. Me_4NBr was found to be less active for this reaction under these conditions, whereas Bu_4NBr almost converted the epoxide to the corresponding cyclic carbonate. The trend for the catalytic activity is n-Bu_4NBr> Pr_4NBr> Et_4NBr > Me_4NBr. Previous studies have made similar observations, with combined experimental and computational studies [37], as mentioned in Section 1.5.1. The bulkiness of the tetrahedral ammonium ion $[NR_4]^+$ forces the Br anion away from the cation more effectively than the smaller alkyl group, which then results in a smaller amount of electrostatic interaction between Br^- and the cation, and which therefore results in greater nucleophilicity of the anion [37].

Table 5.1: Effect of the cations structure on cyclic carbonate synthesis

R_4NBr	Conversion of 1,2-epoxydecane (%)	Cyclic carbonate selectivity (%)	Cyclic carbonate yield (%)[b]
blank	0	0	0
Me_4NBr (4.8 mmol%)[a]	28	93	26
Et_4NBr (3.5 mmol%)[a]	46	95	44
Pr_4NBr (2.8 mmol%)[a]	82	97	80
Bu_4NBr (2.3 mmol%)[a]	98	97	95

Reaction conditions: R_4NBr (0.2 g), $ZnBr_2$ (0.355 mmol, 0.08 g), 1,2-epoxydecane (26.88 mmol, 5 mL), 80°C, 20 bar CO_2, reaction time 4 h, rate of stirring 800 rpm. (a): amount of R_4NBr relative to 1,2-epoxydecane. (b) Yield obtained by using GC analysis.

Regarding the effect of the anion in the quaternary ammonium salt, it was demonstrated that the order of activity was found to be $Bu_4NBr > Bu_4NI \approx Bu_4NCl > Bu_4NF$. In the case of Bu_4NI, when it was added into the reaction mixture of TBHP and styrene, the colour of the mixture changed to dark orange, which indicates the formation of iodine by oxidation with TBHP [29].

5.2.1.1. Effect of the reaction time on cyclic carbonate synthesis

As shown in Table 5.2, the conversion of 1,2-epoxydecane increased with reaction time. 58% conversion was found after a 1 h reaction time, whereas almost all the epoxide was converted to the corresponding CC within 4 h reaction time with 97% selectivity for the CC. Notably, selectivity for the CC remained similar (95%-97%) for the entire course of the reaction.

Table 5.2: Effect of the reaction time

Reaction time (hour)	Conversion (%)	Cyclic carbonate selectivity (%)	Cyclic carbonate yield (%)[a]
1	58	95	55
2	70	95	67
3	91	97	88
4	98	97	95

Reaction conditions: Bu_4NBr (0.62 mmol, 0.2 g), $ZnBr_2$ (0.355 mmol, 0.08 g), 1,2-epoxydecane (26.88 mmol, 5 mL), 80°C, 20 bar CO_2, rate of stirring 800 rpm. (a) Yield obtained by using GC analysis.

5.2.1.2. Effect of CO_2 pressure on cyclic carbonate synthesis

Table 5.3 shows the effect of CO_2 pressure on the synthesis of CC using a Bu_4NBr (2.3 mmol%, amount of Bu_4NBr relative to the 1,2-epoxydecane amount.) and $ZnBr_2$ (1.32 mmol%, amount of $ZnBr_2$ in relation to the 1,2-epoxydecane amount) catalysts. The cyclic carbonate selectivity was slightly increased (93% to 97%) with an increase in CO_2 pressure in the range of 10-20 bar, whereas there was a significant increase in the epoxide

conversion from 80% to 98% when the CO_2 pressure was increased from 10 to 20 bar, respectively.

Table 5.3: Effect of CO_2 pressure on cyclic carbonate synthesis

CO_2 pressure (bar)	Conversion (%)	Cyclic carbonate selectivity (%)	Cyclic carbonate yield (%)[a]
10	80	93	74
15	90	94	84
20	98	97	95

Reaction conditions: Bu_4NBr (0.62 mmol, 0.2 g), $ZnBr_2$ (0.355 mmol, 0.08 g), 1,2-epoxydecane (26.88 mmol, 5 mL), 80°C, reaction time 4 h, rate of stirring 800 rpm. (a) Yield obtained by using GC analysis.

5.2.1.3. Effect of the reaction temperature on cyclic carbonate synthesis

To investigate the catalytic activity at different temperatures, experiments in the range of 70-90°C were carried out. This range was found to provide the optimum reaction temperature for epoxidation of 1-decene, as there should be compatibility between the reaction temperatures for both epoxidation and carbonate formation reactions in a one pot process. The epoxide conversion was affected by the reaction temperature. As shown in Table 5.4, with an increase in reaction temperature from 70°C to 80°C, the conversion of 1,2-epoxydecane increased from 87% to 98% within 4 h reaction time. With a further increase in the reaction temperature to 90°C, the reaction was almost completed within 2 h (99% conversion).

Table 5.4: Effect of the reaction temperature on cyclic carbonate synthesis

T (°C)	Time (hour)	Conversion (%)	Cyclic carbonate selectivity (%)	Cyclic carbonate yield (%)[a]
70	4	87	95	83
80	4	98	97	95
90	2	99	98	97

Reaction conditions: Bu_4NBr (0.62 mmol, 0.2 g), $ZnBr_2$ (0.355 mmol, 0.08 g), 1,2-epoxydecane (26.88 mmol, 5 mL), 20 bar CO_2, rate of stirring 800 rpm. (a) Yield obtained by using GC analysis.

5.2.1.4. Different linear epoxides

In order to survey the scope of substrates, the cycloaddition of CO_2 with other terminal epoxides was examined by performing the reaction under the same conditions with different reaction temperatures. It is clear from Table 5.5 that at 50°C and 70°C, almost all the 1,2-epoxyhexane and 1,2-epoxyoctane were converted to the corresponding CCs respectively within 4 h under solvent-free conditions using 20 bar CO_2 and a Bu_4NBr-$ZnBr_2$ catalysts. Shorter linear epoxide required lower temperature to be converted to the corresponding cyclic carbonate.

Table 5.5: Cycloaddition of CO_2 with different linear epoxides

Epoxide	T (°C)	Conversion (%)	Cyclic carbonate selectivity (%)	Cyclic carbonate yield (%)[a]
1,2-epoxyhexane (41.5 mmol)	50	98	97	95
1,2-epoxyoctane (32.72 mmol)	70	98	98	96
1,2-epoxydecane (26.88 mmol)	80	98	97	95

Reaction conditions: Bu_4NBr (0.62 mmol, 0.2 g), $ZnBr_2$ (0.355 mmol, 0.08 g), epoxide (5 mL), 20 bar CO_2, reaction time 4 h, rate of stirring 800 rpm. (a) Yield obtained by using GC analysis.

5.2.1.5. Mechanism for the cycloaddition of CO_2 with the epoxide for cyclic carbonate synthesis using Bu_4NBr and $ZnBr_2$

A possible mechanism for the cycloaddition of CO_2 with the epoxide for CC synthesis using Bu_4NBr and $ZnBr_2$ is well-known from previous studies [37-42]. The initiation of this reaction is by coordination of the epoxide with $ZnBr_2$ to form the adduct of the zinc-epoxide complex (1) (Scheme 5.2). Afterwards, the Bu_4NBr cation coordinates with the oxygen atom of the coordinated epoxide, which then enhances the nucleophilic attack of the bromide ion at the less-hindered carbon atom of the epoxide. This results in opening of the epoxide ring and generation of an O^- species (2). The carbon atom of CO_2 is partially positive; therefore, this carbon atom is attacked by this newly formed O^- to give $NBu_4OCOOCHRCH_2Br$ (3) as the key intermediate; the bond Zn-O breaks then cyclises *via* intermolecular nucleophilic attack (5) to yield the CC and regenerate the catalyst (Scheme 5.2).

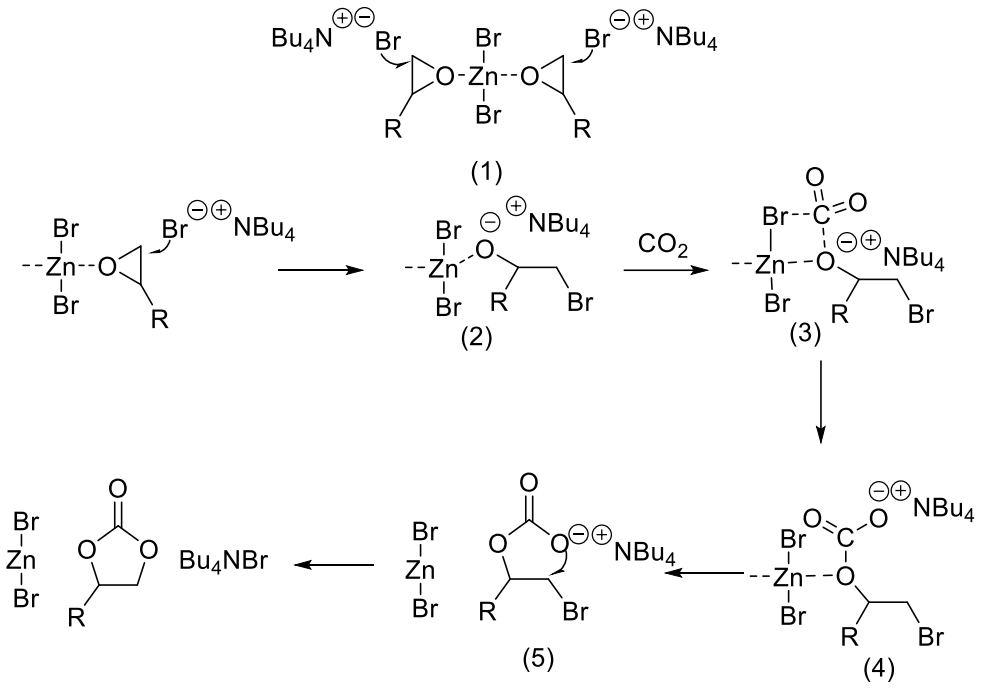

Scheme 5.2: Proposed mechanism for cyclic carbonate synthesis using Bu_4NBr and $ZnBr_2$. R: C_8H_{17}. Adapted from [37-42, 43].

Homogeneous catalysts such as Bu_4NBr are dissolved in a reaction mixture containing CCs. Therefore, separation of the catalysts from the reaction mixture may require more energy through a purification process [44]. A strategy to improve this is to heterogenise Bu_4NBr by dispersing it on a support to achieve better separation of the catalyst from the reaction products [44].

5.2.2. Cycloaddition of CO_2 with the epoxide for cyclic carbonate synthesis using supported Bu_4NBr catalysts

Bu_4NBr was immobilised on supports following the previously reported work in the literature, where silica gel was used as a support [44]. In the current work, MgO, hydrotalcite and silica gel were used as supports (Table 5.6). Hydrotalcite and MgO have been observed to be good catalysts for this reaction as they have more basic sites on their surfaces which can help to adsorb CO_2 as mentioned in Section 1.5.2 [19, 45]. MgO and hydrotalcite were calcined at 400°C, which was observed to be an optimum calcination temperature [19, 45]. Table 5.6 clearly shows that hydrotalcite and MgO supports were not active under these conditions and the reason behind this may be that hydrotalcite and MgO catalysts usually require a polar organic solvent, high temperature and long reaction time in order to produce a good yield of CC [19, 45]. Bu_4NBr was dispersed on MgO and hydrotalcite supports according to previously reported work [44]. It is clear that fresh 15% Bu_4NBr/MgO and 15% Bu_4NBr/hydrotalcite catalysts were active and displayed high conversion of 1,2-epoxydecane and selectivity for the CC. However, the reusability

study shows that no activity was observed for these catalysts, which suggests all the active components leached into the solution in contrast to what was observed in a previous study [44]. Further investigation for the cycloaddition of CO_2 with 1,2-epoxydecane by using high surface area silica-gel as a support for Bu_4NBr. Silica gel alone did not show any activity for this reaction under these conditions. Again, the fresh 15% Bu_4NBr/silica-gel catalyst displayed high conversion of 1,2-epoxydecane (97%) and selectivity for the cyclic carbonate (97%) at 90°C within 4 h. However, all the active components leached into the solution, leading to catalyst deactivation.

Table 5.6: Cycloaddition of carbon dioxide with 1,2-epoxydecane using 15% Bu_4NBr/support

Catalyst	T (°C)	Conversion (%)	Cyclic carbonate selectivity (%)	Cyclic carbonate yield (%)[b]
Blank	80	0	-	0
MgO	80	2	-	0
15% Bu_4NBr/MgO	80	94	92	86
	90	95	94	89
15% Bu_4NBr/MgO (reused)[a]	80	3	-	0
Hydrotalcite	80	1	-	0
15% Bu_4NBr/ hydrotalcite	80	88	93	82
	90	92	93	86
15% Bu_4NBr/ hydrotalcite (reused)[a]	90	2	-	0
silica gel	80	1	-	0
15% Bu_4NBr/silica gel	80	84	95	80
15% Bu_4NBr/silica gel	90	92	94	86
15% Bu_4NBr/silica gel (0.45 g)	90	95	95	90
15% Bu_4NBr/silica gel (reused)[a]	90	3	-	0

Reaction conditions: catalyst (0.3 g), 1,2-epoxydecane (26.88 mmol, 5 mL), 20 bar CO_2, reaction time 4 h, rate of stirring 800 rpm. (a) Reused catalyst: the catalyst was filtered off, then washed with acetone (1 L) and then dried in the oven at 110°C for 16 h. (b) Yield obtained by using GC analysis.

From previous results, quaternary ammonium salts are still the best catalyst for cycloaddition reactions. However, when immobilising or supporting Bu_4NBr on different supports (to make heterogeneous catalyst), all the active components leached into the solution. Therefore, finding a material which can share the effectiveness of Bu_4NBr as well as being insoluble in organic solvents would be the perfect solution for the leaching problem in the liquid phase. It was reported that polydiallyldimethylammonium halides can catalyse the cycloaddition of CO_2 with propylene oxide and could be reused 10 times without significant loss of activity [46].

5.2.3. Cycloaddition of CO_2 with the epoxide for cyclic carbonate synthesis using polydiallyldimethylammonium bromide supported catalysts

In the previous discussion, it was shown that Bu_4NBr has been supported on different supports to synthesise a heterogeneous catalyst for cyclic carbonate synthesis. However, the leaching of the active species still exists with this catalyst. Therefore, using a catalyst which can share the effectiveness of quaternary ammonium salts and being insoluble in organic substrate is valuable in solving the leaching issue. Polydiallyldimethylammonium bromide has these valuable properties [46]. More interestingly, this catalyst is non-toxic as it is used for drinking water pre-treatment [47].

5.2.3.1. Catalyst characterisations

The procedure for the preparation of polydiallyldimethylammonium bromide has been reported previously [46]. From the N_2 adsorption analysis, the surface areas of SiO_2 support alone, and fresh and used PDDA-Br/SiO_2 are summarised in Table 5.7. For SiO_2 the surface area is 345 m^2 g^{-1}, whereas the surface area for 20% PDDA-Br/SiO_2 and 40% PDDA-Br/SiO_2 decreased to 185 m^2 g^{-1} and 143 m^2 g^{-1} respectively, which may indicate the incorporation of PDDA-Br in the support pores. The surface area for reused 40% PDDA-Br/SiO_2 decreased to 88 m^2 g^{-1}, which may result of the adsorption of the products on the catalyst surface.

Table 5.7: Nitrogen physisorption analysis of the surface area using BET method for Polydiallyldimethylammonium bromide supported on SiO_2

Catalyst	Surface area m^2 g^{-1}
SiO_2	345
20% PDDA-Br/SiO_2	185
40% PDDA-Br/SiO_2	143
Reused 40% PDDA-Br/SiO_2	88

XRD patterns for pure silica, 20% PDDA-Br/SiO_2, 40% PDDA-Br/SiO_2 and pure PDDA-Br are shown in Figure 5.1. The main diffraction peaks of PDDA-Br are shown in the range 17°-72°. After impregnating PDDA-Br on the SiO_2 support with 20% loading, the diffraction peaks of PDDA-Br disappear, and a clear peak is only shown between 15° and 25°; these reflection patterns can be assigned to the silica. With 40% PDDA-Br/SiO_2, diffraction peaks of PDDA-Br appear slightly at 23°, 27°, 30°, 44° and 54°.

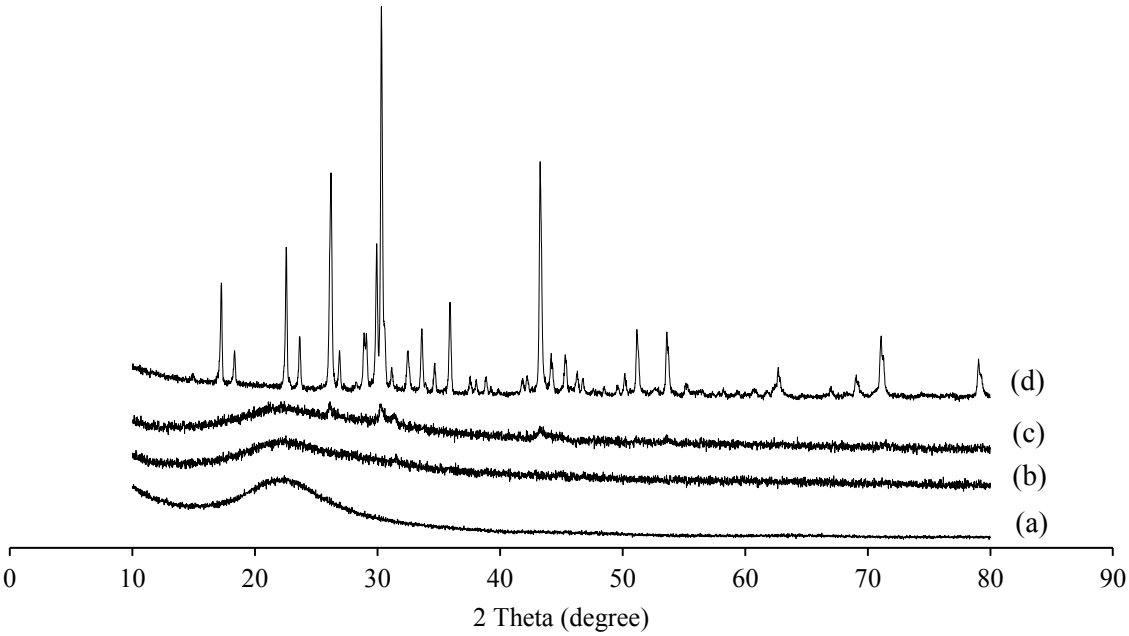

Figure 5.1: XRD patterns for: (a) SiO_2 (b) 20% PDDA-Br/SiO_2 (c) 40% PDDA-Br/SiO_2 (d) pure PDDA-Br.

Thermogravimetric analysis was carried out and the results are shown in Figure 5.2. It was found that there was around 2% weight loss below 100°C, which may be due to the removal of water that was adsorbed on the SiO_2 surface. The PDDA-Br/SiO_2 decomposition starting temperature was 250°C; this decomposition might be due to the gradual degradation of polymeric quaternary ammonium salt, as mentioned in the previous study [46]. The degradation increased with increasing temperature. The whole decomposition of PDDA-Br/SiO_2 catalyst was completed near 900°C and the total weight loss was around 36%.

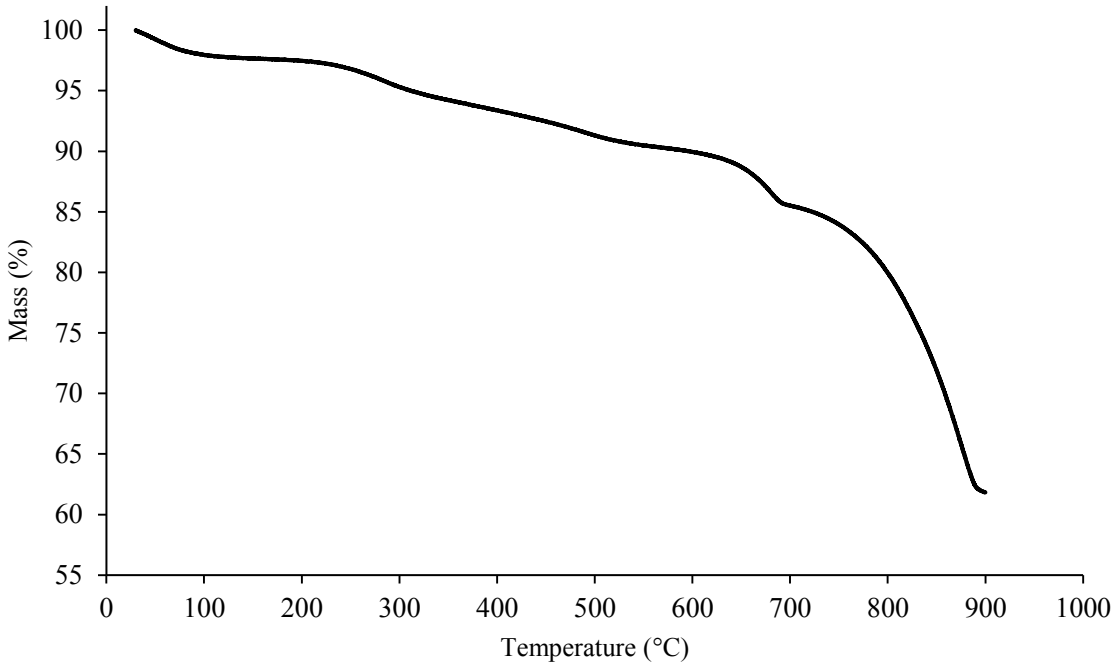

Figure 5.2: TGA for PDDA-Br/SiO_2 catalyst (6.5 mg).

The SEM images (Figure 5.3 and Figure 5.4) show that the surface morphologies of undoped silica and fresh 40% PDDA-Br/SiO_2 are indistinguishable from each other.

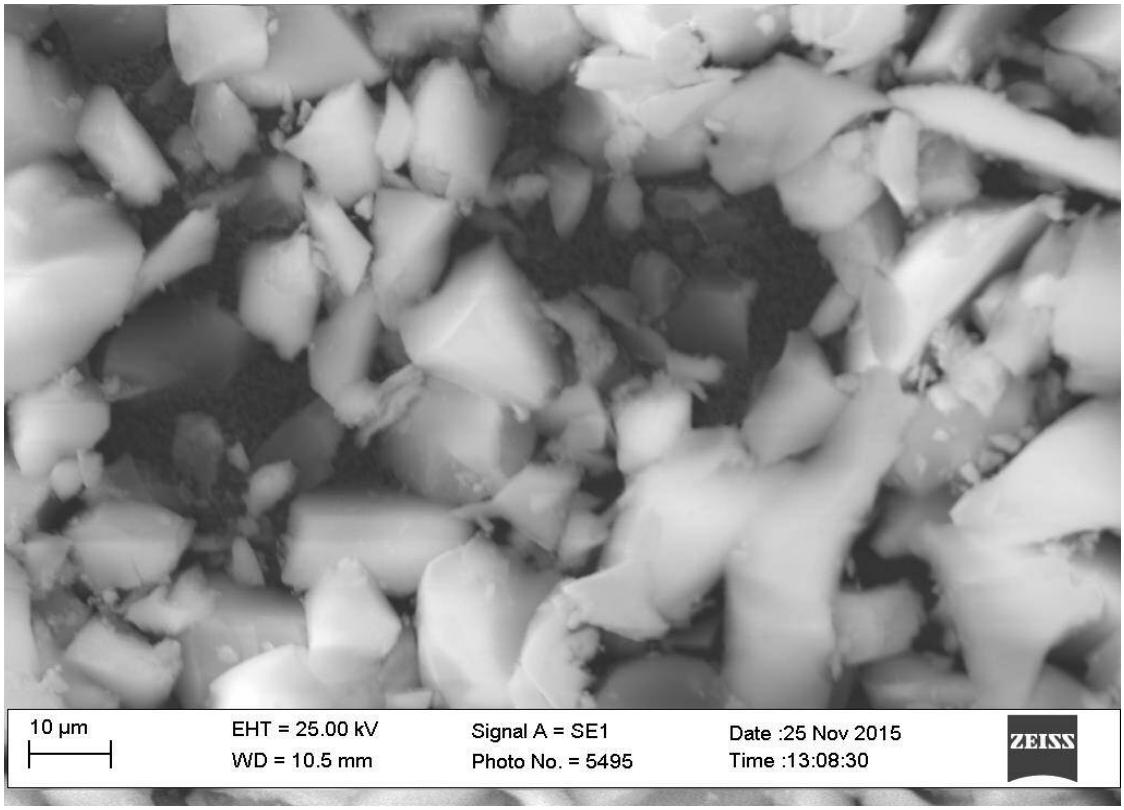

Figure 5.3: SEM image for: SiO_2 support.

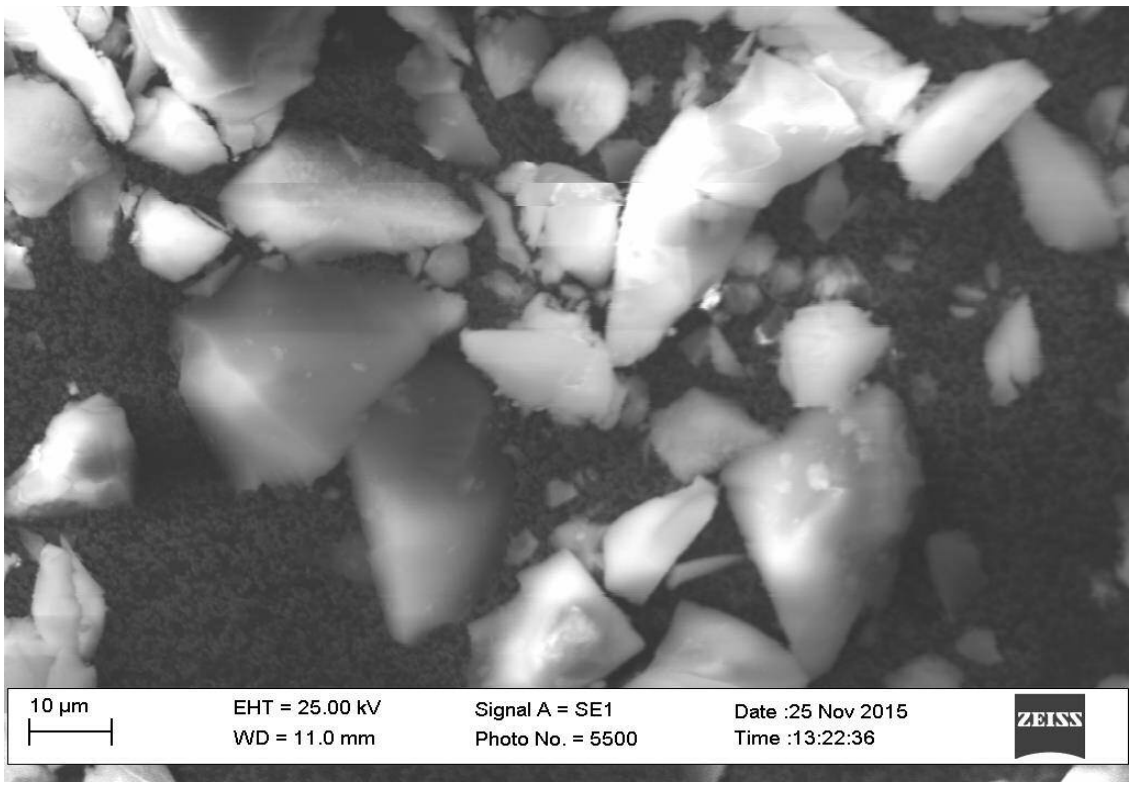

Figure 5.4: SEM image for: 40% PDDA-Br/SiO_2.

5.2.3.2. Cycloaddition of CO_2 with 1,2-epoxydecane using PDDA-Br/SiO_2 catalysts

The results of cycloaddition of CO_2 with 1,2-epoxydecane are summarised in Table 5.8. It is clear that in the absence of the catalyst no activity was observed. Furthermore, SiO_2 alone did not show any activity for this reaction under these conditions. It was suggested that the addition of $ZnBr_2$ plays an important role in enhancing the activity of PDDA-Br/SiO_2 [46]. $ZnBr_2$ alone results in only 2% conversion of 1,2-epoxydecane within a 4 h reaction time. However, the addition of 20% PDDA-Br/SiO_2 with $ZnBr_2$ resulted in a significant improvement in the activity, which gave 30% conversion of the epoxide and a slight increase in the cyclic carbonate selectivity from 89% to 92% within a 4 h run time. Furthermore, the influence of the catalyst loading on the activity of the reaction was studied. It was found that a conversion of 30% was achieved with 20% PDDA-Br/SiO_2 and $ZnBr_2$, while a 42% conversion of 1,2-epoxydecane was observed when the catalyst loading increased to 40% PDDA-Br/SiO_2 within a 4 h reaction time. Additionally, the amount of 40% PDDA-Br/SiO_2 influenced the performance of the reaction. Conversion of 38% was detected when using 0.2 g of 40% PDDA-Br/SiO_2 and $ZnBr_2$, whereas increasing the catalyst mass to 0.3 g and 0.5 g resulted in a subsequent increase in the epoxide conversion to 42% and 50% respectively, and the selectivity in the range 89-94%. The reaction time also increased from 4 to 6 h with a 40% PDDA-Br/SiO_2 catalyst, to increase the epoxide conversion from 42% to 47%

respectively. Interestingly, a further increase in the reaction time to 16 h showed significant conversion of 1,2-epoxydecane of 91% and 97% selectivity for cyclic carbonate. This confirms that the conversion of 1,2-epoxydecane is highly time-dependent under these conditions.

Table 5.8: Cycloaddition of CO_2 with 1,2-epoxydecane using PDDA-Br/SiO_2 catalysts

Catalyst	Conversion (%)	Cyclic carbonate selectivity (%)	Cyclic carbonate yield (%)[c]
Blank[a]	0	0	0
SiO_2[a]	1	0	0
$ZnBr_2$	2	89	1.8
20% PDDA-Br/SiO_2 (0.3 g)	30	92	28
40% PDDA-Br/SiO_2 (0.2 g)	38	91	35
40% PDDA-Br/SiO_2 (0.3 g)	42	89	37
	47[a]	91[a]	43
	91[b]	97[b]	88
40% PDDA-Br/SiO_2 (0.5 g)	50	94	47

Reaction conditions: $ZnBr_2$ (0.355 mmol, 0.08 g), 1,2-epoxydecane (26.88 mmol, 5 mL), 90°C, 20 bar CO_2, reaction time 4 h, rate of stirring 800 rpm. (a) 6 h reaction time (b) 16 h reaction time. (c) Yield obtained by using GC analysis. (a) no $ZnBr_2$ was present in the reaction.

5.2.3.3. The reusability of the 40% PDDA-Br/SiO_2 catalyst

The recycling of 40% PDDA-Br/SiO_2 catalyst was examined. In each cycle, the solid catalyst was recovered by filtration, followed by rinsing with acetone (1 L) and then drying. The recovered 40% PDDA-Br/SiO_2 catalyst was reused in the next reaction and the results are summarised in Figure 5.5. A significant decrease was observed in the conversion after the first cycle of the reused 40% PDDA-Br/SiO_2 from a 42% conversion of the fresh catalyst to give a conversion of 25% on the reused catalyst. However, there was no obvious effect on the cyclic carbonate selectivity, which remained similar (88-89%). The second cycle of cycloaddition of CO_2 with 1,2-epoxydecane displayed a slight decrease in the epoxide conversion from 25% to 20% as well as some decrease in the cyclic carbonate selectivity. Furthermore, the third cycle of this catalyst showed a small decrease in the epoxide conversion to 16%, whereas the cyclic carbonate was still the same value around 80%.

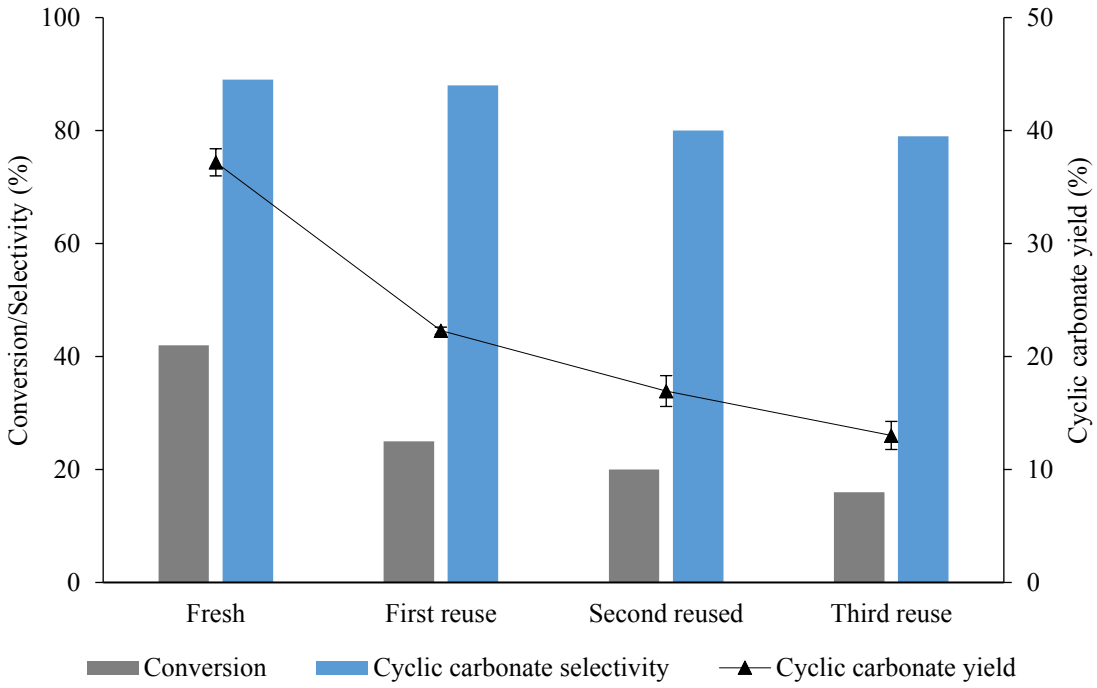

Figure 5.5: The reusability of the 40% PDDA-Br/SiO_2 catalyst. Reaction conditions: 40% PDDA-Br/SiO_2 (0.3 g), $ZnBr_2$ (0.355 mmol, 0.08 g), 1,2-epoxydecane (26.88 mmol, 5 mL), 90°C, 20 bar CO_2, reaction time 4 h, rate of stirring 800 rpm. Error bars indicate range of data based on three repeat experiments.

A similar observation of the reusability of the 40% PDDA-Br/SiO_2 catalyst was found, with an increase in the catalyst mass to 0.5 g instead of 0.3 g (Figure 5.6). Again, the first used cycle displayed a notable decrease in epoxide conversion from 50% with fresh 40% PDDA-Br/SiO_2 catalyst to 30% with the reused one. Furthermore, there was a drop in the cyclic carbonate selectivity from 94% to 87% respectively. A small drop was shown in the epoxide conversion and cyclic carbonate selectivity with the second cycle from 30% to 25% and from 87% to 83% respectively. The decrease in the reused catalyst activity may result of the adsorption of the products and remaining substrate on the catalyst surface, which may have blocked the active sites of the catalyst.

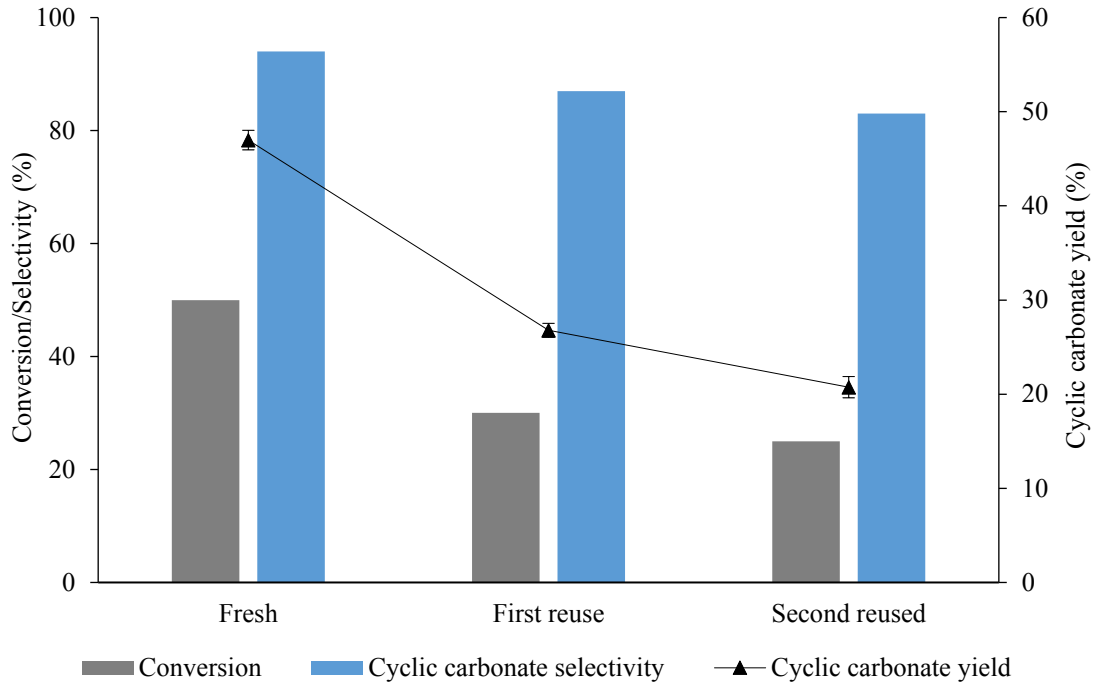

Figure 5.6: The reusability of the 40% PDDA-Br/SiO_2 catalyst. Reaction conditions: 40% PDDA-Br/SiO_2 (0.5 g), $ZnBr_2$ (0.355 mmol, 0.08 g), 1,2-epoxydecane (26.88 mmol, 5 mL), 90°C, 20 bar CO_2, reaction time 4 h, rate of stirring 800 rpm. Error bars indicate range of data based on three repeat experiments.

A filtration experiment could allow us to draw conclusions about the nature of the 40% PDDA-Br/SiO_2 catalyst in this reaction whether it is acting as a homogeneous or heterogeneous catalyst or a combination of both. Filtration tests were conducted after running for 2 h reaction time, which ended up with 20% epoxide conversion. Then filtering the solid 40% PDDA-Br/SiO_2 catalysts, then continuing to either 4 h or 16 h reaction times. Comparing the standard reaction within a 4 h reaction time with the filtered one at the same reaction time (4 h), it can be seen in Figure 5.7 that the reaction proceeds after catalyst removal, but with a significantly reduced conversion of the epoxide from 42% of the standard reaction to 25% with an after-filtration reaction. A similar observation was made when comparing the 16 h standard reaction with the filtered one, a conversion of 91% for the standard reaction, while a 16 h reaction after filtration of solid 40% PDDA-Br/SiO_2 gave 37% conversion of 1,2-epoxydecane. Therefore, the main catalytic route is heterogeneous with significant contribution from homogeneous catalysis.

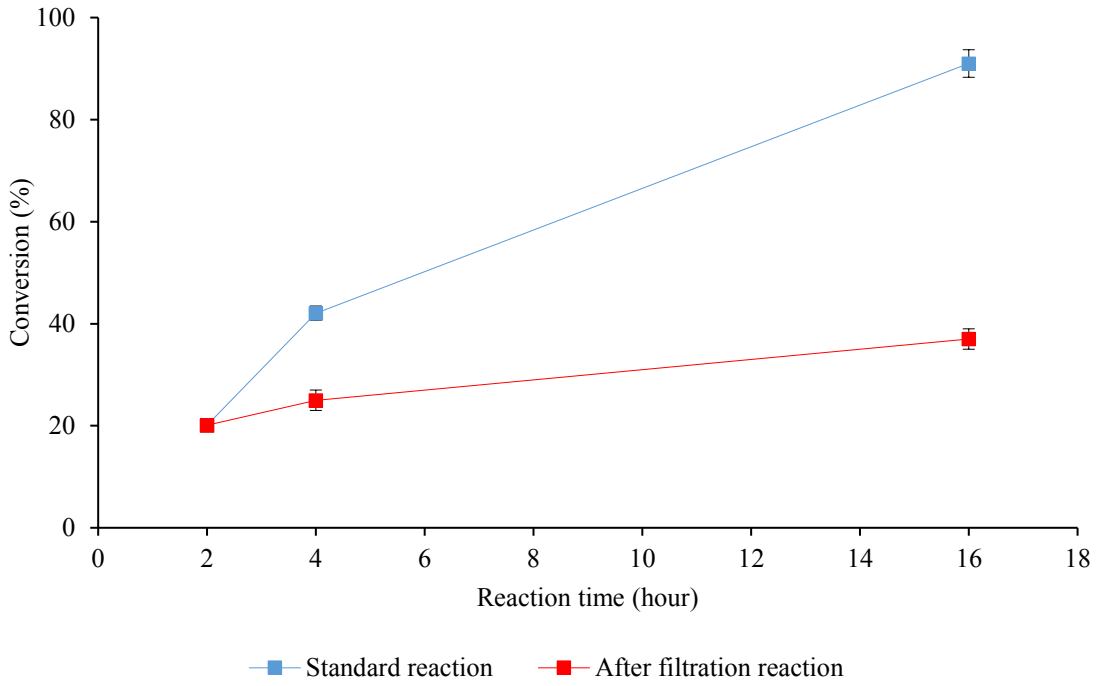

Figure 5.7: Heterogeneous versus homogeneous 40% PDDA-Br/SiO_2 catalyst. Reaction conditions: 40% PDDA-Br/SiO_2 (0.3 g), $ZnBr_2$ (0.355 mmol, 0.08 g), 1,2-epoxydecane (26.88 mmol, 5 mL), 90°C, 20 bar CO_2, rate of stirring 800 rpm. Error bars indicate range of data based on three repeat experiments.

5.2.4. Cycloaddition of CO_2 with the epoxide for cyclic carbonate synthesis using imidazole supported on SiO_2 (Imid/SiO_2)

It was reported that imidazolium-based ionic liquids are active catalysts for cyclic carbonate synthesis [23, 48-50]. In a previous study [23], a supported imidazole catalyst was used as a heterogeneous catalyst for cycloaddition reaction. It was proposed that this catalyst has many advantages over the supported ionic liquid based catalysts, as it is effective in producing cyclic carbonate under solvent-free conditions, easy to synthesise and cost effective. Therefore, supported imidazole catalyst (Imid/SiO_2) was prepared according to the previous work [23]. For the cycloaddition of CO_2 with 1,2-epoxydecane using Imid/SiO_2, the effect of various reaction parameters such as reaction time and catalyst mass were investigated. The aim was to determine the conditions which give the highest conversion of the epoxide and cyclic carbonate selectivity. From Table 5.9 it can be seen that the amount of Imid/SiO_2 catalyst influences the performance of the reaction. Increasing the catalyst mass from 0.1 g to 0.4 g resulted in an increase in the epoxide conversion from 5% to 17% respectively and the selectivity for cyclic carbonate in the range 86-90%. The remaining products such as 1,2-decanediol were formed by opening the epoxide ring.

Table 5.9: Effect of the catalyst mass on cycloaddition of CO_2 with 1,2-epoxydecane

Catalyst mass (g)	Conversion (%)	Cyclic carbonate selectivity (%)	Cyclic carbonate yield (%)[a]
0.1	5	86	4.3
0.2	8	88	7
0.4	17	90	15.3

Reaction conditions: 1,2-epoxydecane (26.88 mmol, 5 mL), 90°C, 20 bar CO_2, reaction time 4 h, rate of stirring 800 rpm. (a) Yield obtained by using GC analysis.

The influence of the reaction time on the conversion and cyclic carbonate selectivity was studied and the results are tabulated in Table 5.10. At a 4 h reaction time, a 17% conversion was recorded; when the reaction time was prolonged to 16 and 24 h, the conversion significantly increased to 58% and 67% respectively. The reusability of Imid/SiO_2 was demonstrated as follows: the Imid/SiO_2 catalyst was recovered by filtration, then washed with CH_2Cl_2 to remove any adsorbed material from products and remaining substrate. It was then dried in the oven at 110°C for 16 h. The conversion of 1,2-epoxydecane with reused Imid/SiO_2 showed a significant drop from 67% to 30% within a 24 h reaction time. However, the cyclic carbonate selectivity remained almost the same at 94-95%, as shown in Table 5.10.

Table 5.10: Effect of the reaction time and reusability study

Reaction time (hour)	Conversion (%)	Cyclic carbonate selectivity (%)	Cyclic carbonate yield (%)[a]
4	17	90	15.3
16	58	98	57
24	67	95	64
24 Reused catalyst	30	94	28

Reaction conditions: Imid/SiO_2 (0.4 g), 1,2-epoxydecane (26.88 mmol, 5 mL), 90°C, 20 bar CO_2, rate of stirring 800 rpm. (a) Yield obtained by using GC analysis.

A filtration experiment was used to determine the nature of the Imid/SiO_2 catalyst in this reaction, whether it was acting as a homogeneous or heterogeneous catalyst or a combination of both. Filtration tests were conducted after running the normal 4 h reaction time, which ended with a 17% epoxide conversion; the catalyst was filtered off after 4 h reaction time and then the reaction was run for another 12 h, as shown in Figure 5.8. Comparing the 16 h standard reaction with the filtered one at the same reaction time (16 h), it can be seen in Figure 5.8 that the reaction proceeds after catalyst removal, but with some reduced conversion of the epoxide from 58% of the standard reaction to 35% for after-filtration reaction. Therefore, the catalytic route is heterogeneous and homogeneous.

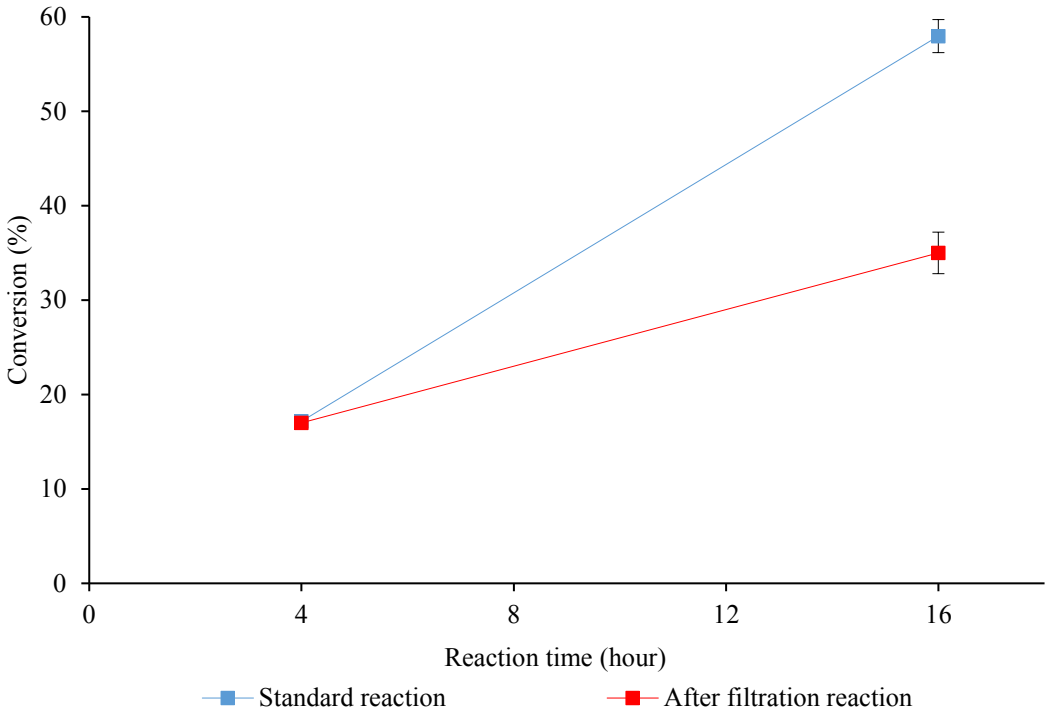

Figure 5.8: Heterogeneous versus homogeneous Imid/SiO_2 catalyst. Reaction conditions: Imid/SiO_2 (0.4 g), 1,2-epoxydecane (26.88 mmol, 5 mL), 90°C, 20 bar CO_2, rate of stirring 800 rpm. Error bars indicate range of data based on three repeat experiments.

It was proposed that the Lewis base site in imidazole has a major role in catalytic activity [23] (Scheme 5.3). As N in the imidazole-supported catalyst has a pair of electrons (Lewis base), it can activate the 1,2-epoxydecane ring through the less hindered carbon, which results in opening of the epoxide ring and generation of an O^- species. The carbon atom of CO_2 is partially positive; therefore, this carbon atom is attacked by this newly formed O^-. The bond N-C breaks then cyclises to yield the CC and regenerate the catalyst. The OH groups of the silica support could play an encouraging role in this cycloaddition reaction, which could act in tandem with the Lewis base sites in imidazole for catalysing this cycloaddition reaction [23].

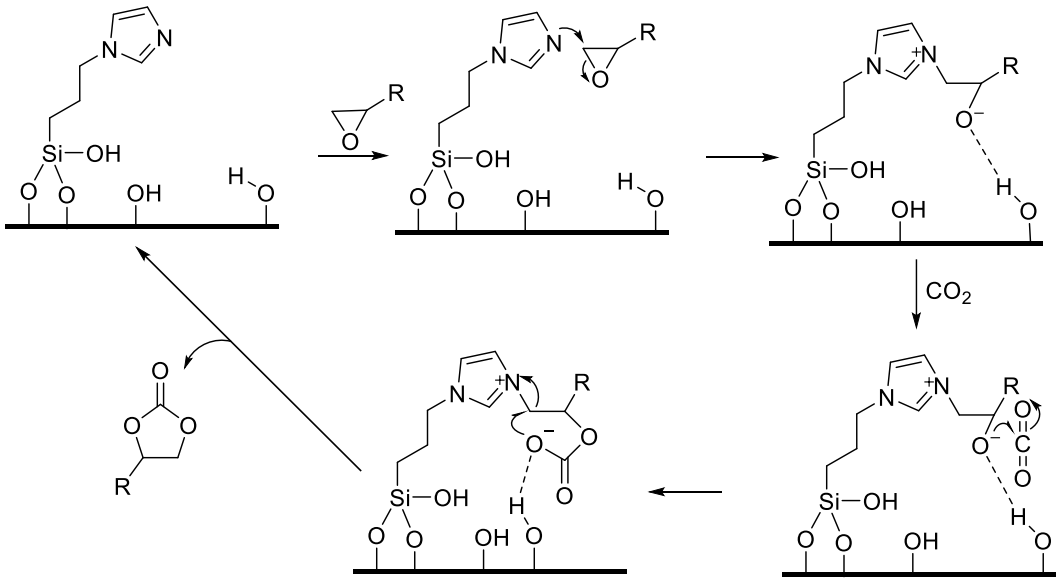

Scheme 5.3: Proposed mechanism of cycloaddition of CO_2 with epoxide on the surface of Imid/SiO_2. Adapted from [23].

The next step before the oxidative carboxylation of 1-decene is the investigation the effect of Bu_4NBr and $ZnBr_2$, 40% PDDA-Br/SiO_2 or Imid/SiO_2 on the epoxidation of 1-decene as well as studying the effect of supported gold catalysts on the cycloaddition of CO_2 with 1,2-epoxydecane.

5.2.5. Epoxidation of 1-decene in the presence of Bu_4NBr and $ZnBr_2$

The epoxidation of 1-decene was carried out in the presence of Bu_4NBr and $ZnBr_2$ using supported gold catalysts and a small amount of AIBN and the results are tabulated in Tables 5.11 and 5.12 respectively. It was found that adding Bu_4NBr markedly reduced the selectivity of the epoxide from 19% to 2% when using 1% Au/SiO_2 as catalyst under 15 bar of O_2. There was at the same time also an increase in the diol selectivity from 2% to 7%; furthermore, trace amounts of epoxide ring opening products such as bromoalcohol were detected in addition to a slight increase in the selectivity for some of the normal products such as alcohols from 1-decene oxidation reaction. Furthermore, as shown in Table 5.12, similar observations were found, the presence of Bu_4NBr in the epoxidation reaction results in a significant decrease in the epoxide selectivity from 34% to 9% when using 1% Au/SiO_2 as catalyst and from 34% to 12% when using1% Au/TiO_2 under atmospheric pressure of air. These observations suggest that Bu_4NBr and $ZnBr_2$ have a negative effect on the epoxidation reaction (they open the epoxide ring). These results are in contrast to a previous study for direct synthesis of cyclic carbonate from styrene [29]. They observed that the addition of Bu_4NBr and $ZnBr_2$ did not have any negative effect on the epoxide production during the epoxidation reaction, as mentioned in Section 1.5.3.

Table 5.11: Effect of Bu_4NBr and $ZnBr_2$ on 1-decene epoxidation step under 15 bar O_2

Catalyst	Co-catalyst	1-Decene conversion (%)	Selectivity (%)			
			Epoxide	Allylic products	Diol	Others
Blank	-	22	17	28	0	40
1% Au/SiO_2	-	24	19	24	2	41
1% Au/SiO_2	Bu_4NBr (1.24 mmol, 0.4 g) + $ZnBr_2$ (0.71 mmol, 0.16 g)	21	2	26	7	55

Reaction conditions: 1% Au/SiO_2 (0.1 g), 1-decene (53 mmol, 10 mL), AIBN (0.036 mmol, 6 mg), 90°C, 15 bar O_2, reaction time 24 h, rate of stirring 800 rpm. Allylic products=∑ (1-decen-3-one, 1-decen-3-ol, 2-decenal, 2-decen-1-ol). Others=∑ (C_7+C_8+C_9 acids, C_8+C_9 aldehyde, C_7+C_8 alcohols, 3-nonen-1-ol, 3-nonanone, cyclododecane, 2-decenoic acid, epoxide ring opening products such as bromoalcohol).

Table 5.12: Effect of Bu_4NBr and $ZnBr_2$ on 1-decene epoxidation step under atmospheric pressure of air

Catalyst	Co-catalyst	1-Decene conversion (%)	Selectivity (%)			
			Epoxide	Allylic products	Diol	Others
Blank	-					
1% Au/SiO_2	-	13	34	28	1	27
1% Au/SiO_2	Bu_4NBr (1.24 mmol, 0.4 g) + $ZnBr_2$ (0.71 mmol, 0.16 g)	10	9	32	7	39
1% Au/TiO_2	-	13	34	30	2	24
1% Au/TiO_2	Bu_4NBr (1.24 mmol, 0.4 g) +$ZnBr_2$ (0.71 mmol, 0.16 g)	10	12	32	6	44

Reaction conditions: catalyst (0.1 g), 1-decene (53 mmol, 10 mL), AIBN (0.036 mmol, 6 mg), 90°C, atmospheric pressure air, reaction time 24 h, rate of stirring 800 rpm. Allylic products=∑ (1-decen-3-one, 1-decen-3-ol, 2-decenal, 2-decen-1-ol). Others=∑ (C_7+C_8+C_9 acids, C_8+C_9 aldehyde, C_7+C_8 alcohols, 3-nonen-1-ol, 3-nonanone, cyclododecane, 2-decenoic acid, epoxide ring opening products such as bromoalcohol).

In a time online study, the epoxidation of 1-decene in the presence of Bu_4NBr and $ZnBr_2$ was investigated under atmospheric pressure of air to see whether there was any effect on the epoxidation mechanism. It was shown in Chapter 4 that during the oxidation of 1-decene, allylic products such as 1-decen-3-one, 1-decen-3-ol, 2-decenal and 2-decen-1-ol are the predominant products at the beginning of the reaction, and lower selectivity for the epoxide was detected. Then, the epoxide selectivity gradually increased with the reaction time and was accompanied by a significant decrease in allylic products selectivity. Compared with the previous standard reaction (without addition of Bu_4NBr and $ZnBr_2$) as shown in Figure 5.9, it is shown in Figure 5.10 that in the presence of Bu_4NBr and $ZnBr_2$, the epoxide selectivity was significantly reduced, whereas there was

an increase in the diol concentration with the increase in the reaction time. Moreover, with the increase in the reaction time, there was a small increase in the selectivity of the normal products from the 1-decene oxidation reaction, such as alcohols and ketone, in addition to the slight increase in the selectivity for trace amounts of epoxide ring opening products such as bromoalcohol.

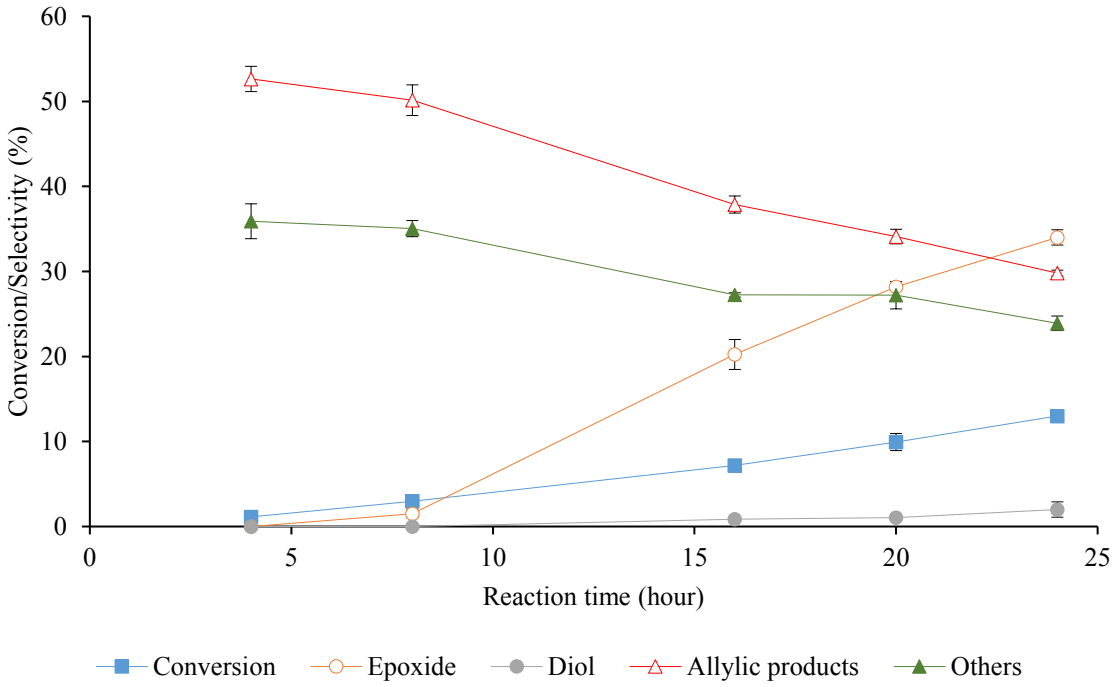

Figure 5.9: Time online study for epoxidation of 1-decene using 1% Au/TiO_2 catalyst. Reaction conditions: 1% Au/TiO_2 (0.1 g), 1-decene (53 mmol, 10 mL), AIBN (0.036 mmol, 6 mg), 90°C, atmospheric pressure air, rate of stirring 800 rpm. Allylic products=∑ (1-decen-3-one, 1-decen-3-ol, 2-decenal, 2-decen-1-ol). Others=∑ (C_7+C_8+C_9 acids, C_8+C_9 aldehyde, C_7+C_8 alcohols, 3-nonen-1-ol, 3-nonanone, cyclododecane, 2-decenoic acid). Error bars indicate range of data based on three repeat experiments.

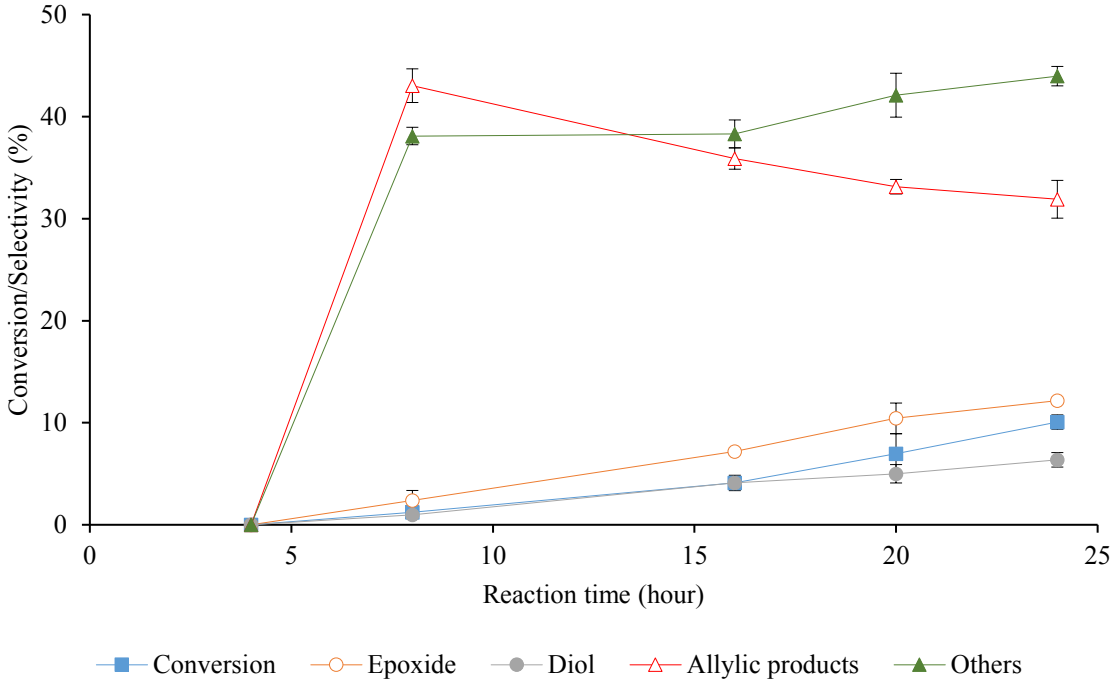

Figure 5.10: Time online study for epoxidation of 1-decene in the presence of Bu_4NBr and $ZnBr_2$. Reaction conditions: 1% Au/TiO_2 (0.1 g), 1-decene (53 mmol, 10 mL), AIBN (0.036 mmol, 6 mg), Bu_4NBr (1.24 mmol, 0.4 g), $ZnBr_2$ (0.71 mmol, 0.16 g), 90°C, atmospheric pressure air, rate of stirring 800 rpm. Allylic products=∑ (1-decen-3-one, 1-decen-3-ol, 2-decenal, 2-decen-1-ol). Others=∑ (C_7+C_8+C_9 acids, C_8+C_9 aldehyde, C_7+C_8 alcohols, 3-nonen-1-ol, 3-nonanone, cyclododecane, 2-decenoic acid, epoxide ring opening products). Error bars indicate range of data based on three repeat experiments.

5.2.6. Epoxidation of 1-decene in the presence of 40% PDDA-Br/SiO_2

Studying the compatibility between the catalysts for epoxidation and cycloaddition steps before coupling them in a one-pot reaction is an essential process. Therefore, the epoxidation of 1-decene reaction was carried out in the presence of 40% PDDA-Br/SiO_2 using 1% Au/TiO_2 and a small amount of AIBN at 90°C for 24 h under atmospheric pressure of air. A similar effect of Bu_4NBr was found with 40% PDDA-Br/SiO_2 towards the epoxidation of 1-decene. From Table 5.13 it can be seen that in the presence of 40% PDDA-Br/SiO_2 there was a significant decrease in the epoxide selectivity from 34% to 8% with a slight decrease in the conversion of 1-decene from 13% to 11%. The presence of 40% PDDA-Br/SiO_2 resulted in opening the formed epoxide ring, which led to increasing the 1,2-decanediol selectivity from 2% to 6% and some increase in selectivity to alcohol products.

Table 5.13: Study the effect of 40% PDDA-Br/SiO_2 on 1-decene epoxidation step

Catalysts	Conversion (%)	Selectivity (%)			
		Epoxide	Allylic products	Diol	Others
1% Au/TiO_2	13	34	30	2	24
1% Au/TiO_2 + 40% PDDA-Br/SiO_2	11	8	32	6	40

Reaction conditions: 1% Au/TiO_2 (0.1 g), 1-decene (53 mmol, 10 mL), AIBN (0.036 mmol, 6 mg), 40% PDDA-Br/SiO_2 (0.3 g), $ZnBr_2$ (0.71 mmol, 0.16 g), 90°C, atmospheric pressure air, reaction time 24 h, rate of stirring 800 rpm. Allylic products=∑ (1-decen-3-one, 1-decen-3-ol, 2-decenal, 2-decen-1-ol). Others=∑ (C_7+C_8+C_9 acids, C_8+C_9 aldehyde, C_7+C_8 alcohols, 3-nonen-1-ol, 3-nonanone, cyclododecane, 2-decenoic acid, epoxide ring opening product such as bromoalcohol).

Again, to gain more details about the reaction, a time online study for epoxidation of 1-decene in the presence of 40% PDDA-Br/SiO_2 was completed. It is shown in Figure 5.11 that with increased reaction time, the epoxide selectivity slightly increased in parallel with increased selectivity for the diol, which is in contrast to the standard reaction (Figure 5.9), where the selectivity for the epoxide significantly increases with an increase in the reaction time and very low selectivity for the diol was detected. Furthermore, from Figure 5.11 it can be seen that there was an increase in other products such as alcohols and products from the epoxide ring opening.

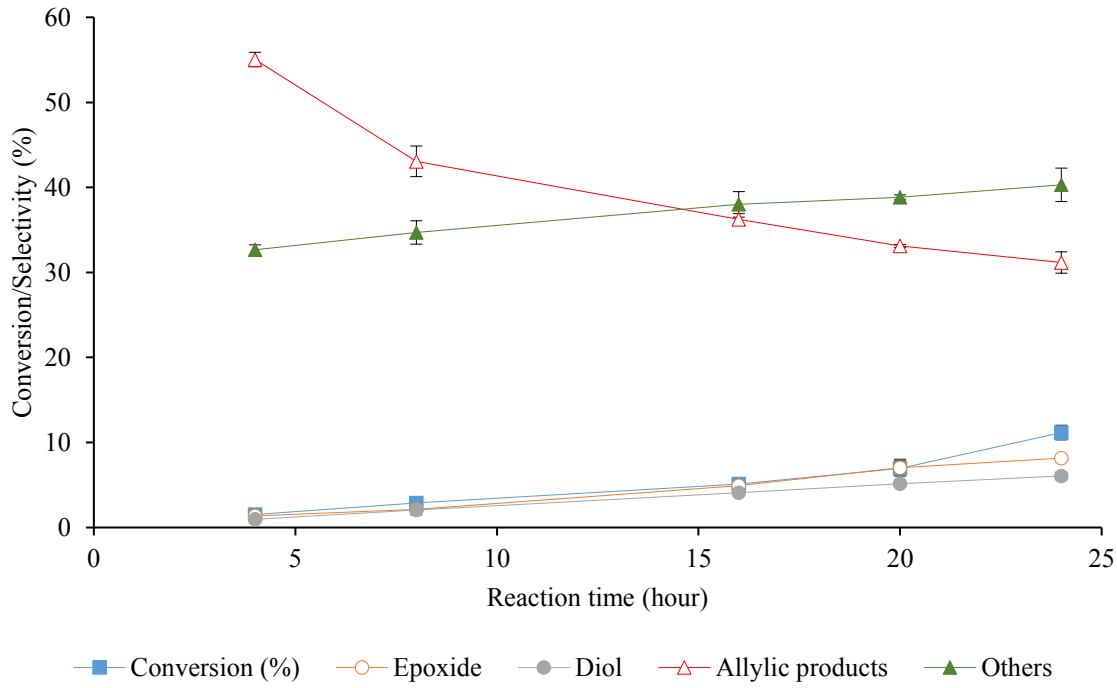

Figure 5.11: Time online study for epoxidation of 1-decene in the presence of 40% PDDA-Br/SiO_2 catalyst. Reaction conditions: 1% Au/TiO_2 (0.1 g), 1-decene (53 mmol, 10 mL), AIBN (0.036 mmol, 6 mg), 40% PDDA-Br/SiO_2 (0.3 g), $ZnBr_2$ (0.71 mmol, 0.16 g), 90°C, atmospheric pressure air, rate of stirring 800 rpm. Allylic products=∑ (1-decen-3-one, 1-decen-3-ol, 2-decenal, 2-decen-1-ol). Others=∑ (C_7+C_8+C_9 acids, C_8+C_9 aldehyde, C_7+C_8 alcohols, 3-nonen-1-ol, 3-nonanone, cyclododecane, 2-decenoic acid, bromoalcohol). Error bars indicate range of data based on three repeat experiments.

5.2.7. Epoxidation of 1-decene in the presence of Imid/SiO_2

The epoxidation of 1-decene reaction was carried out in the presence of Imid/SiO_2 using 1% Au/TiO_2 or 1% Au/SiO_2 and a small amount of AIBN at 90°C for 24 h under atmospheric pressure of air (Table 5.14). When using 1% Au/TiO_2 and 0.2 g of Imid/SiO_2, the conversion of 1-decene decreased slightly from 13% to 8%, as well as reducing the epoxide selectivity from 34% to 22%. A further increase in the amount of Imid/SiO_2 to 0.4 g resulted in a further reduction in conversion to 5% and epoxide selectivity to 9%. A similar observation was found with 1% Au/SiO_2 in the presence of Imid/SiO_2 where the conversion reduced from 13% to 7% and epoxide selectivity decreased from 34% to 22%, as shown in Table 5.14. These observations suggest that Imid/SiO_2 had a negative effect on the epoxidation reaction.

Table 5.14: Study the effect of Imid/SiO_2 on 1-decene epoxidation step

Catalyst	Conversion (%)	Selectivity (%)			
		Epoxide	Allylic products	Diol	Others
1% Au/TiO_2	13	34	30	2	24
1% Au/TiO_2+Imid/SiO_2 (0.2 g)	8	22	33	4	30
1%Au/TiO_2+ Imid/SiO_2 (0.4 g)	5	9	35	6	35
1% Au/SiO_2	13	34	28	1	27
1% Au/SiO_2+ Imid/SiO_2 (0.2 g)	7	22	34	4	33

Reaction conditions: 1% Au/support (0.1 g), 1-decene (53 mmol, 10 mL), AIBN (0.036 mmol, 6 mg), 90°C, reaction time 24 h, atmospheric pressure air, rate of stirring 800 rpm. Allylic products=∑ (1-decen-3-one, 1-decen-3-ol, 2-decenal, 2-decen-1-ol). Others=∑ (C_7+C_8+C_9 acids, C_8+C_9 aldehyde, C_7+C_8 alcohols, 3-nonen-1-ol, 3-nonanone, cyclododecane, 2-decenoic acid, epoxide ring opening products).

Therefore, as seen in the previous results, the combination of the supported gold catalysts with any catalysts for the cycloaddition step under epoxidation conditions gave only small amounts of the epoxide.

5.2.8. Cycloaddition of CO_2 with 1,2-epoxydecane in the presence of supported gold catalysts

As mentioned earlier, it is important to study the compatibility between the catalysts for the epoxidation and cycloaddition steps before coupling them in a one-pot reaction; therefore, the cycloaddition of CO_2 with 1,2-epoxydecane reaction was conducted in the presence of 1% Au/G, 1% Au/hydrotalcite, 1% Au/MgO, 1% Au/TiO_2 and 1% Au/SiO_2, as shown in Table 5.15. It can be seen that supported gold catalysts were not active during CO_2 cycloaddition with epoxide. Furthermore, the presence of the supported gold catalysts had no influence on the catalytic performance of Bu_4NBr in the cycloaddition of CO_2 with 1,2-epoxydecane oxide (Table 5.15).

Table 5.15: Cycloaddition of carbon dioxide with 1,2-epoxydecane using different catalysts: activity data

Catalyst	T (°C)	Time (hour)	Conversion (%)	Cyclic carbonate selectivity (%)
Blank	80	4	0	0
Hydrotalcite	80	4	1	0
1% Au/hydrotalcite	80	4	1.9	2.1
MgO	80	4	2	0
1% Au/MgO	80	4	2	2.5
Graphite	80	4	0	0
1% Au/G	80	4	1	0
TiO_2	90	4	0	0
1% Au/TiO_2	90	4	1	0
SiO_2	90	4	0	0
1% Au/SiO_2	90	4	1	0
Bu_4NBr (0.62 mmol, 0.2 g) + $ZnBr_2$ (0.335 mmol, 0.08 g)	80	4	98	98
1% Au/SiO_2+ Bu_4NBr (0.62 mmol, 0.2 g) + $ZnBr_2$ (0.335 mmol, 0.08 g)	80	4	98	98
1% Au/TiO_2+ Bu_4NBr (0.62 mmol, 0.2 g) + $ZnBr_2$ (0.335 mmol, 0.08 g)	80	4	98	97

Reaction conditions: catalyst (0.2 g), 1,2-epoxydecane (26.88 mmol, 5 mL), 20 bar CO_2, rate of stirring 800 rpm.

5.2.9. Direct synthesis of cyclic carbonate starting from 1-decene

Despite the usefulness and interest in direct synthesis of cyclic carbonate from alkene, few studies have been published in the literature. The reason might be the need for compatibility between general conditions, components and catalysts for both reactions. The epoxidation and cycloaddition reactions were investigated separately to find the optimum reaction conditions for the one-pot system. From the previous results, it was found that Bu_4NBr and $ZnBr_2$ have a negative effect on the epoxide selectivity. Therefore, the one-pot synthesis of cyclic carbonate from 1-decene, O_2 and CO_2 using 1% Au/support-$Bu_4NBr/ZnBr_2$ catalysts was carried out, employing the one pot multistep process (sequential oxidation and carboxylation) as well as the one-pot process (simultaneous oxidation and carboxylation). The results are summarised in Table 5.16. For the direct synthesis of cyclic carbonate in the one-pot (simultaneous oxidation and carboxylation), 1% Au/support, a small amount of AIBN, Bu_4NBr-$ZnBr_2$, 1-decene, O_2 and CO_2 were added into the same reactor at the same time. From Table 5.16 it can be seen that the selectivity for cyclic carbonate is sensitive to the reaction temperature and time. At 80°C, when using 0.2 g of Bu_4NBr and 0.08 g $ZnBr_2$, only around 3% selectivity for cyclic carbonate was observed with reduced epoxide selectivity. However, a further

increase in the temperature to 90°C and in the amount of Bu_4NBr and $ZnBr_2$ to 0.4 g and 0.16 g respectively led to a further increase in the conversion of 1-decene from 14% to 18% as well as an increase in carbonate selectivity from 3% to 8% with a concomitant decrease in epoxide selectivity (Table 5.16). Further increasing in the reaction time led to a slight increase in 1-decene conversion to 20% but had no notable effect on the cyclic carbonate selectivity. The remaining products observed beside cyclic carbonate are from the epoxidation step and a few products from opening the epoxide ring.

Interestingly, higher selectivity of the desired cyclic carbonate product could be achieved by changing to a multistep protocol in which CO_2, Bu_4NBr and $ZnBr_2$ are subsequently added into the reactor after the epoxidation of 1-decene is completed. The epoxidation of 1-decene under atmospheric pressure of air or under 15 bar O_2 using 1% Au/SiO_2 in the absence of CO_2 gave 1,2-epoxydecane with a selectivity of 34% and 19% respectively (Table 5.16). The formed epoxide was converted to the cyclic carbonate after the addition of Bu_4NBr and $ZnBr_2$ catalysts and CO_2. When the reaction was carried out in the one-pot multistep system and epoxidation reaction was carried out under atmospheric pressure of air (epoxide selectivity 34%), there was an improvement in the selectivity for cyclic carbonate to 24%. Epoxidation of 1-decene under 15 bar O_2 became less selective for the epoxide (only 19%) and when the reaction was carried out in the one pot multistep system, 9% selectivity for cyclic carbonate was achieved. Therefore, the one-pot multistep process, where the epoxidation reaction carried out under atmospheric pressure of air, showed good selectivity for cyclic carbonate. Whenever the yield of 1,2-epoxydecane is high, cyclic carbonate is produced under these conditions. As a result, it can be suggested that the efficiency of the cyclic carbonate synthesis in an one-pot process would be determined mostly by the catalytic performance of the supported gold catalyst. Hence, if we find more active and selective catalysts for the 1-decene epoxidation reaction, then it will be a more effective catalyst system for the one-pot multistep reaction (sequential oxidation and carboxylation).

A similar observation was also made with 1% Au/TiO_2 catalyst; as shown in Table 5.16, the epoxide selectivity from epoxidation step was 34%, then after adding the co-catalysts and CO_2, cyclic carbonate was produced with 22% selectivity**.**

Table 5.16: Direct synthesis of cyclic carbonate starting from 1-decene using 1% Au/support-$Bu_4NBr/ZnBr_2$

Reaction starting with 1-decene	T (°C)	1-Decene conversion (%)	Selectivity (%)	
			Epoxide	Cyclic carbonate
One-pot reaction [a, b]: 15 bar O_2+ 15 bar CO_2 (26 h)	80	14	5	3
	90	18	2	8
One pot reaction: 15 bar O_2+ 15 bar CO_2 (28 h)	90	20	3	8
One pot multi-step reaction [c]: (epoxidation under 15 bar O_2)	90	24	2 (19) [e]	9
One pot multi-step reaction: (epoxidation under atmospheric pressure of air)	90	14	3 (34) [e]	24
One pot multi-step reaction: (epoxidation under atmospheric pressure of air) [d]	90	14	3 (34) [e]	22

Reaction conditions: 1% Au/SiO_2 (0.1 g), Bu_4NBr (1.24 mmol, 0.4 g), $ZnBr_2$ (0.71 mmol, 0.16 g), 1-decene (53 mmol, 10 mL), AIBN (0.036 mmol, 6 mg), 24 h reaction time for epoxidation, 4 h reaction time for cycloaddition of CO_2 with the formed 1,2-epoxydecane, 20 bar CO_2 for the one-pot multi step, rate of stirring 800 rpm. (a) One pot reaction: 1% Au/SiO_2, AIBN, Bu_4NBr, $ZnBr_2$,1-decene, O_2 and CO_2 added into the same reactor at the same time. (b) Bu_4NBr (0.62 mmol, 0.2 g), $ZnBr_2$ (0.355 mmol, 0.08 g). (c) One pot multi-step reaction: Bu_4NBr, $ZnBr_2$ and CO_2 are subsequently added into the same reactor after the epoxidation of the 1-decene is completed. (d) 1% Au/TiO_2 (0.1 g) used instead of 1% Au/SiO_2. (e) Selectivity for the epoxide in the epoxidation reaction.

As a result of avoiding interaction between the catalysts themselves for the two steps and intermediate product by addition of catalysts at a different stage, the one-pot multistep synthetic protocol was viewed as a more attractive and practical route for the oxidative carboxylation of 1-decene and CO_2 catalysed by 1% Au/support-$Bu_4NBr/ZnBr_2$ catalytic system. This observation is in agreement with a previous study for direct synthesis of cyclic carbonates from 1-octene [30]. They found that the addition of Bu_4NBr prevented the epoxidation reaction and the expected cyclic carbonate was not obtained. However, a very high yield of cyclic carbonate could be achieved by changing the one pot reaction to a multistep protocol [30].

5.2.10. Proposed mechanism for direct synthesis of cyclic carbonate from 1-decene

The one-pot synthesis of cyclic carbonates through a multistep process is viewed as the combination of epoxidation and cycloaddition reactions catalysed by their respective catalysts. Therefore, the mechanism of direct synthesis of cyclic carbonate from 1-decene over 1% Au/support-$Bu_4NBr/ZnBr_2$ catalysts is proposed in Scheme 5.4. The mechanism of the epoxidation reaction catalysed by supported gold catalysts was studied previously by our group [51] and explained in more detail in Chapters 3. Over a supported gold

catalyst in the presence of AIBN as radical initiator, the radical abstracts an allylic hydrogen atom from the 1-decene molecule and produces the allylic radical (1), which further reacts with oxygen to produce peroxy radical (2). This peroxy species reacts with 1-decene molecule to produce hydroperoxide (3) and one mole of C_{10} radical (1) again. When a supported gold catalyst is present in the reaction mixture, the hydroperoxide thus formed completes the reaction to produce allylic and epoxide products *via* (4) and (5) respectively. The formed epoxide coordinates to $ZnBr_2$ to form the adduct of zinc-epoxide complex and Bu_4NBr cation coordinates with the oxygen atom of the coordinated epoxide, which results to open the epoxide ring and generate O^- species (7). The carbon atom of CO_2 is partially positive and the oxygen atoms are partially negative. Therefore, the carbon atom of the carbon dioxide is attacked by this newly formed O^- to give $NBu_4OCOOCHRCH_2Br$ (9) as the key intermediate. The bond Zn-O breaks then cyclises to yield the CC and regenerate the catalyst.

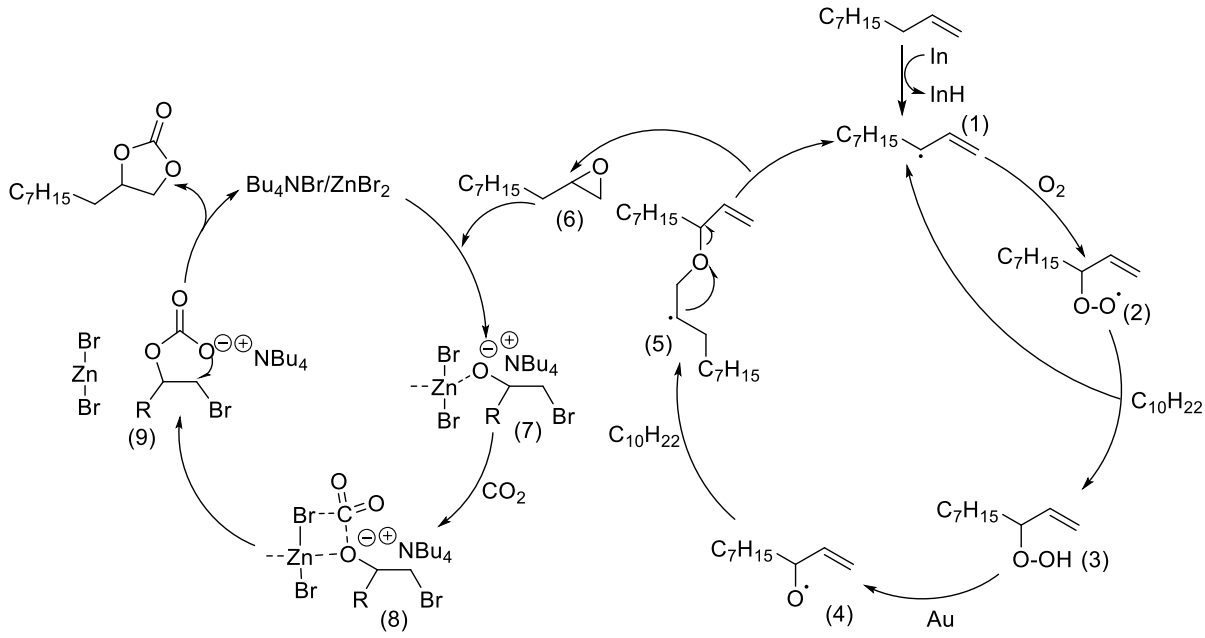

Scheme 5.4: Proposed mechanism for direct synthesis of cyclic carbonate from 1-decene. In: radical initiator, R: C_8H_{17}.

5.3. Cycloaddition of CO_2 with cycloalkene oxide

The epoxidation of cycloalkenes was investigated in more detail using supported gold and gold–palladium nanoparticles catalysts under solvent-free conditions, using air as the oxidant with a small amount of radical initiator [52]. A range of substrates varying the size of ring (C_5 to C_{12}) was tested and it was found that the selectivity for epoxide increased with increase in the ring size of cycloalkenes. In order to perform an one pot reaction, the cycloaddition of CO_2 with cycloalkene oxides reactions have been investigated. It has been demonstrated that the cycloaddition of CO_2 with various sized

cyclic alkene oxides can be completed using Bu_4NBr and $ZnBr_2$ without solvent. The reactivity of the cyclic alkene oxides is related to the ring size, with the smaller rings more reactive than the larger one using the same temperature (90°C). The selectivity for the cyclic carbonate is dependent on the size of the cyclic alkene oxide ring. In particular, the cyclic carbonate selectivity is lower with increasing the ring size of cycloalkene oxide. The experimental findings of cycloaddition of CO_2 with different cycloalkene oxides were verified with the DFT calculations as will be explained in the following Section.

5.3.1. DFT calculations for cycloaddition of CO_2 with cycloalkene oxide

The DFT calculations were completed by Luke T. Perrott and Dr. David J. Willock to consider the effect of ring size on the production of cyclic carbonate [53]. The reaction mechanism followed in the DFT calculations is similar to what was shown in scheme 5.2 for the incorporation of CO_2 into the epoxide catalysed by the quaternary ammonium salt and $ZnBr_2$ catalyst system. A $[Zn_2Br_5]^-$ anion is formed when the quaternary ammonium salt donates a Br^- that connects to one of the Zn centres of a dimer to create an active form. The epoxide first coordinates to the $[Zn_2Br_5]^-$ species via a dative bond with a Zn Lewis acid centre. The epoxide ring opening then follows the transfer of the bromide ion at the less hindered carbon atom of the epoxide. A carbonate intermediate is then formed when the CO_2 is incorporated, causing the ring to close, forming the cyclic carbonate product and regenerating the catalyst. In order to gain computational efficiency, Bu_4NBr was replaced by Et_4NBr as the counter ion and cyclopentene oxide was considered as a model reagent. Figure 5.12 shows calculated potential energy for each reaction stage. Chemical structure diagrams and atomic coordinates for each structure are shown in the Appendix 7.1, which also explained in more detail in our recent publication [53]. It is energetically favourable to co-ordinate the cyclopentene oxide to the Zn centre as this causes the system's energy to lower by around 87 kJ mol^{-1} (**Int. 1**). High energy transition states were found when the cyclopentene oxide ring opened in isolation when following the S_N1 pathway. The exact energy depends on the orientation of the resulting carbocation with respect to the $[Zn_2Br_5]^-$ complex with energies ranging between 38 and 46 kJ mol^{-1} higher than the reference state of the isolated reagents (**S_N1, TS-1t and S_N1,TS-1b**) and 133 kJ mol^{-1} above the co-ordinated epoxide (**Int. 1**). With the addition of a bridging or a terminal Br^- ion, the co-ordination of bromide ion to the three co-ordinate C atom which is exposed on the epoxide ring opening can occur. Figure 5.12 utilises 't' and 'b' labels to distinguish the terminal or bridging cases. A second barrier at 65 kJ mol^{-1} (**S_N1, TS-1b'**) is necessary when a bridging Br^- is added along the S_N1

pathway; however, no such barrier is required with a terminal Br^- ion, which leads to **Int. 2t**. Alternatively, the epoxide ring opening from **Int. 1** can follow pathways leading to transition states for a concerted S_N2 type mechanism in which the new C–Br bond is formed as the epoxide ring opens and these were found to be noticeably lower in energy. Similar to that shown in Figure 5.12, either a terminal or bridging Br^- ion can be used to promote the bromination of the epoxide carbon atom; however, a terminal Br^- ion was preferable as this allowed for the generation of a transition state whereby there was a simultaneous alignment of the Br^- nucleophile with the receiving C atom and stabilisation of the epoxide oxygen atom on the Lewis acid Zn centre. As a result, the terminal Br^- structure used in the S_N2 step (**S_N2, TS-1b**) generated an energy of −32 kJ mol^{-1} (**S_N2, TS-1t**) relative to the initial reference state whereas a structure with a bridging Br^- ion generated 18 kJ mol^{-1}. Depending on the formation of the new C-Br bond (either with the terminal (**Int. 2t)** or bridging Br^- ion **(Int. 2b)**), the intermediate formed following the bromination of the epoxide resulted in two possible chemical structures.

Four distinct intermediates are shown in Figure 5.12, as the configuration detail is dependent on the way the intermediate was formed. Nevertheless, the two intermediates with a bridging Br-C bond have a higher energy than those with a terminal Br^- ion. All four of the calculated structures have been followed the CO_2 insertion step. All four cases showed a lowering of energy following the initial co-ordination of CO_2 to give the **Int. 3** structures. Furthermore, relatively low barriers were found for the formation of a C-O bond between the C atom of the CO_2 and the oxygen atom originating from the epoxide (the **TS-2** structure set). There was a stabilisation of the transition state through its interaction with the Lewis acid catalyst as there was simultaneous coordination of the CO_2 oxygen atom to the Zn centre during the insertion of the CO_2 into the O-Zn bond. As a result, the generated structure had a bridging carbonate group between the Zn centre and the cyclopentane (**Int. 4b a**nd **Int. 4t).** From this, the Br^- anion returned to the $[ZrBr_5]^-$ cluster following ring closure of the cyclic carbonate as a result of the second C-O bond forming in the cyclic carbonate product. This second C-O bond in the cyclic carbonate product had a choice of oxygen atoms. From any of the **Int. 4** structures it possible to envisage the O atom endocyclic in the intermediate's metallocycle. This means that they will be coordinated to Zn and shift to bond to the C atom. Alternatively, if the C-O bond intermediate rotates, *exo*-cyclic O atom will be utilised for ring closure. Figure 5.12 shows this O atom choice with /e being added to the **TS3** transition state structure to denote exocyclic oxygen and /i to denote endocyclic oxygen. The lowest

energy transition state was found when **Int. 4t** utilised exocyclic oxygen to maintain the coordination with the Zn Lewis acid centre in the transition state. This generated an energy of −53 kJ mol^{-1} (**TS-3t'/e**) when compared to the starting point of the potential energy diagram in Figure 5.12. There was only a marginally higher energy generated with the first endocyclic transition (−49 kJ mol^{-1}); however, this was driven through the S_N1 pathway that has a high initial epoxide ring opening barrier (**S_N1 TS-1b'**). Significantly higher barriers were encountered when the intermediates use the Br^- bridging ion and/or Zn coordinating oxygen for ring closure, therefore suggesting that these pathways are not kinetically relevant. The low energy route for the cyclopentene oxide example through the potential energy diagram followed the S_N2 pathway for the ring opening step and used a terminal Br^- ion and an *exo*-cyclic oxygen for the ring closure step. This resulted in the generation of a cyclic carbonate with a *cis*-arrangement and alkyl ring structures in the product. Alternatively, where high barrier to reaction occurred, the trans-structure was found.

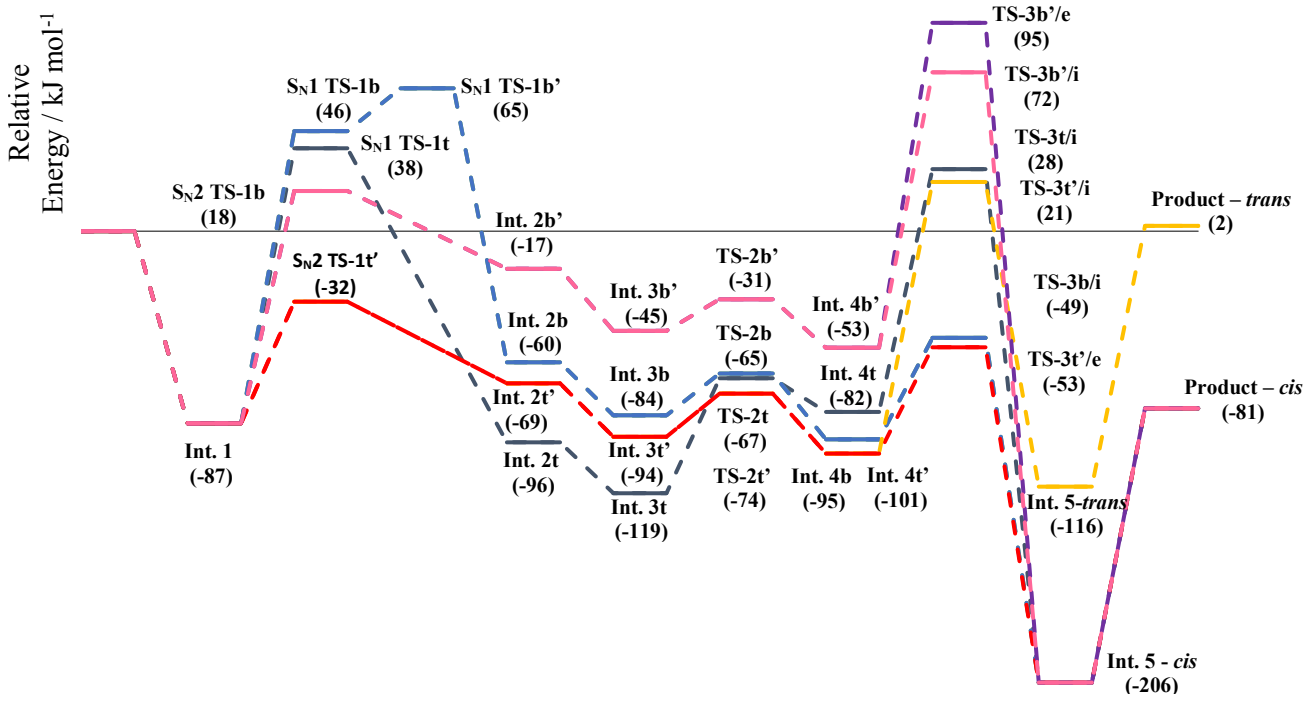

Figure 5.12: Calculated pathways for the addition of CO_2 with cyclopentene oxide to form a cyclic carbonate. Bracketed numbers are energies in kJ mol^{-1} relative to the starting reagents shown to the left.

5.3.2. Cycloaddition of CO_2 with cyclohexene oxide

Extensive studies were published for cyclic carbonate synthesis from epoxide and carbon dioxide as a starting material [19,54-56]. The effect of various reaction parameters such as reaction temperature, reaction time and catalysts mass on the cycloaddition of carbon dioxide with cyclohexene oxide were investigated**.** The target of studying these factors is to determine the most appropriate conditions which give the highest yield of cyclic carbonate. From Table 5.17, it is clear that in the absence of Bu_4NBr and $ZnBr_2$ no reaction occurred at 80°C and at 125°C only a 2% conversion with no observable cyclic carbonate product was seen. This confirms the importance of the Bu_4NBr and $ZnBr_2$ catalysts to produce cyclic carbonates. In the presence of Bu_4NBr and $ZnBr_2$ catalysts, 36% conversion of cyclohexene oxide and a 91% cyclic carbonate selectivity were found at 80°C. Increasing the reaction temperature from 80°C to 90°C resulted in an increase in the conversion from 36 to 43%. Selectivity for cyclic carbonate is independent of these reaction temperatures (80-90°C). A further increase in the reaction temperature to 125°C resulted in a conversion of 49% within 4 h. Increasing the reaction temperature from 80 to 125°C resulted in a similar selectivity for cyclic carbonate in the range (88%-91%). Furthermore, the mass of the catalyst also influences the performance of the reaction, as shown in Table 5.17. Increasing the catalyst mass of Bu_4NBr and $ZnBr_2$ from (0.2 g Bu_4NBr, 0.08 g $ZnBr_2$) to (0.4 g Bu_4NBr, 0.16 g $ZnBr_2$) resulted in an increase in the conversion from 43 to 51% respectively at 90°C. Selectivity for cyclic carbonate slightly decreased from 90% to 85% under these conditions due to the formation of small amounts of epoxide ring opening products. At 125°C when the catalysts mass was increased, a significant improvement in the conversion of cyclohexene oxide was observed from 49 to 80% respectively with a decrease in the cyclic carbonate selectivity from 88% to 83% respectively. Therefore, increasing the reaction temperature to 125°C and doubling the amount of the catalyst are important factors for increasing the conversion. Furthermore, increasing the reaction time from 4 to 8 hour enhanced the conversion from 80 to 89% with no significant effect in the cyclic carbonate selectivity (81-83%). When the reaction was performed for 16 h, 98% of conversion was observed and the cyclic carbonate selectivity slightly dropped to 80% and the formation of small amounts of other by-products such as 1,2-cyclohexanediol, 2-cyclohexene-1-ol and [1,1'-bi(cyclohexylidene)]-2-one was observed.

Table 5.17: Cycloaddition of CO_2 with cyclohexene oxide

Catalyst	T (°C)	Conversion (%)	Cyclic carbonate selectivity (%)	Cyclic carbonate yield (%)[c]
Blank	80	-	-	0
Bu_4NBr (0.2 g) + $ZnBr_2$ (0.08 g)	80	36	91	33
	90	43	90	39
Bu_4NBr (0.4 g) + $ZnBr_2$ (0.16 g)	90	51	85	43
Blank	125	2	-	0
Bu_4NBr (0.2 g) + $ZnBr_2$ (0.08 g)		49	88	43
Bu_4NBr (0.4 g) + $ZnBr_2$ (0.16 g)		80	83	66.4
Bu_4NBr (0.4 g) + $ZnBr_2$ (0.16 g)	125[a]	89	81	72
	125[b]	98	80	78.4

Reaction conditions: cyclohexene oxide (49.4 mmol, 5 ml), reaction time 4 h, 20bar CO_2, rate of stirring 800 rpm. (a) 8 h (b) 16 h. (c) Yield obtained by using GC analysis.

[1]HNMR characterisation of cis-cyclohexene carbonate is shown in Figure 5.13.

[1]H NMR (400 MHz, $CDCl_3$) δ 4.34 (dd, 2H, OCH), 1.54 – 1.48 (m, 2H, CH_2), 1.45 – 1.40 (m, 2H, CH_2), 1.19 – 1.11 (m, 2H, CH_2), 1.05 – 0.97 (m, 2H, CH_2) ppm.

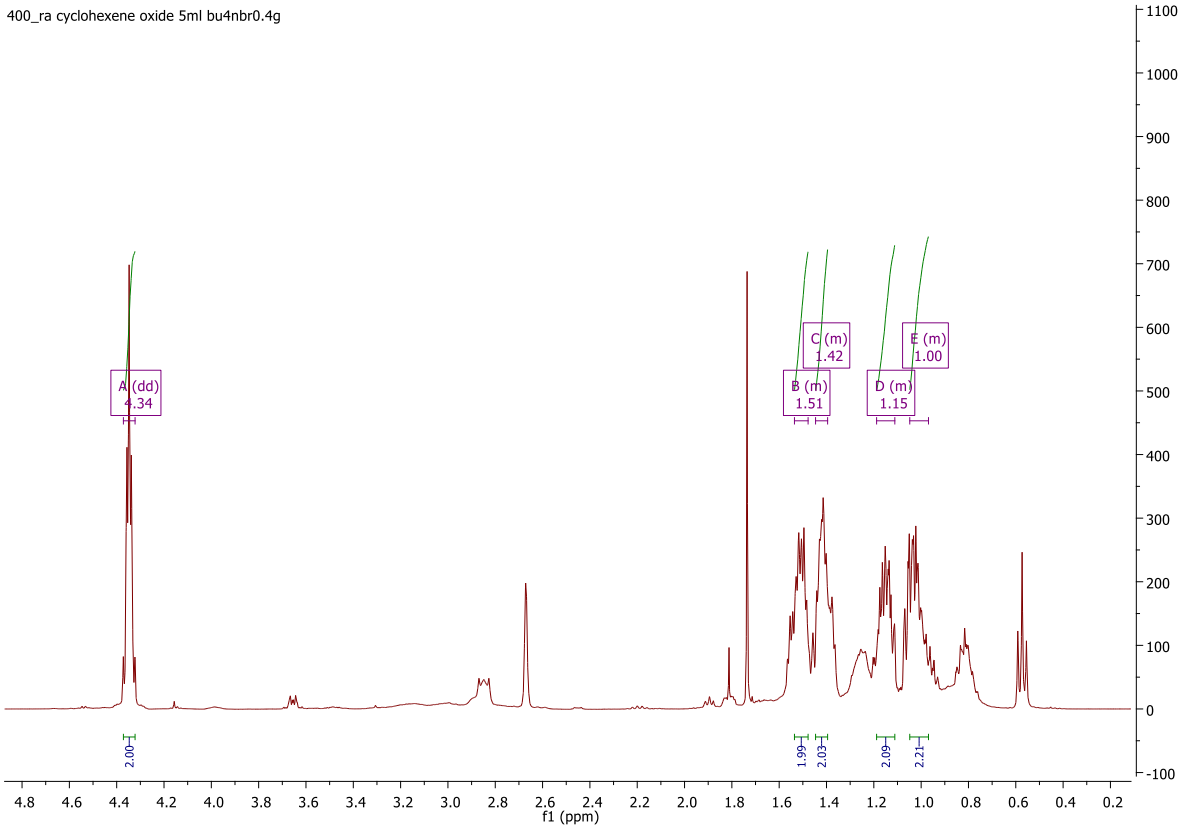

Figure 5.13:[1]H NMR spectrum in $CDCl_3$ of cis-cyclic cyclohexene carbonate.

The by-products can not be identified by NMR but they are detected by GC-MS. The spectroscopic data of GC-MS (obtained by Dr. Rebecca Engel) are described in more detail in the Appendix 7.2.1.

The overall target of this work is the direct synthesis of cyclic carbonate from cyclohexene, which consists of two sequential reaction in which the alkene is first oxidised to the epoxide and then the cyclic carbonate is formed by the reaction with CO_2. These initial reactions show how the cycloaddition of CO_2 with cyclohexene oxide can be optimised to achieve the highest yield of cyclic carbonate. However, for the epoxidation step, earlier work in our group has shown that the epoxidation of cyclohexene is not very selective for cyclohexene oxide using atmospheric oxygen with a small amount of TBHP as a radical initiator over a supported Au or Au-Pd catalysts [52]. Furthermore, it was observed that the higher epoxide selectivity was obtained when larger ring size, such as cyclooctene, was used as the substrate in the oxidation step [52]. Therefore, the investigation continued using cyclooctene oxide, which was formed in high selectivity in the epoxidation step.

5.3.3. Cycloaddition of CO_2 with cyclooctene oxide

Following a similar approach to that employed for cyclohexene oxide, different parameters such as reaction temperature and reaction time were investigated in the cycloaddition of CO_2 with cyclooctene oxide (Table 5.18) to determine the most appropriate conditions, which give the best reaction rate. The influence of temperature was tested over temperatures ranging from 90 to 150°C. After 4 h of reaction at 90°C no conversion of cyclooctene oxide was observed. When the reaction temperature increased from 90°C to 130°C, the conversion increased to 3%. However, no cyclic carbonate was formed and no consumption of CO_2 during the reaction was observed. The product identification by GC-MS (Appendix 7.2.2) indicates that cyclooctanone, cycloocatanol, and 1,2-cyclooctanediol were the major by-products. Furthermore, small amounts of tributylamine, a decomposition product of the quaternary amine catalyst, were found, which may indicate reaction with the Bu_4N^+ cation has taken place. In short reaction time of 4 h, alcohols were the predominant products (total selectivity 59%) with low selectivity for cyclooctanone (20%). With increasing the reaction time to 24 h at 130°C, there was a significant increase in the cyclooctanone selectivity to be 58%. Furthermore, the influence of the reaction time on the conversion of cyclooctene oxide was studied at different temperatures. At 130°C, at 4 h reaction time, 3% conversion was recorded, when the reaction time increased to 24 and 48 h, the conversion of 67% and 99% were obtained. Noticeably, an increase in the reaction time from 4 to 48 h resulted in an increase in selectivity for cyclooctanone from 20% to 61% respectively. Lewis acids are known to catalyse the conversion of epoxides to ketones following the Meinwald rearrangement mechanism [57]. DFT calculations suggest that this can take place through an H shift in intermediates such as **Int 2** (Figure 5.12). The results suggest that, under the reaction conditions used here, this H shift is considerably faster than CO_2 insertion for the cyclooctene oxide substrate [53]. In the case of 150°C, at 4 and 8 h reaction time, the conversion of cyclooctene oxide was 10% and 22% respectively. When the reaction time was prolonged to 16 and 24 h, the conversion significantly increased to 79% and 98% respectively. In general, it can be observed that with increase the reaction temperature and reaction time, the conversion of cyclooctene oxide increased from 3% to 98%. However, no cyclooctene carbonate was observed under any of the conditions used and no consumption of CO_2 during the reactions was observed. It was found in a previous study that the cycloaddition of CO_2 with cyclooctene oxide resulted in very low yield of cyclic carbonate at 180°C within 8 h using 4-dimetheylaminopyridine and lithium chloride as catalysts [33].

Table 5.18: Cycloaddition of CO_2 with cyclooctene oxide

Temperature (°C)	Reaction time (hour)	Conversion (%)	Selectivity (%)	
			Cyclic carbonate	Cyclooctanone
90	4	-	-	-
130	4	3	-	20
	24	67		58
	48	99	-	61
150	4	10		29
	8	22	-	36
	16	79	-	62
	24	98		61

Reaction conditions: cyclooctene oxide (39.6 mmol, 5 g), Bu_4NBr (1.24 mmol, 0.4 g), $ZnBr_2$ (0.71 mmol, 0.16 g), 20 bar CO_2, rate of stirring 800 rpm.

It was reported previously that the role of Bu_4NBr and $ZnBr_2$ is to open the epoxide ring and then activate CO_2 forming linear carbonate intermediate before cyclisation to cyclic carbonate [58]. However, in the case of cyclooctene oxide, no reaction occurred with CO_2 and that may due to high steric hindrance of cyclooctene oxide. Therefore, cycloaddition of CO_2 with cyclooctene oxide to form cyclic carbonate is challenging, and the structure of the cyclooctanone is significantly more stable than the cyclic carbonate.

5.3.4. Cycloaddition of CO_2 with different cycloalkene oxides

Cycloaddition of CO_2 with cyclohexene oxide and cyclooctene oxide have been studied and it was found that a smaller ring size of the cycloalkene oxide converts easily to corresponding cyclic carbonate. In order to confirm the observation of the effect of the ring size of cycloalkene oxide in this reaction, a range of different cycloalkene oxides have been studied. As expected, cycloalkene oxides with smaller ring size such as cyclopentene oxide, showed higher selectivity for cyclic carbonate (91%) at 90°C for 4 h reaction time. Moreover, a small amount of by-products were detected by GC-MS (Appendix 7.2.3) such as cyclopentanone, 1,2-cycopentanediol and 2-bromocyclopentanol which may result from the conversion of intermediates such as **Int 2** in Figure 5.12 to alcohols before the Br^- anion returned to the catalyst [53]. In the

case of larger ring size cyclododecane oxide, even with increasing the reaction time from 8 to 16 h, no cyclic carbonate was produced, and cyclododecanone was the main product for this reaction (selectivity greater than 95%). This is in line with the cyclooctene oxide results. Therefore, it can be demonstrated that with increasing ring size of the cycloalkene oxide, the selectivity towards the corresponding cyclic carbonate decreased and from the C_8 and larger ring size, there is no formation of the cyclic carbonate at all.

Table 5.19: Cycloaddition of CO_2 to different cycloalkene oxides

Substrate	T (°C)	Reaction time (hour)	Conversion (%)	Cyclic carbonate Selectivity (%)	Cyclic carbonate yield (%)
Cyclopentene oxide	90	4	58	91	53
Cyclohexene oxide	125	4	80	83	66.4
Cyclooctene oxide	150	8	22	-	0
Cyclododecane oxide	150	8	13	-	0
		16	48	-	0

Reaction conditions: cycloalkene oxide (26.0-57.3 mmol, 5 ml), Bu_4NBr (1.24 mmol, 0.4 g), $ZnBr_2$ (0.71 mmol, 0.16 g), 20 bar CO_2, rate of stirring 800 rpm.

5.4. The oxidative carboxylation of cycloalkenes

The oxidative carboxylation of cycloalkenes is a challenge. From Table 5.20 it can be noted that starting with cycloalkenes with smaller ring size, it becomes less selective for the epoxide [52]. With increasing the ring size, the epoxide selectivity significantly increased ($C_5<C_6<C_7<<C_8$) using supported gold and gold-palladium catalysts under solvent-free conditions using air as the oxidant [52]. The reason behind this observation is that for the cyclopentene system, the barrier to ring closure to form the cyclopentene oxide was 13 kJ mol^{-1} higher than that for the cyclooctene case [52]. However, regarding the cycloaddition of CO_2 with a range of different cycloalkene oxides, it was found the opposite trend to that in the epoxidation step as shown in Table 5.20. Cyclopentene oxide and cyclohexene oxide have given high selectivity for the cyclic carbonate. However, the insertion of CO_2 in carbonylation of cyclooctene oxide and cyclododecane oxide to form cyclic carbonates is a challenging step, and the structure of ketone is significantly more stable than cyclic carbonate due to the steric hindrance. This suggests that the direct conversion of cycloalkenes to cyclic carbonates is probably only possible for cycloalkenes with a ring size below 8 under these reaction conditions.

Table 5.20: Epoxidation/Carboxylation of different cycloalkenes/cycloalkene oxides

Alkene/Epoxide	Catalyst	Reaction time (h)	T (°C)	Conversion (%)	Selectivity (%)	
					Epoxide	Cyclic carbonate
Cyclopentene	1% Au/G	24	30	8.3	10.9	-
Cyclohexene			60	11.6	5.9	-
Cyclooctene			80	6.8	86	-
Cyclododecene			120	10.2	60.5	-
Cyclopentene Oxide	Bu_4NBr (0.4 g) +$ZnBr_2$(0.16 g)	4	4	58	-	91
Cyclohexene oxide		16	125	98	-	80
Cyclooctene oxide		16	150	79	-	0
Cyclododecane oxide		16	150	48	-	0

5.5. Conclusions

Oxidative carboxylation of olefins is a remarkably economical method because of the use of low-priced olefins as starting materials as well as minimising the use of chemicals, waste production and processing time. The oxidative carboxylation process consists of a combination of two sequential reactions: epoxidation of the olefin, and then the cycloaddition reaction of CO_2 to form epoxide in an one-pot reaction to produce cyclic carbonate. Cycloaddition of CO_2 with 1,2-epoxydecane was studied under solvent-free conditions using different homogeneous and heterogeneous catalysts. Bu_4NBr is the most active quaternary ammonium salts for cyclic carbonate synthesis from epoxides and carbon dioxide. High cyclic carbonate selectivity was achieved even in a short reaction time of 4 h at 80°C using 20 bar CO_2 under solvent-free conditions (as mentioned in Table 5.1). Different linear terminal epoxides have been easily converted to their corresponding cyclic carbonate under these conditions using Bu_4NBr and $ZnBr_2$ as catalysts (as shown in Table 5.5). When immobilising Bu_4NBr on different supports to synthesise heterogeneous catalysts, all the active components leached into the solution leading to the catalyst deactivation. The polydiallyldimethylammonium bromide supported catalysts were tested for this reaction as it was reported to share the effectiveness of Bu_4NBr. This catalyst could be recovered by simple centrifugation after the reaction. Increasing the

catalysts mass and reaction time resulted increasing the conversion of the epoxide. 40% PDDABr/SiO_2 can be reused with some decrease in the activity (as mentioned in Figure 5.5 and Figure 5.6). Imidazole supported onto silica has shown to be an effective catalyst for the cycloaddition of CO_2 with 1,2-epoxydecane to form cyclic carbonate under solvent-free conditions and the catalytic route is heterogeneous with some contribution from homogeneous catalysis.

The epoxidation of 1-decene reaction was conducted in the presence of Bu_4NBr, 40% PDDABr/SiO_2 or imidazole supported catalysts. The presence of these catalysts in the epoxidation reaction resulted in significant reduction in the selectivity for the epoxide. Furthermore, there was no effect from supported gold catalysts on the cycloaddition of CO_2 with 1,2-epoxydecane (as mentioned in Table 5.15). A simple and highly efficient preparation of cyclic carbonates was achieved by the use of 1%Au/support-$Bu_4NBr/ZnBr_2$ catalysts through a one-pot multistep process (sequential oxidation and carboxylation) as shown in Table 5.16.

The oxidative carboxylation process for a range of different cycloalkenes posed a challenge. Smaller ring size such as cyclopentene become less selective to the epoxidation and with an increase in the ring size, the epoxide selectivity significantly increased ($C_5<C_6<C_7<<C_8$). However, regarding the cycloaddition step, the opposite trend was found. Cyclopentene oxide and cyclohexene oxide gave high selectivity for cyclic carbonate. However, the cycloaddition of CO_2 with cyclooctene oxide and cyclododecane oxide to form cyclic carbonate was a challenging step and the structure of ketone is significantly more stable than cyclic carbonate due to the steric hindrance.

5.6. References

[1] Q. Liu, L. Wu, R. Jackstell and M. Beller, *Nat. Commun.*, 2015, **6**, 5933.

[2] S. Fukuoka, M. Kawamura, K. Komiya, M. Tojo, H. Hachiya, K. Hasegawa, M. Aminaka, H. Okamoto, I. Fukawa and S. Konno, *Green Chem.*, 2003, **5**, 497.

[3] A.-A. G. Shaikh and S. Sivaram, *Chem. Rev.*, 1996, **96**, 951.

[4] J. H. Clements, *Ind. Eng. Chem. Res.*, 2003, **42**, 663.

[5] T. Sakakura and K. Kohno, *Chem. Commun.*, 2009, 1312.

[6] A. Khan, L. Yang, J. Xu, L. Y. Jin and Y. J. Zhang, *Angew. Chem., Int. Ed.*, 2014, **53**, 11257.

[7] M. North, R. Pasquale and C. Young, *Green Chem.*, 2010, **12**, 1514.

[8] J. W. Comerford, I. D. V. Ingram, M. North and X. Wu, *Green Chem.*, 2015, **17**, 1966.

[9] C. Martín, G. Fiorani and A. W. Kleij, *ACS Catal.*, 2015, **5**, 1353.

[10] V. B. Saptal and B. M. Bhanage, *Curr. Opin. Green Sustainable Chem.*, 2017, **3**, 1.

[11] R. Martn and A. W. Kleij, *ChemSusChem*, 2011,**4**, 1259.

[12] S.-I. Fujita, B. M. Bhanage, Y. Ikushima, M. Shirai, K. Torii and M. Arai, *Catal. Lett.*, 2002, **79**, 95.

[13] R. L. Paddock and S. T. Nguyen, *J. Am. Chem. Soc.*, 2001, **123**,11498.

[14] X. B. Lu, Y. J. Zhang, K. Jin, L. M. Luo and H. Wang, *J. Catal.*, 2004, **227**, 537.

[15] Y. M. Shen, W. L. Duan and M. Shi, *J. Org. Chem.*, 2003, **68**, 1559.

[16] Y. J. Kim and R. S. Varma, *J. Org. Chem.*, 2005, **70**, 7882.

[17] H. Kawanami, A. Sasaki, K. Matsui and Y. Ikushima, *Chem. Commun.*, 2003, 896.

[18] H. S. Kim, J. J. Kim, H. Kim and H. G. Jang, *J. Catal.*, 2003, **220**, 44.

[19] K. Yamaguchi, K. Ebitani, T. Yoshida, H. Yoshida and K. Kaneda, *J. Am. Chem. Soc.*, 1999, **121**, 4526.

[20] K. Mori, Y. Mitani, T. Hara, T. Mizugaki, K. Ebitani and K. Kaneda, *Chem. Commun.*, 2005, 3331.

[21] T. Yano, H. Matsui, T. Koike, H. Ishiguro, H. Fujihara, M. Yoshihara and T. Maeshima, *Chem. Commun.*, 1997, 1129.

[22] M. Tu and R. J. Davis, *J. Catal.*, 2001, **199**, 85.

[23] M. Sankar, T. G. Ajithkumar, G. Sankar, P. Manikandan, *Catal. Commun.*, 2015, **59**, 201.

[24] M. Alvaro, C. Baleizao, D. Das, E. Carbonell and H. Garcia, *J. Catal.*, 2004, **228**, 254.

[25] T. Sakai, Y. Tsutsumi and T. Ema, *Green Chem.*, 2008, **10**, 337.

[26] Y. Xie, Z. F. Zhang, T. Jiang, J. L. He, B. X. Han, T. B. Wu and K. L. Ding, *Angew. Chem., Int. Ed.*, 2007, **46**, 7255.

[27] T. Takahashi, T. Watahiki, S. Kitazume, H. Yasuda and T. Sakakura, *Chem. Commun.*, 2006, 1664.

[28] P. A. Wender and F. E. McDonald. *Tetrahedron Lett.*, 1990, **31**, 3691.

[29] J. Sun, S.-I. Fujita, F. Zhao, M. Hasegawa and M. Arai, *J. Catal.*, 2005, **230**, 398.

[30] F. Chen, T. Dong, T. Xu, X. Li and C. Hu, *Green Chem.*, 2011, **13**, 2518.

[31] J. A. Verdol, US Patent 3,025,305, Mar. 13, 1962.

[32] H. Yasuda, L. N. He, T. Sakadura and C. Hu, J. Catal., 2005, 233, 119.

[33] V. Calo, A. Nacci, A. Monopoli and A. Fanizzi, *Org. Lett.*, 2002, **4**, 2561.

[34] P. Ramidi, P. Munshi, Y. Gartia, S. Pulla, A. S. Biris, A. Paul and A. Ghosh, *Chem. Phys. Lett.,* 2011, **512**, 273.

[35] K. Kossev, N. Koseva and K. Troev, *J. Mol. Catal. A: Chem.*, 2003, **194**, 29.

[36] J. M. Sun, S. Fujita, F.Y. Zhao, M. Hasegawa and M. Arai, *J. Catal.*, 2005, **230**, 43.

[37] J.-Q. Wang, K. Dong, W.-G. Cheng, J. Sun and S.-J. Zhang, *Catal. Sci. Technol.*, 2012, **2**, 1480.

[38] H. Xie, S. Li and S. Zhang, *J. Mol. Catal. A: Chem.*, 2006, **250**, 30.

[39] J. Sun, L. Wang, S. Zhang, Z. Li, X. Zhang, W. Dai and R. Mori, *J. Mol. Catal. A: Chem.*, 2006, **256**, 295.

[40] J. He, T. Wu, Z. Zhang, K. Ding, B. Han, Y. Xie, T. Jiang and Z. Liu, *Chem. Eur. J.*, 2007, **13**, 6992.

[41] H. Xie, H. Duan, S. Li and S. Zhang, *New J. Chem.*, 2005, **29**, 1199.

[42] S.-S. Wu, X.-W. Zhang, W.-L. Dai, S.-F. Yin, W.-S. Li, Y.-Q. Ren and C.-T. Au, *Appl. Catal. A*, 2008, **341**, 106.

[43] M. North, and R. Pasquale, *Angew. Chem.*, 2009, **121**, 2990.

[44] P. Tundo and M. Selva, *Green Chem.*,2005, **7**, 464.

[45] B. M. Bhanage, S. I. Fujita, Y. Ikushima and M. Arai, *Appl. Catal. A: Gen.*, 2001, **219**, 259.

[46] B. Song, L. Guo, R. Zhang, X. Zhao, H. Gan, C. Chen, J. Chen, W. Zhu and Z. Hou, *J. CO_2 Util.*, 2014, **6**, 62.

[47] X. Zhao and Y. Zhang, *Clean: Soil, Air, Water*, 2013, **41**, 37.

[48] W. Dai, L. Chen, S. Yin, W. Li, Y. Zhang, S. Luo and C. Au, *Catal. Lett.*, 2010, **137**, 74.

[49] J. Wang, X. Yue, F. Cai and L. He, *Catal. Commun.*, 2007, **8**, 167.

[50] W. Dai, L. Chen, S. Yin, S. Luo and C. Au, *Catal. Lett.*, 2010, **135**, 295.

[51] U. N. Gupta, N. F. Dummer, S. Pattisson, R. L. Jenkins, D. W. Knight, D. Bethell and G. J. Hutchings, *Catal. Lett.*, 2015, **145**, 689.

[52] H. Alshammari, P. J. Miedziak, D. W. Knight, D. J. Willock and G. J. Hutchings, *Catal. Sci. Technol.*, 2013, **3**, 1531.

[53] R. Alsaiari, L. T. Perrott, E. Nowicka, R. V. Engel, P. J. Miedziak, S. A. Kondrat, J. K. Edwards, D. J. Willock and G. J. Hutchings, *Catal. Sci. Technol.*, 2017, **7**, 1433.

[54] D. Xiang, X. Liu, J. Sun, F-S Xiao and J. Sun, *Catal. Today*, 2009, **148**, 383.

[55] T. Zhao, Y. Han and Y. Sun, *Phys. Chem. Chem. Phys.*, 1999,**1**, 3047.

[56] J. Q. Wang, D. L. Kong, J. Y. Chen, F. Cai and L. N. He. *J. Mol. Catal. A: Chem.*, 2006, **249**, 143.

[57] J. M. Fraile, J. A. Mayoral and L. Salvatella, *J. Org. Chem.*, 2014, **79**, 5993.

[58] D. J. Darensbourg and M. W. Holtcamp, *Coord. Chem. Rev.*, 1996, **153**, 155.

Chapter 6: Conclusions and future work

6.1. Conclusions

Carbon dioxide utilisation technology can contribute to reducing the CO_2 level by using carbon dioxide as a starting material and transforming it into valuable chemicals such as cyclic carbonates (CCs) [1, 2]. Cyclic carbonates are usually prepared *via* the cycloaddition reaction of CO_2 with an epoxide. Cyclic carbonates can be produced directly from CO_2 and olefins, which has been shown to be a remarkably economical method because of the use of low-priced olefins as starting materials and minimisation of the use of chemicals, waste production and processing time [3].

The one-pot synthesis of cyclic carbonate from olefin and CO_2 consists of two sequential reactions in one pot: epoxidation of the olefin, and the subsequent cycloaddition reaction of CO_2 to the formed epoxide. To obtain information about the roles of the catalyst components, epoxidation of 1-decene (first step) and the cycloaddition of CO_2 with 1,2-epoxydecane (second step) were conducted individually. In all of these studies, the reactions were carried out under solvent-free conditions. Therefore, this thesis was divided into different parts.

In Chapter 3, the liquid phase epoxidation of 1-decene using supported cobalt catalysts was reported. It was shown that supported cobalt catalysts are active in the epoxidation of 1-decene under solvent-free conditions in the presence of TBHP as a radical initiator and oxygen from air as the primary oxidant at 80°C. An investigation was conducted to determine how 1-decene oxidation was affected by the reaction temperature in the absence of both the radical initiator and the catalyst. The results indicated that 1-decene oxidation commenced instantly at a temperature of 110°C, whereas it did not commence when the temperature was lower than 100°C. The effect of the choice of radical initiator on the oxidation of 1-decene in the absence of a catalyst was then studied. TBHP exhibited the lowest activity at 80°C when compared to the other radical initiators (CHP, AIBN). Therefore, we decided to perform further studies using this particular initiator. A number of catalysts with cobalt loading from 0.5 to 10% were prepared and tested for 1-decene epoxidation and 2% Co/MgO was found to give the highest epoxide yield. Catalyst activity and stability are depending on the properties of the support. The most active and stable catalyst was found to be 2% Co/TiO_2. At the start of the reaction with reduced epoxide selectivity, the main products were allylic products (e.g. 1-decen-3-one, 1-decen-3-ol, 2-decenal, and 2-decen-1-ol). As the reaction time increased, the epoxide

selectivity improved, while the allylic products displayed a considerable reduction in selectivity. In the absence of TBHP and presence of the 2% Co/MgO catalyst, traces of the conversion were observed, which indicates the importance of the radical initiator in this reaction. Using 2,6-di-*tert*-butyl-4-methylphenol (BHT) as a radical scavenger leads to the termination of the reaction. This suggests free radicals are involved in the catalytic cycle in the liquid phase epoxidation of 1-decene. FTIR and XPS indicated the adsorption of products on the used catalyst surface resulting in decreased catalyst activity.

In Chapter 4, 1-decene epoxidation was performed over supported gold catalysts in the presence of a very small amount of radical initiator (AIBN, 6 mg) under mild, solvent-free conditions using oxygen as the oxidant. Oxidation did not occur in the absence of the radical initiators. Supported gold catalysts prepared by the sol-immobilisation method, which produced small particles of Au in the range 3–4 nm, displayed the highest activity and selectivity for the epoxide. The effect of O_2 pressure was studied and it was found that as the O_2 pressure increased, the conversion of 1-decene increased correspondingly, but no effect was detected on 1,2-epoxydecane selectivity. Gold nanoparticles were supported on graphite, TiO_2, SiO_2 and MgO. TiO_2 and SiO_2 supported gold catalysts showed the highest conversion and selectivity for 1,2-epoxydecane whereas the supports alone yielded low activity. Oxygen consumption in the reaction was validated by a reaction under a nitrogen gas atmosphere.

In Chapter 5, the cycloaddition of CO_2 with different epoxides was studied under solvent-free conditions with the use of both homogeneous and heterogeneous catalysts. For cyclic carbonate synthesised from epoxide and carbon dioxide, the quaternary ammonium salt with the highest activity was determined to be Bu_4NBr. High cyclic carbonate yield was achieved even in a short reaction time of 4 hours at 80°C using 20 bar CO_2 under solvent-free conditions. Furthermore, under such conditions, Bu_4NBr and $ZnBr_2$ as catalysts facilitated the conversion of various linear terminal epoxides into their corresponding cyclic carbonates. However, Bu_4NBr are dissolved in a reaction mixture containing CCs. Therefore, separation of the catalysts from the reaction mixture may require more energy through a purification process. The polydiallyldimethylammonium bromide supported catalysts were tested for this reaction as they share the effectiveness of Bu_4NBr and are insoluble in organic solvents, which would reduce the leaching of the active components in the liquid phase. This catalyst could be recovered by a simple centrifugation after the reaction. The production of cyclic carbonate could be enhanced by increasing the mass of the catalyst and reaction time. The reusability of a

40% PDDABr/SiO_2 catalyst was tested and some decrease in activity was found, which may be due to the adsorption of products on the surface or due to some leaching of the active species. Furthermore, it was observed that the main catalytic route is heterogeneous with some contribution from homogeneous catalysis. The formation of cyclic carbonate based on carbon dioxide cycloaddition with 1,2-epoxydecane was effectively catalysed by imidazole supported onto silica, the catalytic route exhibiting heterogeneity alongside partial input from homogeneous catalysis. Bu_4NBr or 40% PDDABr/SiO_2 or Imid/SiO_2 were present during the performance of 1-decene epoxidation, considerably diminishing epoxide selectivity. Furthermore, the cycloaddition of carbon dioxide with 1,2-epoxydecane was not affected by supported gold catalysts.

The one-pot synthesis of cyclic carbonate from 1-decene, O_2 and CO_2 using 1% Au/support-$Bu_4NBr/ZnBr_2$ catalysts was carried out, employing the one-pot multistep process (sequential oxidation and carboxylation) as well as the one-pot (simultaneous oxidation and carboxylation). Higher selectivity for cyclic carbonate product could be achieved by using one-pot multistep protocol. However, it was difficult to conduct the process of oxidative carboxylation for various cycloalkene oxides. Epoxide selectivity was low when the ring size was small (e.g. cyclopentene), but it improved substantially ($C_5<C_6<C_7<<C_8$) when the ring size was enlarged. However, regarding the cycloaddition step, the opposite trend was found. Cyclopentene oxide and cyclohexene oxide provided high selectivity for cyclic carbonate, whereas the cycloaddition of CO_2 with cyclooctene oxide and cyclododecane oxide to form cyclic carbonate was a challenging step and the structure of ketone is significantly more stable than cyclic carbonate due to the steric hindrance.

Therefore, starting with an inexpensive alkene instead of an expensive epoxide should be attractive as it will make the synthesis of cyclic carbonate economical as well as avoid the preliminary synthesis and isolation of the epoxide. For the epoxidation step, most published works used the reactive forms of oxygen. In this study, the reaction proceeds using oxygen as the primary oxidant under solvent-free green conditions. Performing this reaction under solvent-free conditions is a significant improvement as it decreases the level of waste as well as the level of toxicity. By using CO_2 as a chemical starting material rather than toxic phosgene, we would reduce the risk to the environment and contribute to the reduction of global warming.

6.2. Future work

The research described in this thesis has demonstrated epoxidation of the olefin, and the cycloaddition reaction of CO_2 to the epoxide. These two steps studied in more detail to find the optimum reaction conditions for the one-pot reaction. Based on the results of this research, it is recommended that further studies should be conducted on some of the topics in this thesis. To this end, it is recommended that the following areas be investigated to improve the activity and performance of catalysts in the epoxidation and cycloaddition steps.

6.2.1. Epoxidation of 1-decene using supported cobalt catalysts

- A cobalt nitrate precursor has been used for the preparation of supported cobalt catalysts. Using a different cobalt precursor may increase the activity and stability of cobalt catalysts.
- In the present research, cobalt catalysts have been prepared using a wet-impregnation method. However, other preparation methods which produce much smaller particles, such as sol-immobilisation, may lead to the synthesis of more active and selective catalysts for the epoxidation of 1-decene. When a catalyst is prepared by different preparation methods, it displays different catalytic activities. Investigation of this point, in addition to finding more active and selective catalysts for the epoxidation of 1-decene, would also help establish a general relationship between the structure of catalysts and catalytic reactivity.
- The heat treatment for this catalyst is calcination under static air at 400°C for 3 h. No other heat treatment conditions have been considered. Since it is an important factor that influences catalytic performance, reduction of cobalt may improve its activity and stability by reducing the leaching of supported cobalt catalysts.
- One of the main limitations, which arose during this study, concerned the reuse of cobalt catalysts. Upon reuse, the supported cobalt catalyst displayed reduced activity due to adsorption of the products. It is suggested that this issue could be addressed by improving the method of preparation as well as improving the washing step after use.
- A variation in activity and stability was observed with different supports. It is recommended that more research be carried out to examine and address this effect.

6.2.2. Epoxidation of 1-decene using supported gold catalysts

- Differences in activity and selectivity were observed when using different supports for an Au catalyst for the epoxidation of 1-decene. The importance of

support for Au catalysts for their effect is well known. Additional investigations on this point would examine the support effect as well as the interface effect between gold nanoparticles and supports and also the role of support during a reaction.

- There are a number of bimetallic systems which could be considered for optimising the activity of gold catalysts. There are some bimetallic systems which may provide more active or selective catalysts suitable for the epoxidation of alkenes, e.g. Au-Cu, Au-Ag and Au-Co. Additional consideration should also be given to developing a method of preparation for bimetallic systems.
- A detailed investigation of the preparation and optimisation of supported Au catalysts using different supports was conducted to achieve optimal Au catalytic activity. However, using a promoter which exhibits highly selective activity in other chemical processes in specific ratio with Au may help obtain a more selective catalyst for the epoxidation of alkenes.
- Epoxidation of 1-decene under atmospheric pressure of air exhibited high selectivity for the epoxide. It is worth to increase the air pressure and study its effect on the epoxidation reaction.

6.2.3. Cycloaddition of CO_2 with epoxide

- Bu_4NBr was found to be the best quaternary ammonium salt for the cycloaddition of CO_2 with different types of epoxides as a homogeneous catalyst. Determination of how to bind Bu_4NBr strongly with supports such as covalent bonding to make heterogeneous catalyst is further required.
- Study the effect of reduce the amount of Bu_4NBr and $ZnBr_2$ in cycloaddition of CO_2 with 1,2-epoxydecane.
- 40% PDDABr/SiO_2 and Imid/SiO_2 catalysts displayed good activity as heterogeneous catalysts. However, reused catalysts exhibited a decrease in activity that may be due to the adsorption of the products and remaining substrate on the catalyst surface. Therefore, additional investigation of the washing step for the reused catalyst may improve its activity.

6.2.4. Oxidative carboxylation of alkenes

- A higher yield of cyclic carbonate from 1-decene was found in a one pot multi-step (sequential oxidation and carboxylation) as compared to a one pot (simultaneous oxidation and carboxylation). Further research is recommended to

improve the selectivity for cyclic carbonate in this multi-step reaction by increasing the selectivity of the epoxide.

- It was shown that the catalysts for the second step have a negative effect on the epoxidation step. Therefore, in the oxidative carboxylation of alkene, it is recommended that a catalyst be identified for the cycloaddition step which does not start catalysis until the epoxidation step is finished. Such a catalyst would catalyse the CO_2 addition to the formed epoxide.

6.3. References

[1] Q. Liu, L. Wu, R. Jackstell and M. Beller, *Nat. Commun.*, 2015, **6**, 5933.

[2] L. L. Jin, H. W. Jing, T. Chang, X. L. Bu, L. Wang and Z. L. Liu, *J. Mol. Catal. A: Chem.*, 2007, **261**, 262.

[3] M. Sun, J. Fujita, S. I. Zhao, F. Hasegawa and M. Arai, *J. Catal.*, 2005, **230**, 398.

Chapter 7: Appendix

7.1. Chemical structure diagrams and atomic coordinates for DFT calculations

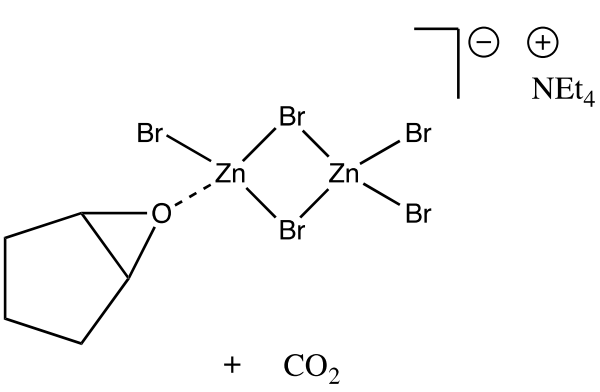

Int. 1

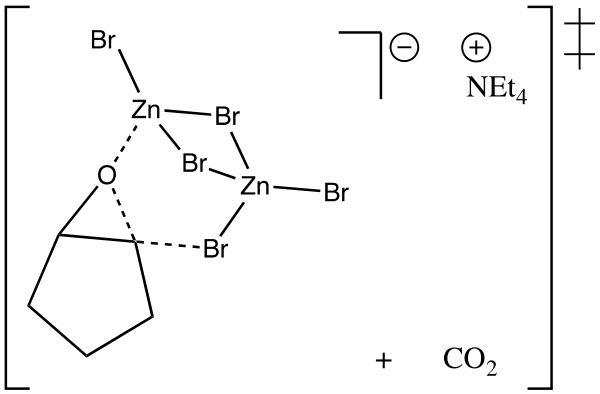

S_N2 TS-1t'

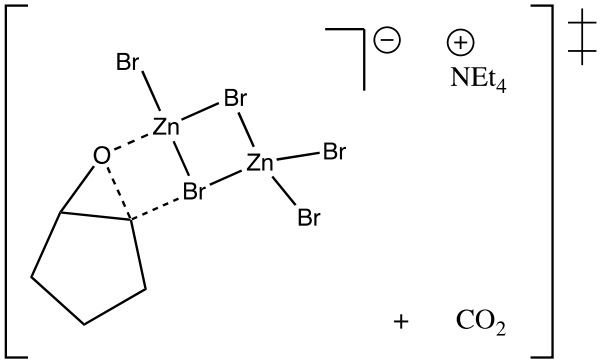

S_N2 TS-1b

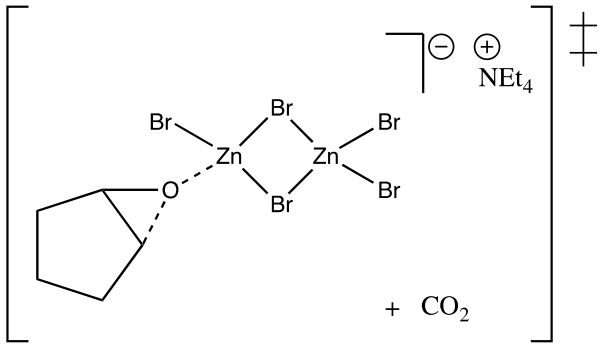

S_N1 TS-1t

S_N1 TS-1b

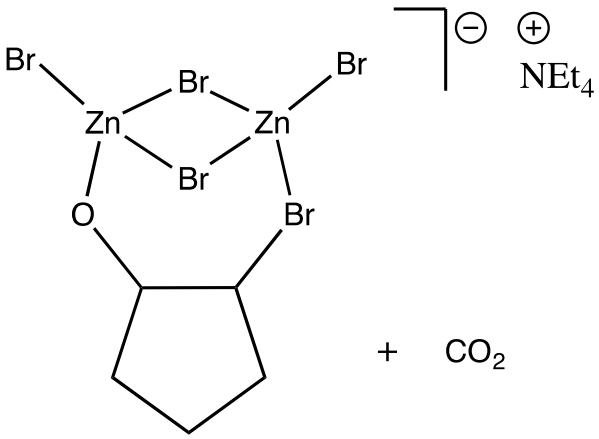

Int. 2t

Int. 2t'

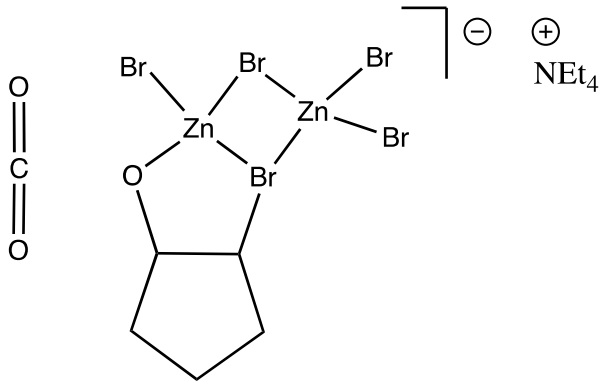

Int. 3b

Int. 3b'

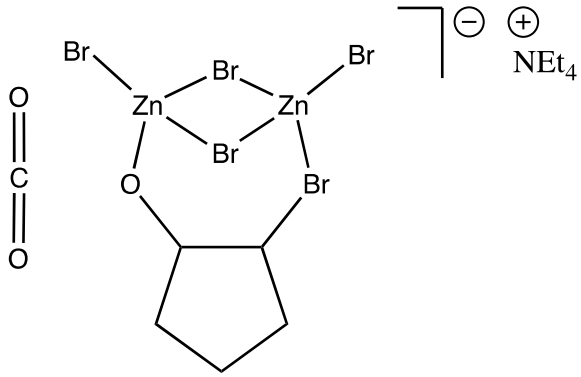

Int. 3t

Int. 3t'

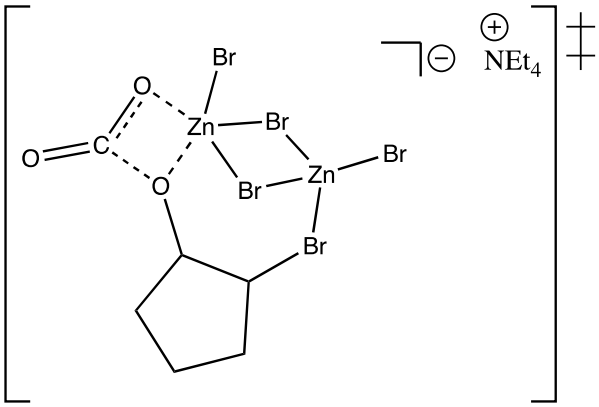

Int. 3t'

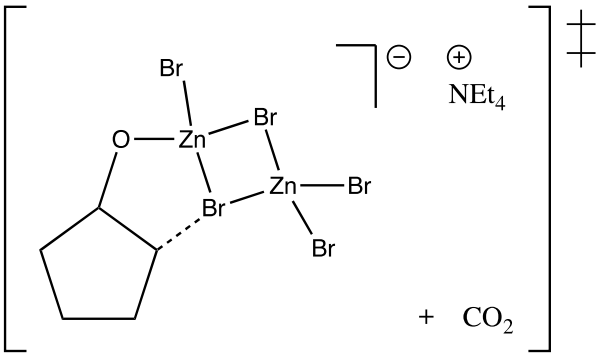

SN1 TS-1b'

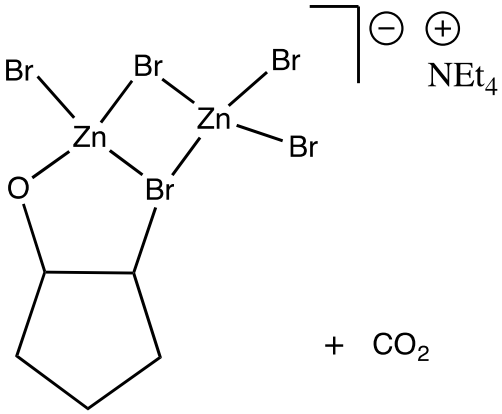

Int. 2b

Int. 2b'

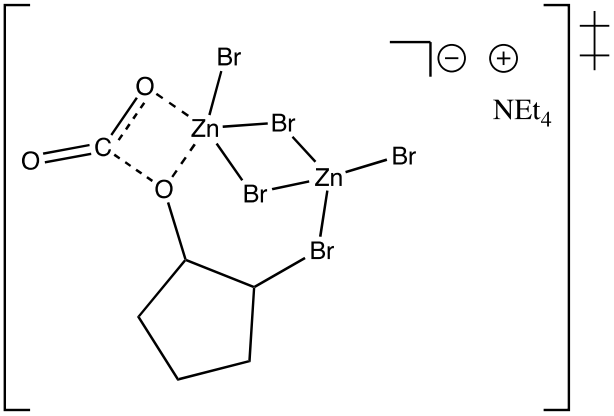

TS-2t

TS-2t'

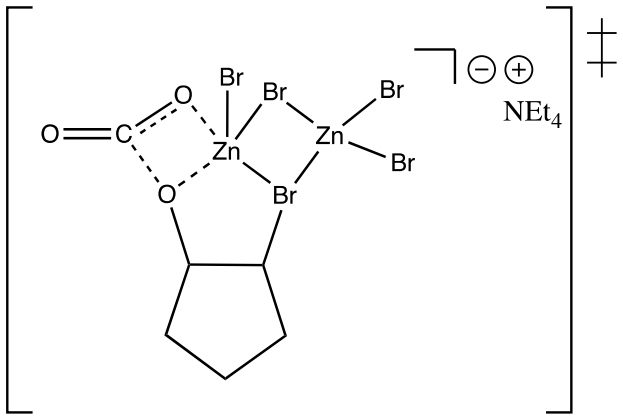

TS-2b

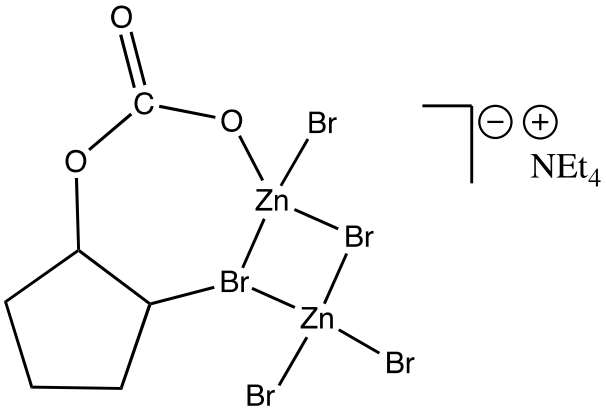

Int. 4b

Int. 4b'

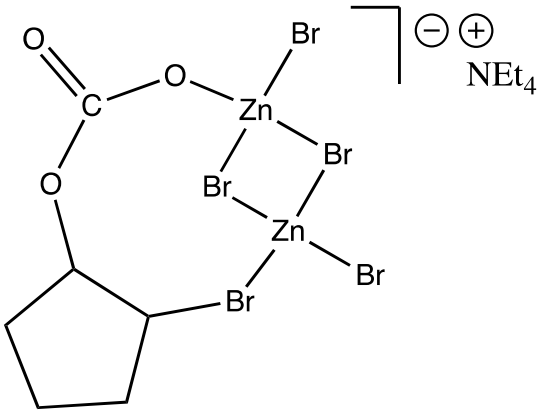

Int. 4t

Int. 4t'

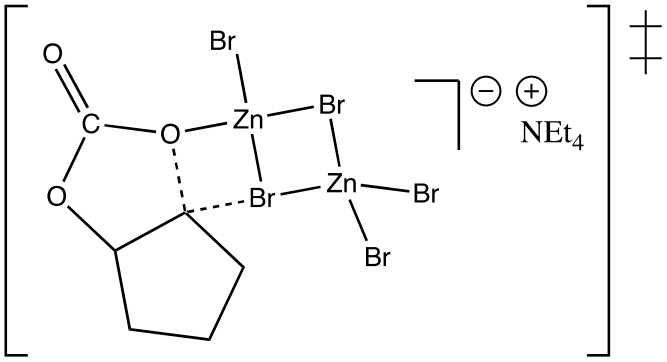

TS-3 (all)

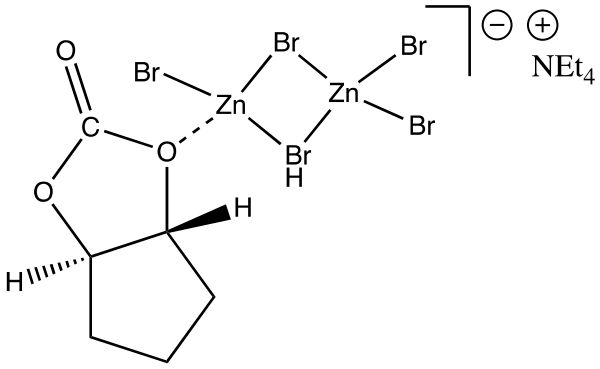

Int.5 - Trans

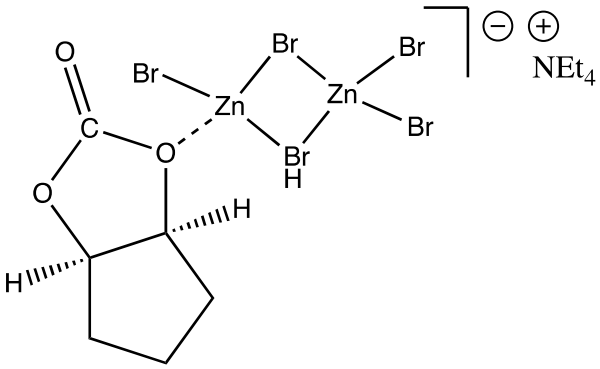

Int.5 – Cis

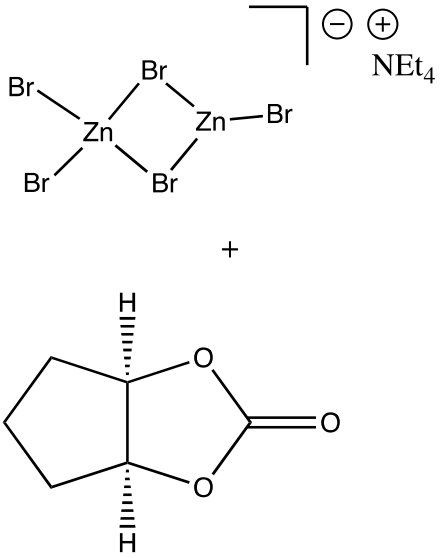

Product – Cis

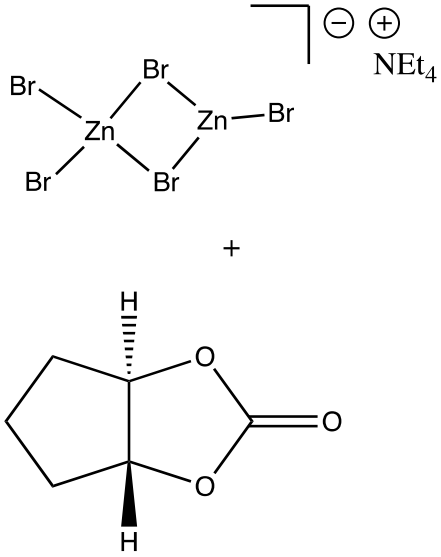

Product – Trans

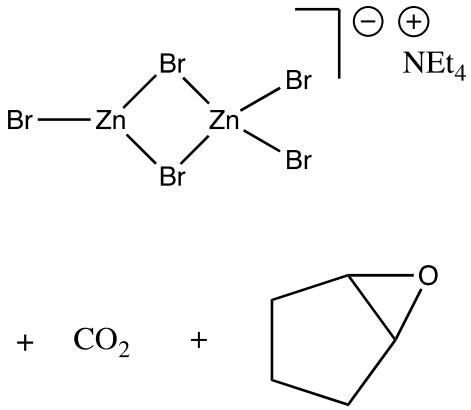

Isolated Reagents

7.2. Spectroscopic data for cycloaddition of CO_2 with different cycloalkene oxides: suggested assignments of products are shown on the spectra where it was possible.

7.2.1 Cycloaddition of CO_2 with cyclohexene oxide experiment (125°C, 20 bar CO_2, 16 h)

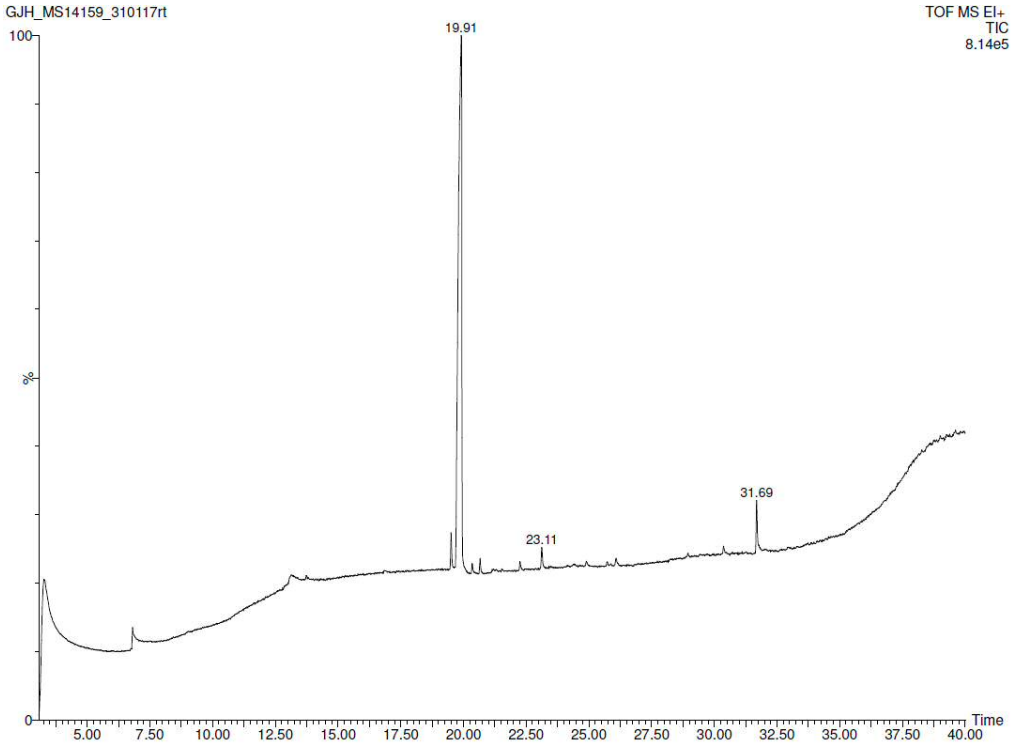

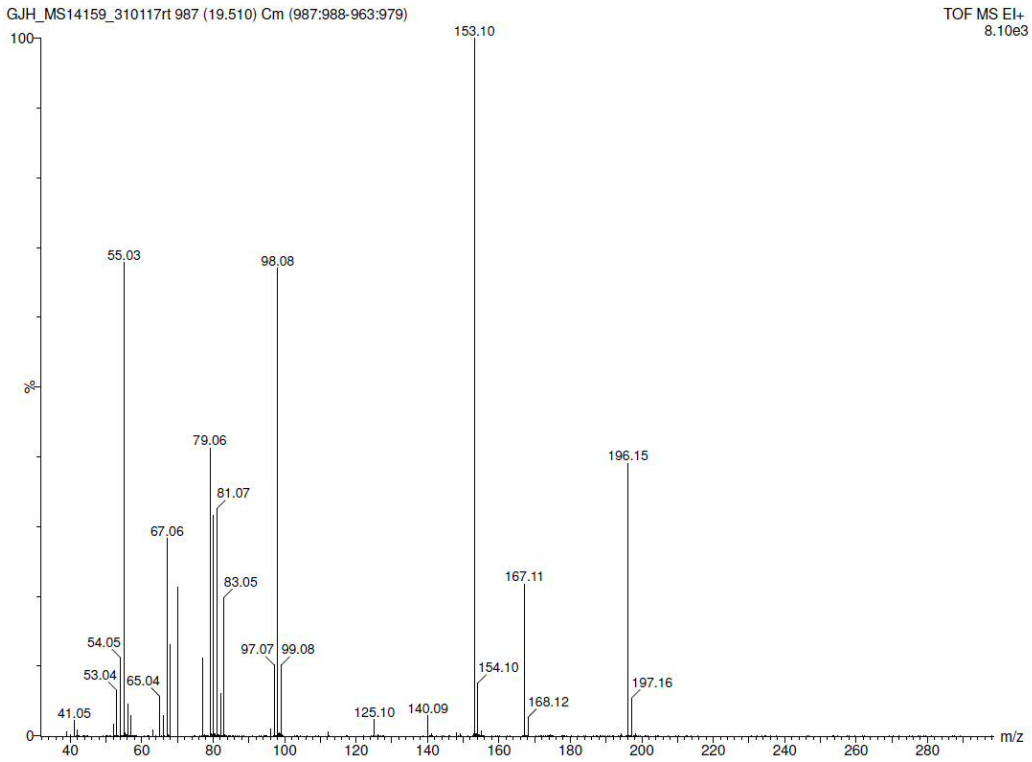

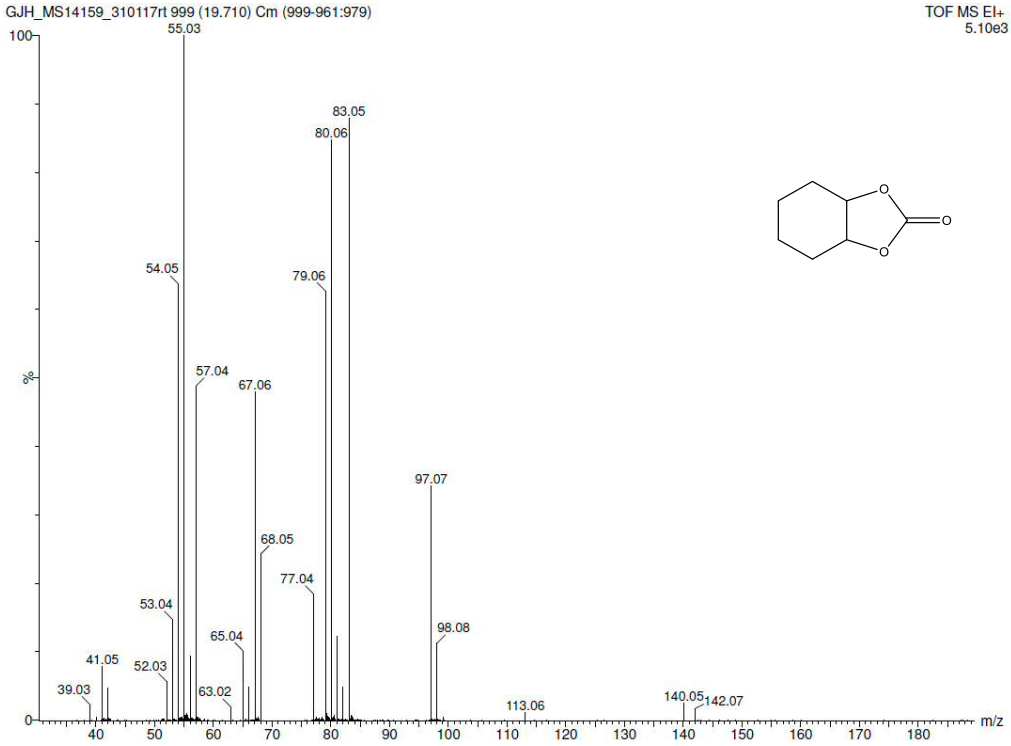
GJH_MS14159_310117rt 999 (19.710) Cm (999-961:979)
TOF MS EI+
5.10e3
100
%
0
55.03
83.05
80.06
54.05
79.06
57.04
67.06
97.07
68.05
77.04
53.04
98.08
65.04
41.05
52.03
39.03
63.02
113.06
140.05
142.07
40 50 60 70 80 90 100 110 120 130 140 150 160 170 180
m/z
O
O
O

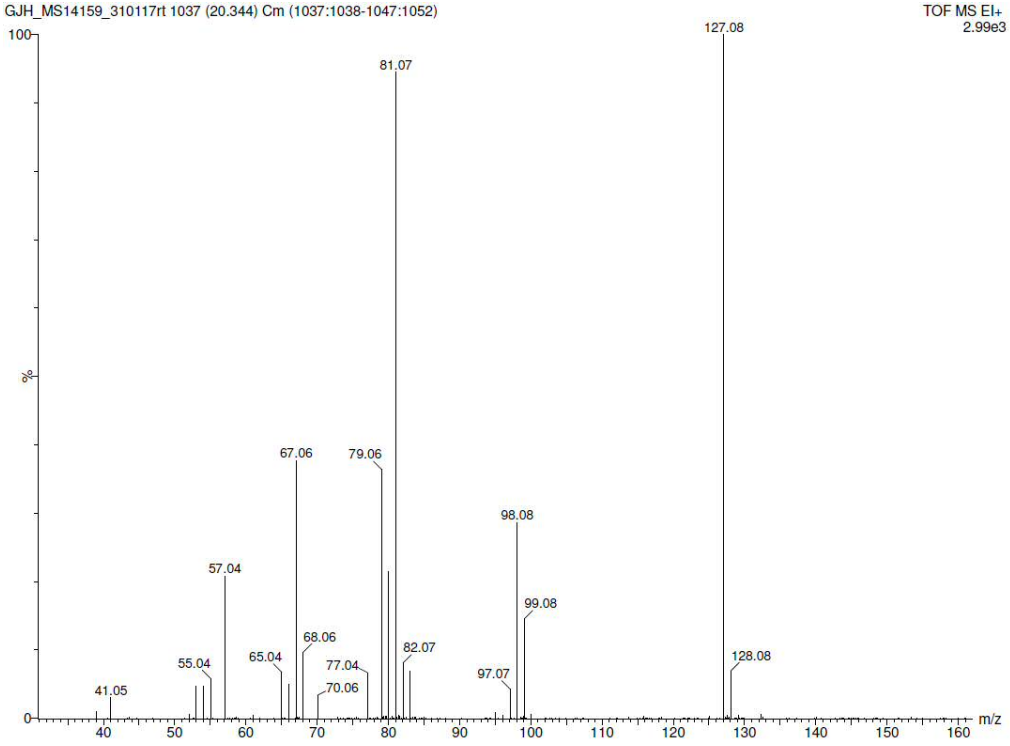
GJH_MS14159_310117rt 1037 (20.344) Cm (1037:1038-1047:1052)
TOF MS EI+
2.99e3
100
%
0
127.08
81.07
67.06
79.06
98.08
57.04
99.08
68.06
82.07
55.04
65.04
77.04
128.08
97.07
41.05
70.06
40 50 60 70 80 90 100 110 120 130 140 150 160
m/z

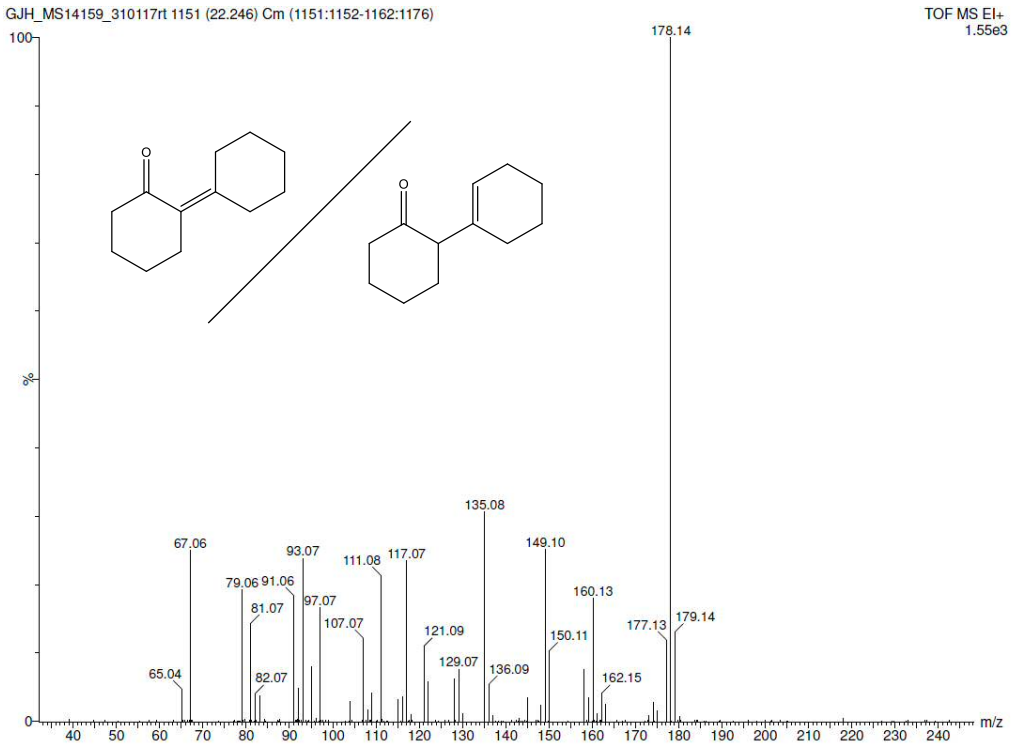
GJH_MS14159_310117rt 1151 (22.246) Cm (1151:1152-1162:1176)
TOF MS EI+
1.55e3
100
%
0
178.14
135.08
67.06
93.07
111.08
117.07
149.10
79.06
91.06
160.13
81.07
97.07
177.13
179.14
107.07
121.09
150.11
129.07
65.04
82.07
136.09
162.15
40 50 60 70 80 90 100 110 120 130 140 150 160 170 180 190 200 210 220 230 240
m/z

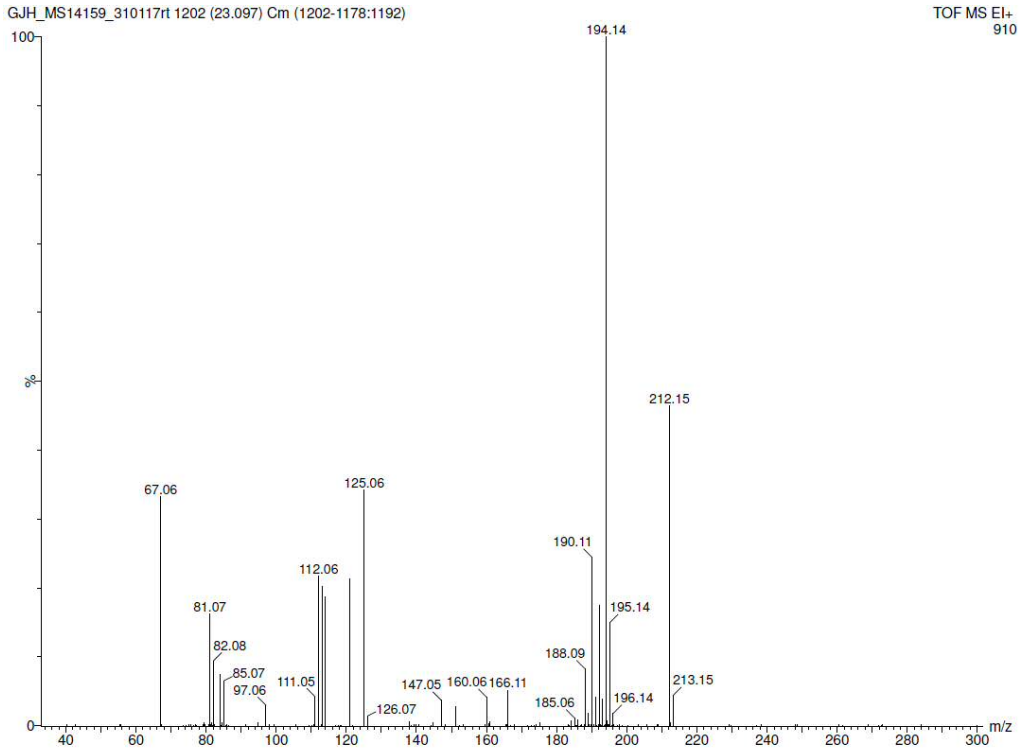
GJH_MS14159_310117rt 1202 (23.097) Cm (1202-1178:1192)
TOF MS EI+
910
100
%
0
194.14
212.15
67.06
125.06
190.11
112.06
81.07
195.14
82.08
188.09
85.07
111.05
147.05
160.06
166.11
213.15
97.06
126.07
185.06
196.14
40 60 80 100 120 140 160 180 200 220 240 260 280 300
m/z

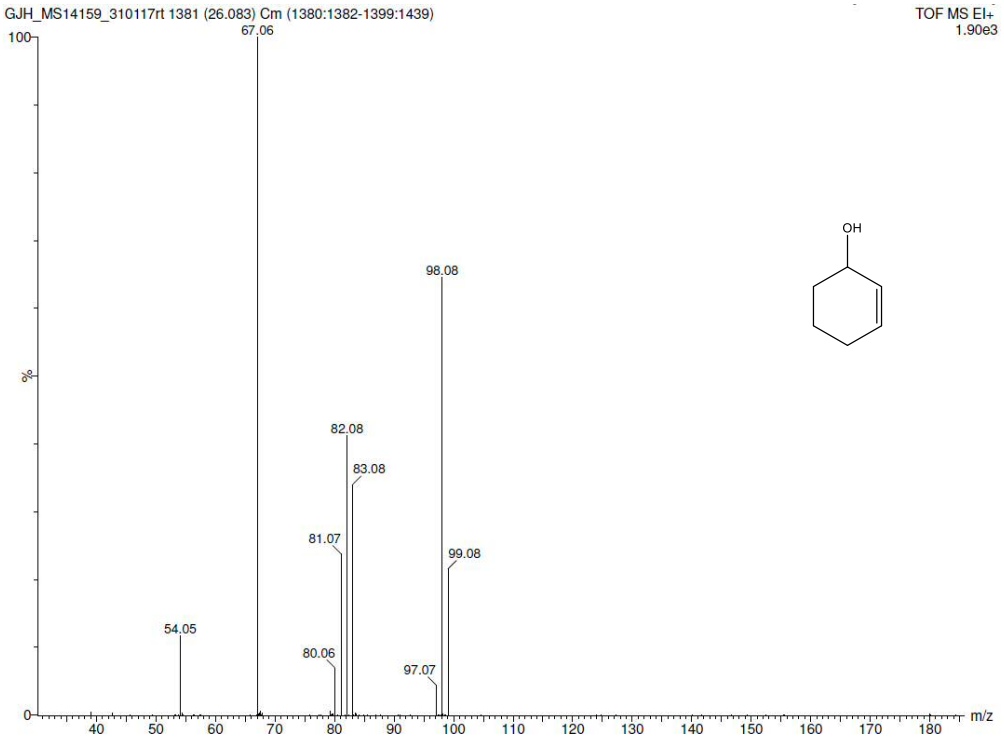

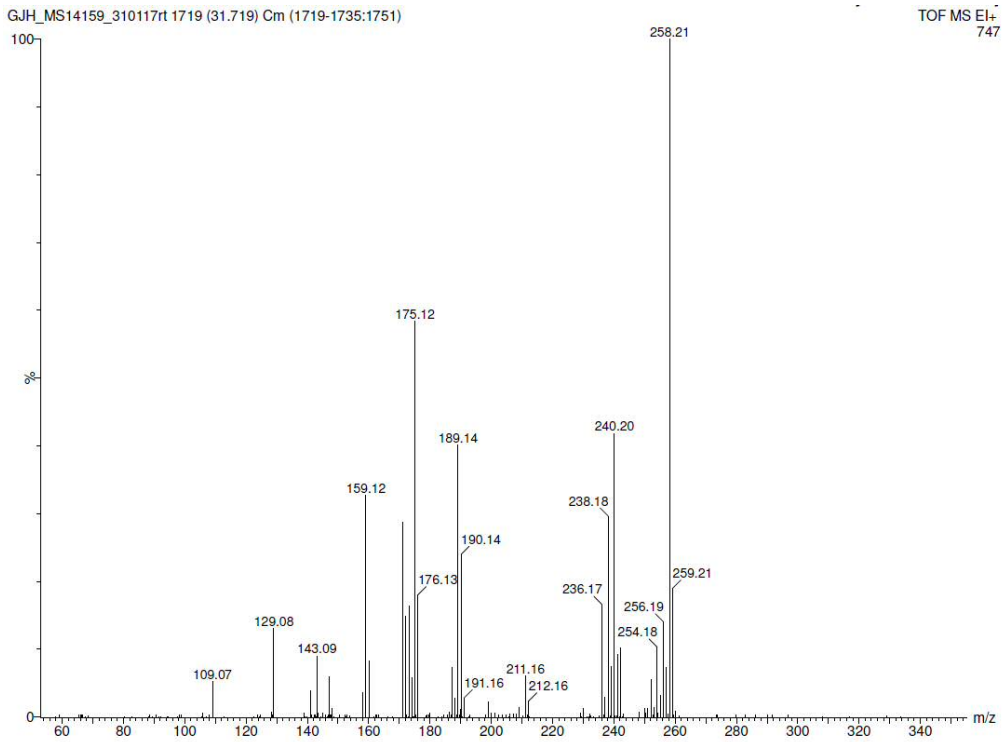

A more concentrated sample shows further side products and the starting material:

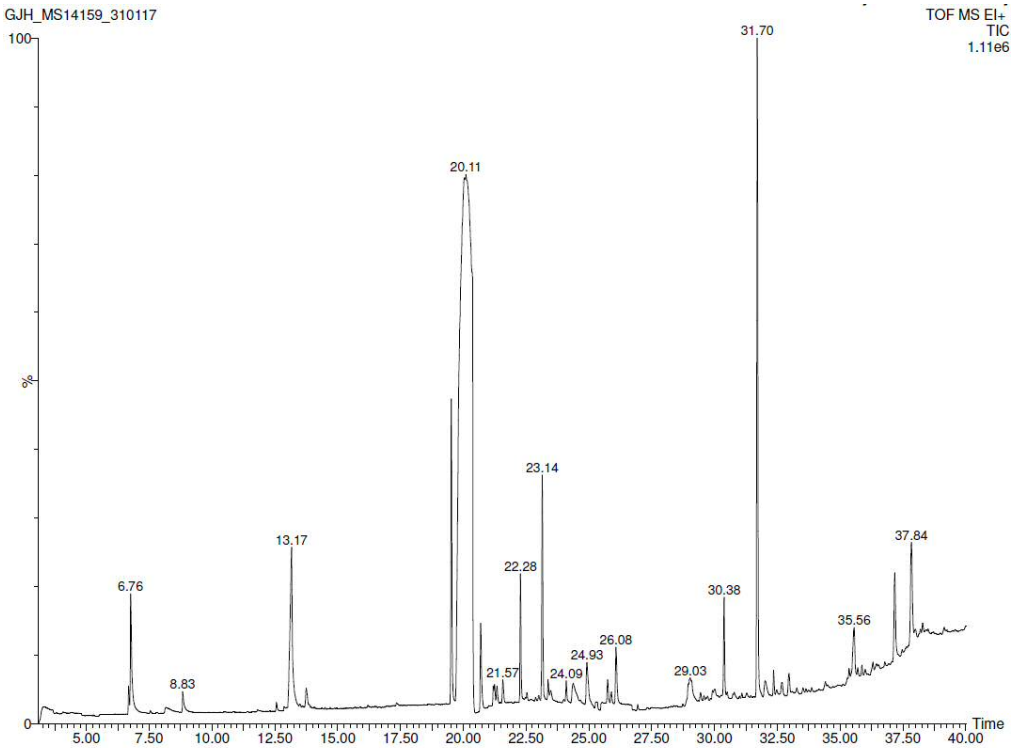
GJH_MS14159_310117
TOF MS EI+
TIC
1.11e6
100
%
0
31.70
20.11
23.14
13.17
37.84
22.28
6.76
30.38
35.56
26.08
24.93
8.83
21.57
24.09
29.03
Time
5.00
7.50
10.00
12.50
15.00
17.50
20.00
22.50
25.00
27.50
30.00
32.50
35.00
37.50
40.00

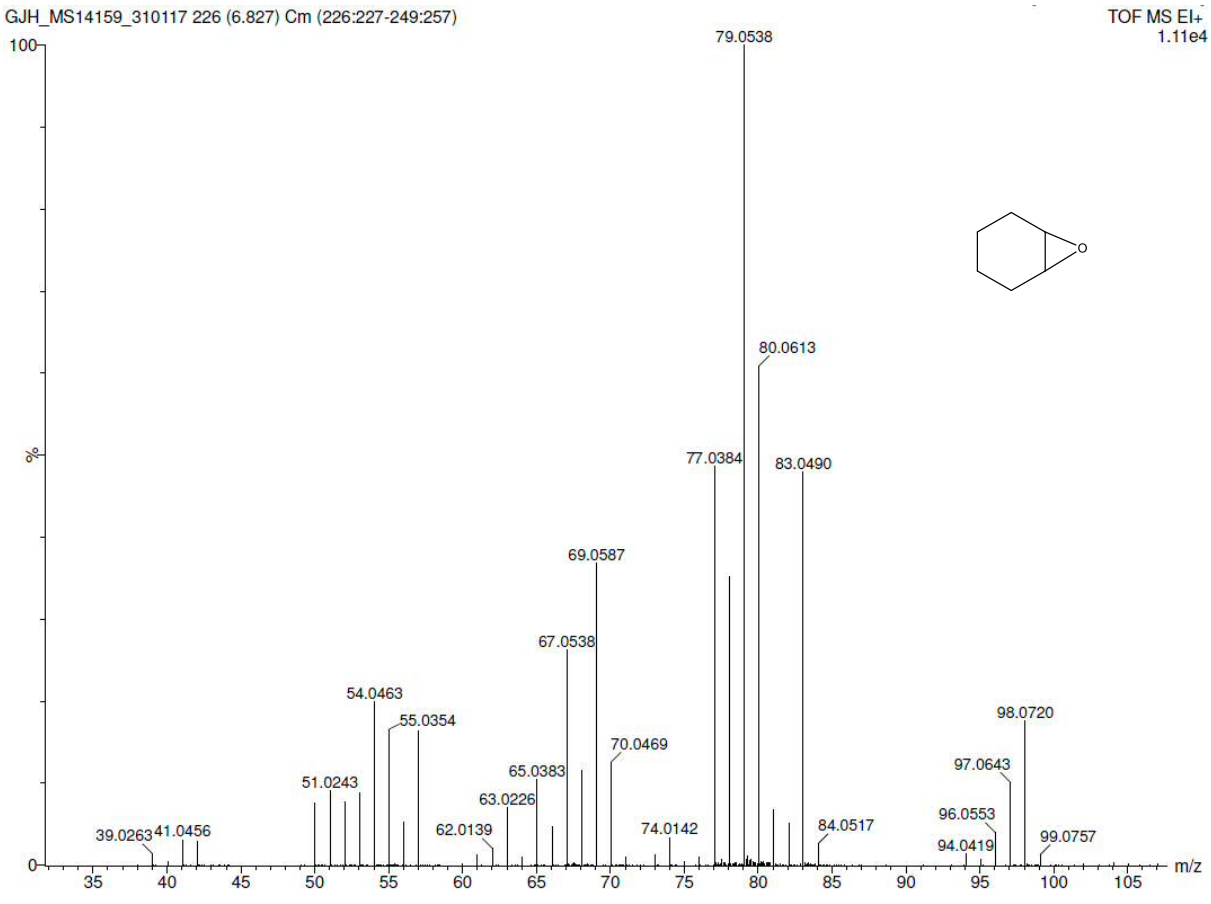
GJH_MS14159_310117 226 (6.827) Cm (226:227-249:257)
TOF MS EI+
1.11e4
100
%
0
79.0538
80.0613
77.0384
83.0490
69.0587
67.0538
54.0463
55.0354
98.0720
70.0469
97.0643
65.0383
51.0243
63.0226
96.0553
39.0263
41.0456
62.0139
74.0142
84.0517
94.0419
99.0757
m/z
35
40
45
50
55
60
65
70
75
80
85
90
95
100
105

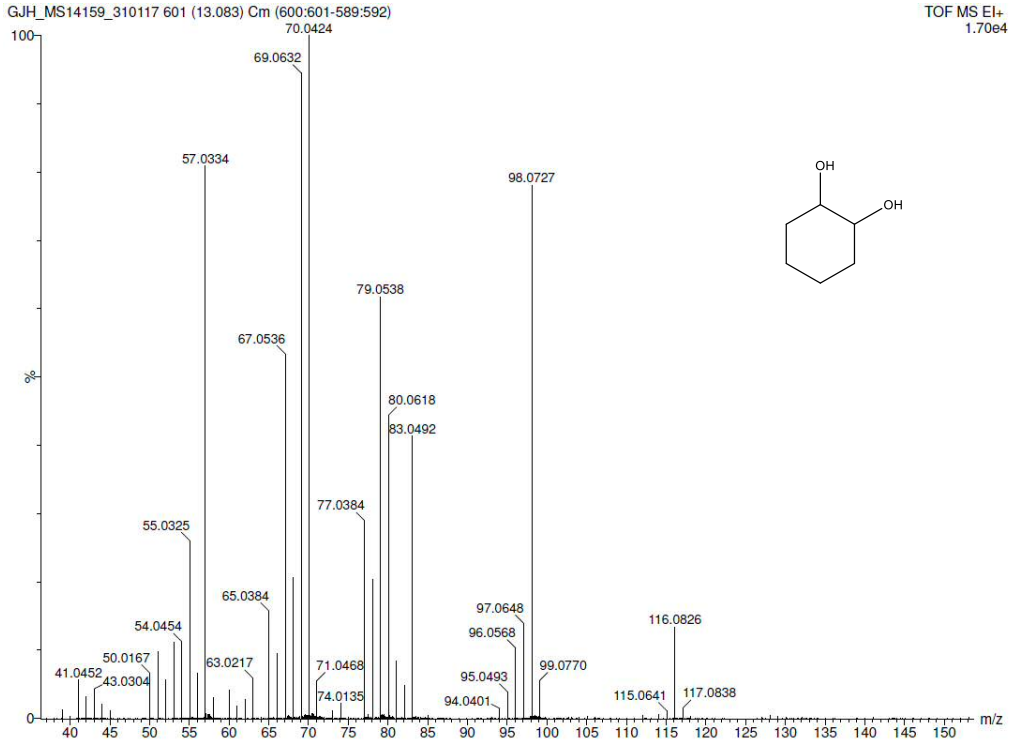

7.2.2. Cycloaddition of CO_2 with cyclooctene oxide experiment (130°C, 20 bar CO_2, 24 h)

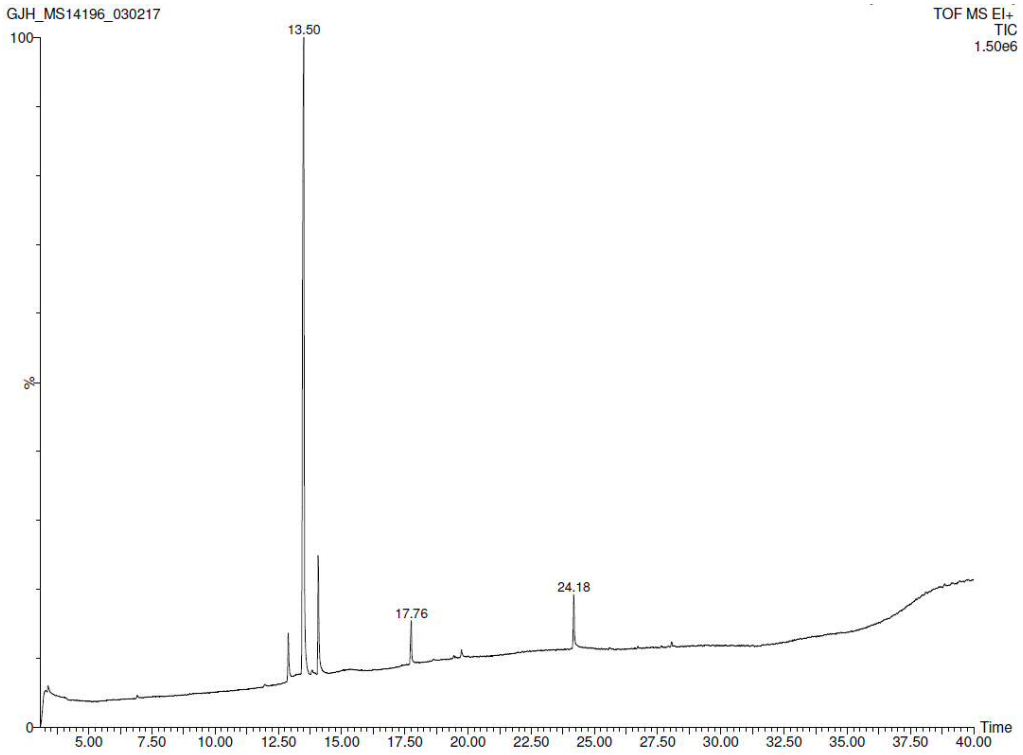

At 12.9 min two compounds are co-eluting, an isomer of the starting material and tributylamine.

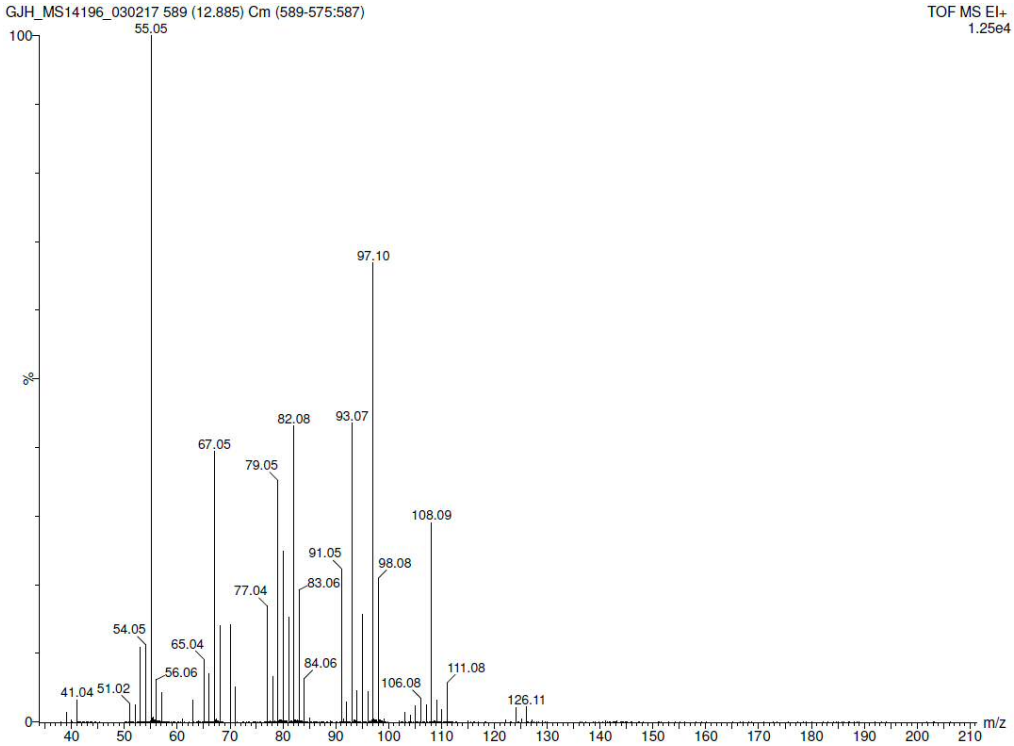
GJH_MS14196_030217 589 (12.885) Cm (589-575:587)
TOF MS EI+
1.25e4
100
%
0
55.05
97.10
82.08
93.07
67.05
79.05
108.09
91.05
98.08
83.06
77.04
54.05
65.04
84.06
111.08
56.06
106.08
41.04
51.02
126.11
m/z
40 50 60 70 80 90 100 110 120 130 140 150 160 170 180 190 200 210

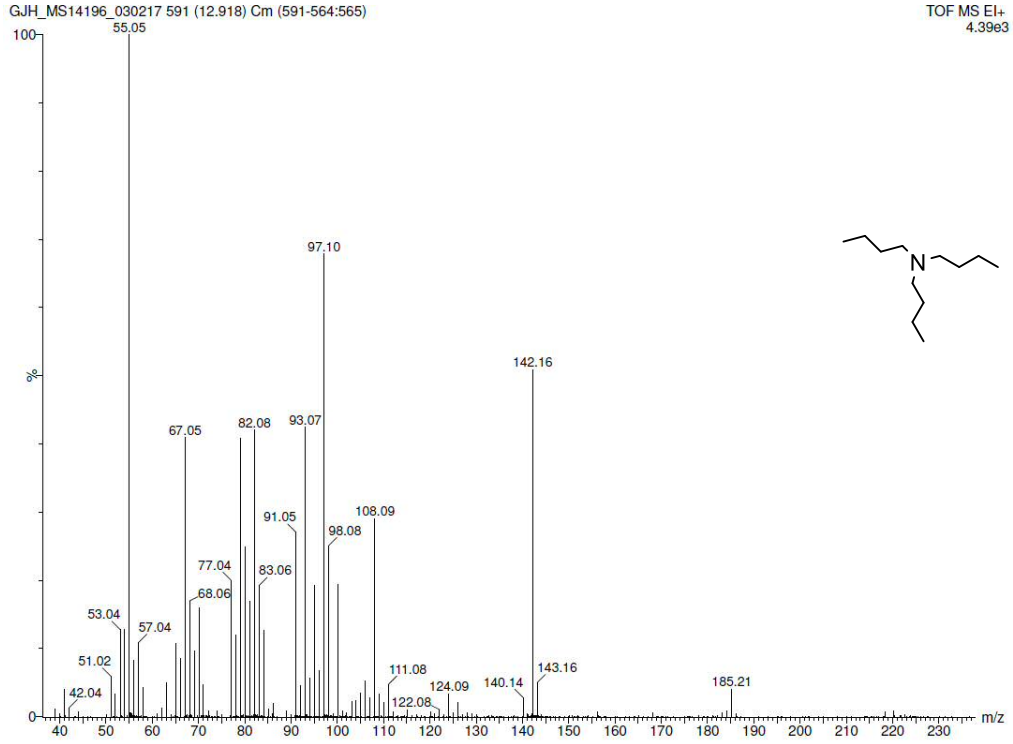
GJH_MS14196_030217 591 (12.918) Cm (591-564:565)
TOF MS EI+
4.39e3
100
%
0
55.05
97.10
142.16
82.08
93.07
67.05
91.05
108.09
98.08
77.04
83.06
68.06
53.04
57.04
51.02
111.08
143.16
124.09
140.14
185.21
42.04
122.08
m/z
40 50 60 70 80 90 100 110 120 130 140 150 160 170 180 190 200 210 220 230

N

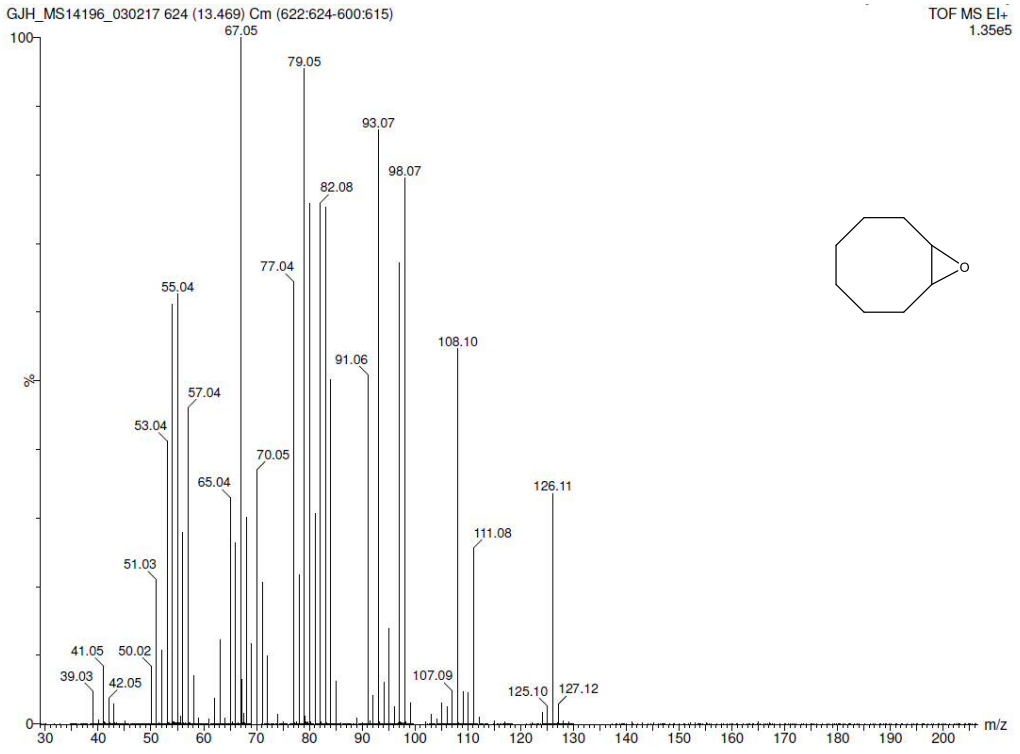
GJH_MS14196_030217 624 (13.469) Cm (622:624-600:615)
TOF MS EI+
1.35e5
100
%
0
67.05
79.05
93.07
98.07
82.08
77.04
55.04
108.10
91.06
57.04
53.04
70.05
65.04
126.11
111.08
51.03
41.05
50.02
39.03
42.05
107.09
125.10
127.12
O
30 40 50 60 70 80 90 100 110 120 130 140 150 160 170 180 190 200
m/z

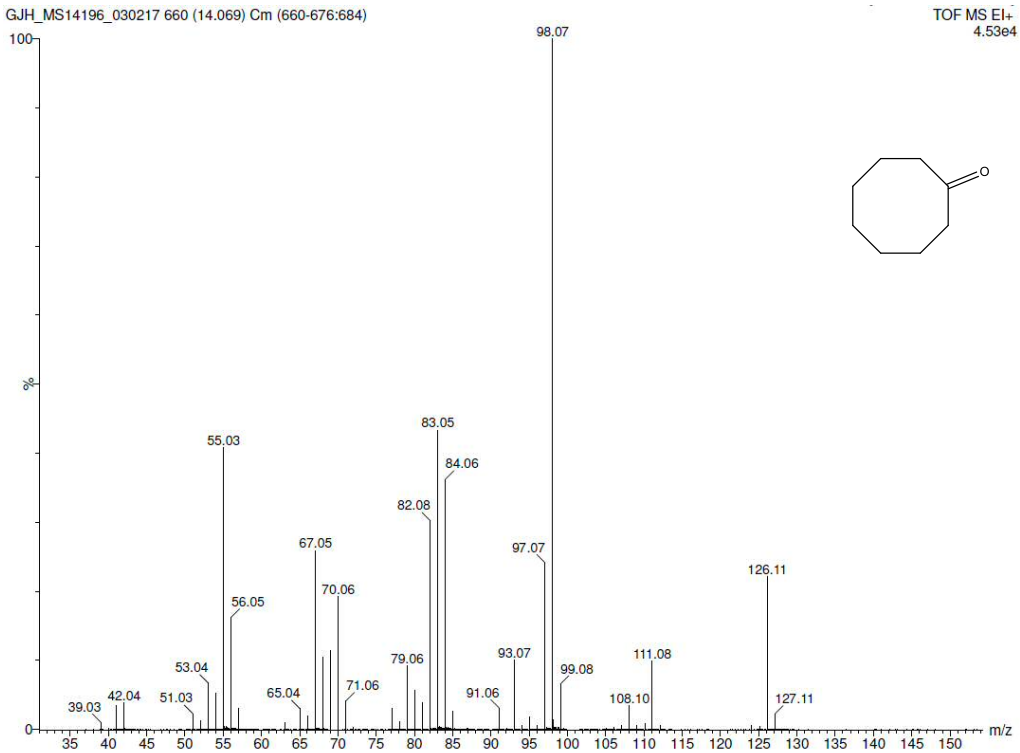
GJH_MS14196_030217 660 (14.069) Cm (660-676:684)
TOF MS EI+
4.53e4
100
%
0
98.07
83.05
55.03
84.06
82.08
67.05
97.07
126.11
70.06
56.05
79.06
93.07
111.08
53.04
99.08
71.06
65.04
91.06
108.10
127.11
39.03
42.04
51.03
O
35 40 45 50 55 60 65 70 75 80 85 90 95 100 105 110 115 120 125 130 135 140 145 150
m/z

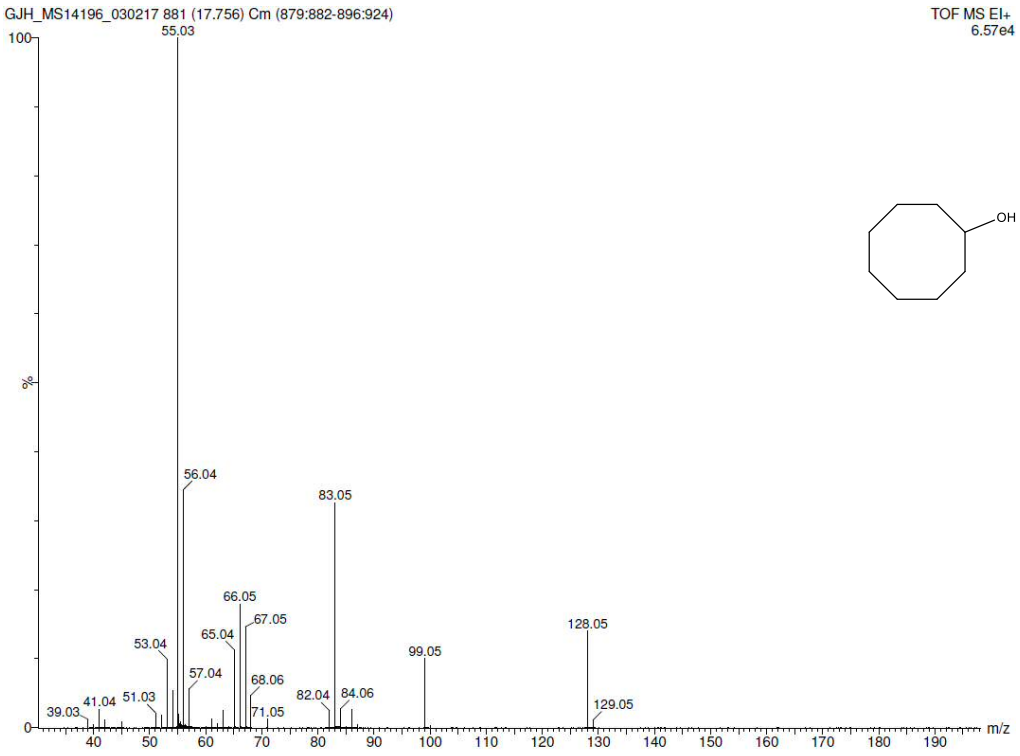
GJH_MS14196_030217 881 (17.756) Cm (879:882-896:924)
TOF MS EI+
6.57e4
100
%
0
55.03
56.04
83.05
66.05
67.05
65.04
53.04
57.04
68.06
71.05
82.04
84.06
99.05
128.05
129.05
39.03
41.04
51.03
OH
40 50 60 70 80 90 100 110 120 130 140 150 160 170 180 190
m/z

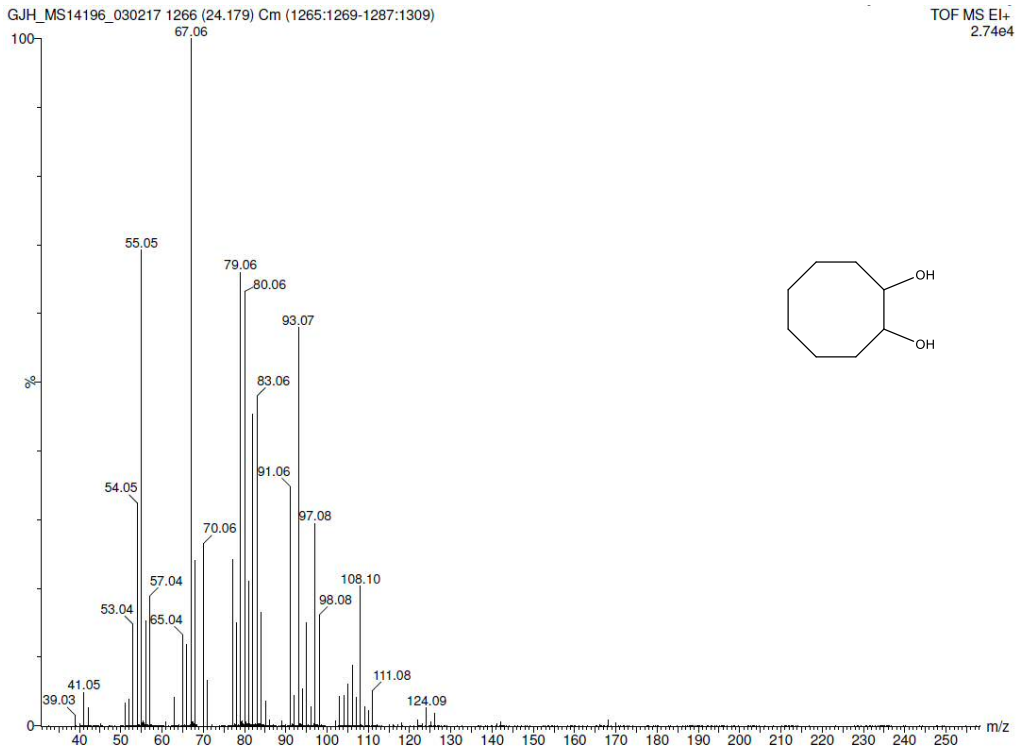
GJH_MS14196_030217 1266 (24.179) Cm (1265:1269-1287:1309)
TOF MS EI+
2.74e4
100
%
0
67.06
55.05
79.06
80.06
93.07
83.06
91.06
54.05
97.08
70.06
57.04
108.10
98.08
53.04
65.04
111.08
41.05
39.03
124.09
OH
OH
40 50 60 70 80 90 100 110 120 130 140 150 160 170 180 190 200 210 220 230 240 250
m/z

7.2.3. Cycloaddition of CO_2 with Cyclopentene oxide experiment (90°C, 20 bar CO_2, 4 h)

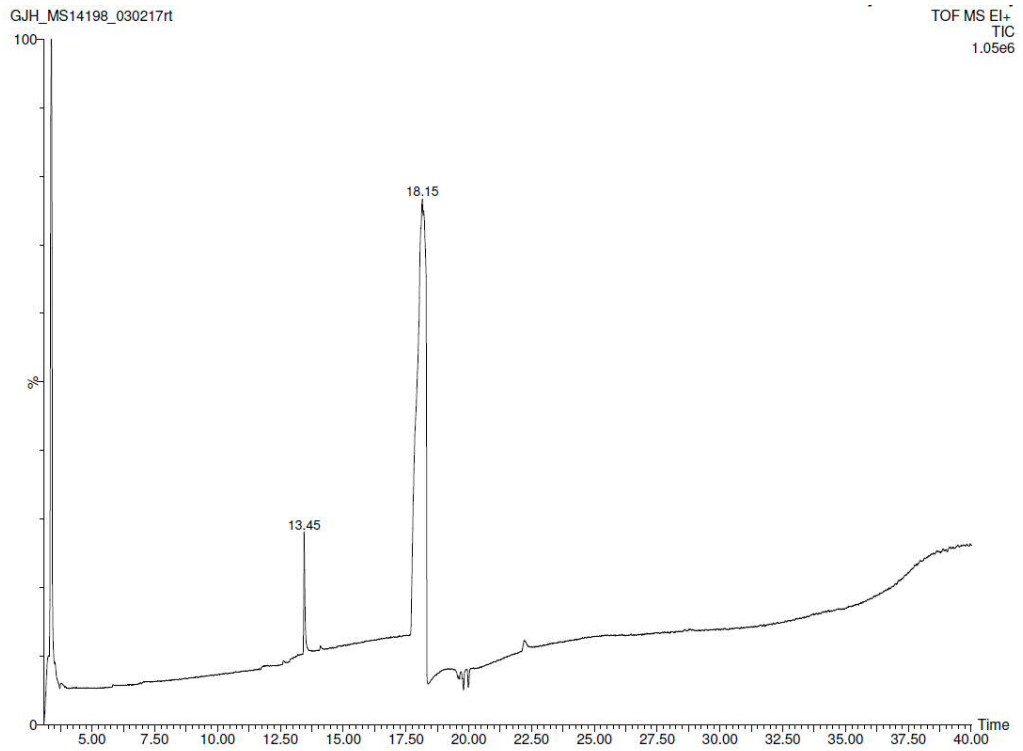

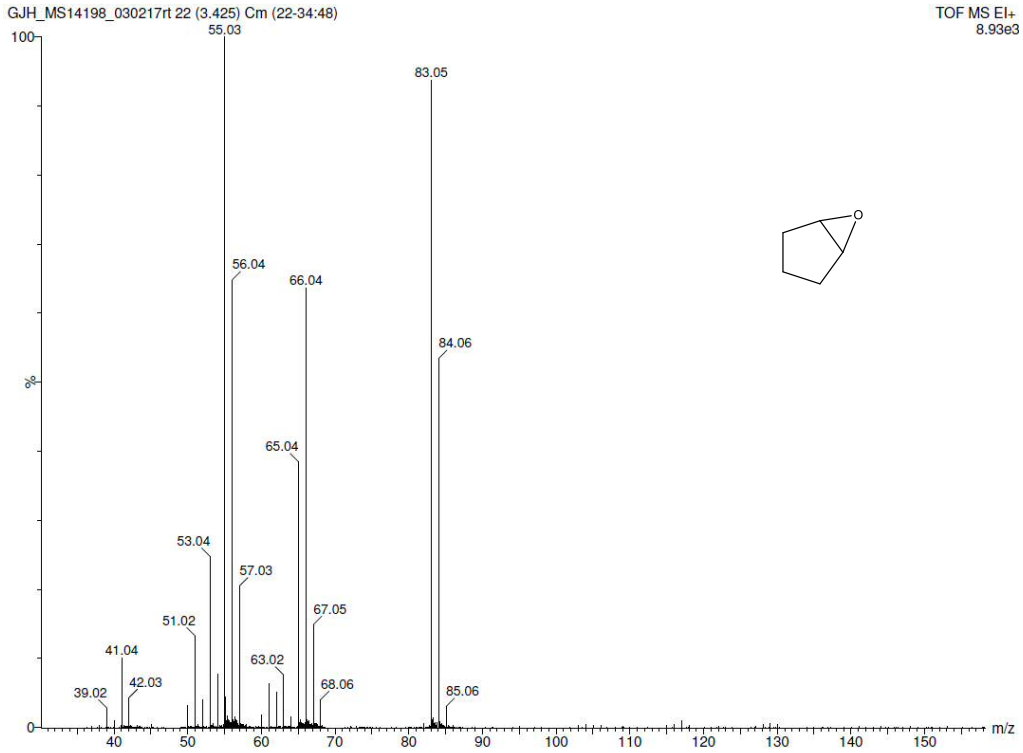

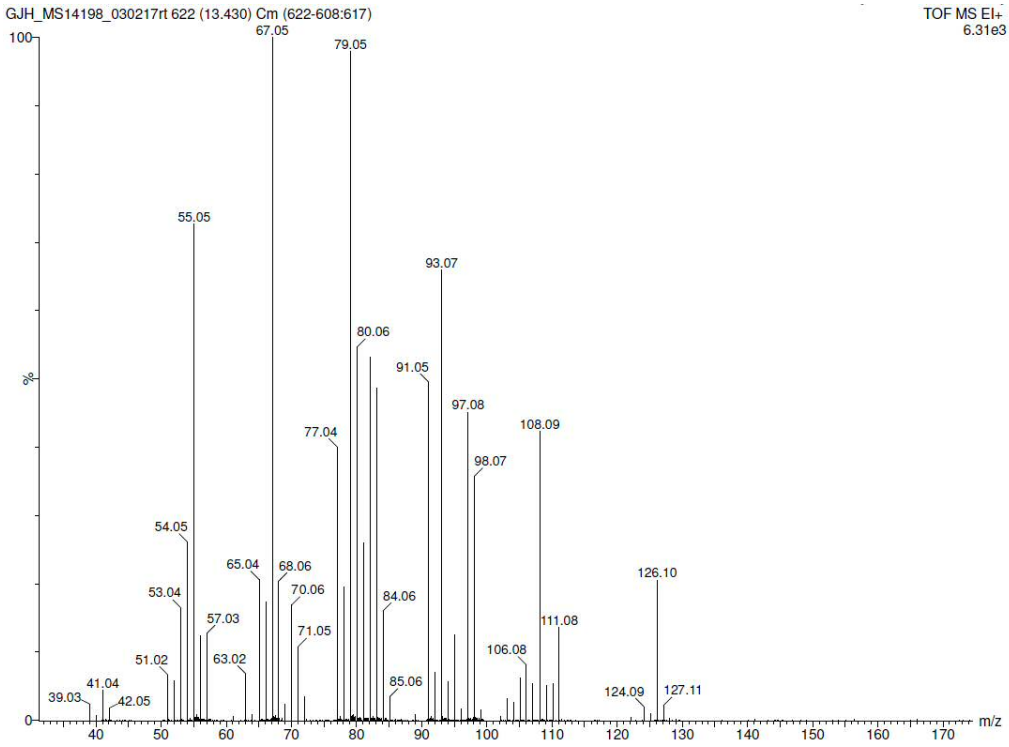
GJH_MS14198_030217rt 622 (13.430) Cm (622-608:617)
TOF MS EI+
6.31e3
100
%
0
67.05
79.05
55.05
93.07
80.06
91.05
97.08
108.09
77.04
98.07
54.05
65.04
68.06
126.10
53.04
70.06
84.06
57.03
111.08
71.05
106.08
51.02
63.02
85.06
41.04
39.03
42.05
124.09
127.11
40
50
60
70
80
90
100
110
120
130
140
150
160
170
m/z

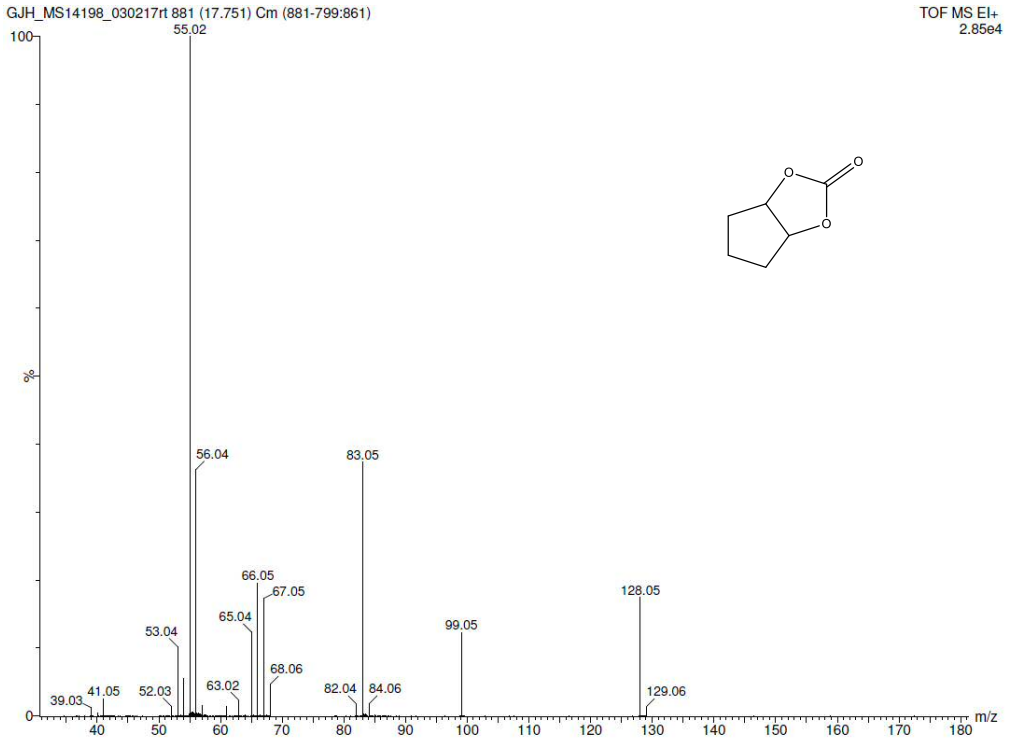
GJH_MS14198_030217rt 881 (17.751) Cm (881-799:861)
TOF MS EI+
2.85e4
100
%
0
55.02
56.04
83.05
66.05
67.05
128.05
65.04
99.05
53.04
68.06
63.02
82.04
84.06
129.06
39.03
41.05
52.03
40
50
60
70
80
90
100
110
120
130
140
150
160
170
180
m/z

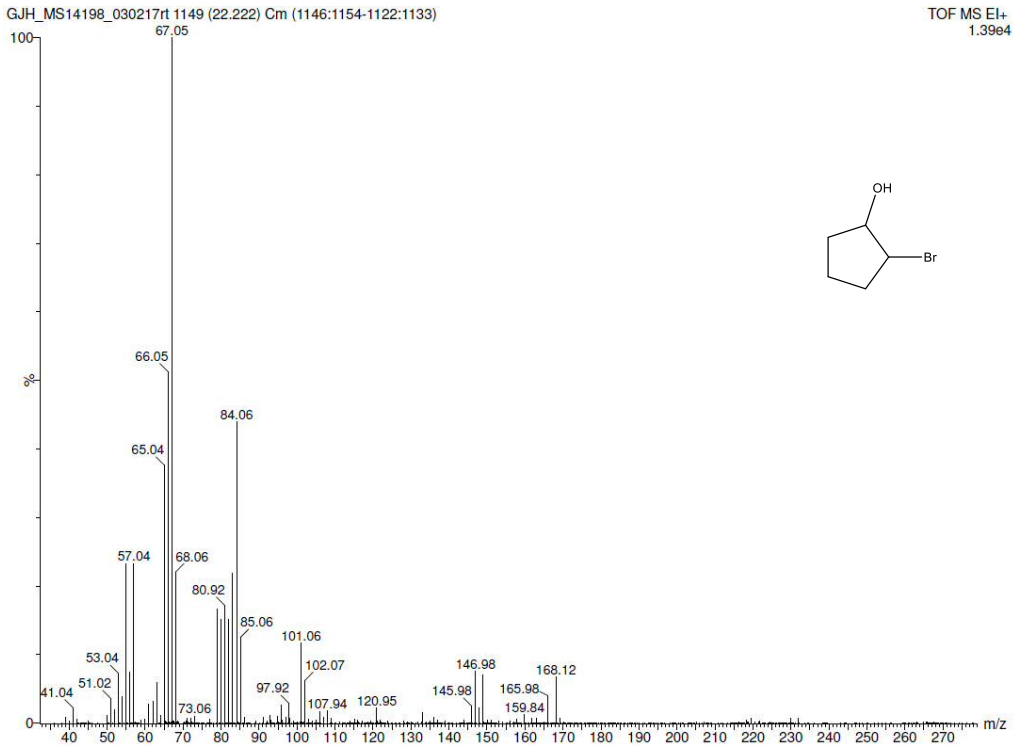

A more concentrated sample shows further side products:

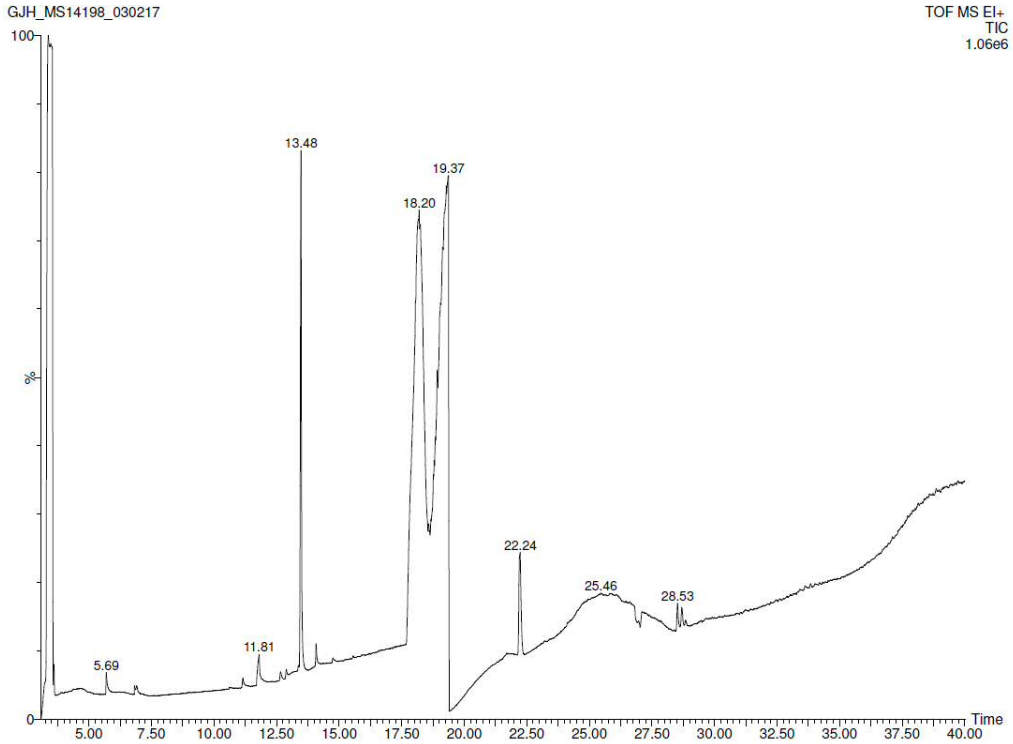

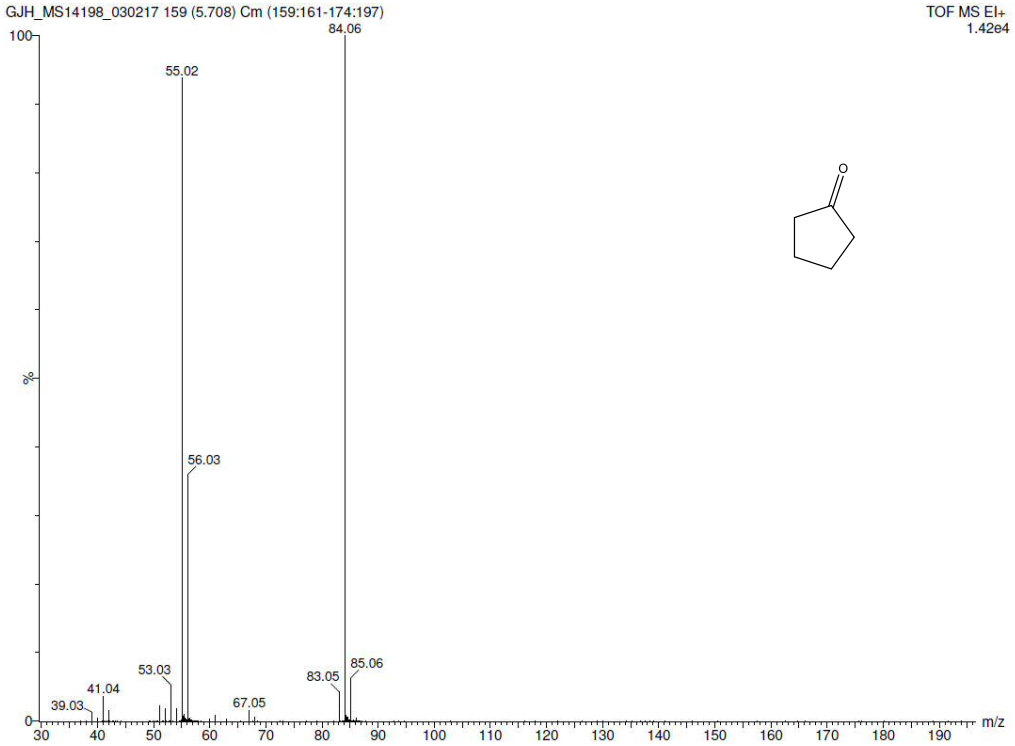
GJH_MS14198_030217 159 (5.708) Cm (159:161-174:197)
TOF MS EI+
1.42e4
100
%
0
84.06
55.02
56.03
53.03
41.04
39.03
67.05
83.05
85.06
O
30 40 50 60 70 80 90 100 110 120 130 140 150 160 170 180 190
m/z

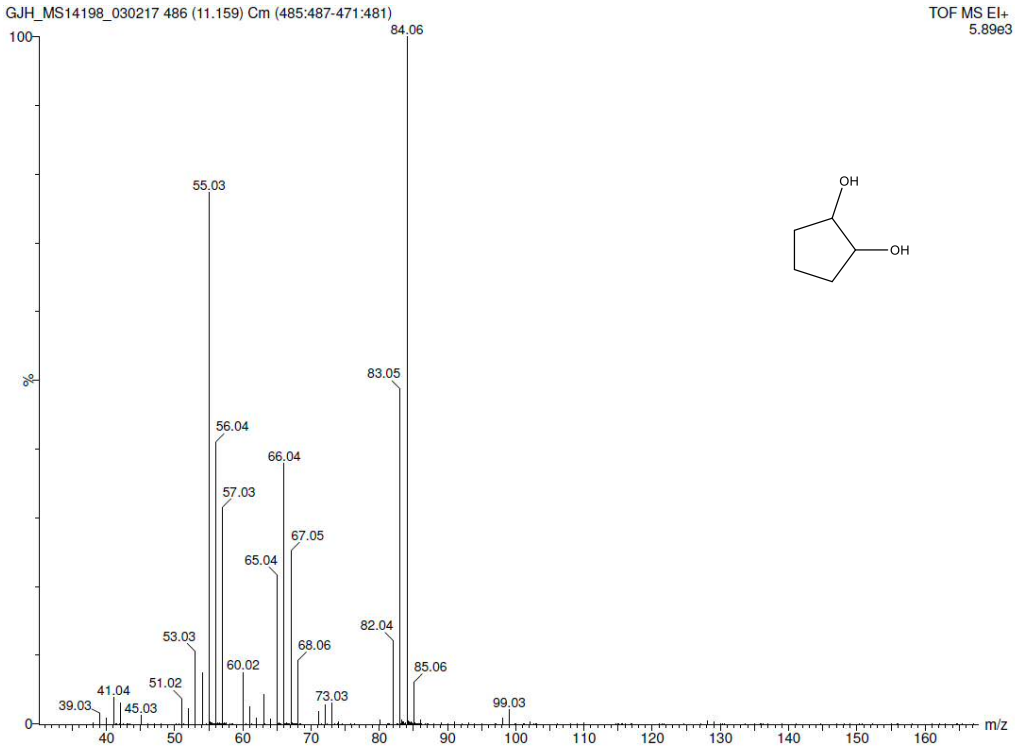
GJH_MS14198_030217 486 (11.159) Cm (485:487-471:481)
TOF MS EI+
5.89e3
100
%
0
84.06
55.03
83.05
56.04
66.04
57.03
67.05
65.04
82.04
53.03
68.06
60.02
85.06
41.04
51.02
73.03
39.03
45.03
99.03
OH
OH
40 50 60 70 80 90 100 110 120 130 140 150 160
m/z